Report
R-19-18
December 2019

Biosphere parameters used in radionuclide transport modelling and dose calculations in SE-SFL

Sara Grolander
Benedict Jaeschke

SVENSK KÄRNBRÄNSLEHANTERING AB

SWEDISH NUCLEAR FUEL
AND WASTE MANAGEMENT CO

Box 3091, SE-169 03 Solna
Phone +46 8 459 84 00
skb.se

SVENSK KÄRNBRÄNSLEHANTERING

ISSN 1402-3091
SKB R-19-18
ID 187883

December 2019

Biosphere parameters used in radionuclide transport modelling and dose calculations in SE-SFL

Sara Grolander, Kemakta Konsult AB
Benedict Jaeschke, AFRY

Keywords: SFL, Long-lived low- and intermediate-level waste, Safety evaluation, Post-closure safety, Surface ecosystem, Biosphere, Dose, Landscape, Model, Laxemar.

Summary

This report is produced as a part of the biosphere assessment of the safety evaluation SE-SFL and describes all biosphere parameters used in the radionuclide model for the biosphere, the BioTex. The report consists of several chapters where different parameter types are described (Chapter 2 – Radionuclide specific parameters, Chapter 3 – Landscape geometries, Chapter 4 – Regolith properties, Chapter 5 – Surface hydrological fluxes, Chapter 6 – Element-specific parameters, Chapter 7– Aquatic ecosystem parameters, Chapter 8 – Terrestrial ecosystem parameters, Chapter 9 – Human characteristics, Chapter 10 to 12 – Parameters used in alternative evaluation cases). Chapter 1 gives a general introduction to the SE-SFL safety evaluation and presents the conditions for parameterisation and the general assumption made in the parameterisation process. The parameterisation methods and the selected data relies to a large extent on the work done in previous safety assessment, SR-PSU (Grolander 2013) although some updates of the radionuclide model have been made that had implications for the parameters that are presented in this report.

No site has yet been selected for the SFL repository. In this evaluation of post-closure safety, the Laxemar site was chosen as an example model site for SFL. This ensures that there is a realistic and consistent site description based on a detailed and coherent dataset. Several of the parameters respond to changes in temperature, precipitation, hydrology, Quaternary geology or geochemical conditions at the modelled site, and these conditions differ between sites in Sweden and also between the Forsmark and Laxemar sites. How the site-specific conditions affect the parameter values was interpreted individually for each parameter. It was concluded that a large number of parameters will be affected significantly by changes in site conditions, these parameters are regarded as site-specific and extensive site-specific information is required in order to be able to undertake a safety evaluation or safety assessment and minimise the uncertainty in the results.

Sammanfattning

Denna rapport produceras som en del av biosfärbedömningen i säkerhetsutvärderingen SE-SFL och beskriver alla biosfärparametrar som används i radionuklidmodellen för biosfären, BioTex. Rapporten består av flera kapitel där olika parametertyper beskrivs (kapitel 2 – Radionuklidspecifika parametrar, kapitel 3 – Landskapsgeometrier, kapitel 4 – Regolitegenskaper, kapitel 5 – Ythydrologiska flöden, kapitel 6 – Elementspecifika parametrar, kapitel 7 – Vattenekosystemparametrar, kapitel 8 – Terrestriska ekosystemparametrar, kapitel 9 − Människans egenskaper, kapitel 10 till 12– Parametrar som används i alternativa utvärderingsfall). Kapitel 1 ger en allmän introduktion till SE-SFL säkerhetsutvärderingen och presenterar villkoren för parametreriseringen och det allmänna antagandet som gjorts i parameteriseringsprocessen. Parameteriseringsmetoderna och de valda parametervärdena förlitar sig i stor utsträckning på det arbete som utförts i tidigare säkerhetsbedömning, SR-PSU (Grolander 2013), även om vissa uppdateringar av radionuklidmodellen har gjorts som haft konsekvenser för parametrarna som presenteras i denna rapport

Ingen plats har ännu valts för SFL. I denna utvärdering av säkerheten efter förslutning valdes Laxemar som en exempelplats för SFL. Detta säkerställer att det finns en realistisk och konsekvent platsbeskrivning baserad på detaljerad och sammanhängande data. Flera av parametrarna är beroende av förändringar i temperatur, nederbörd, vattenflöden, kvartärgeologi eller geokemiska förhållanden på den modellerade platsen, och dessa förhållanden skiljer sig mellan platser i Sverige och även mellan Forsmark och Laxemar. Hur de platsspecifika villkoren påverkar parametervärdena utvärderades individuellt för varje parameter och det kunde konstateras att ett stort antal parametrar kommer att påverkas avsevärt av förändringar i platsförhållandena. Dessa parametrar betraktas som platsspecifika och omfattande platsspecifik information krävs för att kunna göra en säkerhetsvärdering eller säkerhetsanalys och minimera osäkerheten i resultaten.

Contents

1 Introduction 9
1.1 Background 9
1.2 The SE-SFL safety evaluation 11
1.3 The SE-SFL report hierarchy 12
1.4 The role of this report in SE-SFL 13
1.4.1 Structure of this report 14
1.5 The parameterisation method 15
1.6 Quality assurance procedure 15
1.7 Biosphere evaluation cases 16

2 Radionuclide-specific parameters 17
2.1 Effects of site characteristics of parameter values 18
2.2 Dose coefficients 18
2.3 Half-lives 19

3 Landscape development and biosphere object geometries 21
3.1 Biosphere objects and biosphere evaluation cases 22
3.2 Parameterisation of biosphere objects representing present conditions in Laxemar 23
3.2.1 Geometrical features of a biosphere object 23
3.2.2 Regolith thickness 23
3.3 Streams in biosphere objects 26
3.4 Parameters changing during biosphere object development in Laxemar 26
3.4.1 Regolith Lake Development Model (RLDM) 28
3.4.2 A simplified model to describe non-modelled biosphere object stages 29
3.4.3 Lake development 32
3.4.4 Threshold parameters for modelling ecosystem transitions 34
3.5 Permanent aquatic objects to assess long-term release 36
3.6 A coastal site with a flatter topography in comparison to Laxemar 36

4 Regolith properties 39
4.1 Effect of site-specific characteristics on parameter values 40
4.2 Selection of parameter values 40
4.3 Densities and porosities of non-cultivated soils and aquatic sediments 41
4.4 Properties of cultivated soils 41
4.4.1 Densities and porosities of cultivated gyttja clay and peat 41
4.4.2 Compactation of clay gyttja and peat 41
4.4.3 Degree of saturation of clay gyttja and peat 41

5 Surface hydrological fluxes 43
5.1 Introduction 43
5.2 Residence times of water in coastal basins from 10 000 BC to 9 000 AD 45
5.3 MIKE SHE Water balances 48
5.4 Stylised water balance models for biosphere objects 50
5.4.1 Sea stage 51
5.4.2 Lake – Mire stages 52
5.4.3 Drained and cultivated stage 53
5.5 Net precipitation and cross-boundary flows 53
5.5.1 Net precipitation and horizontal surface- and groundwater flows during the land stage 54
5.5.2 Vertical distribution of discharge from the local catchment 55
5.5.3 Bedrock discharge 57
5.6 Downward groundwater fluxes 58
5.6.1 The vertical profile of percolation 59
5.6.2 Percolation rates at reference levels 61
5.6.3 Percolation through the surface of the upper regolith layers in lake and mire ecosystems 63

5.7 Discharge in the biosphere object 64
5.8 Biosphere model parameters for present climatic conditions 67
5.9 Biosphere model parameters for other climatic conditions 68
5.9.1 Impact of moderate changes in temperature and precipitation on runoff and deep groundwater recharge in Southeast Sweden. 68
5.9.2 Parameter values for object 206 for other temperate climate conditions 70
5.9.3 Hydrology in periglacial conditions 71
5.9.4 Parameter values for permafrost conditions 71
5.10 Discussion and conclusions 73

6 Element-specific parameters 75
6.1 Parameter definitions 75
6.2 Effect of site-specific properties on parameter values 77
6.3 Comparison between Laxemar and Forsmark data 78
6.3.1 Limnic *CR*s 81
6.3.2 Marine *CR*s 83
6.3.3 Terrestrial *CR*s 84
3.3.4 K_d values 84
6.4 Selected data for element-specific parameters 84
6.5 Updated *CR* and K_d values for Laxemar 86
6.5.1 *CR* for limnic fish (CR_lake_fish) 86
6.5.2 *CR* for limnic primary producers (cR_lake_pp_macro, cR_ lake_ pp_ micor, cR_Lake_pp_plank) 87
6.5.3 *CR* for marine fish (CR_sea_fish) 87
6.5.4 *CR* for marine primary producers (sea_pp_macro) 87
6.5.5 *CR* for terrestial vegetation and fodder (cR_ter_pp, cR_agri_fodder) 87
6.5.6 *CR* for terrestial herbivores (cR_food_to_herbivore) 88
6.5.7 K_d for particulate matter in lake water (Kd_PM_Lake) 88
6.5.8 K_d for particulate matter in seawater (Kd_PM_Sea) 88
6.5.9 K_d for aquatic sediment (Kd_regoUp_aqu) 88
6.6 Selected data for Be and K 89

7 Aquatic ecosystem parameters 91
7.1 Effects of site-specific characteristics on parameter values 91
7.2 Selection of parameter values 93
7.3 Generic parameters 93
7.4 Site-dependent parameters 93
7.4.1 Site-specific parameters for which Forsmark data are used 93
7.4.2 Site-specific data where updated data are used 94
7.4.3 Time-dependent parameters describing biomass and net primary productivity of aquatic primary producers 96
7.4.4 Updates in BioTEx since SR-PSU 100

8 Terrestrial ecosystem parameters 101
8.1 Effects of site characteristics on parameter values 101
8.2 Selection of parameter data 101
8.3 Generic parameters 102
8.4 Site-specific parameters 105
8.4.1 Site-specific parameters for which Forsmark data are used 105
8.4.2 Site-specific parameters where Laxemar data are assigned 106
8.5 Updates in the BioTEx since SR-PSU 107
8.5.1 Water uptake in growing crops 107
8.5.2 Time period of irrigation 108
8.5.3 Fraction of inorganic chlorine in primary producers 108
8.5.4 Biomass of crops 108
8.5.5 Yields of tubers and vegetables 108
8.5.6 Net primary production 108
8.5.7 Translocation of radionuclides during irrigation of the garden plot 108
8.5.8 Soil respiration in different types of regolith 109

8.5.9 Removal of deposited radionuclides from the plant leaf surface 109
8.5.10 Diffusivity of CO_2 in air 109
8.5.11 Concentration in air after combustion of peat and wood in a small household 109
8.5.12 Stable element concentrations in vegetation and regolith layers 110

9 Human characteristics 113
9.1 Parameters and dependencies of exposure route 113
9.2 Effects of site characteristics on parameter values 113
9.3 Selection of parameter values 114

10 Alternative regional climate evaluation case 117
10.1 Parameters changed in the Alternative regional climate evaluation case 118
10.1.1 Water uptake in crops 118
10.1.2 Amount of irrigation 118
10.1.3 Percolation 118

11 Increased greenhouse effect evaluation case 121
11.1 Water deficit and irrigation practice 121
11.1.1 The drained mire 121
11.1.2 The garden plot 122
11.2 Parameters changed or added in the increased greenhouse effect climate case 122
11.2.1 Number of irrigation events for large scale agriculture 122
11.2.2 Number of irrigation events for a garden plot 122
11.2.3 Time period for irrigation for large-scale agriculture 123
11.2.4 Time period for irrigation of the garden plot 123
11.2.5 Amount of irrigation 123
11.2.6 Water uptake in crops 123
11.2.7 Percolation 123
11.2.8 Concentration of CO_2 in the atmosphere 124
11.2.9 Wash off coefficient for fodder 124
11.2.10 Leaf storage capacity for fodder 124
11.2.11 Translocation of radionuclides to cereals 124
11.2.12 Threshold describing the length of the “greenhouse” climate (threshold_IGE) 124

12 Simplified glacial cycle 125

13 Concluding summary 129

References 133

Appendix A Radionuclide-specifc parameters 139

Appendix B Landscape geometries 143

Appendix C Regolith parameters 145

Appendix D Hydrological fluxes 147

Appendix E Element-specific parameter values 149

Appendix F Aquatic ecosystem parameters 187

Appendix G Terrestrial ecosystem parameters 189

Appendix H Human characteristics 193

Appendix I Alternative regional climate 195

Appendix J An increased greenhouse effect 197

Appendix K Simplified glacial cycle 199

1 Introduction

This report constitutes one of the references supporting the safety evaluation for a proposed concept for the repository for long-lived waste (SFL) in Sweden. The purpose of the SFL safety evaluation (SE-SFL) is to provide input to the subsequent, consecutive steps in the development of SFL. This chapter gives the background to the project and an overview of the safety evaluation. Moreover, the role of this report is described in the context of the evaluation.

1.1 Background

The Swedish power industry has been generating electricity by means of nuclear power for more than 40 years. The Swedish system for managing and disposal of the waste from operation of the reactors has been developed over that period. When finalised, this system will comprise three repositories: the repository for short-lived radioactive waste (SFR), the repository for long-lived waste (SFL), and the Spent Fuel Repository.

The system for managing radioactive waste is schematically depicted in Figure 1-1. SKB currently operates SFR at Forsmark in Östhammar municipality to dispose of low- and intermediate-level waste produced during operation of the various nuclear power plants, as well as to dispose waste generated during applications of radioisotopes in medicine, industry, and research. Further, SFR is planned to be extended to permit the disposal of waste from decommissioning of nuclear facilities in Sweden. The spent nuclear fuel is presently stored in the interim storage facility for spent nuclear fuel (Clab) in Oskarshamn municipality. Clab is planned to be complemented by the Encapsulation Plant, together forming Clink. SKB has also applied to construct, possess and operate the Spent Fuel Repository at Forsmark in Östhammar municipality. The current Swedish radioactive waste management system also includes a ship and different types of casks for transport of spent nuclear fuel and other radioactive waste.

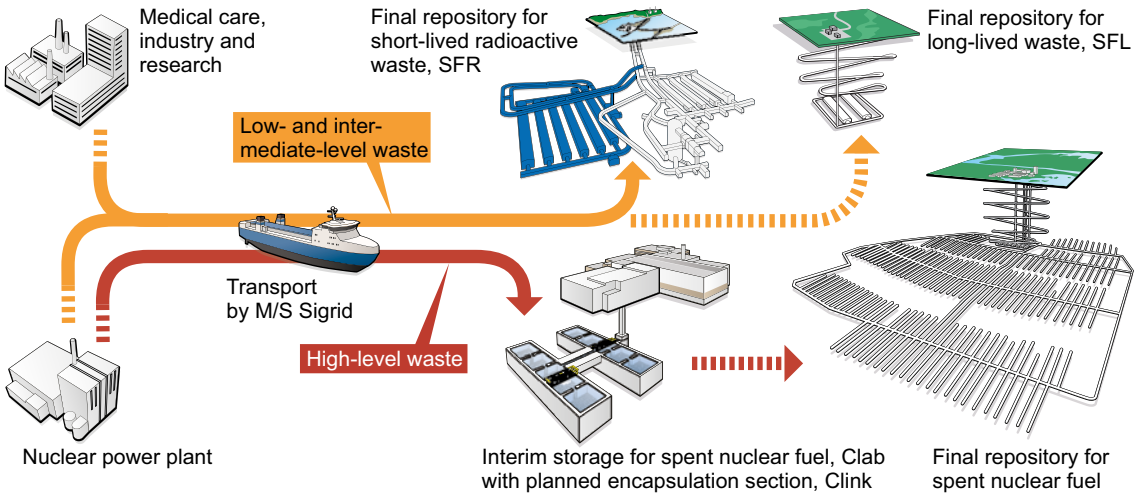

Figure 1-1. *The Swedish system for radioactive-waste management. Dashed arrows indicate future waste streams to facilities planned for construction.*

SFL will be used for disposal of the Swedish long-lived low- and intermediate-level waste. This comprises long-lived waste from the operation and decommissioning of the Swedish nuclear power plants, from early research in the Swedish nuclear programmes (legacy waste), from medicine, industry, and from research which includes the European Spallation Source (ESS) research facility. The long-lived low- and intermediate-level waste from the nuclear power plants consists of neutron-activated components and control rods and constitutes about one third of the waste planned for SFL. The rest originates mainly from the Studsvik site, where Studsvik Nuclear AB and Cyclife Sweden AB both produce and manage radioactive waste from medicine, industry and research. The legacy waste to be disposed of in SFL is currently managed by the company AB SVAFO.

In 1999, a preliminary safety assessment for SFL was presented (SKB 1999). The objective was to investigate the capacity of the facility to act as a barrier to the release of radionuclides and the importance of the repository location. The assessment was reviewed by the authorities (SKI/SSI 2001). One of the main comments was a lack of a clear account of the basis for the selection of the design and that no design alternatives had been considered. Reflecting the comments from the authorities on the preliminary safety assessment, possible solutions for management and disposal of the Swedish long-lived low- and intermediate-level waste were examined in the SFL concept study (Elfwing et al. 2013). After a first screening, four waste vault concepts were evaluated with respect to two evaluation factors; post-closure safety and robustness of the barrier safety functions (Evins 2013). Based on the evaluation, a system was proposed as a basis for further assessment of post-closure safety. According to this system, SFL is designed as a deep geological repository with two different sections:

- one waste vault, designed with a concrete barrier, BHK, for metallic waste from the nuclear power plants, and
- one waste vault, designed with a bentonite barrier, BHA, for the waste from Studsvik Nuclear AB, Cyclife Sweden AB and AB SVAFO.

A schematic illustration of the proposed facility layout and waste vault concepts for SFL is displayed in Figure 1-2. BHK is approximately 135 m long and BHA is approximately 170 m long. Both vaults have a cross sectional area of approximately 20×20 m^2. It is assumed that the waste vaults are located at 500 m below the surface and that this depth is sufficient to avoid adverse effects by permafrost during future glacial cycles, i.e. at a depth sufficient to exclude the possibility of freezing of the repository.

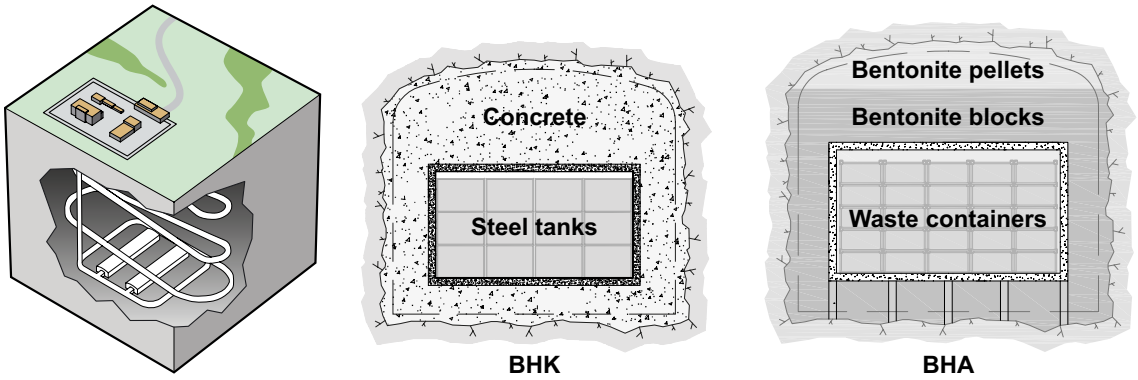

Figure 1-2. *Preliminary facility layout and the proposed repository concept for SFL (left), with one waste vault for metallic waste from the nuclear power plants (BHK, centre) and one waste vault for waste from Studsvik Nuclear AB, Cyclife Sweden AB and AB SVAFO (BHA, right).*

1.2 The SE-SFL safety evaluation

The purpose of SE-SFL is to provide input to the subsequent, consecutive steps in the development of SFL. These consecutive steps include further development of the design of the engineered barriers and the site-selection process for SFL. More specifically, there are two main objectives for SE-SFL. The first is to evaluate conditions in the waste, the barriers, and the repository environs under which the repository concept has the potential to fulfil the regulatory requirements for post-closure safety. The second is to provide SKB with a basis for prioritising areas in which the level of knowledge and adequacy of methods must be improved in order to perform a full safety assessment for SFL. This is in line with the iterative safety analysis process that the SFL repository programme follows, in which the results from post-closure safety analyses and related activities (e.g. information from a site selection process and development of numerical methods) are used to successively inform and improve the analysis. In accordance with the Nuclear Activities Act (1984:3), important research needs for the SFL programme that emerge as a result of SE-SFL will be reported in the research, development and demonstration (RD&D) programme. An important aspect of this is to ensure that the industry has well founded information to support long-term planning.

To reflect its status as a preliminary analysis the present analysis is denoted *safety evaluation*. The safety analysis methodology as applied in SE-SFL is a first evaluation of post-closure safety for the repository concept proposed by Elfwing et al. (2013) and is not part of a license application. As such, the methodology follows the methodology established by SKB for the most recent safety assessments for the extended SFR (SR-PSU; SKB 2015a) and for the Spent Fuel repository (SR-Site; SKB 2011a) but is adapted in view of the objectives of SE-SFL. The adaption of the methodology for the purposes of SE-SFL is described in Section 2.5 of the **Main report**.

To the extent applicable, SE-SFL builds on knowledge from SR-PSU and SR-Site. There are commonalities regarding the waste, engineered barriers, bedrock, surface ecosystems and external conditions relevant to post-closure safety. For instance, SE-SFL and SR-Site both address timescales of one million years (see Section 2.3 of the **Main report**). A further similarity is the proposed depth of 300–500 m. There are similarities between SFR and SFL regarding the waste and waste packaging and the proposed engineered barriers.

No site has yet been selected for SFL and therefore data from SKB's site investigation programmes for the Spent Fuel Repository and for the extension of SFR have been utilised in SE-SFL. In order to have a realistic and consistent description of a site for geological disposal of radioactive waste, data from the Laxemar site in Oskarshamn municipality (see Figure 1-3), for which a detailed and coherent dataset exists, are used. Based on an initial hydrogeological analysis for SE-SFL, the location for the SFL repository was selected to be a part of the rock volume that was earlier found most suitable for a potential Spent Fuel Repository within the Laxemar site (SKB 2011b). Data from Forsmark are included in the analysis to extend the ranges of situations and parameter values addressed, while preserving the overall context defined for Laxemar.

SE-SFL is further developed in comparison to the previous assessment (SKB 1999). Important improvements are an updated inventory and a more comprehensive and detailed account of internal and external processes. Moreover, in SE-SFL the description of biosphere has focused on vertical transport from the geosphere and accumulation in discharge areas (including ecosystem conversion), as compared with the stylised modules in SFL 3-5, which primarily described the upper parts of ecosystems. Moreover, the availability of data from the SR-Site and SR-PSU site investigations also allows for a more detailed representation of the biosphere (and the geosphere).

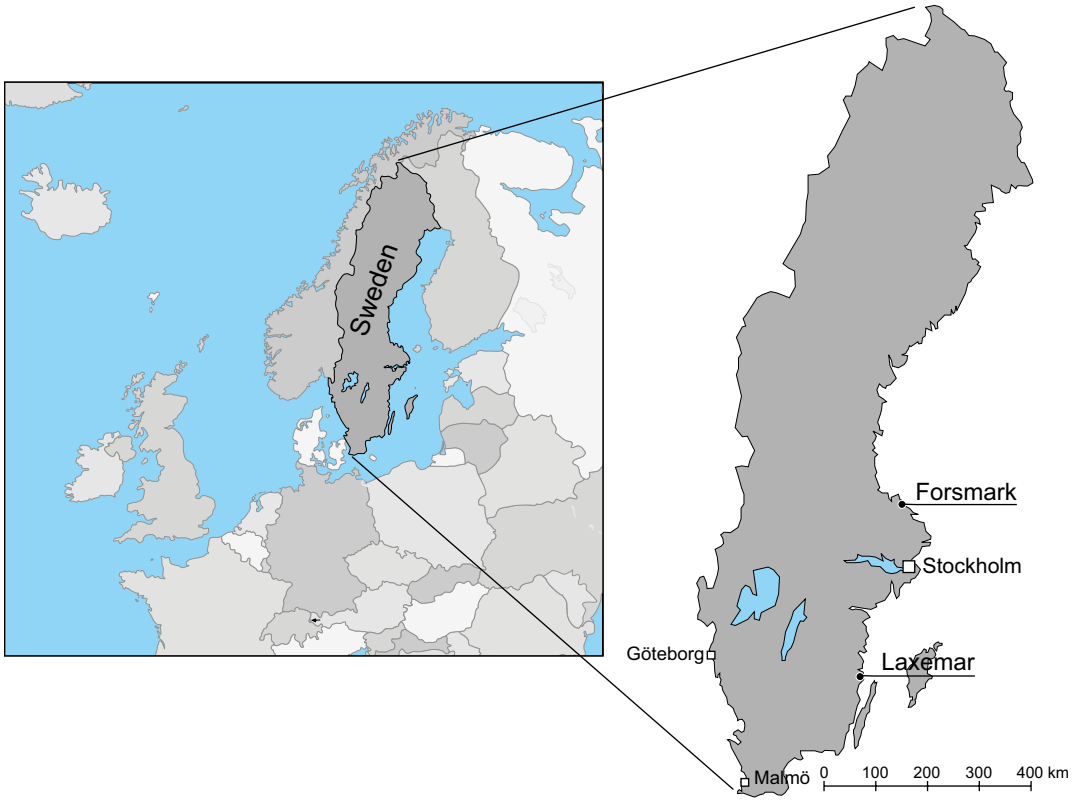

Figure 1-3. *Map showing the location of Laxemar and Forsmark. Data from the site investigations in Laxemar, along with the data from the SR-Site and SR-PSU assessments from Forsmark, are used in SE-SFL in order to have a realistic and consistent description of a site for geological disposal of radioactive waste, for which a detailed and coherent dataset exists.*

1.3 The SE-SFL report hierarchy

The **Main report** and main references in SE-SFL are listed in Table 1-1, also including the abbreviations by which they are identified in the text (abbreviated names in bold text). It can be noted that there are no dedicated process reports for the different systems in SE-SFL but there is a FEP-report. The SFR and SFL waste and repository concepts have many similarities, for instance the use of similar barrier materials and thus similar process interactions with the surrounding bedrock environment (Section 2.5.4 in the **Main report**). Therefore, the descriptions of internal processes for the waste (SKB 2014d) and the barriers (SKB 2014c) in SR-PSU are used in SE-SFL. For the bedrock system, the descriptions of internal processes for the geosphere in SR-Site (SKB 2010a) and SR-PSU (SKB 2014a) are used. This report is part of the additional references, which include documents compiled within SE-SFL. In addition, SE-SFL also relies on references to documents that have been compiled outside of the project, either by SKB or other similar organisations, or are available in the scientific literature. In Figure 1-4 the hierarchy of the **Main report**, main references and additional references within SE-SFL is shown.

Table 1-1. Main references in SE-SFL and the abbreviations by which they are identified in the text, shown in bold.

Abbreviation used when referenced in this report	Text in reference list
Main report	**Main report, 2019.** Post-closure safety for a proposed repository concept for SFL. Main report for the safety evaluation SE-SFL.SKB TR-19-01, Svensk Kärnbränslehantering AB.
Biosphere synthesis	**Biosphere synthesis, 2019.** Biosphere synthesis for the safety evaluation SE-SFL. SKB TR-19-05, Svensk Kärnbränslehantering AB.
Climate report	**Climate report, 2019.** Climate and climate-related issues for the safety evaluation SE-SFL. SKB TR-19-04, Svensk Kärnbränslehantering AB.
FEP report	**FEP report, 2019.** Features, events and processes for the safety evaluation SE-SFL. SKB TR-19-02, Svensk Kärnbränslehantering AB.
Initial state report	**Initial state report, 2019.** Initial state for the repository for the safety evaluation SE-SFL. SKB TR-19-03, Svensk Kärnbränslehantering AB.
Radionuclide transport report	**Radionuclide transport report, 2019.** Radionuclide transport and dose calculations for the safety evaluation SE-SFL. SKB TR-19-06, Svensk Kärnbränslehantering AB.

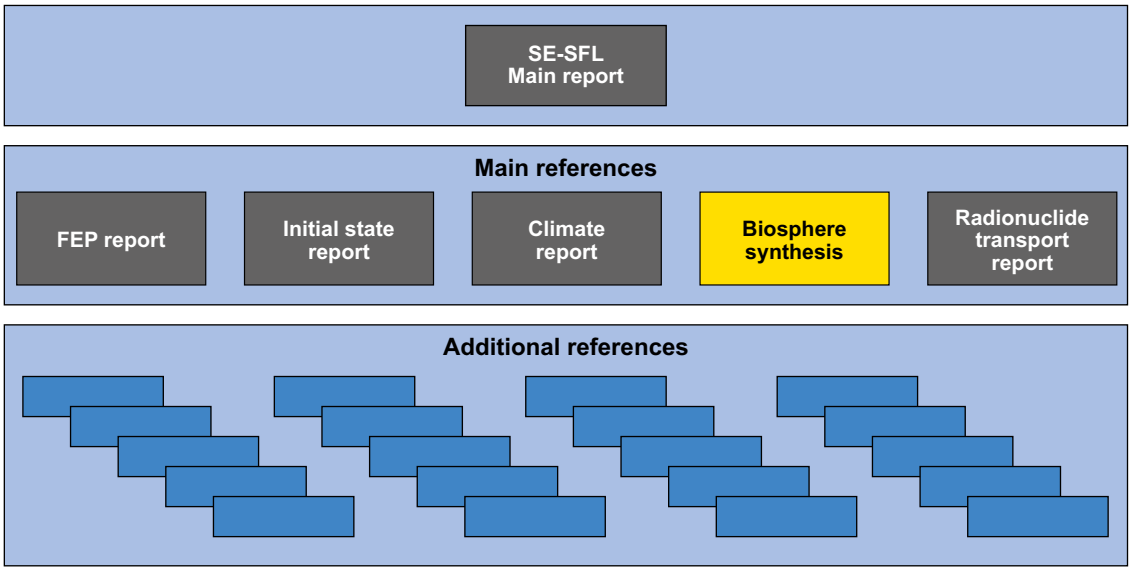

Figure 1-4. *The hierarchy of the Main report, main references and additional references in the safety evaluation of post-closure safety SE-SFL. The additional references either support the Main report or one or more of the main references.*

1.4 The role of this report in SE-SFL

This report is part of the biosphere assessment performed as an integral part of the safety evaluation of SFL. The main purpose of the biosphere assessment within SE-SFL is to allow the evaluation of the conditions under which the repository concept has the potential to fulfil the regulatory requirements for post-closure safety. To this end, the biosphere assessment allows estimations of the annual effective dose for a representative individual in the most exposed group that reflect a robust description of the biosphere and a credible handling of associated uncertainties.

The biosphere assessment is conducted by means of the Biosphere Model for Transport and Exposure (BioTEx) which describes transport and accumulation in areas where radionuclides from a geological repository potentially could be discharged (biosphere objects). The BioTEx is populated with parameter values for different properties and processes in the biosphere. These parameters, their values and the underpinning methodology and reasoning for the derivation of parameter values are described in this report. BioTEx itself is described in Chapter 8 of the **Biosphere synthesis**.

The work done within the SE-SFL biosphere project has been conducted by several people. The main contributing authors to this report are shown in Table 1-2 along with the chapters for which they were responsible.

Table 1-2. Contributors to SE-SFL Biosphere and the main chapters in this report with which they have been associated.

Chapter	Parameters/function	Main authors
	Editors	Sara Grolander, Kemakta Konsult AB, Ben Jaeschke, AFRY
2	Radionuclide-specific dose coefficient and half-lives	Per-Anders Ekström, Kvot AB
3	Landscape development and biosphere object geometries	Peter Saetre, SKB, Olle Hjerne, SKB, Anders Löfgren, EcoAnalytica
4	Regolith characteristics	Gustav Sohlenius, SGU
5	Surface hydrological fluxes	Peter Saetre, Mona Sassner, DHI Sverige AB
6	Element-specific K_d and *CR* parameters	Sara Grolander
7	Aquatic ecosystem parameters	Olle Hjerne, Anders Löfgren,
8	Terrestrial ecosystem parameters	Anders Löfgren
9	Human characteristics	Peter Saetre
10	Alternative regional climate	Anders Löfgren, Peter Saetre
11	An increased greenhouse effect	Anders Löfgren, Peter Saetre
12	Simplified glacial cycle	Anders Löfgren, Peter Saetre
	All maps and GIS in this report	Mårten Strömgren, Umeå University
	Review work	Mike Thorne, Ari Ikonen, Thomas Hjerpe

1.4.1 Structure of this report

The BioTEx used in this safety evaluation is based on the model used in the recent safety assessments conducted by SKB for the extension of the SFR repository, SR-PSU (Saetre et al. 2013). The parameters needed in this evaluation are therefore mainly the same as those used in SR-PSU (Grolander 2013). However, some updates of the BioTEx since SR-PSU (described in Chapter 8 of the **Biosphere synthesis**) had implications for the parameters that are presented in this report.

The parameters used in the BioTEx can be divided into eight categories. Each of these categories is described in a separate chapter (Chapters 2 to 9).

- Radionuclide-specific parameters.
- Landscape development and biosphere object geometries.
- Regolith characteristics.
- Hydrological fluxes.
- Element-specific K_d and *CR* parameters.
- Aquatic ecosystem parameters.
- Terrestrial ecosystem parameters.
- Human characteristics.

In addition to the parameters used in the biosphere base case, which is an evaluation case for present-day conditions throughout the evaluation period, several additional evaluation cases have been identified to address different issues and are presented in separate chapters (10–12); an alternative regional climate, an increased greenhouse effect and a simplified glacial cycle evaluation case. These evaluation cases are also described in Chapter 7 of the **Biosphere synthesis.**

Each chapter contains tables describing the parameters, whereas the parameter values are presented in the tables in the Appendixes to the report.

1.5 The parameterisation method

The basis for the parameterisation method used in SE-SFL has been taken from SKB's earlier safety assessment for the extension of SFR facility in Forsmark, SR-PSU (Grolander 2013).

In earlier safety assessments, e.g. SR-Site and SR-PSU, the assessment related to a selected site and, consequently, the site provided the context for many aspects of parameterisation e.g. shoreline displacement, topography and soil chemistry. No site has yet been selected for the SFL repository. In this evaluation of post-closure safety, the Laxemar site was chosen as an example model site for SFL. This ensures that there is a realistic and consistent site description based on a detailed and coherent dataset (Chapter 3 in the **Biosphere synthesis**).

Several of the parameters respond to changes in temperature, precipitation, hydrology, Quaternary geology or geochemical conditions at the modelled site, and these conditions differ between sites in Sweden and also between the Forsmark and Laxemar sites. How the site-specific conditions affect the parameter values was interpreted individually for each parameter, some parameters will not be affected significantly by changes in site conditions, these parameters are regarded as generic and valid for a larger region (see Chapter 13). For the generic parameters, the SR-PSU parameter values (and ranges) derived for Forsmark can be assumed to be representative for a generic site and also for the modelling site of Laxemar.

The parameters values that are expected to vary between sites are regarded as site-specific, this means that, for each parameter, values representative for the specific conditions at the modelled site need to be selected. In this evaluation, Laxemar is selected as an example of a possible site and site-specific parameter data representative of Laxemar were selected, if possible. For some of these cases, site-specific parameter values from the safety assessment SR-Site conducted for the Laxemar site were used, in other cases, data from the literature were used to derive representative parameter values. If the difference between the parameter values representing Forsmark and Laxemar was less than 10 %, this difference was regarded as of little significance and the Forsmark value was used. These parameters are still assumed to be site-specific and might need to be assigned updated values if another site were to be selected as a basis for modelling. The parameterisation method are summaries in the bullet list below and in Figure 1-5:

- For generic parameters, data from Forsmark are used (Grolander 2013)
- For site-specific parameters:
  - Data for Forsmark (SR-PSU) are used in cases were the differences in parameter values between Forsmark and Laxemar are regarded as of little significance.
  - SR-Site data for Laxemar are used to calculate new parameter values
  - Other additional data are used for deriving parameter values representative for Laxemar.

Consequently, each chapter describing a set of parameter contains a discussion as to what extent parameters will be affected by specific site-conditions, which will thereby motivate the choice of the selected parameter value.

1.6 Quality assurance procedure

Controlled handling of data and workflow is crucial to guarantee the quality of data and model results. The biosphere analysis in SE-SFL follows the quality plan for the safety evaluation project (Section 2.6 in the **Main report**). According to this plan, all reports go through a traceable factual review by experts and a quality review step. In addition, a QA process has been developed to ensure that data are complete and correct, and that the usage, sources, review, and storage of data are traceable.

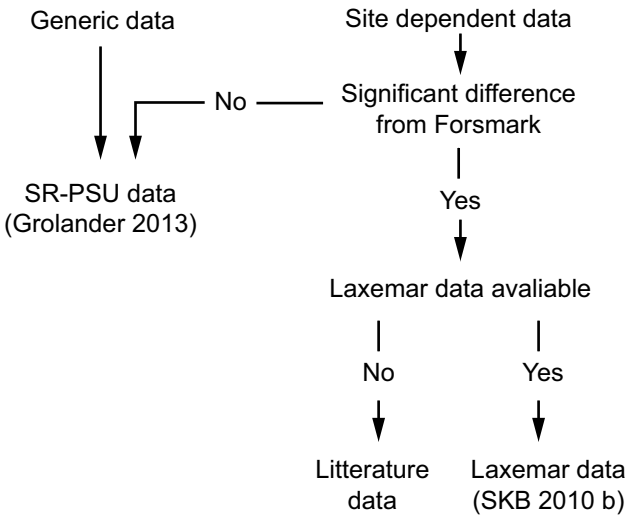

Figure 1-5. *The parameterisation method is summaries in this figure, showing how data are selected for generic and site-specific parameter respectively.*

The QA process includes a factual review of all selected parameter values and a quality control of delivery. Data files for the selected parameter group are stored on the Subversion, (SVN), server, ensuring full version handling and traceability. In short, the QA procedure includes the roles of a data deliverer, a data reviewer and QA-coordinator. Each delivery file contains a macro-controlled review system and all additions, changes and deletions to the data entries are logged. The QA process will make sure that information on the following questions is available:

- Which values were finally selected to be used in the safety evaluation?
- How have the data been derived (reference to source report)?
- How have the data been reviewed (methods for reviewing, side calculations)?
- Who (data deliverer, a data reviewer and QA-coordinator) has done what, and when?
- Where are files stored?

Data used for Forsmark, taken from the previous assessment SR-PSU were not included in the present factual review and QA procedure; these data are already quality assured within the SR-PSU assessment (Grolander 2013).

1.7 Biosphere evaluation cases

In SE-SFL, different evaluation cases were used to investigate effects of altered conditions or alternative assumptions on dose results (Section 2.4.7 in the **Biosphere synthesis).** The six different biosphere evaluation cases were; the *Present-day evaluation case* (base case) which used the present conditions in Laxemar, the *Alternative discharge area evaluation case* which investigated effects using multiple types of ecosystems and their succession in response to shoreline displacement representing conditions at Laxemar and Forsmark in the past/far future and also included release to permanent aquatic objects, the *Initially submerged evaluation case* which investigated how a release below the sea level and different periods of sea cover would affect dose, the *Alternative regional climate evaluation case* which investigated the effects of regional climate on dose, the *Increased greenhouse effect evaluation case* which investigated the effects of increased temperatures and changes in precipitation and the *Simplified glacial cycle evaluation case* which investigated the effects of glaciation, including both periods of periglacial and glacial conditions. These evaluation cases are further described in the **Biosphere synthesis** (Chapter 7), whereas this report describes the selected parameter data for all evaluation cases.

For the *Alternative discharge area evaluation case* hydrological fluxes and landscape parameters were altered and these are described in Chapters 5 and 3 respectively. The other parameters were the same as for the present-day evaluation case.

2 Radionuclide-specific parameters

The radionuclide-specific parameters used in the radionuclide transport model are the half-lives of radionuclides, ingrowth of radionuclides in soils and the dose coefficients used in the calculations of potential doses to humans for converting the activity intakes (Bq) of ingested or inhaled radionuclides as well as the activity concentrations in environmental media (Bq m^{-3}) to effective doses to humans (Sv). Three different types of coefficients are used:

1. dose coefficients for external exposure from radionuclides in the ground, doseCoef_ext (Sv h^{-1} per Bq m^{-3})
2. dose coefficients for ingestion, doseCoef_ing (Sv Bq^{-1}), and
3. dose coefficients for inhalation, doseCoef_inh (Sv Bq^{-1}).

The dose coefficients represent committed effective dose per unit intake for adults. The model approach used in SFL is the same as in recent SKB safety assessments SR-PSU (SKB 2015a), SR-Site, (SKB 2011a) and SAR-08 (SKB 2008) and the definitions of the dose coefficients are identical, see Table 2-1. However, a different set of radionuclides was considered in the present SE-SFL assessment (see Table 2-2) than in SR-PSU.

The dose coefficients for ingestion are independent of the ingestion pathway, i.e. via food or water. The only exception is carbon-14, for which different dose coefficients are used for ingestion via food and via water. This is because carbon is present in different chemical forms in water and food. That is, the ICRP dose coefficient for ingestion is based on the assumption that the C-14 is in the form of organic compounds that can be readily metabolised and incorporated into body tissues and organs. This is an appropriate assumption for ingestion of food. However, in drinking water, the carbon will be predominantly present as dissolved carbon dioxide or dissolved bicarbonate or carbonate. In these forms almost all ingested C-14 will be lost by exhalation as carbon dioxide without ever having been metabolised and incorporated in body tissues. Therefor dose coefficients for ingestion of water are taken from a model that is consistent with the biokinetics of bicarbonate and carbon dioxide (Leggett 2004). This approach has also been proposed by Smith and Thorne (2015) and endorsed by Harrison and Leggett (2016).

The values used for external exposure from a volumetric source are based on homogeneous distribution of the radionuclides in a soil layer of infinite depth and infinite lateral extent.

The annual dose from exposure to contaminated air resulting from combustion of peat or wood was calculated based on the dose coefficient for inhalation of contaminated air and the activity concentration in air. The activity concentration in the air was based on a conversion factor (f_combust) converting the activity concentration in the fuel (peat or wood) to the activity concentration in the air (Stenberg and Rensfeldt 2015, Section 2.3).

In addition to these parameters, scaling factors for ingrowth of radioactive daughter in agricultural soils are used. The radionuclide transport model analytically calculates activity concentrations in agricultural soils depending on different source terms. These activity concentrations are either a steady state solutions or an average activity concentration during the 50-yearperiod of which agriculture practice is assumed to be sustainable or. As outlined in the description of the radionuclide transport model (**Radionuclide transport report**), these activity concentrations do not include ingrowth of activity from longer-lived radioactive daughter that may build up during this 50-year period. To handle the potential dose contribution due to exposure from longer-lived radioactive daughters, the scaling factors (dose_ingrowth_agri_ext/inh/ing, unitless) are used. These scaling factors are calculated as the ratio between the 50-year average of the exposure due to a unit concentration considering ingrowth and exposure to longer-lived daughter and the 50-year average of corresponding exposure not considering ingrowth of longer-lived daughter radionuclides.

Table 2-1. Summary of radionuclide-specific parameters used; the data values are presented in Appendix A.

Name	Unit	Description
doseCoef_ext	$(Sv\ h^{-1})\cdot(Bq\ m^{-3})^{-1}$	Dose coefficient for external exposure
doseCoef_ing	$Sv\ Bq^{-1}$	Dose coefficient for ingestion
doseCoef_ing_water_14C	$Sv\ Bq^{-1}$	Dose coefficient from ingestion of carbon-14 in water
doseCoef_inh	$Sv\ Bq^{-1}$	Dose coefficient for inhalation
dose_ingrowth_agri_ext	Unitless	Average relative contribution from external exposure including daughter radionuclides in agricultural land
dose_ingrowth_agri_ing	Unitless	Average relative contribution from ingested radionuclides including daughter radionuclides in agricultural land
dose_ingrowth_agri_inh	Unitless	Average relative contribution from inhaled radionuclides including daughter radionuclides in agricultural land
Half-life	year	Radionuclide half-life

Table 2-2. Radionuclides included in the radionuclide transport calculations.

Ac-227	Cd-113m	Eu-150	Nb-94	Pu-240	Tb-157	U-234
Ag-108m	Cl-36	Eu-152	Ni-59	Pu-241	Tb-158	U-235
Am-241	Cm-242	Gd-148	Ni-63	Pu-242	Tc-99	U-236
Am-242m	Cm-243	H-3	Np-237	Ra-226	Th-228	U-238
Am-243	Cm-244	Ho-166m	Pa-231	Ra-228	Th-229	Zr-93
Ar-39	Cm-245	I-129	Pb-210	Re-186m	Th-230	
Ba-133	Cm-246	K-40	Pd-107	Se-79	Th-232	
Be-10	Co-60	La-137	Po-210	Si-32	Ti-44	
C-14	Cs-135	Mo-93	Pu-238	Sm-151	U-232	
Ca-41	Cs-137	Nb-93m	Pu-239	Sr-90	U-233	

2.1 Effects of site characteristics of parameter values

The dose coefficients are not affected by site-specific characteristics and are assumed to be representative for any modelled site in Sweden.

2.2 Dose coefficients

Because the modelling approach used in SE-SFL is identical to the approach used in previous assessments the same method for deriving dose coefficients was used. Also, the same references as in SR-PSU were used for deriving the dose coefficients, that is, ICPR Publication 119 (ICRP 2012) for dose coefficients for ingestion and inhalation and Eckerman and Ryman (1993) and Eckerman and Leggett (1996)[1] for dose coefficients external exposure. See Chapter 3 of Grolander (2013) for a detailed description of the method used in SR-PSU.

Some of the radionuclides included in the assessment decay to radioactive daughter radionuclides. The dose contributions from daughter radionuclides are included applying the same method as in SR-PSU. This means that long-lived daughter radionuclides that are not assumed to be in secular equilibrium with the parent radionuclide are explicitly modelled in the radionuclide transport model

[1] USEPA 2019 published dose coefficients for external exposure in august 2019 (after the modelling work was completed in this project). The updated values has been evalauated and will not affect the results in any significant way

(these are included in the list of radionuclides in Table 2-2). For short-lived daughter radionuclides that are assumed to be in secular equilibrium with the parent radionuclide, the contribution of the daughter radionuclide is included in the dose coefficient of the parent radionuclide. This is described detail in Section 3.3 in Grolander (2013).

For the radionuclides assumed to be in secular equilibrium, the decay chains and the relative activity ratios for the daughter radionuclides are listed in Table 2-14 in Shahkarami (2019). The dose contribution from the daughter radionuclide is added to the dose coefficient of the parent radionuclide using the relative activity ratios. The information on the decay chains and the activity ratios are derived from ICRP Publication 107 (ICRP 2008), which is an updated table compared with the one used in SR-PSU.

The complete list of used dose coefficients is given in Appendix A.

2.3 Half-lives

The half-lives of the modelled radionuclides are presented in Appendix A. The data are selected from four different references; Firestone et al. (1998), Schrader (2004), Jörg et al. (2010) and ICRP (2008). The complete list of the half-lives that were used is given in Table 2-12 in Shakarami (2019).

3 Landscape development and biosphere object geometries

In this chapter, the selection of landscape parameter values for the biosphere transport and exposure model (BioTEx) used in SE-SFL are described. The parameters presented below are those describing the biosphere objects (BO) in the landscape, which are the identified potential discharge areas for radionuclides. The identification of biosphere objects in the landscape was made as a part of the SR-Site evaluation of the Laxemar site (Figure 3-1; see **Biosphere synthesis,** Section 5.2). The parameters are listed in Table 3-1 and the parameter definitions are also the same as presented in Chapter 4 in Grolander (2013).

In this chapter, the description of the parameter values and method used to derive the parameter values are given, whereas the assigned parameter values are listed in Appendix B.

Table 3-1. Summary of landscape parameters used.

Name	Unit	Description
area_basin	m^2	Surface area of the basin, including the biosphere object
area_obj	m^2	Area of the lake object
area_obj_aqu	m^2	Surface area of an aquatic object
area_obj_aqu_agri	m^2	Surface area of the stream in agricultural land
area_obj_ter	m^2	Surface area of a terrestrial object
area_obj_ter_agri	m^2	Surface area of agricultural land (excluding stream)
area_obj_ter_init	m^2	Initial area of the terrestrial part of the object
area_watershed	m^2	Surface area of the watershed, including the basin
res_rate	$m^3\ m^{-2}\ year^{-1}$	Gross resuspension rate per unit surface area
sed_rate	$m^3\ m^{-2}\ year^{-1}$	Gross sedimentation rate per unit surface area
threshold_end	year	The last year of terrestrial ingrowth
threshold_isolation	year	The year a bay becomes isolated from regular seawater intrusions
threshold_start	year	The year a bay starts developing into a lake
threshold_stop	year	The year a bay finishes developing into a lake
threshold_well	year	The time point when the first land that appeared in the object is 1 m above the sea level, which is equal to threshold_stop
wat_ret	year	Water retention time
z_regoGL	m	Thickness of glacial clay
z_regoLow	m	Thickness of regolow (till)
z_regoPeat_equlib	m	Thickness of peat
z_regoPeat_init	m	Initial thickness of peat
z_regoPG_agri	m	Thickness of terrestrial post-glacial sediments in present agricultural land at the year 2000
z_regoPG_aqu	m	Thickness of aquatic post-glacial sediments
z_regoPG_ter	m	Thickness of terrestrial post-glacial sediments
z_regoSub_agri	m	Thickness of sub-regolith in present agricultural land at the year 2000
z_regoUp_agri	m	Thickness of the oxygenated active regolith layer in agricultural land (ploughing depth)
z_water	m	Average depth of water

3.1 Biosphere objects and biosphere evaluation cases

Depending on the evaluation case, biosphere objects and landscape parameter values were used differently and the derivation of these are described in this chapter

The *present-day evaluation case* represents present biosphere conditions using the most probable discharge area of deep groundwater from a hypothetical SFL repository in the example site Laxemar, which is biosphere object 206 (Figure 3-1; see also the **Biosphere synthesis**, Section 5.3).

The *Alternative discharge area evaluation case* includes nine biosphere objects from Laxemar (Figure 3-1); one mature mire (203), five cultivated fields (204, 206, 210, 212, 213), one lake (207), and two sea bays (201, 208). For the purpose of the safety evaluation, the six terrestrial objects were assumed to have reached a stable successional stage, and thus their properties (i.e. soil thicknesses and surface hydrology) did not vary with time. However, the two sea bays are expected to develop into lakes because of land rise, and present and future lakes are expected to develop into mires within around ten thousand years. Therefore, the properties of these objects (e.g. area and depth of the water body, the area of the wetland and the thickness of regolith layers) changed over time in accordance with the ecosystem succession described by the SR-Site Regolith Lake Development Model (RLDM) (See below and Brydsten and Strömgren 2010). As the actual location of a future repository is still to be determined, biosphere objects from a site with a relatively flatter topography than Laxemar were also included in the assessment. That is, six biosphere objects from the Forsmark site were used in this evaluation case (Section 3.6). The natural succession of these objects from a sea basin, through a lake phase, to a mire, were described as part of the SR-PSU safety assessment (Brydsten and Strömgren 2013). In the context of this safety evaluation, these objects are not viewed as representing specific discharge areas above the SFL repository, and thus there is no pre-set time anchor to the time series describing the development of these discharge areas. Therefore, they were anchored in time so as to just include the last phase of the shallow bay and the successional stages thereafter (Section 7.3.3 in the **Biosphere synthesis**).

The biosphere objects in all evaluation cases were designed to evaluate dose consequences for a static (time-independent) mire or agricultural land at a coastal or inland repository location, or a developing landscape at a coast repository location. Due to isostatic land rise, the sea period is a transient successional stage. Moreover, as the RLDM describes the natural lake-mire succession, a lake is also a transient feature of a biosphere object. Thus, to evaluate a situation where radionuclides are directly released into the sea for a long period of time, or a situation where radionuclides reach a large freshwater body in a mature terrestrial landscape (e.g. as a consequence of human damming activities) an additional set of non-changing time-invariant sea and lake biosphere objects were constructed and added to the *Alternative discharge area* evaluation case (Section 3.5).

In the time perspective that is relevant for a safety assessment of long-lived radioactive waste (1 million years) one or several periods of glaciation may occur. The fifth biosphere evaluation case illustrates potential dose consequences after the area has been submerged under a future sea. In this case, biosphere object 206 is taken to develop from a deep-sea basin, through a coastal basin and lake, to a final mire stage. The development of biosphere object 206 was only described for the submerged period in the SR-Site RLDM. Consequently, a schematic description was constructed from the two sea basins (201 and 208) and the one lake (207) that were described in SR-Site RLDM for Laxemar. This was done by characterising the lake development in terms of simple algebraic expressions and then applying these functions to describe the initial conditions of the lake stage and the subsequent sedimentation and ingrowth of vegetation for biosphere object 206. This is described in Section 3.4 below.

3.2 Parameterisation of biosphere objects representing present conditions in Laxemar

In the *present-day evaluation case*, characterisation of one cultivated field (206) is based upon descriptions from the identified biosphere objects of today (Figure 3-1). An alternative state of this discharge area is also evaluated as a mire in the lake basin of 206 that may be drained and used as a cultivated area during the modelled time period. The same methodology was used to derive data for parameterising the present conditions for the other eight biosphere objects and these biosphere objects were used in other evaluation cases.

3.2.1 Geometrical features of a biosphere object

The spatial delimitation of the biosphere objects was made in accordance with earlier safety assessments (SKB 2015a, Lindborg 2010). That is, the biosphere objects were outlined based on topography to represent clearly defined ecosystems, reflecting reasonably homogenous biotic properties (e.g. type of vegetation, and rates of primary production and decomposition) and abiotic characteristics (e.g. regolith stratification and groundwater hydrology) (Figure 3-1). In contrast to previous assessments, most of the biosphere objects in Laxemar are above the present sea level, such as agricultural land, mires and lakes. There are also two semi-enclosed sea basins, where the sea basins set the boundary for the aquatic part of the biosphere object today, but their future lake basins are also shown in Figure 3-1, within the delineated area.

Generally, a biosphere object can be divided into two geometrical areas depending on development stage: (1) the basin-associated future lake or mire, and (2) the catchment of this basin. In the marine stage, the biosphere object is always the basin of a future lake or mire. In the lake or terrestrial stage, the same biosphere object is a lake or a mire. The areal delimitation of the biosphere object when it is above the sea level (area_obj) approximately reflects the original lake basin or is a sum of the lake area (area_obj_aqu) and the mire area (area_obj_ter) depending on the successional stage (Figure 3-2). In the fully developed mire the area_obj_aqu represents the stream area running within the biosphere object and area_obj_aqu_agri represents the same for the agricultural land.

The watershed or the basin is the upstream area at the biosphere object outlet including the area of the object itself (area_watershed, see also Figure 3-2). A watershed can contain other basins if they are located upstream of the biosphere object defining the watershed (the watershed in Figure 3-2 does not have an upstream basin). If a biosphere object is located close to a water divide or has no other basins upstream, the watershed area equals the basin area (as in Figure 3-2). The basin (area_basin) is therefore the watershed of a biosphere object minus the watershed of any upstream basins. These areas are presented in Table 5-1 of the **Biosphere synthesis** and are used in the hydrological parameterisation, which is further described in Chapter 5. The geometrical measures of the nine objects of Laxemar are shown in in Appendix B.

3.2.2 Regolith thickness

The regolith is defined as all inorganic and organic Quaternary deposits/soil layers on top of the bedrock and is divided into different layers based on their properties. In BioTEx each regolith layer corresponds to a specific model compartment (see Saetre et al. 2013). These layers/compartments are till, glacial clay, postglacial sediments, peat and two fractions of cultivated soil. The regolith layer thicknesses were calculated from the regolith depth model (RDM), which is based on empirical observations in the Laxemar area (Nyman et al. 2008). In Figure 3-3, the geological layers in the RDM and the corresponding regolith compartments in BioTEx are illustrated. There is a 1:1 correspondence between spatially averaged thicknesses of Z-layers (Z6 and Z5) of the RDM within an object and the thickness parameter values of the model compartments for the two deepest geological layers, till (z_regoLow) and glacial clay (z_regoGL) (Figure 3-3). The Radionuclide transport model for the biosphere used in SR-PSU did not contain a separate representation for coarse-grained postglacial sediments (Z4). In agreement with SR-PSU, the thickness of this layer was combined with that of postglacial fine sediments (Z3), to represent the thickness of the postglacial sediment layer (z_regoPG).

In RDM, grid cells with a peat thickness exceeding 0.5 m, the topmost layer of the RDM is defined as peat (Z2). In all other cells, the surface layer is called the Z1 layer. On bedrock outcrops, Z1 is assumed to be 0.1 m and in other areas it is 0.6 m and contains the uppermost regolith layers down to the bedrock if the thickness is less or equal to 0.6 m. Consequently, Z1 is the only layer in the RDM if the regolith thickness is less than 0.6 m. By definition, Z1 and Z2 cannot coexist in a cell, but they can after averaging over cells within an object. To determine the regolith thickness of BioTEx regolith compartments, the parent material of the Z1-layer was assigned based on the object type. In the mature mire (object 203), the Z1 layer was assumed to consist of peat and consequently added to Z2. In BioTEx, the peat layer was divided into an upper more biologically active and oxic layer (z_ regoUp) with a thickness of 0.3 m (partly unconsolidated) and a lower anoxic layer with a thickness described by z_regoPeat. Similarly, this oxic and partly unconsolidated regoUp layer is also found on the lake and sea bottoms. All the agricultural areas (objects 204, 206, 210, 212, 213) are assumed to originate from drained lakes and mires (based on soil profiles from agricultural land), and the thickness of this organic soil layer (i.e. a Histosol) is the sum of both the Z1 and the Z2 layers. However, in the model, cultivated soil is further divided into two soil layers: an upper highly biologically active layer which is affected by ploughing, RegoUp_ agri (thickness = 0.25m), and a lower soil layer RegoSub (thickness = thickness [Z1+Z2] −0.25 m). In the lake (object 207) and in the sea basins (201 and 208), Z1 and Z3 were taken from modelled regolith thicknesses (RLDM, see below).

The thicknesses of regolith layers in the six terrestrial objects of Laxemar are shown in Figure 3-4 and listed in Appendix B.

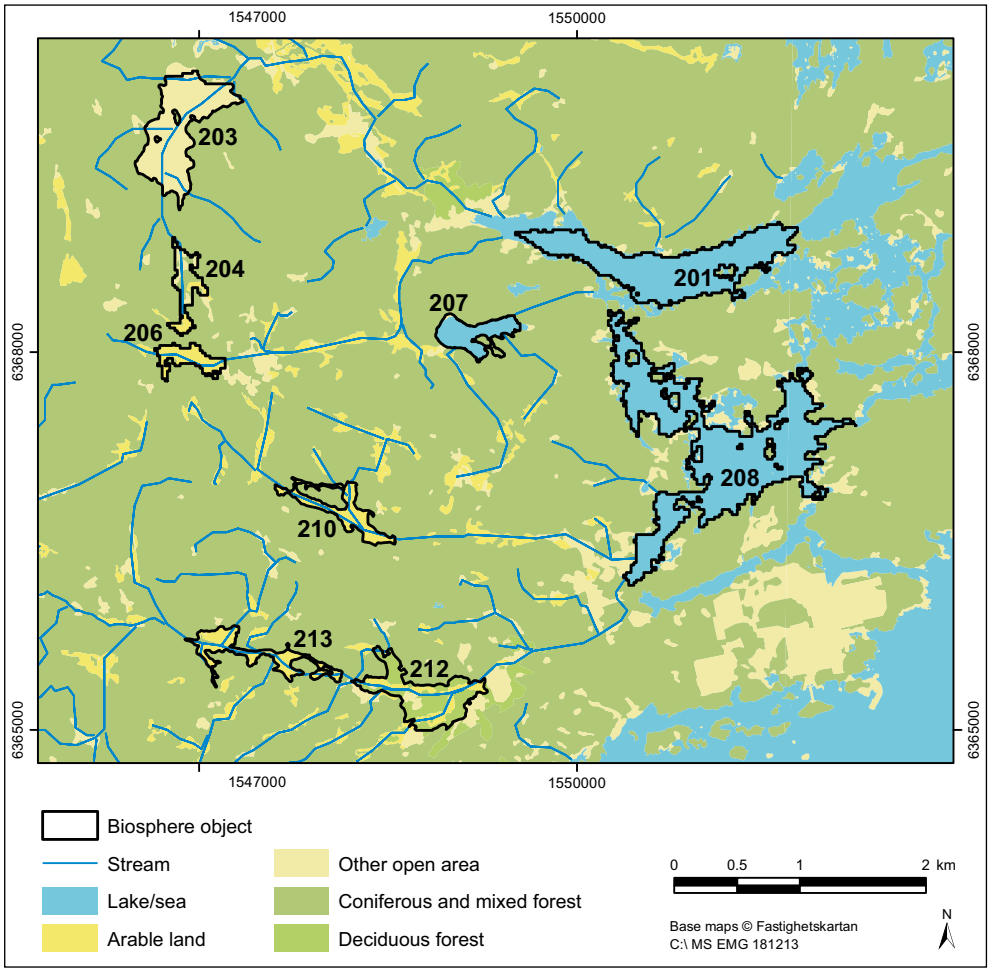

Figure 3-1. *The nine biosphere objects projected onto the present land-use map in the Laxemar area. The objects represent different ecosystems and locations in the landscape, and deep groundwater could potentially be discharged in all of them. The areas of biosphere objects 201 and 208 correspond to the future lake basins and are therefore somewhat smaller than the sea basins present today (see also Chapter 5 in the Biosphere synthesis).*

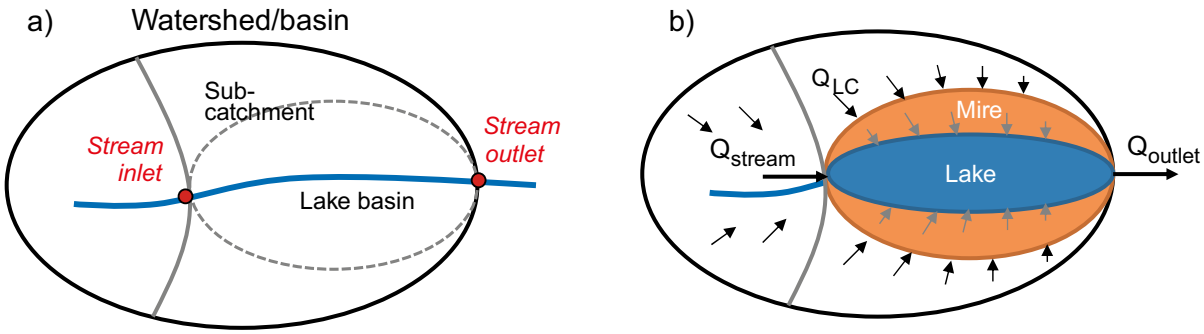

Figure 3-2. *Conceptual model of the (a) geometrical features of the biosphere object and it's water generating areas, (b) water flows (Q) into and out of a biosphere object containing a lake (blue) and a mire (orange) part. Black ellipse represents the watershed/basin. If the stream carries water from upstream basins, then the watershed is larger than the basins. Grey line divides the basin into the catchment of the inlet (left) and the catchment of the outlet (also known as the sub-catchment, right). Note that the sub-catchment includes the lake basin (which outlines the object in the land stage). Note that the water flow from the local catchment (QLC) does not include water generated from net precipitation within the lake basin (e.g. grey arrows in (b)). Figure modified from Werner et al. (2013) (this figure is the same as Figure 5-4).*

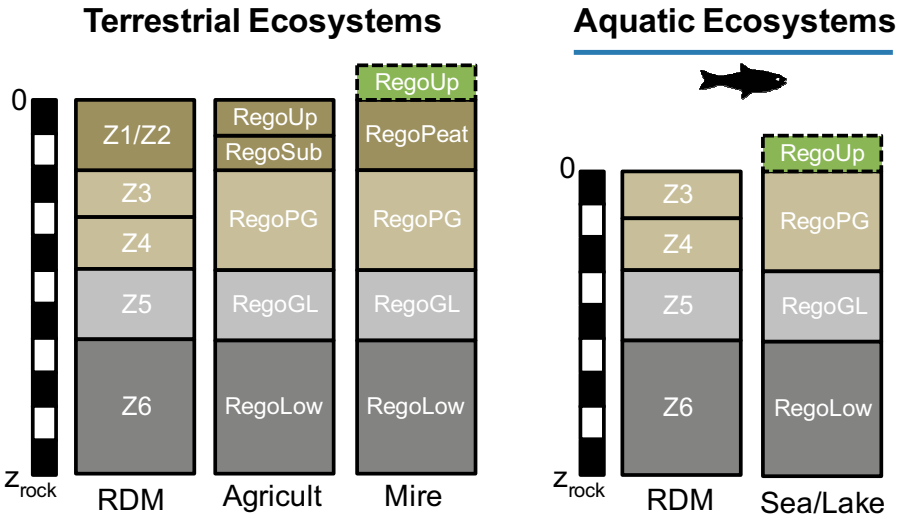

Figure 3-3. *Correspondence between geological layers in the regolith depth model (RDM) for Laxemar (Sohlenius and Hedenström 2008) and regolith compartments in BioTEx (Saetre et al. 2013) (this figure is the same as Figure 5-5).*

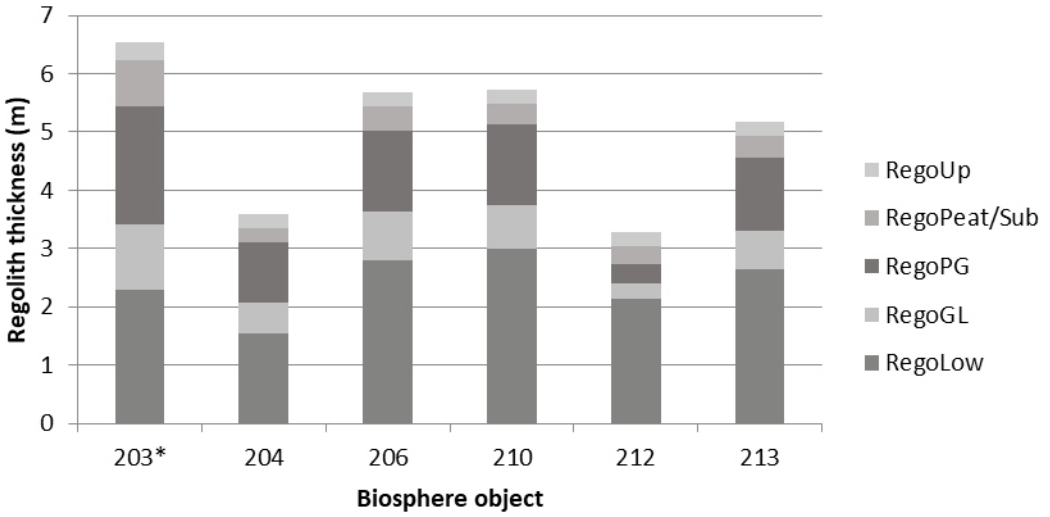

Figure 3-4. *Thickness (z) of regolith compartments of BioTEx for six terrestrial biosphere objects based on the regolith depth model (RDM) describing the present conditions of Laxemar. RegoUp represents the biologically active layer with a high rate of decomposition and root uptake. * mire ecosystem (the other objects are agricultural ecosystems).*

3.3 Streams in biosphere objects

The final stage of the lake succession occurs when the lake basin has been filled with mire vegetation and the only open water that remains in the object is a stream. Similarly, when a lake or mire has been drained, a stream will typically remain in the cultivated area. Lengths of present (and future) streams in the biosphere objects in Laxemar were directly extracted from the stream network (Figure 3-5). Average depths and widths of existing streams were determined from field measurements (Figure 3-6, Strömgren et al. 2006). The length and the width of the stream were used to calculate the surface area (area_obj_aqu_agri) of the stream within the biosphere object (area_obj_aqu_). Objects 201 and 208 are presently sea bays with large catchments, and future streams in these objects were assumed to have a cross-section similar to that of Laxemarån (i.e. relatively wide and deep). As in previous safety assessments (SR-Site, SR-PSU). the average stream depth (z_water_agri) was approximated to be half of the maximum depth. The parameter values are listed in Appendix B.

3.4 Parameters changing during biosphere object development in Laxemar

In the *Alternative* d*ischarge area evaluation case* biosphere objects 201, 207 and 208 developed from present-day condition until their mire stage based on the RLDM. For biosphere objects 204, 206, 210, 212 and 213, which are agricultural land today, there was a need to also describe the mire stages. These biosphere objects therefore needed additional information similar to the results from the RLDM. Therefore, an additional simple model was created based on the results from the RLDM for the fully modelled objects. The RLDM modelling is described in Section 3.4.1, whereas the additional modelling for the objects not included in the RDLM is described in Sections 3.4.2 and 3.4.3. Section 3.4.4 describes threshold parameters that determined the different developmental stages of the biosphere objects.

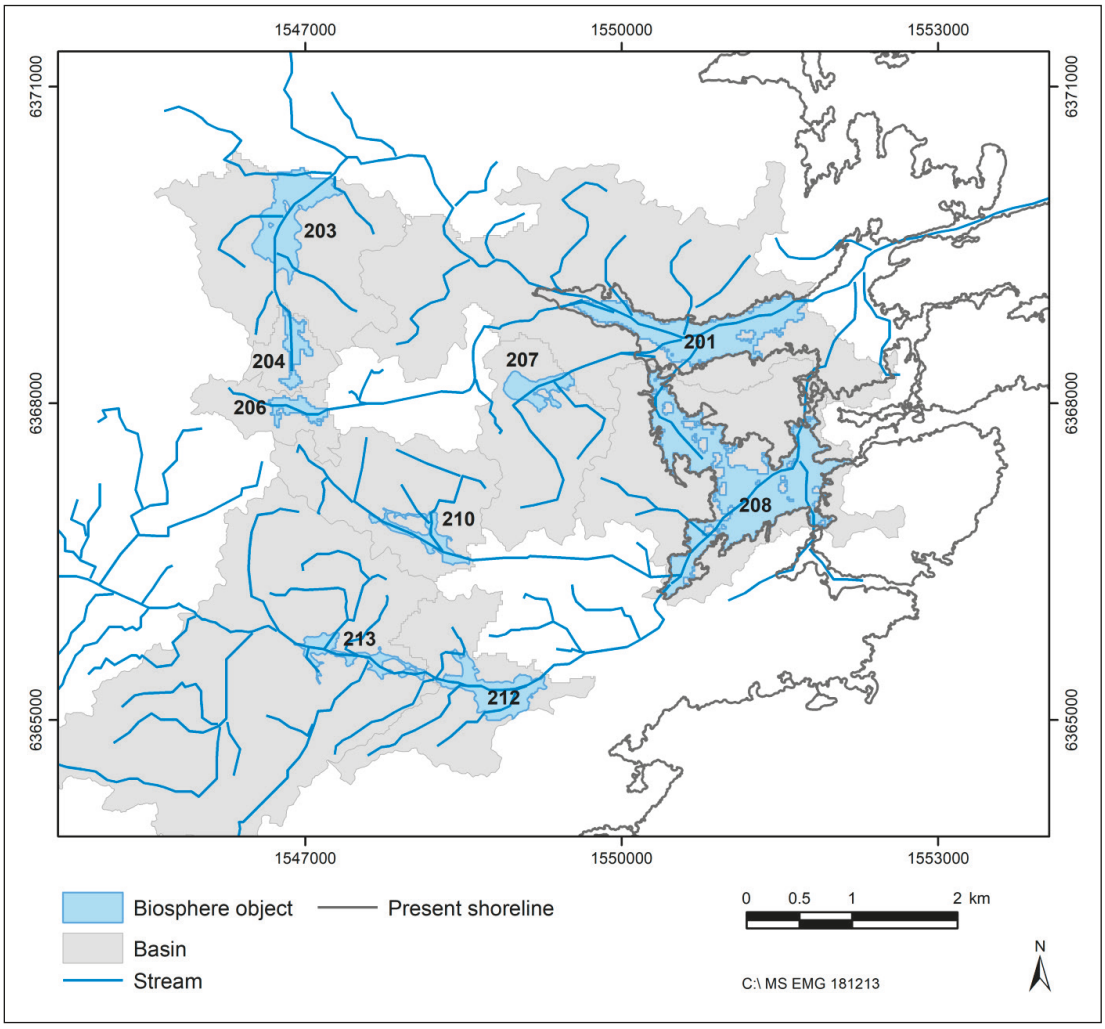

Figure 3-5. *The surrounding basin in grey for each biosphere object. The present streams as well as the projected future streams (Bosson et al. 2009, Sassner et al. 2011) are shown. These all end in one large river gathering the discharge of a future landscape at Laxemar.*

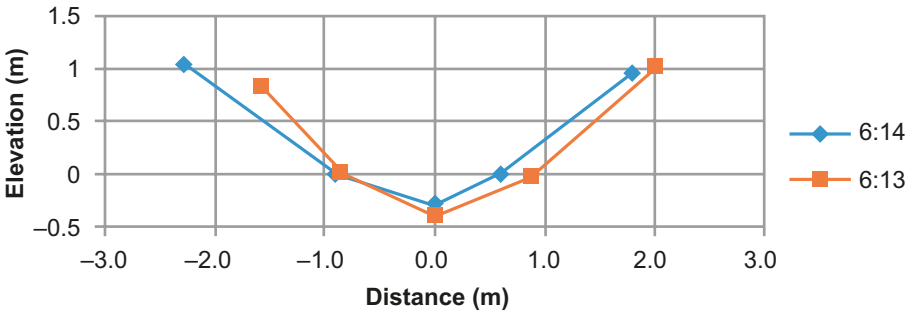

Figure 3-6. *Two cross-sections (numbered as 6:13 and 6:14) of the present stream in object 206 (Mederhultsån). The outermost points represent the banks, the centre-most point represents the deepest section of the stream, and the points in between represent depths at locations across the width of the stream. The stream field investigation is described in detail in Strömgren et al. (2006). Data from SICADA.*

3.4.1 Regolith Lake Development Model (RLDM)

In SR-Site, a coupled regolith-lake development model (RLDM) describing landscape development at a coastal site during an interglacial was developed (Brydsten and Strömgren 2010). The model was applied to both Forsmark (Grolander 2013) and Laxemar (unpublished). The model output included maps, with 20 m resolution, and spatial average data, describing the development of biosphere objects in terms of time dependent model parameters. In Laxemar, three biosphere objects (201, 207 and 208) have a full RLDM development history simulated. The remaining objects (203, 204, 206, 210, 212, 213) had only the sea phase modelled (see further below) and the lake phases were described in accordance with the three fully modelled biosphere objects. The development of the lake phase for the remaining objects is described in detail below.

The RLDM consists of two modules: a marine module that predicts the sediment dynamics caused by wind and waves, and a lake module that predicts the lake infill processes caused by sedimentation and vegetation ingrowth. The marine module was run for all biosphere objects from fully submerged conditions (~10 000 BC), and the output was recorded at 500-year intervals. Parameters that described average conditions for the biosphere objects during the sea period included: area (area_obj, area_obj_ter, area_obj_aqu), average and maximum water depth (z_water, z_water_max), and the area of the photic zone of sea basins (area_photic), average thickness of postglacial fine sediments (z_regoPGC), and rates of sedimentation and resuspension (sed_rate, res_rate).

The lake module was run from the point of lake isolation until the lake had been filled in, and outputs were recorded for every 100th years. However, this module was only applied to three of the biosphere objects as a part of the SR-Site study in the Laxemar area (SKB 2010b), namely the two sea objects (201, 208) and Lake Frisksjön (207). The module predicted the same parameters as the sea module for the open lake water area, and in addition similar parameters were calculated for the mire part of the lake basin. These included the area covered by mire vegetation (area_obj_ter), the average thickness of postglacial fine sediments (z_regoPGC_ter) and the final peat thickness in the mature mire (z_regoPeat_equilib, the peat thickness when the lake basin is fully filled with peat).

The ecosystem succession, where the mire grows into the lake, was described for the three fully modelled biosphere objects (201, 207, 208) in Laxemar by vegetation ingrowth (Ter_growth, $m^2\ year^{-1}$) as from Brydsten (2006):

$$\text{Ingrowth rate} = IGR_{min} + ß_{ALB} \times Area_{Lakebas} \qquad \text{Equation 3-1}$$

Where

IGR_{min}($m^2\ year^{-1}$) is the minimum rate of vegetation ingrowth (given a sufficient availability of shallow lake bottoms) [16.5]

$Area_{lakebas}$ (m^2) is the area of the lake basin

$ß_{ALB}$ ($year^{-1}$) is a constant that describes how the rate of ingrowth increases with the size of the lake basin [2.4×10^{-4}]

The rate given by Equation 3-1 is a maximum value for the lake, as the vegetation ingrowth in the RLDM is limited by the availability of the area of shallow lake bottoms for reed colonisation (water depth less than 2 m).

Reeds will also colonise the shallow part of the sea basin before lake isolation, and in the RLDM a water depth limit of 1.3 m was used for allowing vegetation ingrowth (area_obj_ter). The lower ingrowth depth of 1.3 m compared with that applicable to the isolated lake ecosystem (2 m) is due to the higher exposure to wave action and ice drift in the sea bay (Brydsten and Strömgren 2013). For the biosphere objects lacking a full RLDM description, the vegetation ingrowth was approximated by assuming ingrowth to start at the time point when the biosphere object was first isolated at low sea water level (−0.9 m is the mean yearly lowest sea water level, i.e. threshold_start, see Section 3.4.4).

Moreover, the volumetric net sedimentation rate (vol_net_sed m^3 $year^{-1}$) was calculated with an empirical relationship valid for small (<100 ha and <4 m deep) lakes (Brydsten 2006 and Brydsten L, personal communication):

$$vol\_net\_sed = ß_1\ Volume_{water} - ß_2\ (Volume_{water})^2 \qquad \text{Equation 3-2}$$

Where

$Volume_{water}$ (in 10^6 m^3) is the volume of water in the lake basin, and

$ß_1$ and $ß_2$ (m^3 $year^{-1}$ $[10^6\ m]^{-3}$ and m^3 $year^{-1}$ $[10^6\ m]^{-6}$) are empirical constants [193, 14.2]

In BioTEx, sedimentation and resuspension rates are expressed per unit lake area. Moreover, the resuspension (res_rate, m^3 m^{-2} $year^{-1}$) was assumed to be 65 % of the net sedimentation rate (Grolander 2013). The gross sedimentation rate (sed_rate, m^3 m^{-2} $year^{-1}$) is by definition the sum of the net sedimentation and resuspension rates.

The thickness of regolith layers below the modelled post glacial fine sediments (regoPG) were assumed to be constant throughout the development of the object. The parameter values for till (z_regoLow), glacial clay (z_regoGL) and coarse-grained postglacial sediments were taken from the RDM (Nyman et al. 2008, Figure 3-7). As BioTEx did not have a separate representation for coarse-grained postglacial sediments, the time-independent thickness of this layer was added to the time-dependent thickness of postglacial fine sediments (z_regoPGC) predicted by the RLDM, and the sum represented the thickness of postglacial clay (z_regoPG).

3.4.2 A simplified model to describe non-modelled biosphere object stages

The biosphere objects 201, 207 and 208 were modelled using the RLDM, as described in the previous section. The other biosphere objects were only modelled until the start of their lake stage in the RDLM, and their further lake development was described using a simplified model based on the three fully modelled objects. That simplified model is explained in this section.

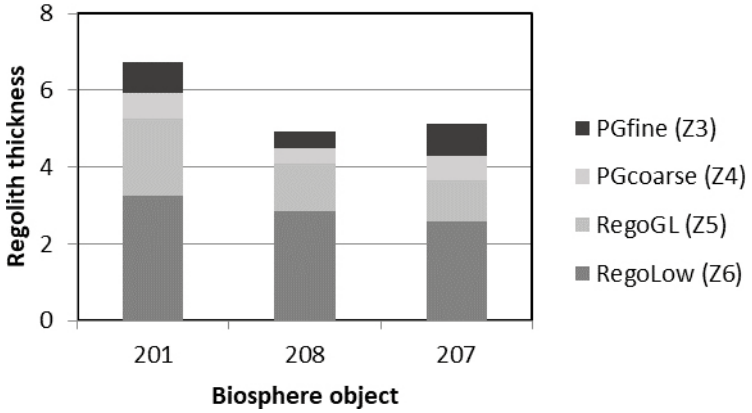

Figure 3-7. *The average regolith thickness of three aquatic biosphere objects. The thicknesses of the three lowest regolith layers were treated as constant over time. The thicknesses of postglacial fine sediments (z_PG_{fine}, Z3) were modelled with the RLDM, and coarse- and fine-grained postglacial sediments (Z4+Z3) from the RDM were summed to yield z_regoPG.*

The initial conditions for the lake stage

The area and volume of the lake basin

The lake basin area (area_obj) of a biosphere object was assumed to be equal to the object area during the land period (see Section 3.2.1). As the bathymetry of former lakes Laxemar has not been measured, the initial volume of the lake basin before any sediment accumulation had to be estimated. Thus, the volume above the layer of the coarse sand and gravel sediments (Z4) was estimated as the product of the surface area of the lake basin and the average thickness of the organic sediment column at the completion of the mire stage. The latter term was approximated from the present day soil profile (Figure 3-4), by assuming that the present Z1 and Z3 layers corresponded to a compacted layer of postglacial fine sediments (65 % of the original thickness due to drainage of the wetland), and that this layer was originally covered by a 1.6 m thick peat layer (i.e. the Z2 layer). The thickness of the peat layer was close to the mean (1.8 m) of the three RLDM-modelled biosphere objects at the mire completion. Today, the mean peat thickness is close to 1 metre in the coastal area (Sohlenius and Hedenström 2008), but this value is only characteristic of relatively young mires.

Time of lake isolation

The RLDM described the development of the basins during the sea phase in time steps of 500 years. The end of the sea stage in the lake basins was defined as the last record for the marine stage predicted by the RLDM.

Vegetation

The shallow parts of a sea bay will be colonised with reeds, and a substantial part of the lake area may already be covered by mire vegetation (reed) at the time of isolation. The vegetation cover of the sea bay will depend on the bathymetry of the basin, as well as on the physical exposure (e.g. waves, ice) and bottom substrate both less easily predictable in the long term and deemed potentially adding only detail to the picture in the level of the development of the biosphere objects. Using data from the three Laxemar objects with a full RLDM history (201, 207 and 208), the cover of vegetation (area_obj_ter) at the time of lake isolation, VegCover ($m^2 \cdot m^{-2}$), was described as a linear function of the average water depth of the sea bay immediately prior to isolation (Figure 3-8):

$$VegCover = Cover_{max} - ß_{depth} \times Depth_{seabay} \qquad \text{Equation 3-3}$$

where:

$Cover_{max}$ (fraction of lake basin) is a constant describing the maximum cover of mire vegetation at threshold_isolation (with a value of 0.68 $m^2\ m^{-2}$ used here]

$ß_{depth}$ ($m^2\ m^{-2}\ m^{-1}$) is a constant that describes how the fraction of the lake basin covered by vegetation decreases with the water depth in the sea basin prior to isolation [0.11]

$Depth_{seabay}$ (m) is the average water depth of the biosphere object prior to the time point threshold_isolation.

The vegetation cover at the time point for isolation of the lake basin (threshold_isolation) was then interpolated backwards to the time at which the biosphere object was first isolated at low water levels (−0.9 m, i.e. threshold_start, see Section 3.4.4) in accordance with the RLDM modelled biosphere objects. The average thickness of the peat layer was estimated to be 1 m at the time of lake isolation (average across objects 201, 207 and 208)[2]. In the RLDM, the initial volume under vegetation is also the volume that will finally be filled with mire peat and is hereafter simply referred to as peat volume.

[2] It can be noted that the estimated value of 1 m also equals the expected average water depth for a lake bottom with an even slope colonised by reed to a depth of 2 m, which is the depth limited for reed colonisation in the RLDM (Brydsten and Strömgren 2013).

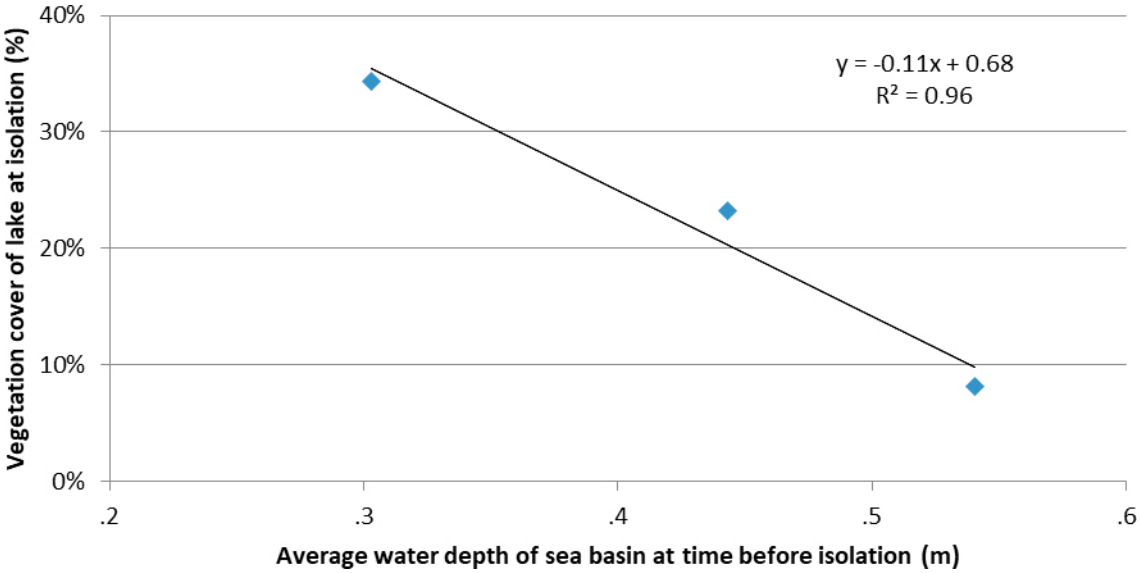

Figure 3-8. *Relation between vegetation cover (%) of a lake basin at the point of isolation and average water depth in the sea basin at the time point prior to isolation based on RLDM results for the three biosphere objects 201, 207 and 208. Also, the linear regression of the three datapoints, the function for the linear relationship as well as its coefficient of determination are shown.*

Postglacial fine sediments

Postglacial fine sediments accumulate during the sea stage (regoPG_aqu), and at the time of isolation a substantial layer of organic sediments may have developed in the lake basin. The layer of fine sediments will be thickest in the deepest part of the basin. The shallower parts of the basin have a shorter history of wind and wave sheltered conditions needed for accumulation, and thus the layer of fine sediments tends to be thinner along the shores than in the central parts of the basin.

The initial thickness of post-glacial fine sediments (z_regoPG_aqu) in the basin of a historic lake was calculated for the six biosphere objects (203, 204, 206, 210, 212 and 213) as a function of the sediment thickness in the sea basin (prior to the time point threshold_isolation) and the surface area relationship between the sea basin and the lake basin. For the three RLDM-modelled biosphere objects an empirical relationship for the relative lake sediment thickness was derived as a linear function of the inverse of the relative lake area as follows (Figure 3-9):

$$\frac{Z_{PGC,lakebas}}{Z_{PGC,seabay}} = R_0 + \beta_{area}\frac{Area_{seabay}}{Area_{lakebas}} \qquad \text{Equation 3-4}$$

where

$Z_{PGC,lakebas}$ (m) is the average thickness of postglacial clay gyttja in the lake basin at the point of isolation

$Z_{PGC,seabay}$ (m) is the average thickness of postglacial clay gyttja in the sea basin prior to isolation

$Area_{lakebas}$ (m^2) is the area of the lake basin

$Area_{seabay}$ (m^2) is the area of the sea basin prior to isolation

$ß_{area}$ (unitless) is a constant that describes how the initial value of the relative sediment thickness increases with the inverse of relative area of the lake basin [0.78]

R_0 (unitless) is a constant that equals $1-ß_{area}$ [0.22]

The initial thickness of postglacial fine sediments covered by mire vegetation (z_regoPGC_ter) was assumed to be 65 % of the average thickness of the postglacial fine sediment in the whole lake basin, which was an average from the modelled objects 201, 207 and 208). The initial sediment thickness under open water (z_regoPGC_aqu) was calculated from volume balance (vol_sed_PGC-area_obj_ter*z_regoPGC_ter), and the area of the open water (given by $Area_{lakebase}$[1-VegCover]).

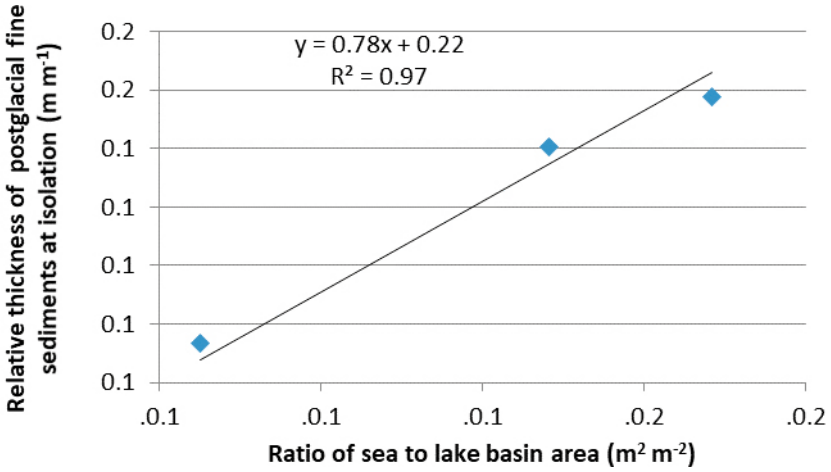

Figure 3-9. *Relative thickness of postglacial fine sediments at the point of isolation as a function of the ratio of the sea basin (prior to isolation) and the lake basin.*

3.4.3 Lake development

Sedimentation and resuspension

The volumetric net sedimentation rate, NetSed (m^3 $year^{-1}$), the resuspension rate (res_rate, m^3 m^{-2} $year^{-1}$) and the gross sedimentation rate (sed_rate, m^3 m^{-2} $year^{-1}$) were modelled as in the three objects with the full RLDM lake stage development (see Section 3.4.1).

Ingrowth of vegetation into the lake

Vegetation expands into the lake, and in the RLDM the rate of expansion depends on the lake basin size and the bathymetry of the lake. That is, the maximum rate of ingrowth is a linear function of the lake basin area, but the ingrowth is limited by water depth and no ingrowth occurs on lake bottoms with a water depth exceeding 2 m (Brydsten and Strömgren 2010).

In Laxemar, the topography is more pronounced than in Forsmark, and consequently the rate of ingrowth (ter_growth, m^2 $year^{-1}$) predicted by the RLDM is significantly lower than the maximum rate (obtained by Equation 3-1 and originally calibrated against Forsmark). The average rate of ingrowth, between the point of isolation and the time when 95 % of the lake is covered with vegetation was calculated for objects 201, 207 and 208 (Figure 3-10). The rate of ingrowth for the three objects was approximately proportional to the lake basin area, and an average relative rate of ingrowth of 1 % per 100 years was used to estimate an initial rate of vegetation ingrowth for all historic lakes. The rate of ingrowth was then kept constant at this level until the lake was completely overgrown by vegetation. That is, for a historic lake with a basin area of 10 ha (100 000 m^2), vegetation was assumed to expand at a constant rate of 10 m^2 per year.

However, for the small lake (206, 17 ha) this slow rate of ingrowth resulted in an extended period of a shallow water depth (<2 m) towards the end of the simulated lake succession. This was deemed highly unrealistic, and therefore the average rate was adjusted to 1.5 %. A pattern of larger relative rate of ingrowth for small lakes is consistent with the function used for maximum ingrowth in Forsmark (Figure 3-10); however, this rate is still much lower than the maximum rate used in the RLDM for Forsmark.

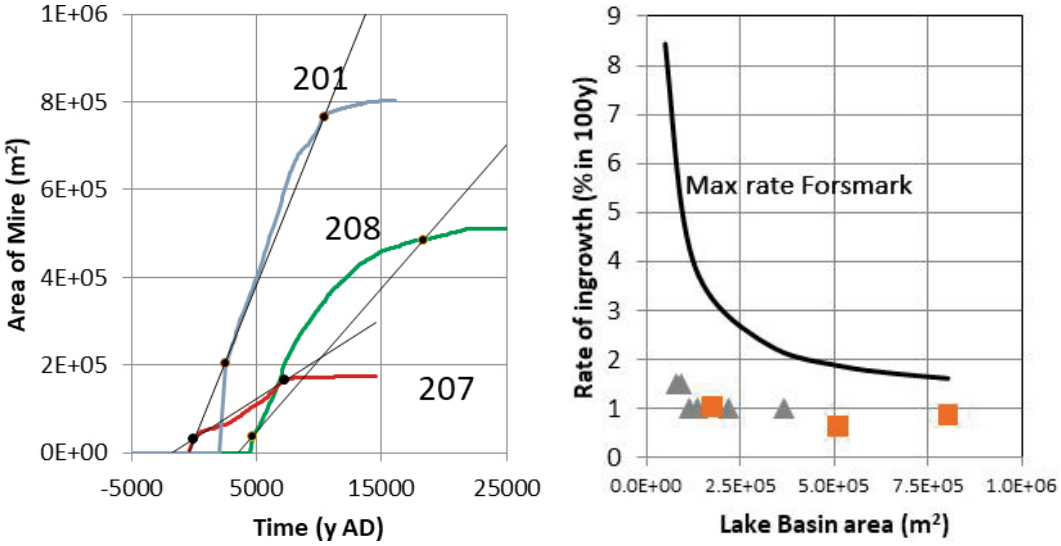

Figure 3-10. *Rate of mire vegetation ingrowth in Laxemar. Left) Ingrowth predicted by the RLDM for three biosphere objects (ID numbers shown in the graph). The slopes of the black lines correspond to the average rates of ingrowth. Right) Relative ingrowth rate as a function of lake basin area. Orange squares represent the three lakes on the left, grey triangles represent the parameter values used for the six historic lakes, and the black line represents the maximum rate for lakes in Forsmark (FM).*

Modelling the lake-mire succession

The development of the historic lakes was modelled in time-steps of 100 years. For each time step the volume (vol_obj_aqu), area (area_obj_aqu) and average depth (z_water) of open water, area of mire vegetation (area_obj_ter), peat thickness (z_regoPeat) and thickness of postglacial fine sediments (total and subdivided with respect to water or mire vegetation, z_regoPGC_aqu and z_regoPGC_ter) were updated. This was processed in the following order:

1. The total volume of post-glacial sediments (m^3) was updated by adding the volume produced by net sedimentation since the previous time step. Sediment production was calculated as the product of net sedimentation rate of the previous time step (Eqation 2) and the time interval between steps (100 years).
2. The mire area (area_obj_ter, m^2) was updated by adding the area colonised by mire vegetation since the previous time step. The recently colonised area was calculated as the product of a constant relative ingrowth rate (% per 100 year) and the lake basin area. The lake area (m^2, i.e. the open water surface, area_obj_aqu) was decreased by the same area.
3. The total volume of peat (vol_obj_ter) was updated by adding the water volume that had been covered by mire vegetation since the previous time step. The lake bottom depth of the colonised area was assumed to be 2 m, if the average water depth (z_water) of the lake exceeded 2 m. Otherwise the average depth of the lake was also used for the depth colonised by reeds.
4. The volume of open water (vol_obj_aqu) was estimated as the total lake basin volume less the volume of peat (vol_obj_ter) and postglacial fine sediments (vol_sed_PGC) at each time step.
5. The volume of postglacial fine sediments under the mire (vol_PGC_ ter, m^3) was updated by adding the volume covered by vegetation since the latest time step. The volume of the recently covered sediments was calculated as the product of the area colonised by vegetation since the latest time step (calculated under 2), and the average thickness of the postglacial fine sediments under open water (z_regoPGC_ aqu) from the previous time step.
6. The volume of postglacial fine sediments under open water was calculated by subtracting the sediment volume under the mire (calculated under 5) from the total amount of postglacial fine sediments (calculated under 1). Similarly, the volume of open water was calculated by subtracting the total volume of postglacial fine sediments (calculated under 1) and the total amount of peat (calculated under 3) from the lake basin volume (above the glacial clay and coarse-grained postglacial sediments, Figure 3-3).

7. Finally, the average water depth (z_water), and the average thicknesses of peat (z_regoPeat) and post glacial fine sediments (in the mire and lake parts, respectively, z_regoPGC_ter and z_regoPGC_aqu) were updated for the time step by dividing the respective volumes by areas.
8. The procedure was repeated until the lake had been completely covered with vegetation (time = T_end)[3].
9. In the, a stream was always present as the last stage of the lake surface water area. The estimation of stream geometry is described under Section 3.3.

The thickness of postglacial fine sediments and the gross rate of sedimentation in the stream were assumed to be similar to those in the last time step of the lake stage. Finally, bottom sediments in the stream were assumed to have reached equilibrium, and thus the resuspension rate was set equal to the gross sedimentation rate.

Assessing fit of simplified model

To assess to what extent the simplified calculations could reproduce the dynamics of the RLDM, the development of object 207 was described from isolation of the lake to the final mire stage (Figure 3-11).

The constant rate of ingrowth matched the ingrowth dynamics of mire vegetation, fairly well, based on the hypsographic map, but the average water depth of the lake derived from simplified assumptions did not match the dynamics of the RLDM. However, the overall patterns of a steadily increasing mire area, and a steadily decreasing water depth, were captured with the simple calculations, and the fit was judged to be sufficiently good for the purpose of an assessment. Moreover, the development of the average thickness of peat and postglacial fine sediments matched the output of the RLDM very well.

The mire peat thickness at mire maturity (z_regoPeat_equilib) varied between 1.4 m and 1.7 m in the six historic lakes, and the thickness of the postglacial fine sediments (z_regoPG) correlated well with the thickness of the corresponding layers of present biosphere objects (Figure 3-12). This demonstrates that the outputs from the calculations are reasonably consistent with the initial assumptions used to estimate the volume of the lake basin (i.e. a peat thickness of 1.6 m, and a fine sediments (claygyttja) compactation of 65 %).

3.4.4 Threshold parameters for modelling ecosystem transitions

The transitions of biosphere objects from marine basins to shallow sea bays, lakes and mires are driven by land-rise. These transitions are initiated when certain thresholds for the biosphere object are reached. The time at which a threshold is reached, for instance the year when the isolation of a lake starts, is used to specify the occurrence of a transition, in this case when a bay turns into a lake. These times of exceedance of thresholds are also used to determine when certain activities, e.g. draining of a mire, are possible. The thresholds are also used to interpolate other parameters between sea and lake stages, e.g. water fluxes and net primary production. See Grolander (2013) for a more detailed description of the parameters describing different developmental stages listed in Appendix B.

[3] T_end = T_isolation + (AreaLake -($Cover_{max}$ -$ß_{depth} \times Depth_{seabay}$))/($Area_{lakebas} \times Rate_{ingrowth}$), where $Rate_{ingrowth}$ is the relative ingrowth rate [% $year^{-1}$].

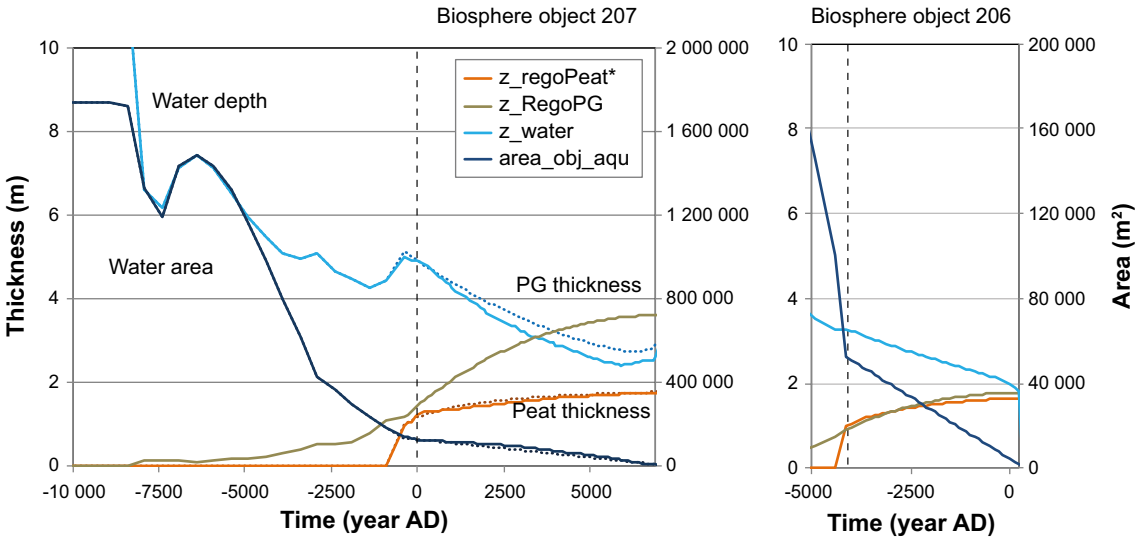

Figure 3-11. *Development of biosphere objects according to the RLDM and a simplified version describing lake infilling. Left panel: Development of Lake Frisksjön (207). Solid lines represent lake area (dark blue, area_obj_aqu), water depth (light blue, z_water), peat thickness (orange, z_regoPeat*) and the average depth of post-glacial fine sediments in the object (brown, z_regoPG). Dotted lines represent the same properties calculated with the simplified model. Lake isolation occurs at year 0 AD. Right panel: Development of the historical lake in biosphere object 206 as predicted by the simplified model. Lake isolation occurs at year 0 and −4100 AD, respectively (dashed vertical line).*

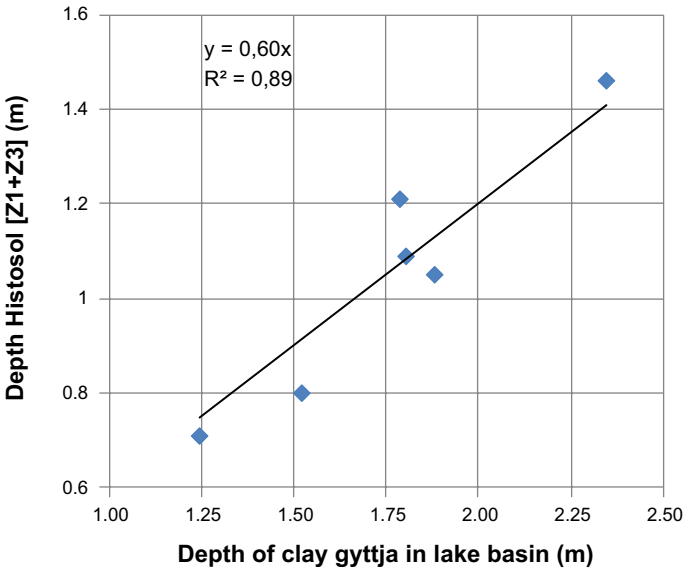

Figure 3-12. *Present-day fine sediment thickness in the biosphere objects as a function of modelled thickness of the post glacial clay gyttja in six historic lakes. The Z1 layers corresponds to the upper soil layer (excluding peat), and the Z3 layers corresponds to a layer of fine sediments below the surface soil layer (see also Figure 3-3).*

The time for lake isolation (threshold_isolation) was defined as the time when the lake basin threshold (the physical regolith formation present at the forthcoming outlet of the lake) reached the yearly average sea level. The thresholds of future and historic lakes were determined from measurements. The height of thresholds of future lakes basins were manually levelled during a field-campaign in August 2005 (Lindborg 2006). For present biosphere objects, the lake basin threshold was estimated in the field and represents the lowest point found today (Strömgren et al. 2006). This threshold may be the result of artificial lowering in order to drain potential agricultural land. The threshold for the present lake 207 represents the undrained lake and was estimated by measuring the altitude of the old outlet from the lake (the new outlet is located in another part of the lake). The shoreline displacement, i.e. the net effect of the glacio-isostatic uplift and the global eustatic sea level rise, was described by the expressions presented in Påsse (2001) (see **Climate report** and SKB (2014b) for a more detailed description). Start of isolation (threshold_start) was defined as the time point when the lake threshold reached the sea level at low water level, and isolation was defined as completed when the lake threshold reached sea level at high water level (threshold_stop). The values used for high and low water level were based on data from Kungsholmsfort in the southern part of the Baltic Sea between 1887-1983 (lowest low-water (LLW) −0.9 m and highest high-water (HHW) 1.3 m, Sjöfartsverket 1992).

Threshold_end is the time point when the lake basin is completely filled with peat. Threshold_well is the year when it is possible to use a well in the object; for most biosphere objects, this occurs at the same moment as the object fully transforms from a sea basin to a lake or land and thus seawater intrusion into well water becomes unlikely (i.e. it is the same year as threshold_stop). In some cases it might occur later depending on the topography.

3.5 Permanent aquatic objects to assess long-term release

To allow the assessment of long-term release of radionuclides to a sea basin, two static versions of the sea basins 201 and 208 were included as separate biosphere objects. The time slices used to represent the bathymetry of the two objects where chosen to span a large interval of water exchange rates. Thus, for object 208, which is a semi-enclosed embayment, the present state was used, and, for the other end of the range, an early time point (9 500 BC) was selected for object 201, representing a sea basin with a high rate of water exchange. Moreover, to evaluate a situation where radionuclides reach a freshwater body in a mature terrestrial landscape (e.g. as a consequence of human damming activities) static versions of three lakes, based on the RLDM, were introduced as separate biosphere objects. These objects were the present lake Frisksjön (object 207, 2 000 AD), and objects 201 and 208 at their times of isolation (5 100 AD and 2 500 AD).

In the evaluation case where these five aquatic objects developed over time, the parameters for water depth, water volume, and rates of sedimentation and resuspension were taken from the RLDM predictions. Present conditions, as described in the RDM of the site (Nyman et al. 2008), were used to characterise the thickness of regolith layers in Lake Frisksjön (207) and the coastal basin 208. The parameter data are presented in Appendix B.

3.6 A coastal site with a flatter topography in comparison to Laxemar

With the aim of contrasting different landscapes and properties of biosphere objects, six biosphere objects (116, 121_1, 121_2, 157_1, 157_2 and 159) located in Forsmark, northern Uppland, which were readily analysed in SR-PSU assessment were used to illustrate a coastal site with a flat topography (Figure 3-13). These biosphere objects are today located below the present sea level and will emerge because of the shoreline regression. These biosphere objects are described in SKB (2015a, Section 6.3) and their parameterisation is described in Grolander (2013). Figure 3-14 below describe the biosphere object sizes and regolith thicknesses.

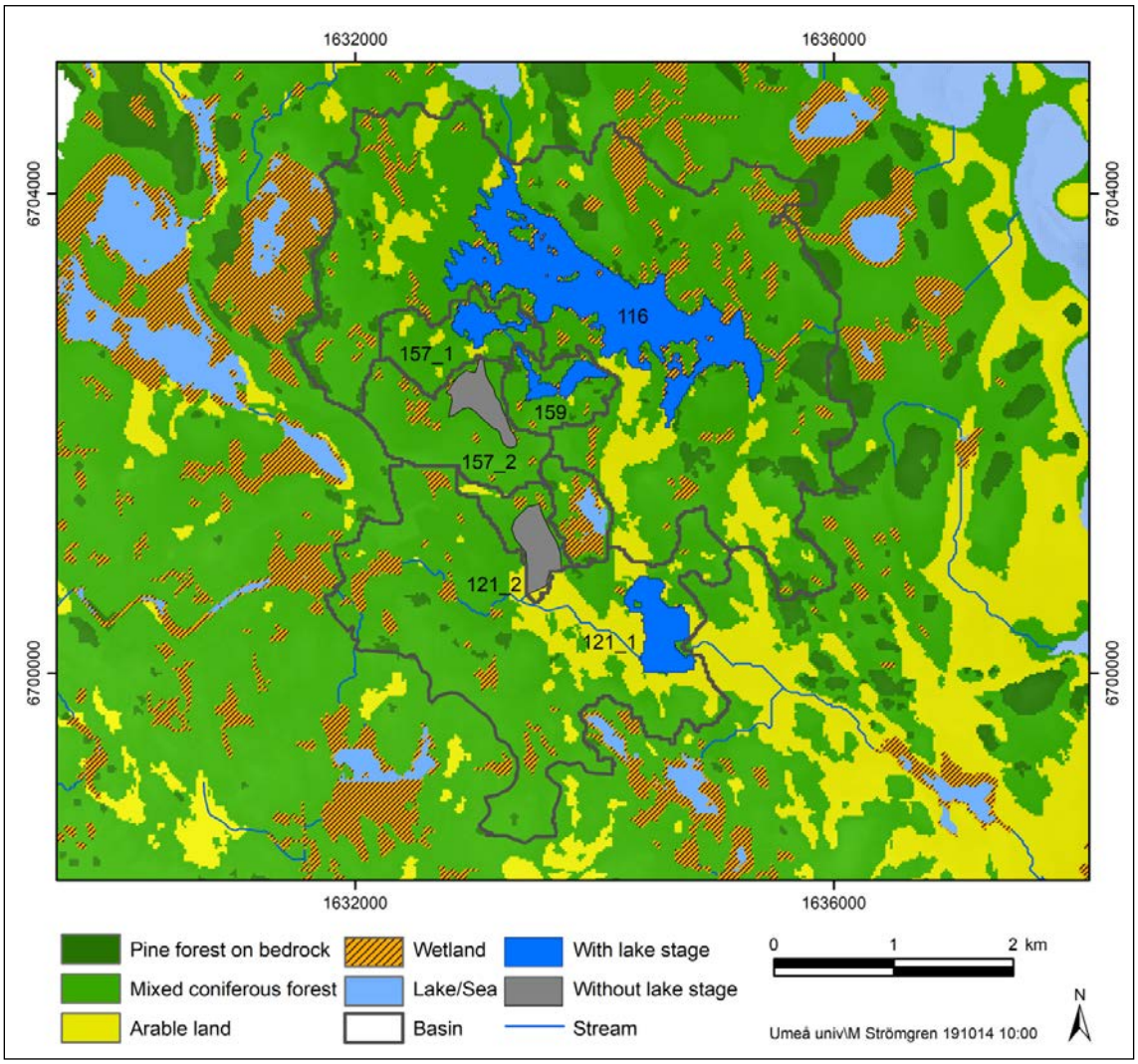

Figure 3-13. *The six biosphere objects in the Forsmark area included in SE-SFL and are here illustrated at 4500 AD. At present, all of the objects are located in the sea. Grey biosphere objects will turn directly into mire objects when they become terrestrial as a result of shore-line regression, and blue areas are biosphere objects that will go through a lake stage before turning into mires.*

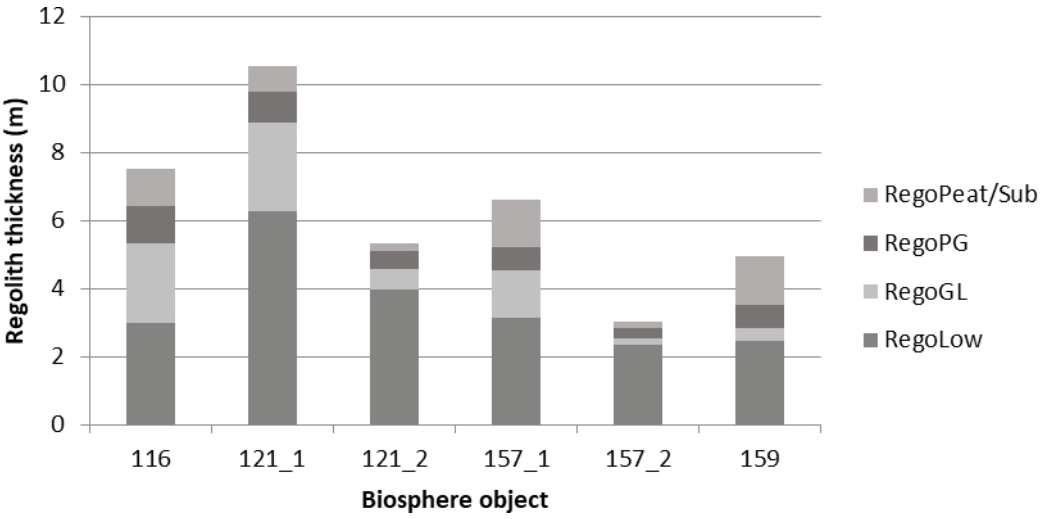

Figure 3-14. *Regolith thickness among different regolith types for the six future biosphere objects in SR-PSU representing the mire stage in the successional development.*

4 Regolith properties

This chapter presents the parameters in BioTEx for SFL-SE used to represent the physical regolith properties within the assessed biosphere objects. The parameters include, for instance, porosity and density of the natural regolith types and agricultural soils as well as properties that are relevant for the safety assessment of agricultural soils such as degree of saturation and compaction of peat and gyttja. Chemical properties are described in Chapter 6 and hydraulic properties used in the hydrological modelling are described in Chapter 5. Descriptions of all physical regolith parameters addressed in this Chapter are given in Table 4-1. The effect of site-specific characteristics on the selected parameter values is described in Section 4.1.

The regolith/soil compartments in the BioTex for Laxemar are defined based on the regolith depth model for Laxemar presented in Nyman et al. (2008). According to the regolith depth model the general stratigraphy above the bedrock is till, glacial clay, a thin layer of sand, postglacial clay gyttja, peat and a top layer that is affected by soil-forming processes. The stratigraphy of soil/regolith layers in the Laxemar model area is similar to the stratigraphy at the Forsmark site. This is illustrated in Figure 3-3.

In BioTEx, the regolith/soil layers are defined as five regolith/soil compartments for the terrestrial ecosystem and four compartments for the aquatic ecosystem (Figure 3-3). The RegoLow compartment represents till overlying the bedrock, the RegoGL compartment represents the glacial clay overlying the till. The RegoPG represents the postglacial clay gyttja layer. These lower layers (RegoLow, RegoGL and RegoPG) are identical in both terrestrial and aquatic ecosystems whereas the top layers differ between the ecosystems. In the terrestrial ecosystem, the peat is divided into one anoxic peat layer, RegoPeat, and one layer representing the oxidised top layer of the peat, RegoUp. In the aquatic ecosystem, the RegoUp layer represents the oxidised organic top sediment. Additionally, there is a sand layer present in the Laxemar area, which is found between the RegoGL and the RegoPG layers. This sand layer is usually rather thin and has consequently been included in the RegoPG layer.

Three agricultural land-use variants are assessed in the SFL-SE; modern agricultural practices with draining of wetland, early agriculture with infield-outland practices, and a modern garden plot utilised by a household. These three land-use variants are the same as in SR-PSU and they are further described in the **Biosphere synthesis**. The soil types considered in the three land-use variants differ depending on the available soil types at the modelled site.

In the infield-outland and the garden plot variants, clay-gyttja represents the cultivated areas of today. Such soils are dominating the landscape as an effect of the earlier drainage and cultivation activities. In the case of the infield and outland farming, another possibility is to use the sandier soils that are present in the Laxemar area. In the Present-day evaluation case (**Biosphere synthesis**) the starting point of the assessment is today and therefore the cultivated clay-gyttja areas are of potential interest also for infield and outland farming. Consequently, in this calculation sandy soils were disregarded.

Additionally, there is one variant of the modern agricultural land use, where the ageing agricultural soils present today in six of the biosphere objects are utilised. This agricultural variant is used in the *Present-day evaluation case*. The regolith depths are taken from the present-day description and remain constant over time, instead of a modelled development from a sea bay to a drained mire. The parameters used in this case are porosity and density of the uppermost 25 cm (z_regoUp_agri) of the regolith profile as well as the degree of saturation, compactation (parameter values presented below, see also Chapter 3).

Table 4-1. Definition of regolith parameters used.

Name	Unit	Description
compact_gyttja	m m^{-1}	Initial immediate compactation of agricultural soils (clay gyttja) + reduction due to oxidation
compact_peat	m m^{-1}	Initial immediate compactation of agricultural soils (peat) + reduction due to oxidation
dens_regoGL	kg_{DW} m^{-3}	Density of glacial clay
dens_regoLow	kg_{DW} m^{-3}	Density of the lower regolith layer (till)
dens_regoPeat	kg_{DW} m^{-3}	Density of upper anoxic layer of terrestrial regolith (peat)
dens_regoPG	kg_{DW} m^{-3}	Density of post-glacial sediments
dens_regoUp	kg_{DW} m^{-3}	Density of soil in a modern kitchen garden or glacial clay in early agricultural societies
dens_regoUp_gyttja	kg_{DW} m^{-3}	Density of agricultural soil derived from clay gyttja
dens_regoUp_lake	kg_{DW} m^{-3}	Density of upper 5 cm layer of aquatic regolith (lake)
dens_regoUp_peat	kg_{DW} m^{-3}	Density of agricultural soil derived from peat
dens_regoUp_sea	kg_{DW} m^{-3}	Density of upper 10 cm layer of aquatic regolith (sea)
dens_regoUp_ter	kg_{DW} m^{-3}	Density of upper oxic layer of terrestrial regolith (peat)
poro_regoGL	m^3 m^{-3}	Porosity of glacial clay
poro_regoLow	m^3 m^{-3}	Porosity of lower regolith layer (till)
poro_regoPeat	m^3 m^{-3}	Porosity of upper anoxic layer of terrestrial regolith (peat)
poro_regoPG	m^3 m^{-3}	Porosity of post-glacial sediments
poro_regoUp	m^3 m^{-3}	Porosity of soils in a modern kitchen garden or glacial clay in early agricultural society
poro_regoUp_gyttja	m^3 m^{-3}	Porosity of agricultural soil derived from clay gyttja
poro_regoUp_lake	m^3 m^{-3}	Porosity of upper 5 cm layer of aquatic regolith (lake)
poro_regoUp_peat	m^3 m^{-3}	Porosity of agricultural soil derived from peat
poro_regoUp_sea	m^3 m^{-3}	Porosity of upper 10 cm layer of aquatic regolith (sea)
poro_regoUp_ter	m^3 m^{-3}	Porosity of upper oxic layer of terrestrial regolith (peat)
S_w_regoUp	m^3 m^{-3}	Degree of saturation in soils in a modern kitchen garden or in upper layer of sandy soils in early agricultural society
S_w_regoUp_gyttja	m^3 m^{-3}	Degree of saturation in upper soil layer in a cultivated drain mire
S_w_regoUp_peat	m^3 m^{-3}	Degree of saturation in upper soil layer in in a cultivated drain mire
z_drain_agri	m	Trenching depth after compactation

4.1 Effect of site-specific characteristics on parameter values

The definition of the regolith compartments included in BioTEx is dependent on the local stratigraphy of the regolith layers of the area. The stratigraphy and properties of regolith layers at a site is dependent on the formation history and the ecological and climatic conditions that has been prevailing at the site after formation. Therefore, the regolith properties will differ between sites in Sweden, for instance if the site is located above or below the highest coastline. This means that regolith properties are dependent on the local conditions and are regarded as site-specific.

4.2 Selection of parameter values

The properties of the regolith, i.e. the density and porosity of the regolith layers in Laxemar are expected to be similar to the properties at Forsmark, because the common formation history and similar climatic and ecological conditions at the two sites. It was therefore assumed that the data for regolith parameters used in SR-PSU could be used to represent the properties of the regolith in the Laxemar model area. To evaluate this assumption site-specific data from Laxemar used in SR-Site safety assessment (Löfgren 2010) were compared with site-specific data from Forsmark used both

in SR-Site (Löfgren 2010) and SR-PSU (Grolander 2013). When data on porosity and density of till, glacial clay and postglacial gyttja from the two sites were compared, the differences in mean values were found to be very small (up to 3 %). A similar comparison between other soil types (peat and aquatic sediments) was not possible because no corresponding data were available from Laxemar.

The selected parameters are described in Table 4-1 and the values used are included in Appendix C.

4.3 Densities and porosities of non-cultivated soils and aquatic sediments

For these parameters (dens_regoLow, dens_regoGL, dens_regoPG, dens_regoPeat, dens_regoUp_ter, dens_regoUp_lake, dens_regoUp_sea, poro_regoLow, poro_regoGL, poro_regoPG, poro_regoPeat, poro_regoUp_ter, poro_regoUp_lake, poro_regoUp_sea) the SR-PSU data have been used, see Grolander (2013) Chapter 5.3 and Appendix C for selected data values for each parameter.

4.4 Properties of cultivated soils

At the Laxemar site the modern agricultural land-use variant, utilises drained areas comprising primarily clay gyttja and peat along the valleys in areas which have a history of being shallow bays, lakes and mires. The infield-outland land-use variant and the garden plot land-use variant utilise the same type of areas as in the modern agricultural land-use variant. Cultivated clay gyttja, which is the topsoil after the peat has been oxidised, with a high organic content is also the dominating soil type in the agricultural fields at Laxemar present today. The properties of the cultivated clay gyttja and peat are presented in the following sections.

4.4.1 Densities and porosities of cultivated gyttja clay and peat

Densities and porosities of cultivated clay gyttja measured in the surroundings of Forsmark site are presented in Section 5.4.1 in Grolander (2013). These values are used for the parameterisation of the developing biosphere objects and are similar to the values from Laxemar presented in Lundin et al. (2005) for densities (dens_regoUp, dens_regoUp_gyttja) and porosities (poro_regoUp, poro_regoUp_gyttja) of the cultivated clay gyttja in Laxemar. See Table 4-1 for a description of the parameters and Appendix C for selected data values for each parameter.

4.4.2 Compactation of clay gyttja and peat

The compaction of gyttja and peat (compact_gyttja, compact_peat) is the ratio of dry bulk densities of drained and un-drained gyttja and peat, respectively. The calculated parameter values for Forsmark used in SR-PSU are used also for the Laxemar site, see Section 5.4.3 in Grolander (2013). See Table 4-1 for a description of the parameters and Appendix C for selected data values for each parameter.

4.4.3 Degree of saturation of clay gyttja and peat

The degree of saturation of cultivated clay gyttja and peat (S_w_regoUp, S_w_regoUp_peat, S_w_regoUp_gyttja) is dependent on local conditions and can also differ between years. There are no data available for this parameter from the Laxemar or Forsmark sites. The parameter data used for SR-PSU were based on literature data, these data are used also in this study, see Section 5.4.4 in Grolander (2013). See Table 4-1 for a description of the parameters and Appendix C for selected data values for each parameter.

5 Surface hydrological fluxes

5.1 Introduction

The BioTEx spans over very long time periods and it is therefore needed to account for the effects of for example isostatic and eustatic changes, ecosystem succession and climate variation. The surface and groundwater hydrology for each potential discharge area are therefore described under several different conditions. The stages and ecosystems included in the safety evaluation are: off-shore and coastal sea ecosystems, lake and wetland ecosystems, and agricultural ecosystems (on previously drained lake-mires).

In SE-SFL, the ambition has been to apply the SR-PSU methodology to derive parameters describing surface and groundwater water flows for discharge areas in Laxemar. In SR-PSU inter-basin water exchange for each sea basin was calculated with the MIKE 3 FM model for both off-shore and coastal conditions (Werner et al. 2013). However, the data available for Laxemar were not as detailed as for Forsmark in the SR-PSU assessment. Instead, water exchange rates were based on values reported in 2010, which were calculated with the CouBa-model (Engqvist 2010). The early submerged period was not represented in these simulations, and consequently water residence times before 3 000 BC had to be estimated from present-day open coastal conditions. The resulting residence times and the methods used to derive them are described in the next section.

In SR-PSU, flows of ground and surface water were estimated separately for each biosphere object. Flows across regolith and ecosystem boundaries were derived from MIKE SHE-simulated water balances for three different successional stages. In SE-SFL, detailed water-balances were only available for present-day conditions. Thus, a new methodology for deriving groundwater parameters, which could be used for systematic interpolations to other successional stages, was developed. In short, the SE-SFL methodology starts from a set of stylised water balance models for natural and cultivated ecosystems. Object-specific boundary conditions are calculated based on water balances and catchment properties. Percolation is calculated from empirical rules, and upward groundwater flows and streamflow are inferred from mass balance. Sections 5.4–5.7 describe how hydrological flows were derived from MIKE-SHE water balances. It is demonstrated that parameters for present-day conditions derived with the new methodology are similar to those derived with the SR-PSU methodology (e.g. Figures 5-13, 5-14). However, for future conditions (for which water balance data from Laxemar are lacking) the uncertainties of the derived groundwater flow parameters are potentially large. The parameters used when describing hydrological fluxes are listed in Table 5-2 and parameter values used are presented in Appendix D.

Table 5-1. Summary of hydrological parameters. Note that in models describing ecosystem succession the parameters are identical with those in SR-PSU (m^3 m^{-2} $year^{-1}$).

Name	Description
q_bedrock_low_lake	Water flux from bedrock to lower regolith in the limnic phase
q_bedrock_low_sea	Water flux from bedrock to lower regolith in the marine phase
q_bedrock_low_sea_deep	Water flux from bedrock to lower regolith in the deep marine phase
q_bedrock_low_ter	Water flux from bedrock to lower regolith for the terrestrial part in the mire phase
q_downstream	Water flux from the water column downstream after the marine phase
q_gl_low_lake	Water flux from the glacial clay layer to lower regolith for the aquatic part in the limnic phase
q_gl_low_sea	Water flux from the glacial clay layer to lower regolith in the marine phase
q_gl_low_sea_deep	Water flux from the glacial clay layer to lower regolith in the deep marine phase
q_gl_low_ter	Water flux from the glacial clay layer to lower regolith for the terrestrial part in the mire phase
q_gl_pg_lake	Water flux from glacial clay to the post glacial clay layer for the aquatic part in the limnic phase
q_gl_pg_sea	Water flux from glacial clay to the post glacial clay layer in the marine phase
q_gl_pg_sea_deep	Water flux from glacial clay to the post glacial clay layer in the deep marine phase
q_gl_pg_ter	Water flux from glacial clay to the post glacial clay layer for the terrestrial part in the mire phase
q_low_bedrock_lake	Water flux from lower regolith to bedrock in the limnic phase
q_low_bedrock_sea	Water flux from lower regolith to bedrock in the marine phase
q_low_bedrock_sea_deep	Water flux from lower regolith to bedrock in the marine phase
q_low_bedrock_ter	Water flux from lower regolith to bedrock for the terrestrial part in the mire phase
q_low_gl_lake	Water flux from lower regolith to the glacial clay layer for the aquatic part in the limnic phase
q_low_gl_sea	Water flux from lower regolith to the glacial clay layer in the marine phase
q_low_gl_sea_deep	Water flux from lower regolith to the glacial clay layer in the deep marine phase
q_low_gl_ter	Water flux from lower regolith to the glacial clay layer for the terrestrial part in the mire phase
q_peat_pg_ter	Water flux from peat to the post glacial clay layer for the terrestrial part in the mire phase
q_peat_up_ter	Water flux from peat to the upper peat layer for the terrestrial part in the mire phase
q_pg_gl_lake	Water flux from post glacial clay to the glacial clay layer for the aquatic part in the limnic phase
q_pg_gl_sea	Water flux from post glacial clay to the glacial clay layer in the marine phase
q_pg_gl_sea_deep	Water flux from post glacial clay to the glacial clay layer in the deep marine phase
q_pg_gl_ter	Water flux from post glacial clay to the glacial clay layer for the terrestrial part in the mire phase
q_pg_peat_ter	Water flux from post glacial clay to the peat layer for the terrestrial part in the mire phase
q_pg_up_lake	Water flux from post glacial clay to the upper sediment layer for the aquatic part in the limnic phase
q_pg_up_sea	Water flux from post glacial clay to the upper sediment layer in the marine phase
q_pg_up_sea_deep	Water flux from post glacial clay to the upper sediment layer in the deep marine phase
q_up_peat_ter	Water flux from upper peat to the peat layer for the terrestrial part in the mire phase
q_up_pg_lake	Water flux from upper sediment to the post glacial clay layer for the aquatic part in the limnic phase
q_up_pg_sea	Water flux from upper sediment to the post glacial clay layer in the marine phase
q_up_pg_sea_deep	Water flux from upper sediment to the post glacial clay layer in the deep marine phase
q_up_wat_lake	Water flux from the upper sediment layer to water column for the aquatic part in the limnic phase
q_up_wat_sea	Water flux from the upper sediment layer to water column in the marine phase
q_up_wat_sea_deep	Water flux from the upper sediment layer to water column in the deep marine phase
q_up_wat_ter	Water flux from the upper peat layer to water column for the terrestrial part in the mire phase
q_wat_up_lake	Water flux from water column to the upper sediment layer for the aquatic part in the limnic phase
q_wat_up_sea	Water flux from water column to the upper sediment layer in the marine phase
q_wat_up_sea_deep	Water flux from water column to the upper sediment layer in the deep marine phase
q_wat_up_ter	Water flux from water column to the upper peat layer for the terrestrial part in the mire phase

Table 5-2. Hydrological parameters used to calculate the corresponding flows in time-independent models of mires and agricultural ecosystems.

Name	Unit	Description
b_percol_agri	m^{-1}	Rate of decrease of percolation at reference depth with thickness of the glacial clay layer at the reference level for agricultural ecosystems
b_percol_ter	m^{-1}	Rate of decrease of percolation at reference depth with thickness of the glacial clay layer at the reference level for mire ecosystems
delta_disch	m^{-1}	Rate of change with depth of horizontal discharge of groundwater into an object (applies to all ecosystems)
f_disch_stream_agri	unitless	Fraction of the runoff from the basin that reaches the stream upstream of the discharge area for agricultural ecosystems
f_disch_stream_ter	unitless	Fraction of the runoff from the basin that reaches the stream upstream of the discharge area for mire ecosystems
f_disch_surf	unitless	Fraction of the discharge from the local catchment that reaches the biosphere object as surface (rather than groundwater) discharge.
f_surfperc_LC	unitless	Fraction of the surface water reaching the mire that percolates (and generates groundwater) as opposed to being discharged to the stream within the object
f_surfperc_obj_agri	unitless	Fraction of net precipitation that infiltrates into agricultural soil (as opposed to being discharged to the ditch)
f_surfperc_obj_ter	unitless	Fraction of the net precipitation in the object that percolates to deeper peat layers (as opposed to being discharged directly from surface peat to the stream).
k_percol_agri	m^{-2}	Regression coefficient that describes how percolation decreases with the thickness of glacial clay in agricultural soil
k_percol_ter	m^{-2}	Regression coefficient that determines how percolation below the reference level decreases with the thickness of glacial clay in mire ecosystems
m_percol_agri	m^{-1}	Rate of decrease in percolation with soil depth in the absence of a glacial clay layer in agricultural soil
m_percol_ter	m^{-1}	Rate of decrease in percolation with soil depth in the absence of a glacial clay layer in mire ecosystems

5.2 Residence times of water in coastal basins from 10 000 BC to 9 000 AD

Engqvist (2010) has estimated the residence time of water in coastal basins of the Laxemar site area for the time period 3 000 BC through 9 000 AD by the average age (AvA) of water parcels. The first step of the calculations of this residence time was to partition the coast into basins with interconnecting straits (Figure 5-1). Then the author used the CouBa-model to simulate the water exchange due to advection and mixing of water. The forcing of the model consisted of runoff from land, wind-induced stress, thermal surface dynamics (heating/cooling) and density fluctuations at the open boundary towards the coastal zone.

The residence times of individual basins were expressed relative to the age of water expected to be uncontaminated with radionuclides, i.e. water from land runoff and the coastal zone were assigned an age of 0. The residence times thus include recycling of water parcels between basins. However, once a water parcel passes the boundary of the coastal zone its residence time is no longer tracked (and its age becomes 0). The simulations with the CouBa-model could reproduce the anticipated increases in residence time associated with land rise, as well as temporary recessions caused by the transition of various basins becoming connected to, or disconnected from, the coastal zone (Figure 5-2). The water residence time for the coastal basins outside the basins with biosphere objects was estimated to be 4 days. This time was added to the average age of each basin to ensure that the residence time was not underestimated (Engqvist 2010).

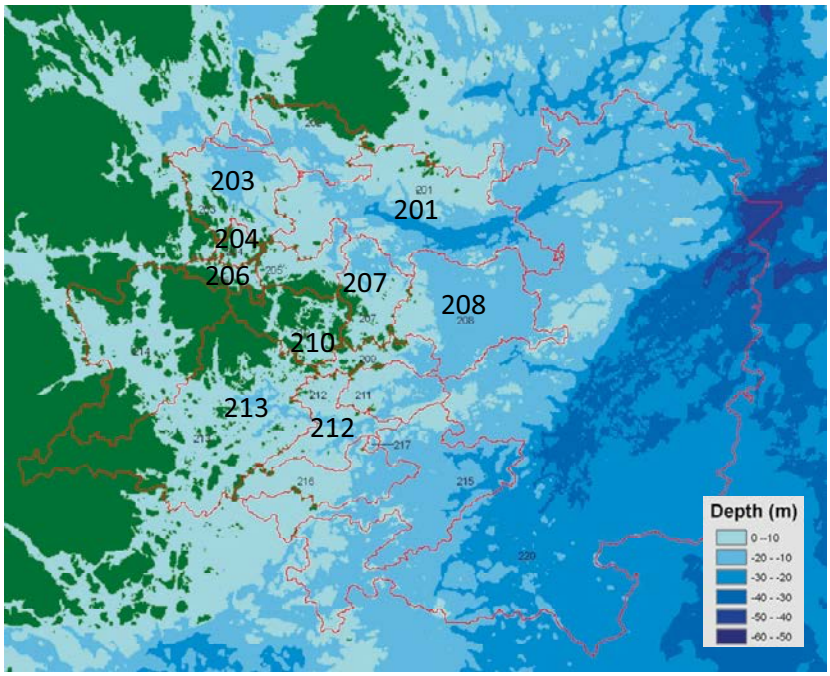

Figure 5-1. *Subdivision of the Laxemar landscape into coastal basins against the background of the former coastal line (6000 BC). Basins included in SE-SFL are indicated by their id-numbers in large font.*

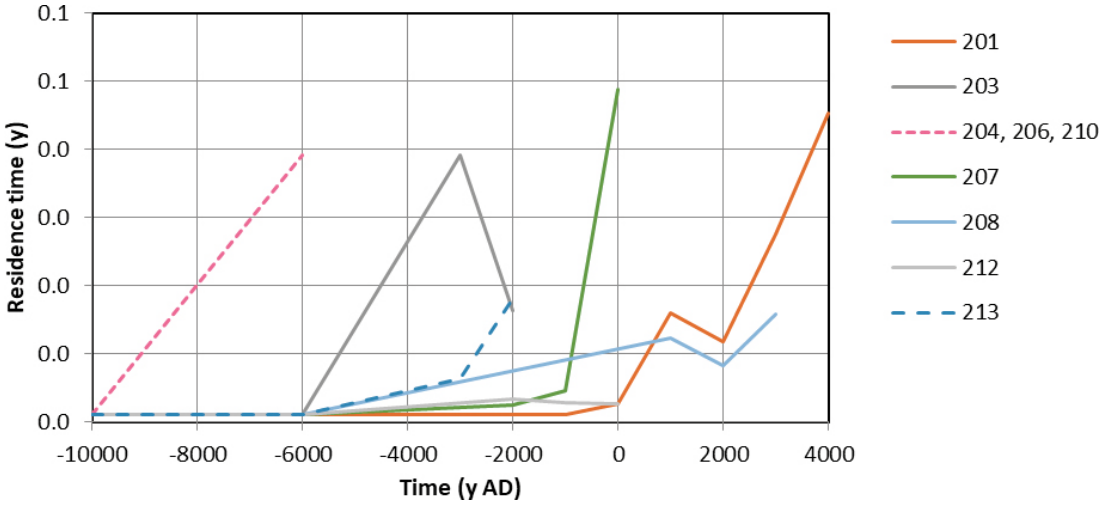

Figure 5-2. *Residence time for coastal basins in Laxemar as a function of calendar year. Data from Engqvist (2010) were cautiously scaled by a factor of 1.5 (see text). For deeply submerged conditions, a coastal zone residence time of 4 days was used for all basins. The lines end at the last 1 000-year step before isolation.*

To quantify how uncertainty with respect to bathymetry affected the average age, the modelled residence times for six basins at the present time (2 000 AD) were compared with those from an earlier study (Engqvist 2006, 2010). The earlier study was partly based on *in situ* soundings, and the two data sets were deemed to be sufficiently independent for an evaluation (Engqvist 2010). The overall correlation between residence times from the two studies was very good ($r^2 = 0.95$), but the residence times calculated in the 2010-study were systematically shorter than those from the earlier study (~2/3). As it could not be determined which of the two studies was more realistic, all values from the 2010 study (which had shorter residence times) were scaled by the factor of 1.5, cautiously making sure that the higher estimates for water age were used in the SE-SFL assessment[4].

[4] A long residence time corresponds to a slow rate of water exchange and a low rate of dilution of radionuclides released to a basin.

No simulations were done for the period before 3 000 BC in Engqvist (2010). For the period after the passage of an inland ice sheet, all basins were expected to be deeply submerged (water depth > 50 m). This period corresponds to the time around 10 000 BC in the historic reconstruction of Laxemar, and thus the residence time of the open coastal zone (i.e. 4 days) was used for this time (Figure 5-2). Considering the limited size of the basins (as compared with the coastal zone), 4 days can be seen as an upper (and cautious) estimate of residence time for deeply submerged basins. Basins at low or intermediate elevations in the landscape (i.e. objects 201, 203, 207, 208, 212 and 213) were assumed to remain mixed with the open coastal zone until 6 000 BC. However, the water exchange of three semi-enclosed basins located in relatively high terrain (204, 206 and 210) was expected to be restricted already at this time. Thus, the residence time for these basins was set to 0.39 years at 6 000 BC, corresponding to the CouBa simulated residence time of the two semi-enclosed basins (202 and 203) at 3 000 BC.

As mentioned above, surface water flows through sea basins (WF_{out}, m^3 $year^{-1}$), used for approximating the dilution of discharging radionuclides (Bq $year^{-1}$), were estimated by dividing the water volume of a basin by corresponding the residence time of the water (Figure 5-3). As the residence time (i.e. average age) includes the time when a water parcel is outside the basin (but inside the coastal zone) it is over-estimating the average time that the water parcels will stay inside a specific basin. Thus, the method used to estimate the exchange of water yields cautious estimates of the dilution of radionuclides within a coastal basin.

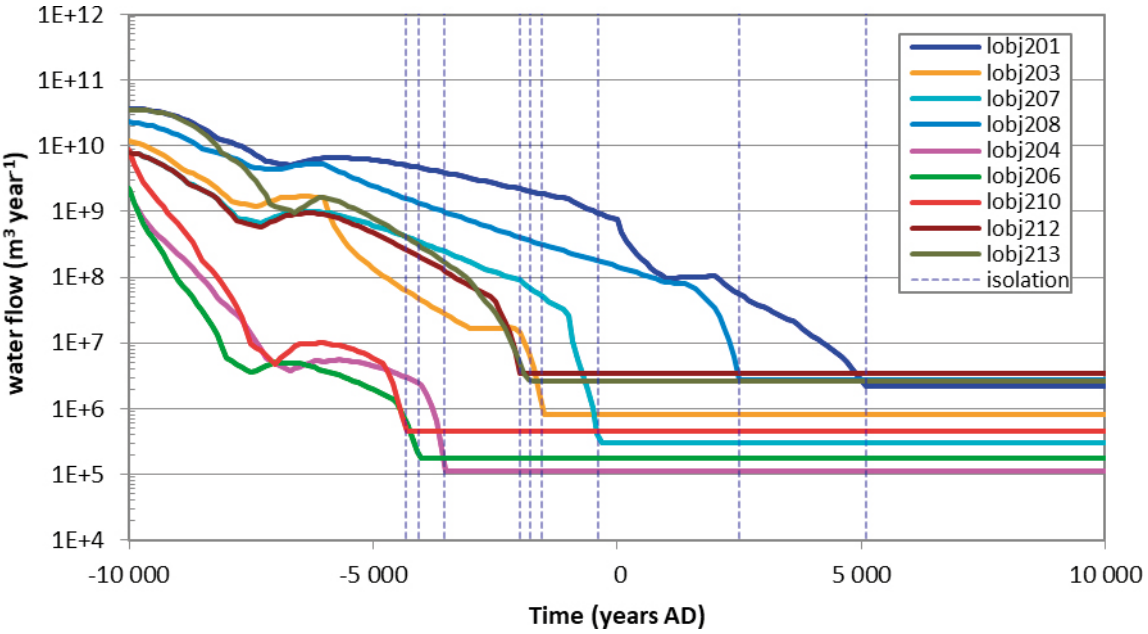

Figure 5-3. *Volumetric flows of surface water through nine biosphere objects in Laxemar (WFout) as a function of calendar year. For sea basins (time before isolation) the water flows were calculated as the water volume of the basin divided by the residence time (or average age) of the water (Figure 5-2). After lake isolation, the water flow (or stream discharge) from the object is assumed to be approximately constant (see Section 5.8 for details).*

5.3 MIKE SHE Water balances

For each biosphere object, water balance components were extracted based on simulations made with the distributed hydrological MIKE SHE model. Two setups of the MIKE SHE model have previously been developed and applied to the Laxemar region with notable differences regarding the extent of the modelling domain and horizontal grid resolution. In the present SE-SFL study, the results from the MIKE SHE SDM-Site model for Laxemar (Bosson et al. 2008), referred to as SDM-Site model below, were used as a first choice. This was motivated as the horizontal grid resolution in SDM-Site model was 20 × 20 m and, thus, four times higher than in the SR-Site MIKE SHE model for Laxemar (Sassner et al. 2011) which was run at a resolution of 40 × 40 m. However, water balance components for biosphere objects 203 and 204 had to be derived from the coarser SR-Site model, as both objects are located outside the SDM-Site model domain. Both MIKE SHE models were run for the period from 2003-10-10 to 2007-12-31 and the water balance results were extracted as annual average values for the last three hydrological years, from 2004-10-01 to 2007-10-01. Water balances for the present conditions of individual biosphere objects were derived from previous MIKE SHE models as a part of the SE-SFL biosphere assessment.

In SR-PSU, an updated methodology for presenting water balance results and extracting parameters for transport calculations of radionuclides in solution was used (Werner et al. 2013, Chapter 7). From the MIKE SHE models, water balances were extracted with the water balance tool. The water-balance included components of horizontal water flows into and out of each object, and across the boundaries of mire and lake/stream parts of the objects. The water balance also described the vertical water flows between surface water and regolith, between the bedrock and the regolith, and between calculation layers within the regolith (see the layers adopted in SE-SFL shown in Figure 5-5.

The methodology builds on a conceptual model of water flows into and within the biosphere object. The biosphere object and the catchment surrounding it can be divided into a number of areas used for different purposes in the safety assessment (Figure 5-4). Each biosphere object belongs to a watershed. The watershed is the upstream area relative to the object outlet including the area of the object itself. If a biosphere object is located close to a water divide or has no other objects upstream, the watershed equals the basin area. A watershed can also contain other biosphere objects and their basins if they are located upstream of the object defining the watershed. The term basin is thus defined in this assessment as the watershed of a biosphere object minus the watershed of any upstream biosphere object(s). The sub-catchment is defined as the catchment of the outlet of a biosphere object minus the catchment of the inlet of the same biosphere object i.e. the area that generates diffuse inflow into the biosphere object. The size of the biosphere object is defined as original lake basin area (see also Section 3.2.1). These different areas generate different water flows separated in the parameterisation of BioTEx (for a comparison of these areas see Table 5-1 in the **Biosphere synthesis**). The open water of the lake is enclosed within the mire (Figure 5-4). That is, there is a border of mire between the lake and the sub-catchment on all sides. Thus, runoff from the basin can reach the mire directly (Q_{LC}) or as water through the stream inlet (Q_{stream}) (Figure 5-4). Runoff from (potentially existing) upstream basins will also reach the object as streamflow ($Q_{upstream}$, not shown in figure). Moreover, all water is assumed to leave the object as concentrated surface water flow (Q_{outlet}) through the lake/ stream outlet of the object.

The MIKE SHE SDM-Site model resolves the regolith domain into two calculation layers. With this resolution, the influence of surface processes on groundwater flows is captured by the uppermost 2 m layer which has been found appropriate for reaching an acceptable agreement between measured and calculated levels of ground and surface water, and of stream discharge (Bosson et al. 2009). However, for transport and dose calculations the model representation of the regolith needs to capture a higher vertical resolution than the calculation layers used to extract the water balances. That is, in BioTEx, radionuclide accumulation in five different regolith layers (with unique biological and/or chemical properties) has the potential to affect human exposures in terrestrial ecosystems.

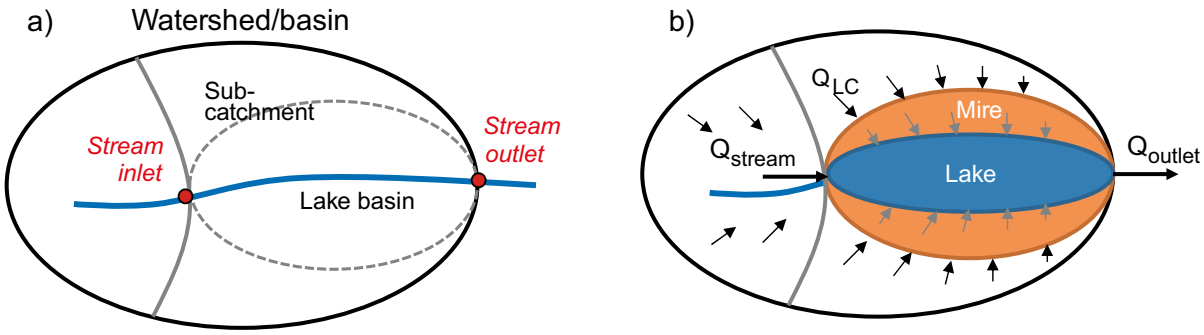

Figure 5-4. *Conceptual model of the (a) geometrical features of the biosphere object and it´s water generating areas, (b) water flows (Q) into and out of a biosphere object containing a lake (blue) and a mire (orange) part. Black ellipse represents the watershed/basin. Grey line divides the basin into the catchment of the inlet (left) and the catchment of the outlet (also known as the sub-catchment, right). Note that the sub-catchment includes the lake basin (which outlines the object in the land stage). Note that the water flow from the local catchment (QLC) does not include water generated from net precipitation within the object/ lake basin (grey arrows). Figure modified from Werner et al. (2013) (this figure is the same as Figure 3-2).*

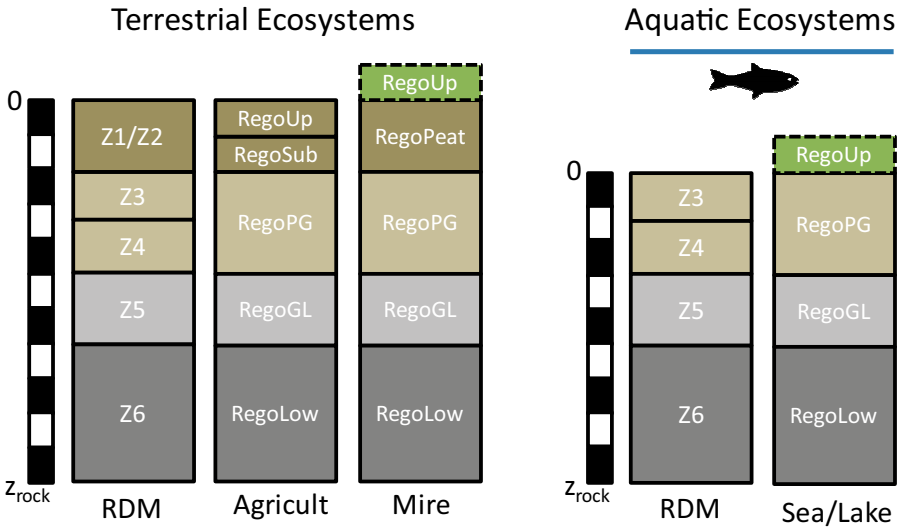

Figure 5-5. *Correspondence between geological layers in the regolith depth model (RDM) for Laxemar (Sohlenius and Hedenström 2008) and regolith compartments in BioTex (Saetre et al. 2013) (this is the same figure as Figure 3-3).*

Thus, to derive water flows at the scale required for transport modelling, water balance components describing flows into or within the regolith column simulated by MIKE SHE had to be rescaled to the vertical resolution of BioTEx. To enable a rescaling of water flows, the average thicknesses of the geological layers were extracted together with the water balance components for each described biosphere object. Most of the regolith layers in the transport model correspond to one (or occasionally two) of the geological Z-layers (Figure 5-5, Figure 5-6). Mapping of the (average) thickness and its vertical position was therefore straight-forward. Two relatively thin, biologically active and unconsolidated regolith layers represented in BioTEx ($RegoUp_{ter}$ and $RegoUp_{aqu}$) are not part of the soil depth model. The thickness of surface peat and aquatic top-sediments were instead fixed to of 0.3m and 0.1 m respectively (Grolander 2013).

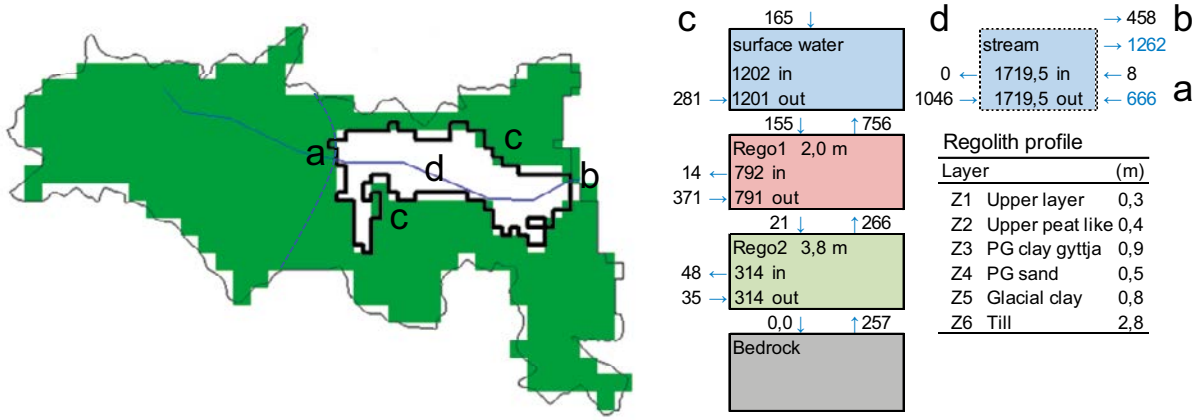

Figure 5-6. *Water balances for present conditions of biosphere object 206 in Laxemar. Map of the biosphere object and its catchment. The thin black line outlines the borders of the basin. The green and the white areas represent the watershed and the object within the basin, respectively. The blue line represents a stream, and the dotted line approximately subdivides the basin into the catchments of the inlet and outlet of the stream, where the latter is the sub-catchment. Right) Stacked boxes represent Mike SHE calculation layers within the object and arrows represent water fluxes across object or regolith layer boundaries. Figures in the boxes show net in- and outflow of water. Blue numbers indicate streamflow (from Mike11). All units are in 10^{-3} m^3 m^{-2} $year^{-1}$ (normalised to the area of the object). Average regolith depth for regolith calculation layers are given in the boxes, and the average depth of geological layers are listed in the table. Letters are used to link components in the left and right panels.*

The water balances for the biosphere object that is used in *the Present day evaluation case* in SE-SFL is presented in Figure 5-6 and upward flows for other objects are shown in Figures 5-13 and 5-14). The biosphere object (206) is located within the headwater catchment of Mederhultsån (Figure 3-5). The stream in this catchment originates upstream of the biosphere object and flows through the object. In the water balance, this is represented by the blue arrows on the righthand side of the stream box. The arrows pointing to the stream box, represent ground- and surface-water flows from the basin to the stream (Q_{stream} in Figure 5-4), whereas the arrows pointing out from the stream represent all water leaving the object (Q_{outlet} in Figure 5-4).The horizontal arrows to the left in the water balance represent surface and groundwater exchange with the local catchment (corresponding to Q_{LC} in Figure 5-4), whereas the horizontal arrows in the middle represent water exchange between the biosphere object and the stream.

The vertical arrows in the water balance represent annual average flows (normalised by the object area) and are, from top to bottom: Net precipitation (top), percolation and discharge to the surface deep percolation and discharge between regolith layers, and groundwater exchange with the bedrock. It can be noted that the percolation within the object (and its local catchment) contributes to the upward flow of water, but that the primarily source for this upward flow is bedrock discharge of groundwater generated outside the boundaries of the object. In the MIKE SHE SDM-model the uppermost calculation layer (Rego1) of the included terrestrial objects typically corresponds to more recently deposited regolith layers (including cultivated organic soils, peat, clay-gyttja and sand), whereas the deeper calculation layer (Rego2) typically corresponds to older deposits (glacial clay and till).

5.4 Stylised water balance models for biosphere objects

Stylised water balance models for the sea and the land stages were developed to estimate water flows under conditions differing from those for which the water balances were originally simulated. This approach is similar to that used in the GEMA model (Kłos 2015). In general, boundary conditions for water laterally entering the biosphere object were taken (or derived) from object-specific water balances, downward groundwater flows (percolation) were calculated using empirical rules, and upward flows (discharge) were calculated from water balance within each model compartment,

cautiously assuming that all water can only leave the biosphere object as surface runoff or streamflow[5]. Below follow brief descriptions of the conceptual water balance models for sea basins (5.4.1), for lake-mire ecosystems (5.4.2) and for drained agricultural land (5.4.3).

5.4.1 Sea stage

During submerged conditions it is assumed that terrestrial recharge has an insignificant effect on groundwater flows in coastal and offshore basins. This means that the groundwater flow is assumed to be driven by local circulation. Moreover, the discharge of groundwater from the bedrock is assumed to be independent of the groundwater flow in the regolith within the object. Thus, by estimating the downward flow from the sea and the percolation through subsequent regolith layers (see Sections 5.6.1 and 5.6.2), the upward groundwater discharge for each regolith layer can be calculated from the water balance (left panel in Figure 5-7).

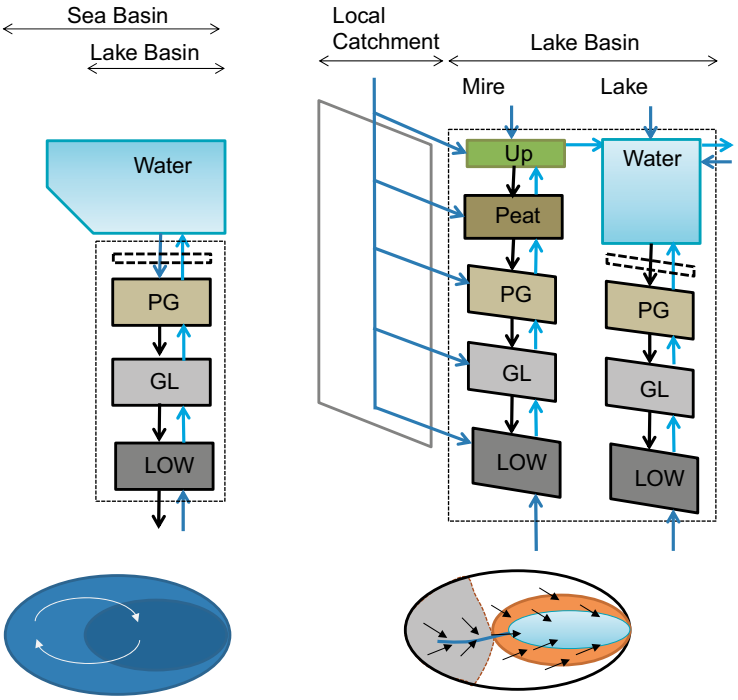

Figure 5-7. *Stylised water balance models for biosphere objects in early successional stages (sea basin and lake-mire complex). Boxes in upper panel represent regolith layers or surface water, and arrows represent flux of water. Dark blue arrows indicate water discharged into the object across its boundary. Black arrows indicate percolating water. Light blue arrows represent upward groundwater return flows within the object. Arrows to the right represent the stream inlet (dark blue) and outlet (light blue). The dashed boxes indicate that flows through the upper part of aquatic sediments (RegoUp) are approximated by the conditions at the water-sediment boundary. Lower panel is a schematic representation of the surface area of the biosphere object and the basin (from above). The dark blue oval represents the part of the basin that will be occupied by the lake-mire ecosystem (i.e. the lake basin). The local catchment (i.e. the area of the sub-catchment less the area of the biosphere object) is indicated in light grey.*

[5] The exclusion of downwards and outgoing horizontal groundwater flows is cautious in a safety assessment perspective, because it implies that groundwater-carried export of radionuclides from biosphere objects is excluded from the analysis (c.f. Section 7.6 in Werner et al. 2013).

5.4.2 Lake – Mire stages

During the terrestrial period, recharge in the local catchment is expected to be a main driver of groundwater fluxes in regolith layers, especially in the upper part of the soil profile. The amount of water that enters the biosphere object as surface runoff or streamflow is expected to be proportional to the area of the watershed, whereas the groundwater inflows from surrounding regolith layers are expected to be proportional to the size of the local catchment. Moreover, the vertical distribution of the groundwater flow originating from the local catchment will depend on properties of the biosphere object (see Section 5.5.2).

A conceptual model of the hydrology of the lake-mire system was developed in SR-PSU (Werner et al. 2013, Chapter 7, and Figure 5-4b above). In this representation of the hydrological system, the open water of the lake is enclosed within the mire. A fraction of the groundwater from the local catchment that enters the mire can thus be expected to reach the lake sediments below the open water. In the MIKE SHE water balances there is frequently a substantial exchange of water in regolith layers at the lake – mire boundary (see for example the water balance for object 116 in Appendix 1 of Werner et al. 2013). However, most of this exchange of groundwater is expected to be limited to a relatively narrow zone, and not to penetrate into the interior of the mire area. Due to a lack of relevant measurement data, the flow-path through the mire part has been simplified, and in the conceptual model all groundwater from the sub-catchment is assumed to reach the lake after flowing through the uppermost regolith layer (Figure 5-7). With this approach, the conceptual model for groundwater fluxes through the mire is the same for an early and a late stage (Figure 5-7 and Figure 5-8).

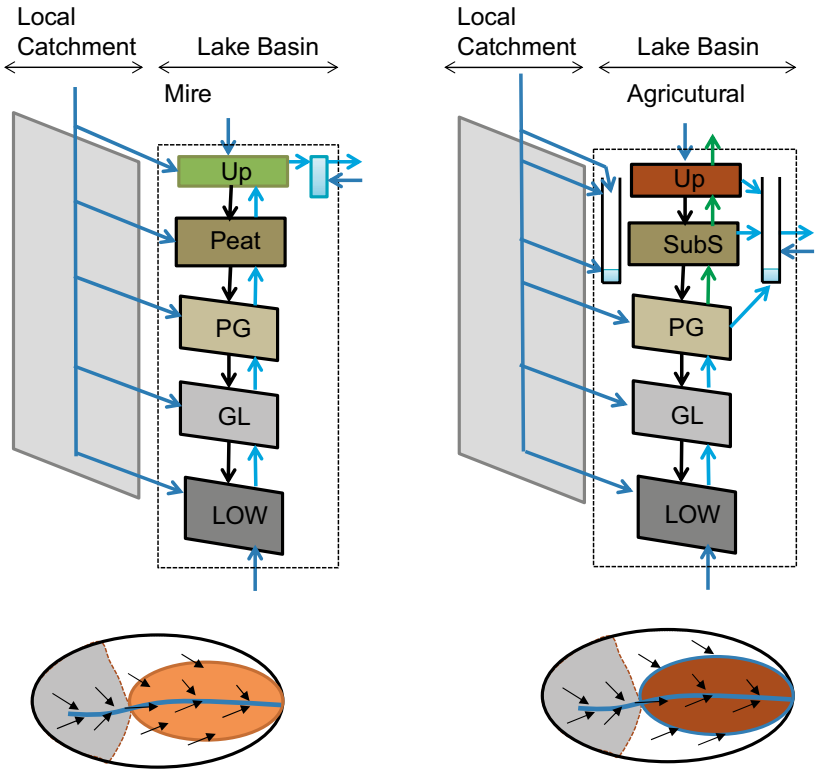

Figure 5-8. *Stylised water balance models for biosphere objects in late successional stages:(mire left and agricultural ecosystem (right)). Symbols and notations of upper and lower panels follows those in Figure 5-7, with the exception of green arrows which here represent plant uptake of water (to cover the plant water deficit) during the vegetation season. Note that when the biosphere object is cultivated (right), all discharge from the upper part of the local catchment (i.e. above the groundwater table), and from the stream inlet, is drained into the ditch surrounding the cultivated area.*

As in the conceptual model for the sea stage, the discharge of groundwater from the bedrock is assumed to be independent of the groundwater flux in the regolith layers of the local catchment. Streamflow from the upstream watershed (excluding the sub-catchment), is assumed to be independent of processes in the local catchment, and streamflow is assumed to have an insignificant effect on groundwater flow paths within the object. Thus by 1) subdividing the runoff from the local catchment into surface water and groundwater flows through separate regolith layers (Section 5.5.2), by 2) estimating the downward groundwater flows in the mire and the lake respectively (Section 0), and by 3) assuming that all water leaves the biosphere object as streamflow, the upward groundwater flow for each regolith layer can be calculated from water balance (Figure 5-7 and Figure 5-8).

5.4.3 Drained and cultivated stage

The conceptual hydrological model of the cultivated land is similar to that of the mire, but it includes the important difference of a system of ditches that lower the groundwater level of the cultivated land. The soil layers above the ditching depth (RegoUp and RegoSub) are consequently unsaturated. The system of ditches is also assumed to isolate the drained and cultivated soil layers from the local catchment above the ditching depth (i.e. above RegoPG), and runoff from the catchment is assumed to be discharged directly to the ditches. Discharge from deeper regolith layers within the biosphere object is likewise assumed to be drained by ditches (Section 6.4 in SKB 2015b). For most of the year, the dominating flow direction of groundwater in the unsaturated soil layers of the cultivated land is downwards. However, for part of the year there is a plant water deficit (i.e. plant needs exceed the soil water supplied by precipitation and soil storage). In the conceptual model, this water deficit is assumed to be covered by an upward flow of groundwater from the saturated to the unsaturated soil layers. The method for translating MIKE SHE water balances into fluxes that corresponds with this conceptual model is further described in Sections 5.5 through 5.7.

5.5 Net precipitation and cross-boundary flows

The difference between precipitation and evapotranspiration is called net precipitation. Net precipitation in the basin surrounding a biosphere object will result in surface runoff (to the stream or to the object), and/or it will percolate and thereafter reach the object (or the stream) as groundwater. The part of the basin where net precipitation primarily results in surface runoff and groundwater discharge directly to the object can be referred to as *the local catchment* and equals the sub-catchment[6], less the area of the object. On the other hand, net precipitation in the watershed upstream the local catchment (either inside or outside the original sea basin) will primarily reach the biosphere object as stream discharge.

For biosphere objects that are presently in the land stage, surface and groundwater flux components could be derived from MIKE SHE water balances. However, for future terrestrial conditions of biosphere objects which are presently below sea level, discharge from the local catchment, from streams and from the bedrock has to be estimated. Similarly, for simulations of times beyond the passage of an inland ice sheet, the groundwater flow for submerged conditions has to be estimated for objects that are presently above the sea level. Thus, a simplified methodology for calculating discharge components and rules for scaling bedrock discharge are developed below.

We start with the water balance of a biosphere object. If changes in long-term storage and percolation to the bedrock are negligible, then the annual average discharge from the object (Q_{outlet}, m^3 $year^{-1}$) will equal the total input. The total annual input of water to a biosphere object can be expressed by four components, namely, net precipitation (Q_{NP}), discharge from the basin (Q_{basin}) where the object is located, stream discharge from basins upstream (if there are any) ($Q_{upstream}$), and discharge from the bedrock ($Q_{bedrock}$):

$$Q_{outlet} = Q_{NP} + Q_{basin} + Q_{upstream} + Q_{bedrock}$$

[6] The definition of the sub-catchments is the catchment for the outlet of a lake/biosphere object minus the catchment for the inlet of the same lake/biosphere object, and the area includes the surface of the lake/biosphere object (e.g. SKB 2010a).

The discharge from the basin can be partitioned into that reaching the object via the stream inlet (Q_{stream}) and discharge from the local catchment directly to the biosphere object (Q_{LC}), with the parameter $f_{disch,stream}$ describing the fraction of the discharge going to the stream. The water flows can be expressed as the product of (area-) specific flows (m year^{-1}) and the area of the object, basin or catchment as follows:

$$Q_{NP} = NetPrec \times area_{object}$$

$$Q_{basin} = Runoff_{basin}\left(area_{basin} - area_{object}\right)$$

$$Q_{stream} = f_{disch,stream} \times Q_{basin}$$

$$Q_{LC} = \left(1 - f_{disch,stream}\right) Q_{basin}$$

$$Q_{upstream} = Runoff_{watershed}(area_{watershed} - area_{basin})$$

$$Q_{bedrock} = q_{Bedrock} \times area_{object}$$

where

NetPrec is the area-specific net precipitation on the biosphere object (m year^{-1}),
$Runoff_{basin}$ is the area-specific discharge from the basin (m year^{-1}),
$Runoff_{Watershed}$ is the area-specific discharge from the upstream watershed (m year^{-1}),
$area_{object}$ is the surface area of the biosphere object (m^2),
$area_{basin}$ is the surface area of the basin, including the biosphere object (m^2),
$area_{watershed}$ is the surface area of the watershed, including the basin (m^2), and
$f_{disch,stream}$ is the fraction of the discharge from the local catchment that reaches the stream within the basin. This scaling factor is unitless.

If the catchments of the stream inlets and outlets are spatially separated, and it is assumed that the specific discharge in the sub-catchment is homogenous, then this scaling factor can be expressed in terms of surface areas:

$$f_{disch,stream} = \frac{Q_{stream}}{Q_{basin}} = \frac{area_{basin} - area_{subcatch}}{area_{basin} - area_{object}}$$

where $area_{subcatch}$ is the area of the catchment of the stream outlet of the object less the area of the catchment of the stream inlet of the object (m^2).

5.5.1 Net precipitation and horizontal surface- and groundwater flows during the land stage

To derive surface and groundwater flows patterns within the assessed biosphere object when this is located above sea level, flow patterns from MIKE SHE SDM-Site water-balances were examined.

The area-specific net precipitation (*NetPrec* m year^{-1}) of the seven terrestrial biosphere objects averaged 0.16 m year^{-1}, and the variation was not systematically related to land use or successional stage (cultivated, lake/mire or mature mire). Given the limited between object variation relative to the mean (CV=0.13), the average value was considered to be representative for all biosphere objects and successional stages.

The discharge generated within the local catchment was derived from the water-balances of the uppermost basins (i.e. headwater catchments) of four watersheds, namely Kärrsviksån (object 204), Mederhultsån (object 206), lake Friskjön (object 207), and Ekerumsån (object 210). For the objects located in these basins the discharge from the local catchment to the object was calculated by summing the horizontal net discharge across the object boundaries. This discharge included the net flow of surface runoff into the object, the net flow of groundwater (into Rego1 and Rego2), and the flow of water from the inlet of the stream (which had formed within the basin). Vertical discharge of groundwater from the bedrock was, however, excluded. The discharge from the basin scaled linearly with the area of the basin less the area of the object, (Figure 5-9), and the average value of

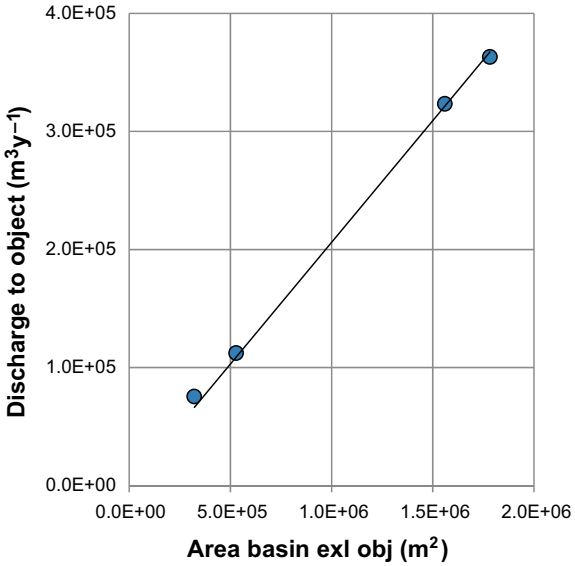

Figure 5-9. *Discharge from the basin as a function of the basin area (less the area of the object). Data obtained from present day MIKE SHE water balances for four terrestrial head water catchments in Laxemar (see text for details). The near perfect match reflects that the spatial variation in runoff is limited and that the net exchanges of water across the outer and lower boundaries are small in the MIKE SHE model.*

the area-specific runoff ($Runoff_{basin}$, m year^{-1}) from the local catchment was 0.21 m year^{-1} (CV = 0.06). Moreover, the area-specific discharge from the basin was somewhat higher than the area-specific net precipitation within the object (see above), which is consistent with the MIKE SHE description of future discharge areas in Forsmark (Tables 7-2 and 7-3 in Werner et al. 2013).

The specific runoff ($Runoff_{watershed}$ m year^{-1}) from the SDM-Site model area (including the surface and groundwater runoff to the sea), has been estimated to be 0.17 m year^{-1} (Bosson et al. 2008). This value is similar to the specific runoff of biosphere objects located near the coast with large watersheds (0.18 m year^{-1} for objects 201, 208 and 213, cf. Figure 3-5), and thus it was considered sound to use the runoff for the whole model area for calculations of discharge from upstream basins of future and present biosphere objects.

5.5.2 Vertical distribution of discharge from the local catchment

The surface flow to the biosphere object ($Q_{disch,surf}$ m^3 year^{-1}) can be described as a fraction of the total discharge from the local catchment :

$$Q_{disch,surf} = Q_{LC} \times f_{disch,surf}$$

Where $f_{disch,surf}$ is a unitless fraction between 0 and 1.

A substantial fraction of the discharge from the local catchment reached the object as surface flow, and the variation between objects was large (range = 0.4–0.9). However, only a minor portion of the variation in the surface discharge could be explained by the object properties (e.g. object area and the thickness of regolith layers), and/or local catchment features (e.g. area or total flow). The fraction of surface runoff is expected to reflect the flow-paths of ground and surface water in the local catchment and these are controlled by a combination of factors (including, topography, regolith stratigraphy and spatial scale). As it was not possible to determine the main driver for the inter-object variation, the fraction calculated from MIKE SHE water balances was used as an object-specific parameter in SE-SFL (Table 5-3). For objects that are presently submerged (201 and 208) the average fraction from the other objects was used for terrestrial conditions (0.75), even though the uncertainty of this value may be substantial.

In SE-SFL calculations the fraction of discharge that reached the object as surface water was treated as being independent of the total discharge from the local catchment. However, if net precipitation changes (e.g. due to climate variation) this is not realistic. For example, if net precipitation were to increase in an object with saturated soil layers, then the fraction of surface water discharge would also be expected to increase. The dependency between surface runoff and total discharge will be explored in future SKB studies.

In all water balances, the horizontal groundwater inflow to the regolith layers decreased with depth. With only two calculation layers (Rego1 and Rego2) in the SDM-Site water-balances it was not possible to determine the shape of this decline in flux. However, in SR-PSU the regolith profile was described by four MIKE SHE calculation layers, and in these water balances the discharge from the local catchment declined exponentially with depth (r^2 varied between 0.86 and 0.99, Figure 5-10). Thus, the horizontal discharge Q (m^3 $year^{-1}$) into a regolith section can be described by the discharge at the top of the regolith stack ($Q_{disch,z0}$, m^3 $year^{-1}$) and the position of the upper and lower boundaries z_1 and z_2 (m) of the section:

$$Q_{disch,rego}(z1,z2) = \int_{z1}^{z2} Q_{disch,z0} \times e^{-\delta_{dis} z} = \frac{Q_{disch,z0}}{\delta_{dis}} \left(e^{-\delta_{dis} z1} - e^{-\delta_{dis} z2}\right)$$

where
d_{dis} is the rate of changed of the discharge with depth [m^{-1}].

The parameter d_{dis} is an object-specific property and was calculated from the water balance for each of the seven terrestrial biosphere objects (Table 5-3). A high rate of decline implies that the horizontal discharge declines strongly with depth. This may, for example, be expected when the horizontal hydraulic conductivity is higher in the upper parts of the regolith horizon than in the lower part. However, the vertical resolution of the SDM-model in Laxemar was limited, and the main drivers for variation in this parameter were not further investigated in this study.

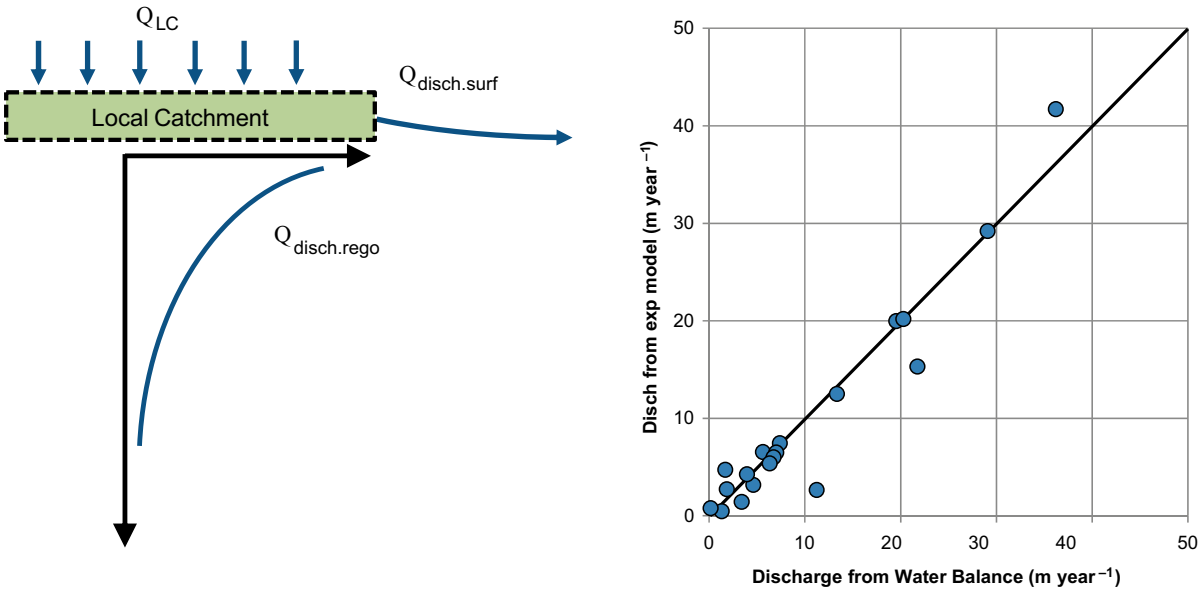

Figure 5-10. *Horizontal inflows from the local catchment to biosphere objects. Left) Conceptual model where net precipitation in the local catchment (Q_{LC}) drives flow paths that results in surface runoff ($Q_{disch,surf}$) and groundwater flows ($Q_{disch,rego}$) which decline exponentially with the regolith depth. Right) Model fit for an exponentially decreasing rate of specific groundwater inflow with regolith depth ($Q_{disch,rego}$) for four regolith layers in five terrestrial ecosystems in Forsmark (former lakes 116, 121_1, 157_1, 159 and 160). The specific groundwater flows modelled by the simplified exponential model are plotted as a function of the values reported in the original water balances for 11 000 AD (mire expansion completed). The line indicates a good agreement between predicted and reported values. The simplified model explains between 86 and 99 percent of the variation of the data of the individual objects.*

From the above equation, it follows that the fraction of groundwater discharge, $f_{disch,i}$ (-) in regolith layer i can be calculated as the ratio between the discharge to the regolith layer and the discharge over the full regolith profile (excluding surface runoff):

$$f_{disch,i} = \frac{\left(e^{-\delta_{dis} z_{top,i}} - e^{-\delta_{dis} z_{bot,i}}\right)}{\left(1 - e^{-\delta_{dis} z_{rock}}\right)}$$

where
$z_{top,i}$ and $z_{bot,i}$ are the positions of the upper and lower boundaries of regolith layer i, and z_{rock} is the position of the lower boundary of the regolith stack [m below the surface].

The discharge from the local catchment (Q_{LC}) can thus be partitioned into surface runoff and groundwater discharge, and the vertical distribution of the horizontal groundwater inflow into one or several regolith horizons can be calculated from the upper and lower depths of the layer:

$$Q_{disch,rego\_i} = Q_{LC} \times \left(1 - f_{disch,surf}\right) \times f_{disch,i}\left(\delta_{dis}, z_{top,i}, z_{bot,i}, z_{rock}\right)$$

Where i is an index for the regolith layer (or layers) of interest, for example i = Peat, PG, GL or Low for mire ecosystems.

5.5.3 Bedrock discharge

The net discharge from the bedrock, $Q_{bedrock}$ (m^3 $year^{-1}$) can be expressed as the product of the area of the object, $area_{object}$ (m^2) and the area-specific discharge from the bedrock, $q_{Bedrock}$ (m $year^{-1}$):

$$Q_{bedrock,i} = q_{bedrock,i} \times area_{object}$$

$$i = \{sea, ter\}$$

Estimates of area-specific bedrock discharge for terrestrial conditions, $q_{bedrock,ter}$ (m $year^{-1}$), were available from the water-balances of seven objects (203, 204, 206, 207, 210, 212 and 213). The remaining two objects (201 and 208) are presently under water, and the discharge rates from the water balances were considered to reflect transitional conditions (between the sea and the land stages).

In SE-SFL, it is assumed that the specific discharge of groundwater from the bedrock to the till (RegoLow) is spatially uniform within a discharge area. This simplifying assumption is reasonable as the modelled specific bedrock discharge to the till layer beneath the mire area in five Forsmark objects hardly differs from the value obtained assuming a uniform distribution (i.e. combining the inflow beneath the mire and the lake in the MIKE SHE water balances) (Figure 5-11).

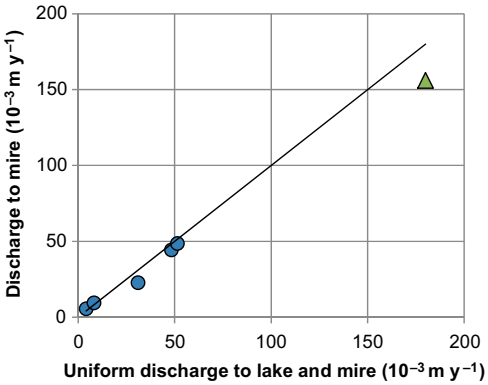

Figure 5-11. *Specific discharge from bedrock under the mire part of the object as a function of the specific discharge averaged over the entire biosphere object during the lake-mire stage. Both flows (y and x axis) were calculated from water balances of five lake-mire biosphere objects in Forsmark (objects 116, 121_1, 157_1, 159 and 160, blue circles) and one object in Laxemar (object 207, green triangle). If the lake area is insignificant, then the (1:1) line indicates that specific discharge is spatially uniform in the object, and that the discharges under the lake and mire parts are similar.*

Figure 5-11. Specific discharge from bedrock under the mire part of the object as a function of the specific discharge averaged over the entire biosphere object during the lake-mire stage. Both flows (y and x axis) were calculated from water balances of five lake-mire biosphere objects in Forsmark (objects 116, 121_1, 157_1, 159 and 160, blue circles) and one object in Laxemar (object 207, green triangle). If the lake area is not insignificant, then the (1:1) line indicates that specific discharge is spatially uniform in the object, and that the discharges under the lake and mire parts are similar.

The change in discharge from bedrock between sea and land conditions was examined by comparing water balances for five lake-mire objects in Forsmark before (3000 AD) and after lake isolation (5000 AD) (Werner et al. 2013). The ratio of bedrock discharge during the terrestrial stage relative to bedrock discharge during the sea stage varied considerably among the studied objects (i.e. between 1.05 and 10, n=5). This variation presumably reflected the degree to which the recharge areas driving the discharge had emerged at 3000 AD. Simulations of bedrock hydrology in Forsmark suggest that the upward flow of deep groundwater at repository depth is substantial also in the 1 000 years prior to 3000 AD (Odén et al. 2014). Thus, due to lack of data covering the full transition period between sea and land, it was assumed that bedrock discharge will be a factor 10 lower during the sea stage as compared with the terrestrial stage ($Scalefact_{q,bedrock,low,sea} = 0.1$ [-]). This value corresponds to the upper limit of the range observed in Forsmark (see above), and it reflects the changed from a submerged state (5.7 m of water) where the catchment is almost completely covered by water (only 2 % of the catchment has emerged) to full land conditions. Thus, the specific discharge from the bedrock to the till during sea stage $q_{bedrock,low,sea}$ (m year^{-1}) can be expresses as:

$$q_{bedrock,low,sea} = Scalefact_{q,bedrock,low,sea} \times q_{bedrock,low,ter}$$

Where

$q_{bedrock,low,twe}$ is the area specific discharge from the bedrock to the till (RegoLow) in the biosphere object (m year^{-1}) and

$Scalefact_{q,bedrock,low,sea}$ is the scale factor describing the ratio between the area-specific flows from the bedrock in the sea and land periods. The scale factor is unitless.

Table 5-3. Parameters used to describe discharge into the biosphere objects in the terrestrial period. Parameter values were derived from MIKE SHE water balances. When parameter values were not available from water balances they were estimated as follows: 1 = Fraction of stream discharge estimated from surface areas in the basin. 2 = average parameter values used for presently submerged objects. 3 = discharge from bedrock has been upscaled from present coastal conditions.

Biosphere object	$f_{disch,stream}$ (-)	$f_{disch,surf}$ (-)	δ_{dis} (m year^{-1})	$q_{bedrock,low,ter}$ (m year^{-1})
203	0.16[1]	0.65	1.2	0.07
204	0	0.86	1.0	0.15
206	0.52	0.45	1.2	0.26
210	0.39	0.80	1.2	0.18
212	0.29	0.84	1.6	0.11
213	0.53	0.93	0.9	0.09
207	0.46	0.69	1.1	0.20
201	0.37[1]	0.75[2]	1.2[2]	0.10[3]
208	0[1]	0.75[2]	1.2[2]	0.05[3]

5.6 Downward groundwater fluxes

The downward groundwater fluxes (percolation) through the regolith column tend to decrease with depth. According to MIKE SHE water balances, a lot of water is exchanged vertically in the upper part of the regolith profile (<0.5m) in lake and mire ecosystems (Werner et al. 2013), but below this zone percolation decreases with a rate that is approximately exponential. Coastal and agricultural

ecosystems lack this hydrologically active zone, and percolation decreases approximately exponentially from the surface. Moreover, the downward flux of groundwater is partially controlled by the thickness of layers with a low hydraulic conductivity. In SE-SFL, these general observations were formalised into a simplified representation of the downward flux of groundwater that is described below.

The functions describing percolation are derived from statistical analysis of available MIKE-SHE water balances. Four water balances from the MIKE SHE SDM-model had a sufficient vertical resolution and could be used to derive parameters describing the percolation rate in agricultural ecosystems in Laxemar. However, the number of water balances established for the other ecosystems was insufficient to assess the fit of the proposed relationships to the available data. Thus, for coastal, lake and mire ecosystems water balances from SR-PSU were utilised to derive plausible descriptions of percolation through the successional stages of natural ecosystems. For this purpose, data from all three time slices available for the lake-mire objects[7] in Forsmark were used (Werner et al. 2013).

The downward flux of percolating water, Q_{percol} (m^3 $year^{-1}$) can be expressed as the product between the area of the object, $area_{object}$ (m^2), and the area-specific rate of percolation, q_{percol} (m $year^{-1}$):

$$Q_{percol} = q_{percol} \times area_{object}$$

5.6.1 The vertical profile of percolation

In the water balances from all ecosystems, the vertical profile of decreasing percolation below some reference level can be described by an exponential function with a reasonable accuracy (see below). Thus, the rate of percolation q (m $year^{-1}$) at depth z (m) below a reference level can be expressed as:

$$q_{percol}(z) = q_0\, e^{-\delta_{percol}\, z}$$

where

z is the depth below the reference level (z_0) [m]

q_0 is the area-specific downward flux of groundwater at the reference level [m $year^{-1}$], and

d_{percol} is the rate of decrease in percolation with depth m^{-1}].

The rate of change is an ecosystem-specific parameter that is likely to vary between biosphere objects. A simple linear expression for the rate of decrease was used to examine whether the between-object variation could be attributed to the thickness of the least hydraulic permeable layer, (i.e. the glacial clay layer):

$$\delta_{percol} = k_{percol} \times z_{regoGL} + m_{percol}$$

where

z_{regoGL} is the average thickness of the glacial clay layer [m],

k is a regression coefficient that determines how d increases with the thickness of glacial clay [m^{-2}], and

m is the rate of decrease that would occur if there was no glacial clay layer [m^{-1}].

The exponential function was least square fitted to the downward water fluxes reported in MIKE SHE water balances, and the fit was assessed on the groundwater flux rates below the reference level.

Percolation rates within agricultural ecosystems were first studied by inspection of four SDM-model water balances describing present conditions in Laxemar. In these water balances, the exponential model could describe the percolation profile from the surface with a good accuracy ($r^2 = 0.95$, Figure 5-12). The rate of decrease varied between 0.55 and 1.0, and the between-object variation could be linearly related to the depth of the glacial clay layer ($k_{percol} = 0.8$ in Table 5-3)

[7] The SR-PSU biosphere objects that developed a lake were 116, 121_1, 157_1, 159 and 160.

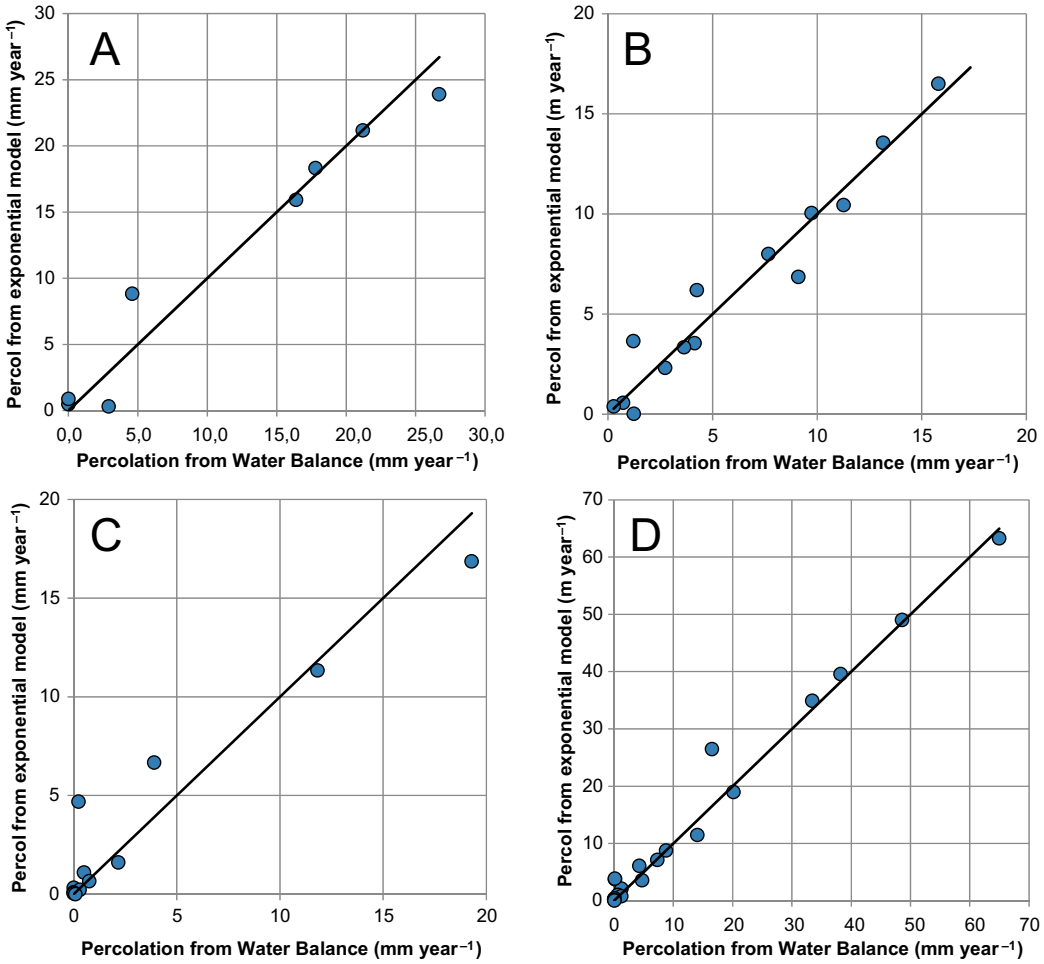

Figure 5-12. *Model fit for an exponentially decreasing rate of percolation below the reference level in four different ecosystems. The modelled percolation rate is plotted as a function of the values reported in the original MIKE SHE water balances. The line indicates a perfect fit between estimates from the stylised model and flows from and the original water-balances. A) Agricultural ecosystems in Laxemar ($n_{obj} = 4$, $n_{layer} = 8$ [4 × 2], $r^2 = 0.95$). B) Coastal ecosystems in Forsmark ($n_{obj} = 5$, $n_{layer} = 15$ [5 × 3], $r^2 = 0.93$). C) Lake ecosystems in Forsmark ($n_{obj} = 3$, $n_{layer} = 12$ [3 × 4], $r^2 = 0.92$). D) Mire ecosystems in Forsmark ($n_{obj} = 5$, $n_{layer} = 20$ [5 × 4], $r^2 = 0.98$).*

Percolation rates of coastal ecosystems were then studied by inspection of five SR-PSU water balances which describe biosphere objects prior to lake isolation in Forsmark (3 000 AD). The exponential model could describe the percolation profile from the sediment surface in these water balances with a good accuracy ($r^2 = 0.93$, Figure 5-12). The rate of decrease varied between 0.35 and 0.67 (m^{-1}), and this between-object variation was not correlated to the thickness of low conductive layers (Table 5-3). When the model was fitted to the SDM water balances for two coastal basins in Laxemar (201 and 208), the resulting rate of decline was considerably higher, namely 0.99 (m^{-1}).

To describe the percolation rate in open lakes, SR-PSU water balances for the time slice 5 000 AD were examined. As the aim was to describe lakes in an early and medium development stage, two objects with an open lake area of less than 10 % of the original lake basin were excluded. The exponential model could describe the percolation profile from 0.5 m below the sediment surface with a good accuracy ($r^2 = 0.92$, Figure 5-12). The rate of decrease varied between 0.26 and 0.57 (m^{-1}), and the between object variation was not correlated with the thickness of the glacial clay (Table 5-4). There is presently only one lake in the Laxemar area (object 207), and the vertical resolution of the SDM-water balance for this object was not sufficient for the corresponding parameter estimation.

To describe the percolation rate in mire ecosystems, SR-PSU water balances for the time slice 11 000 AD were examined. At this time, mire peat covered the entire lake basin in all objects. The exponential model could describe percolation profile from a depth of 0.5 m below the peat surface with a high accuracy ($r^2 = 0.98$, Figure 5-12). The rate of decrease varied between 0.17 and 0.49 (m^{-1}), and the between object variation was not correlated with the thickness of low glacial clay (Table 5-4). There is presently only one mire in the Laxemar area (object 203), and the vertical resolution of the SDM-Site water balance for this object was not sufficient for a corresponding parameter estimation.

5.6.2 Percolation rates at reference levels

Percolation at the reference level q_0 (m $year^{-1}$) tended to scale with the net precipitation in the water balances for terrestrial ecosystems (i.e. agricultural land and mire). Moreover, under saturated conditions, the percolation rate at this level decreased with the thickness of the glacial clay layer.

Thus, for agricultural systems which have unsaturated conditions in the uppermost soil layers, the percolation rate at the reference level (i.e. the surface) was described as a fixed fraction of the net precipitation in the biosphere object (*Netprec*, m $year^{-1}$):

$$q_0 = Netprec \times f_{surfperc,obj}$$

where

$f_{surperc,obj}$ is the fraction of net precipitation that percolates into agricultural soil (-).

However, for sea and mire ecosystems between object variation of percolation at the reference level was better described by an exponential function of the glacial clay thickness:

$$q_{0,i} = q_{0,max,i} e^{-b_{per,i} \times z_{regoGL,i}} \; ; \; i = sea, mire$$

where

$q_{0,max}$ is the maximum percolation rate (m $year^{-1}$),

b_{percol} is the rate of decrease of percolation with thickness of the glacial clay layer [m^{-1}] and

z_{regoGL} (m) is the average thickness of the glacial clay layer in the object

For lake ecosystems the percolation at the reference level (0.5 m below the surface) scaled approximately linearly with the downward flux over the water-sediment boundary ($q_{wat,sed}$, m $year^{-1}$), and the value of the scaling factor decreased with the thickness of the glacial clay layer:

$$q_0 = q_{wat,sed} \times f_{percol,0.5}$$

$$f_{percol,0.5} = f_{percol,0.5,max} \; e^{-b_{percol,lake} \times z_{regoGL,lake}}$$

where

$f_{percol,0.5}$ is the fraction of the flux across the water-sediment boundary that percolates through the regolith column at 0.5 m depth [-].

$f_{percol,0.5,max}$ is the maximum fraction of the flux across the water-sediment boundary that percolates through the regolith column at 0.5 m depth [-], and

$b_{percol,lake}$ is the rate of decrease of the fraction with increasing thickness of the glacial clay [m^{-1}]

The above expressions were used in combination with MIKE SHE water balances to derive parameters describing the percolation rate at the reference level.

For agricultural objects, the SDM-water balances from the cultivated discharge areas were examined. On average 78 % of the net precipitation in these objects percolated into the soil, and as the variation was relatively small (CV = 0.18, n = 4) this number was used as a typical value for all cultivated areas in Laxemar.

For coastal ecosystems an exponential decline of percolation with the thickness of glacial clay could describe the percolation rate at the surface of the sediments of the five Forsmark objects with a reasonable accuracy ($r^2 = 0.75$, Figure 5-13). The maximum rate of percolation was 0.041 m year^{-1}, and the rate of decline was 0.16 (m^{-1}). When the same function was fitted to the SDM water balances for two coastal basins in Laxemar (201 and 208), the maximum rate was almost identical (0.041 m year^{-1}), but the rate of decline was considerably higher, 0.99 (m^{-1}).

For lake ecosystems, the percolation at the reference level (0.5 m below the sediment surface) was described reasonably well by a fraction of the downward flux over the water-sediment boundary, which decreased with the thickness of glacial clay ($r^2 = 0.83$, Figure 5-13). The derived maximum percolation fraction ($f_{percol,0.5,max}$) was 0.033 (-), and the corresponding rate of decline was 0.83 (m^{-1}).

For mire ecosystems the net precipitation generated in the biosphere object (*NetPrec*, m year^{-1}) was used as the upper limit for percolation from the reference depth. The exponential model described the percolation at the reference level (0.5 m below the peat surface) of the water balances with a high accuracy ($r^2 = 0.99$, Figure 5-13), and the rate of decline (with glacial clay thickness) was 0.98 (m^{-1}).

Table 5-4. Parameters used to describe percolation rate at and below the reference level (RL). Parameters were calculated from MIKE-SHE water balances (WB) for biosphere objects in Laxemar (Lx) and Forsmark (Fm). Note that b_{percol}, m_{percol} and k_{percol}, all describe how fast percolation decrease with soil depth. Square brackets indicate variation between objects. a = parameters describing dependencies on the thickness of the glacial clay layer (m^{-1}). b = values in parenthesis from Fm.

			Rate at RL (q_0, m year^{-1})		Rate below RL (δ_{per}, m^{-1})	
Ecosyst.	**Site**	**RL**	**$q_{0,max}$**	**b_{percol}[a]**	**m_{percol}**	**k_{percol}[a]**
Agri	Lx	Water/Rego	0.78 *NetPrecp*	0	0.36	0.80
Coastal[b]	Lx (Fm)	Water/Rego	0.041 (0.041)	0.99 (0.16)	0.99 (0.35-0.67)	0
Lake	Fm	z_{rego}= 0.50 m	0.033 $q_{wat,rego}$	0.80	0.37 [0.26-0.57]	0
Mire	Fm	z_{rego}= 0.50 m	NetPrecp	0.98	0.32 [0.17-0.49]	0

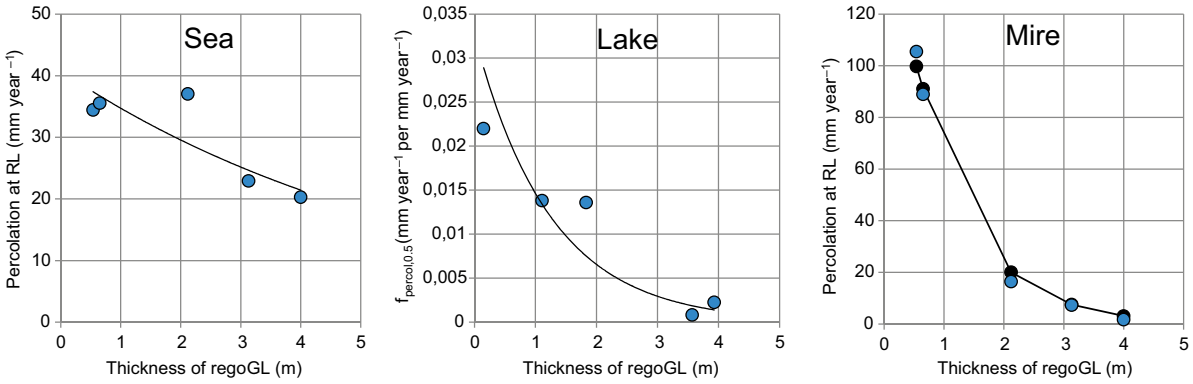

Figure 5-13. *Percolation at the reference depth as a function of glacial clay thickness in three ecosystems. Left) Percolation at the water sediment boundary from the water balance of five coastal basins in Forsmark (blue circles), and the exponential function used to describe the relationship (line, r2 = 0.75). Middle) Percolation at 0.5 m depth from water balances of five Forsmark lakes, expressed relative to the percolation at the water-sediment boundary (blue circles), and exponential function used to describe the relationship (line, r2 = 0.83). Right) Percolation at 0.5 m depth from the water balance of five Forsmark mires (blue circles) and calculated percolation (black circles, r2 = 0.99) as a function of object specific net precipitation and thickness of glacial clay.*

5.6.3 Percolation through the surface of the upper regolith layers in lake and mire ecosystems

In Forsmark, the area-specific rate of percolation across the water sediment boundary ($q_{wat,sed}$, m year^{-1}) of the three relatively open lake ecosystems (i.e. lakes 116, 121_1 and 157_1) varied varied between 0.85 and 2.1 m year^{-1}, and there was a tendency for the rate to increase with the size of the lake. However, the percolation rate in Lake Frisksjön in Laxemar (2.6 m year^{-1}) exceeded the highest rate recorded in Forsmark (in spite of a moderately sized lake area). Moreover, the percolation rate over the water-sediment boundary did not decrease with the thickness of low conductive regolith layers. As it was unclear what the drivers were for the infiltration rate of lake sediments, this rate was simply seen as an object-specific property. Thus, the value from the water balance was used for the rate in Lake Frisksjön, whereas the average rate from the three open Forsmark lakes and Lake Frisksjön (1.7 m year^{-1}, CV=0.48, n=4) was assigned to future and past lakes in SE-SFL.

In the water balances for mire ecosystems, infiltration from the surface appeared to be uncorrelated to the percolation profile in deeper regolith layers. Thus, this rate had to be characterised separately. MIKE SHE water balances from Forsmark suggest that the vertical exchange of water over the boundary between overland water and the regolith column can be substantial in mire ecosystems. On average, the rate of surface percolation is 30 percent larger than the net precipitation but the variation between objects is large (Werner et al. 2013). The data from Laxemar were limited to one object (203), and, for this particular object, the percolation from surface water exceeded the net precipitation by a factor of four.

The infiltration rate from the peat surface ($Q_{Percol,RegoUp,ter}$, m^3 year^{-1}) can thus be seen as the sum of two components, one originating from the net precipitation within the object and one originating from surface runoff from the local catchment. Thus, the total flow can be expressed as a function of the net precipitation, and the surface discharge from the local catchment:

$$Q_{Percol,RegoUp,ter} = f_{surfper,obj} \times NetPerc \times area_{object} + f_{surfper,LC} \times Q_{disch,surf}$$

where

$f_{surfperc,obj}$ is the fraction of the net precipitation that percolates to deeper peat layers (rather than is discharged to the stream), and

$f_{surfperc,LC}$ is the fraction of the surface water reaching the mire that percolates to deep peat within the object (rather than being discharged to the stream).

The parameter values for $f_{surfperc,obj}$ and $f_{surfperc,LC}$ were estimated from the available water balances as follows: For objects where the surface percolation exceeded the net precipitation it was assumed that all net precipitation contributed to the surface percolation (i.e. $f_{surfperc,obj} = 1$). The remaining percolation was attributed to the runoff from the local catchment, and the fraction of the surface runoff from the local catchment, $f_{surfperc,LC}$, was back-calculated from the above expression. For objects where the net precipitation exceeded the surface percolation, the contribution from the local catchment was *assumed* to be negligible ($f_{surfperc,LC} = 0$).

Thus, for the present mire object 203, the value of $f_{surfperc,obj}$ was set to one, and the value for $f_{surfper,LC}$ was calculated to be 0.5. For small mires (corresponding to Lake Frisksjön and the present arable objects in the area), the median value from the mire water balances in Forsmark were used for $f_{surfperc,obj}$ and $f_{surfperc,LC}$, namely 1 and 0.055, respectively. However, for large mires (i.e. 201 and 203) the values from the mire in the large lake basin 116 was used, (i.e. 0.44 and 0 respectivley).

5.7 Discharge in the biosphere object

In SE-SFL the upward groundwater fluxes (discharge) through the regolith column was calculated assuming that change in storage is negligible in each regolith compartment at a scale relevant for assessing the average doses over an adult lifetime (i.e. over 50 year). Thus, for the conceptual models of natural ecosystems presented in Sections 5.4.1 to 5.4.2 the upward flux of groundwater for a regolith compartment (Q_{up}, m^3 year^{-1}) equals the sum of incoming surface and groundwater (Q_{in}, m^3 year^{-1}), less the flux of groundwater which percolates from the layer (Q_{percol}, m^3 year^{-1}):

$$Q_{\uparrow,rego\_i} = \sum Q_{in,rego\_i} - Q_{percol,rego\_i}$$

where

Q_{in} includes percolation from the regolith layer immediately above ($Q_{percol,rego\_i-1}$), horizontal discharge from the local catchment ($Q_{disch,rego\_i}$) and vertical discharge from the regolith layer underneath ($Q_{up,rego\_i+1}$) or from the bedrock ($Q_{bedrock}$).

As in the previous assessment SR-PSU, the uppermost layer of unconsolidated aquatic sediments and peat were regarded as having little or no hydrological resistance. Thus, the upper boundary of the aquatic top sediments (RegoUp$_{aqu}$) was attributed the same fluxes as the upper boundary of the postglacial fine sediments (RegoPG), which both corresponded to the exchange of water across the water-regolith boundary in the MIKE SHE water balances. Moreover, the hydrological exchange with the surface (or overland) water (described in the MIKE SHE water balances) was attributed to the surface peat layer (RegoUp$_{ter}$). Consequently, the net precipitation (Q_{NP}) and the horizontal flux of surface water from the local catchment ($Q_{disch,surf}$) is directed to this compartment, and the flux of water to the lake ($Q_{regoUp,water}$) was calculated from the balance of incoming and outgoing water (Table 5-5).

The above equation was also applied to the deeper regolith profile of agricultural soil (i.e. RegoGL and RegoPG). However, the upward flux into the unsaturated layers of the agricultural ecosystems was assumed to be primarily driven by plant water uptake. This uptake corresponds to the plant water deficit during the vegetation season, and the water (if supplied) is lost from the upper regolith (by transpiration). Thus, the upward flux through RegoSub (i.e. Q$_{,PG}$ and Q$_{,Sub}$) is simply described using the expected water deficit during the vegetation season:

$$Q_{\uparrow,PG} = Q_{\uparrow,Sub} = Q_{\uparrow,Up} = Q_{plantuptake} = q_{up,satSoil,agri} \times area_{object}$$

where

$q_{up,satSoil,agri}$ is the area specific upward flux driven by the plant water deficit, which typically takes a value between 0.02 and 0.07 m year^{-1} for temperate conditions (Grolander 2013).

All discharge from the local catchment above the drainage depth (i.e. $Q_{disch,surf}$ and $Q_{disch,rego}$) was directed to the stream/ditch. Mass-balance of water was then used to calculate the surplus of water entering each of the three uppermost regolith layers (i.e. RegoUp$_{agri}$, RegoSub and RegoPG) and this water was also directed (i.e. drained) to the stream/ditch system.

Thus, for each ecosystem the upward flow from the deepest compartment (RegoLow) can be solved first for any given point in time. This yields the discharge from below to the next compartment (RegoGL). Thus, working in sequence from below to the top, all discharge terms within the object can be calcualted (Table 5-5).

Table 5-5. Overview of water flows in aquatic and terrestrial ecosystem models. The elements in the table correspond to the arrows in Figure 5-7 and Figure 5-8. For each compartment (row) one flow was calculated from flow balance (FB_i), and consequently the sum of incoming water balances the sum of the outgoing water. Note that with this representation all vertical flows between regolith compartments are represented twice (on consecutive rows). * = the vertical flows through the unconsolidated layer of aquatic sediments were assumed to be the same as those of the layer below (RegoPG).

		Water flux into compartment			Water flux out of compartment		
Ecosystem	**i**	→	↓	↑	→	↓	↑
Sea/Coast/Lake							
RegoUp*	0		$Q_{percol,wat}$	$\mathbf{FB}_{i+1}$		$Q_{percol,wat}$	$\mathbf{FB}_{i+1}$
RegoPG	1		$Q_{percol,wat}$	$\mathbf{FB}_{i+1}$		$Q_{percol,PG}$	$\mathbf{FB}_{i}$
RegoGL	2		$Q_{percol,PG}$	$\mathbf{FB}_{i+1}$		$Q_{percol,GL}$	$\mathbf{FB}_{i}$
RegoLow	3		$Q_{percol,GL}$	$Q_{bedrock}$		$Q_{percol,Low}$	$\mathbf{FB}_{i}$
Mire							
Stream	0	$Q_{stream} + Q_{upstr} + FB_{i+1}$			$\mathbf{FB}_{i}$		
RegoUp	1	$Q_{disch,surf}$	Q_{NP}	$\mathbf{FB}_{i+1}$	$\mathbf{FB}_{i}$	$Q_{percol,up}$	
RegoPeat	2	$Q_{disch,peat}$	$Q_{percol,up}$	$\mathbf{FB}_{i+1}$		$Q_{percol,peat}$	$\mathbf{FB}_{i}$
RegoPG	3	$Q_{disch,PG}$	$Q_{percol,peat}$	$\mathbf{FB}_{i+1}$		$Q_{percol,PG}$	$\mathbf{FB}_{i}$
RegoGL	4	$Q_{disch,GL}$	$Q_{percol,PG}$	$\mathbf{FB}_{i+1}$		$Q_{percol,GL}$	$\mathbf{FB}_{i}$
RegoLow	5	$Q_{disch,Low}$	$Q_{percol,GL}$	$Q_{bedrock}$		$Q_{percol,Low}$	$\mathbf{FB}_{i}$
Agricultural							
Stream/ditch	0	$Q_{stream} + Q_{upstr} + Q_{dis,surf} + Q_{dis,up} + Q_{dis,subs} + FB_{i+1} + FB_{i+2} + FB_{i+3}$			$\mathbf{FB}_{i}$		
RegoUp	1		Q_{NP}	Q_{uptake}	$\mathbf{FB}_{i}$	$Q_{percol,up}$	Q_{uptake}
RegoSub	2		$Q_{percol,up}$	Q_{uptake}	$\mathbf{FB}_{i}$	$Q_{percol,subs}$	Q_{uptake}
RegoPG	3	$Q_{disch,PG}$	$Q_{percol,subs}$	FB_{i+1}	$\mathbf{FB}_{i}$	$Q_{percol,PG}$	Q_{uptake}
RegoGL	4	$Q_{disch,GL}$	$Q_{percol,PG}$	FB_{i+1}		$Q_{percol,GL}$	$\mathbf{FB}_{i}$
RegoLow	5	$Q_{disch,Low}$	$Q_{percol,GL}$	$Q_{bedrock}$		$Q_{percol,Low}$	$\mathbf{FB}_{i}$

The parameters used to calculate discharge into a biosphere object, and percolation through the regolith layers within the object (Table 5-3 and Table 5-4), were derived from object-specific water balances. Thus, the system described above can be considered calibrated for the objects and the time slice that were described by MIKE SHE water balances. In Figure 5-14 the performance of the calibrated system is illustrated by comparing the calculated upward flows with those in the original water balance for one object. The object is a small mire in Forsmark (157_1, at 11 000 AD), with a water balance that has a relatively high resolution (i.e. four layers). The calculated upward flows captured the vertical profile of the original water balance and flows across the regolith layer boundaries were in close agreement with linear interpolations from the original water balance (the method used in SR-PSU). Finally, as mass balance was imposed in the calculations, the flow out from the object (to the stream) was also in good agreement with that of the original MIKE SHE water balance.

Similar comparisons were done for biosphere objects in Laxemar (Figure 5-15). The water balances derived from the SDM-model have a limited vertical resolution (two layers), and thus it is hard to evaluate flux rates at boundaries within the uppermost MIKE SHE calculation layer. Nevertheless, in most cases the calculated flows appear to capture the information in the water balances to a sufficient degree. However, in one case the calculated flows deviated notably from the flow in the water balance; the upward flow from sediments to open water in Lake Frisksjön was 25 % larger in the water balance than calculated (marked a in central panel of Figure 5-15). However, this deviation may well reflect limitations in the SDM-model underlying the water balance. The upward flow calculated in this study primarily reflects the percolation from the open water (2.7 m year^{-1}). When the vertical resolution of the MIKE SHE model was increased, then the upward and downward flows across the sediment-water boundary of Lake Frisksjön also approached a balance (Johansson and Sassner 2019, Figure 3-10).

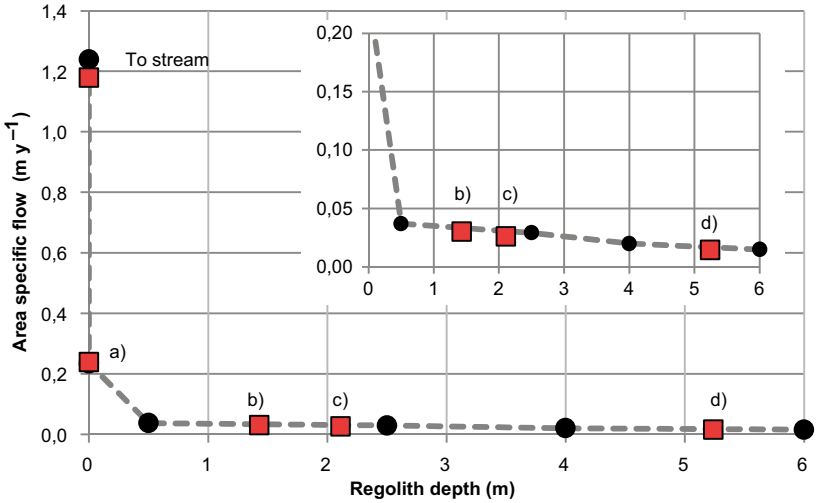

Figure 5-14. *Discharge within and out of a mire biosphere object. Calculated upward specific groundwater flows across regolith boundaries, and out from the object via stream discharge (red squares), are superimposed on the flows from the MIKE SHE water balance for object 157_1 at 11 000 AD (black circles connected by grey dashed line). Letters indicate boundaries between regolith layers; a) RegoUp (or overland water) and RegoPeat, b) RegoPeat and RegoPG, c) RegoPG and RegoGL, and, d) RegoGL and RegoLow.*

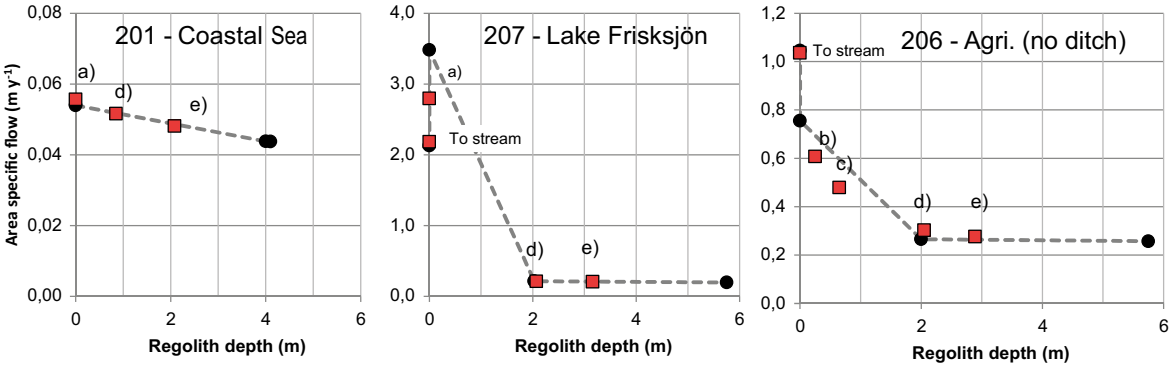

Figure 5-15. *Discharge within and out of Laxemar biosphere objects. Calculated upward groundwater flow across regolith boundaries and out from the object via stream discharge (red squares) were superimposed on the water flows from the MIKE SHE water balance for objects 201, 207 and 206 (black circles connected by grey dashed line). Letter indicates vertical boundaries between; a) Water and aquatic sediments, b) RegoUp and RegoSub (cultivated land), c) RegoSub and RegoPG (cultivated land) d) RegoPG and RegoGL, and, e) RegoGL and RegoLow. Note that water flows to ditches are not explicitly represented in the water balance of object 206 (Figure 5-6) and thus the flows in the unsaturated layers (b and c) have been adjusted to reflect conditions without drainage.*

5.8 Biosphere model parameters for present climatic conditions

To derive parameter values for BioTEx, all components of the water balance were solved for each object and developmental stage included in the safety evaluation. For all objects, present conditions were used to represent the present-day stage of coastal (201, 208), lake (207), mire (203) and agricultural (204, 206, 210, 211 and 212) ecosystems. For other successional stages, object-specific properties (such as the areal extension of the lake and the mire, and the thickness of postglacial fine sediments) were derived for a representative point in time with the RLDM (Chapter 3.4.2) as follows.

To represent offshore *sea conditions* (object 201), the regolith profile from an early time point in the reconstruction of the site (9 400 BC, with water depth of about 50 m) was used to calculate the hydrological parameters. To represent semi-enclosed conditions (object 208), the regolith profile from the last time point before lake isolation was used (2 200 AD, water depth 3.0 m). According to the RLDM description of the site, water depth in basin 206 will be approximately 6 m at 8 400 BC, and the regolith profile from this point in time was selected as representative for the start of coastal conditions (see below).

For historic (206) and future (201 and 208) *lakes*, the time for isolation was used to characterise areal extension of, and regolith thickness under, open lake conditions[8]. The time for isolation was selected since maximum exposure from lakes typically involves C-14, and the dose (per unit release) from this radionuclide in the BioTEx tends to peak at isolation when loss by degassing from the mire is limited.

For historic (206) and future (201, 207 and 208) *mires*, properties (i.e. areal extension and regolith depths) from the time of mire completion were used for calculations of hydrological parameters[9]. At this time point, the area expansion and peat growth are completed. This time point was selected since long-term accumulation of radionuclides is of principal interest in SE-SFL, and the properties of the mature stage prevails for most of the assessment period.

Following the SR-PSU methodology, the effect of shoreline displacement on groundwater fluxes was captured by recognising a sequence of ecosystem stages and using linear interpolation between these stages to represent the flux in the transition period (Saetre et al. 2013). Thus, groundwater hydrology (on the scale of a year) was assumed to be approximately constant during the sea stage. Coastal conditions were seen as a transient stage, and stable conditions were assumed to be re-established when the biosphere object was isolated from the sea, which marks the start of the land period. Simulations of bedrock hydrology in Forsmark suggest that the upward flux of deep groundwater from repository depth increase approximately linearly from present sea-covered conditions until times when the landscape has emerged out of the sea (Odén et al. 2014). For the surface area where the discharge was expected, this period corresponds to the development from a sea basin, with an average depth of 6 m water, to a mire which has emerged fully out of the sea (Object 157_2 in SR-PSU).

In accordance with the patterns in Forsmark, it was assumed that the coastal influence starts when the average water depth reaches 6 m also in Laxemar. This means that the two present coastal bays (201 and 208) were considered to be in a coastal transitional stage. For the historic development of object 206, an average water depth of 6 m coincides with the start of the emergence of the object's local catchment (about 15 % of the final area). Since the runoff from the local catchment is a main driver of the upward groundwater flow, it is judged that this threshold is reasonable to use as the start for upscaling the groundwater flux through the regolith column (Figure 5-16).

[8] The time for isolation predicted by the shoreline displacement curve for the three biosphere objects 206, 201 and 208 are: 4 100 BC, 5 100 AD and 2 500 AD.

[9] The time for completion of mire expansion predicted by the RLDM for the four biosphere objects 206, 207, 201 and 208 are: 900 AD, 9 800 AD, 21 000 AD and 13 200 AD.

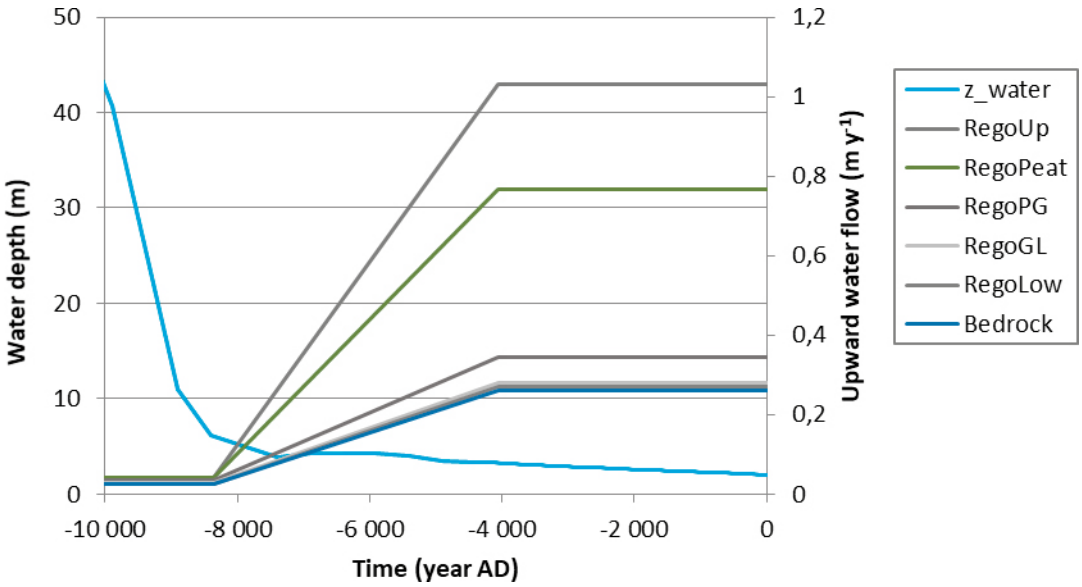

Figure 5-16. *Handling of groundwater flow parameters in response to landscape development. In SE-SFL two stages of the biosphere object were acknowledged (the sea and the land stage), and in between these a coastal transition period is postulated. Downward and upward groundwater fluxes were calculated separately for each stage using the conceptual water balance model (and underlying parameters) described in this report and flows in the transition period were calculated by linear interpolation. The graph shows how the upward flow from the bedrock through the regolith column varies as a function of time in object 206. In the graph, the end of the sea stage occurs when the average water depth is 6 m (~ 8400 BC) and the start of the land stage occurs when the lake threshold is at the sea level (ca 4100 BC). Note that the change in upward flow increases towards the surface of the regolith stack, reflecting an increasing influence of water from the local catchment.*

5.9 Biosphere model parameters for other climatic conditions

In SE-SFL the present climate is assumed in the base evaluation case. However, the effects of a considerably warmer climate and effects of variations in the regional climate were evaluated in the *increased greenhouse effect* (Section 7.4 in the **Biosphere synthesis**) and *the alternative regional climate* (Section 7.5 in the **Biosphere synthesis**) evaluation cases. Moreover, the effects of a considerably colder climate (including permafrost conditions) were examined in the *simplified glacial cycle evaluation case*. The method used to extract hydrological parameters for these conditions are described in this section.

5.9.1 Impact of moderate changes in temperature and precipitation on runoff and deep groundwater recharge in Southeast Sweden.

The impact of moderate climate variation on surface hydrology in Southeast Sweden has previously been studied by the Swedish Meteorological and Hydrological Institute, SMHI. Losjö and co-workers simulated groundwater recharge in two catchments with the HBV-model, using the recorded climate (1961–1996) for the area and five climate scenarios (Losjö et al. 1999) [10]. The simulations showed that moderate climate variation may have an important impact on the seasonal pattern of both runoff and groundwater recharge. For example, an increased temperature may decrease snow accumulation and increase evapotranspiration, which will reduce snow melt peak runoff. A decreased temperature may, on the other hand, decrease runoff and recharge during winter, but increase these fluxes during spring and summer.

[10] The climate scenarios used were; 1) +2 °C (no change in precipitation), 2) +2 °C and −20 % precipitation, 3) −1 °C (no change in precipitation), −1°C and +20 % precipitation, and 4) +3.5 °C and +15 % precipitation (representing global warming). In these first four scenarios, the same adjustment was made to all daily data, whereas in scenario 5 adjustments varied over the year.

To approximate how the combined effects of moderate changes in temperature and precipitation may affect annual hydrological fluxes, the results from the HBV simulations were re-analysed. For this analysis, the small catchment in the Äspö area (near the Laxemar site) was selected to study the impact on runoff, whereas the large catchment of Emån (in the Laxemar region) was was selected to characterise the response in deep groundwater recharge (and discharge). The latter choice was based on the assumption that recharge in a large area drives the upward flux of deep groundwater in local discharge areas. In the analysis, the change in annual flows (relative the recorded climate) were modelled as linear functions of changes in temperature and precipitation.

The analysis showed that a linear approximation could explain most of the response in both runoff and deep groundwater recharge (Figure 5-17, left panel). As expected, runoff increased with precipitation and decreased with temperature. That is, for each percent increase in precipitation the runoff increased by 2.8 % (Standard error, SE = 0.38), whereas runoff decreased by 21 % (SE = 2.6) for each degree increase in annual temperature. The response in deep groundwater recharge was similar to that of the runoff, but the magnitude of the response was smaller. That is, deep groundwater fluxes increased by 0.9 % (SE = 0.21) per percent increase in precipitation and decreased by 7.2 % (SE = 1.4) per degree increase in temperature.

The range of temperature [−1 to +2 °C] and precipitation [−20 % to +20 %] variation used in the SMHI study gave a reasonable cover of the temperate climate conditions examined in SE-SFL. Thus, the relative change in runoff and in deep groundwater recharge were calculated for three alternative regional climates (North, Central and Southwest), and for a warmer climate in Laxemar (ICP 4.5) (right panel in Figure 5-15).

As expected, a colder [−1.4 to −3.8 °C] and wetter climate [10 to 18 %] increased the runoff (North and Central), whereas the outcome in a warmer and wetter climate depended on the balance between the effects of the two climate components. That is, a small increase in temperature and a moderate increase in precipitation (0.9 °C, +33 %) increased runoff (Southwest), whereas a moderate increase in temperature and a relatively small increase in precipitation (2.6 °C, +12 %) resulted in a reduced runoff. The response in deep groundwater recharge was similar in direction, but the magnitude was typically only 30–40 % of the runoff response. It can be noted that the temperature and precipitation changes expected under the alternative temperate climate conditions examined in SE-SFL occasionally were outside the range explored in the SMHI study. Thus, the calculated responses in runoff and deep groundwater recharge are to be interpreted as indications of the hydrological response to an altered climate, rather than robust and precise predictions.

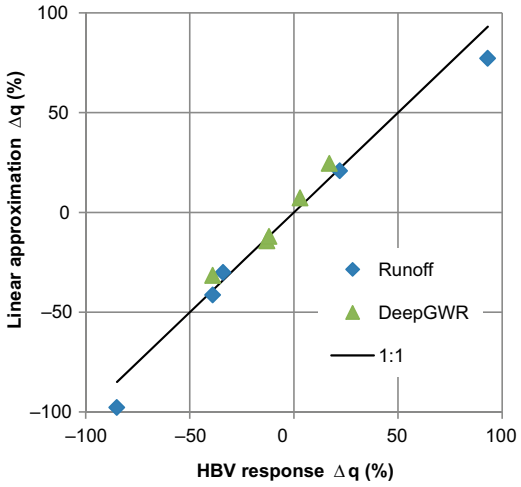

Climate	Δ Temp (°C)	Δ Precip (%)	Response: Δ Runoff (%)	Response: Δ DGWR (%)
North	-3.8	18.3	130.2	43.0
Central	-1.4	9.6	56.0	18.3
Southwest	0.9	33.5	75.7	22.5
Increased GH effect (ICP 4.5)	2.6	12.0	-20.0	-8.3

Figure 5-17. *Impact of moderate climatic variation on groundwater recharge in the Laxemar area. Left) Linear approximations of the response corresponded well to the response predicted by the HBV model for five climate scenarios (r2= 0.98 and 0.93 for runoff and deep groundwater recharge, respectively). Right) Predicted response in runoff and deep groundwater recharge (DGWR) given four different variants of temperate climate conditions, corresponding to the alternative regional climate and the increased greenhouse effect evaluation cases.*

5.9.2 Parameter values for object 206 for other temperate climate conditions

For each of the climate conditions in the biosphere evaluation cases *alternative regional climate* (North, Central and Southwest) and *increased greenhouse effect* (RCP4.5), parameters representing the surface hydrology of object 206 were calculated with the method described in Sections 5.5 to 5.7 (Figure 5-16).

For the calculations, the input parameters representing runoff in object 206 (*Netprec* and $runoff_{basin}$, m year^{-1}) were up- or down-scaled according to the expected temperature and precipitation response (Drunoff, Figure 5-15). Similarly, the area-specific discharge from the bedrock ($q_{bedrock}$, m year^{-1}) was scaled according to the response in deep groundwater recharge (DDGWR, Figure 5-15). Moreover, for agricultural soils the plant water deficit was adjusted according to the climate expected in the vegetation season (Chapter 7), and the deficit was covered by groundwater uptake ($q_{up,satSoil,agri}$, m year^{-1}) or irrigation water (added to the net precipitation). For the present conditions in Laxemar, the plant water deficit was estimated to be 0.069 m year^{-1}, whereas the deficit is expected to be higher for increased greenhouse conditions (0.090 m year^{-1}) and similar or lower for the other regional climate variants (0.070, 0.066, 0.046 m year^{-1} for the South-West, Central and North coastal locations, respectively)

The results of these calculations are presented in Figure 5-18. As the discharge from the bedrock dominated the upward groundwater flow at depth in object 206, the response in the discharge from the till (RegoLow) was similar to that of the upward flux from the bedrock (DDGWR, Figure 5-15). On the other hand, discharge from the catchment dominated the surface discharge from the object, and consequently the response in stream discharge was similar to that in runoff (Drunoff, Figure 5-15). The response in the regolith profile above the till was a mixture of the response in deep groundwater and the surface discharge (with an increased influence of the runoff towards the surface).

In the model of cultivated soil (right panel in Figure 5-18) there is a ditch that drains most of the discharge water from the saturated zone (RegoPG) and disconnects the unsaturated soil layers (RegoSub and RegoUp) from the local catchment. Thus, the response in upward movement of groundwater in the lowest unsaturated layer (RegoSub) reflected the alternative parameter values for water uptake only. The response in discharge from the upper unsaturated layer (RegoUp) to the stream/ditch (and the discharge from the steam) was, on the other hand, primarily reflecting the change in net precipitation/runoff (and the response was consequently similar to that in the mire). The response in the saturated regolith profile (RegoLow to RegoPG) was also similar to that of the mire, although the influence from runoff increased more towards the surface (e.g. RegoPG) as the regolith stack was notably thinner after drainage and cultivation (5.7 vs 7.5 m).

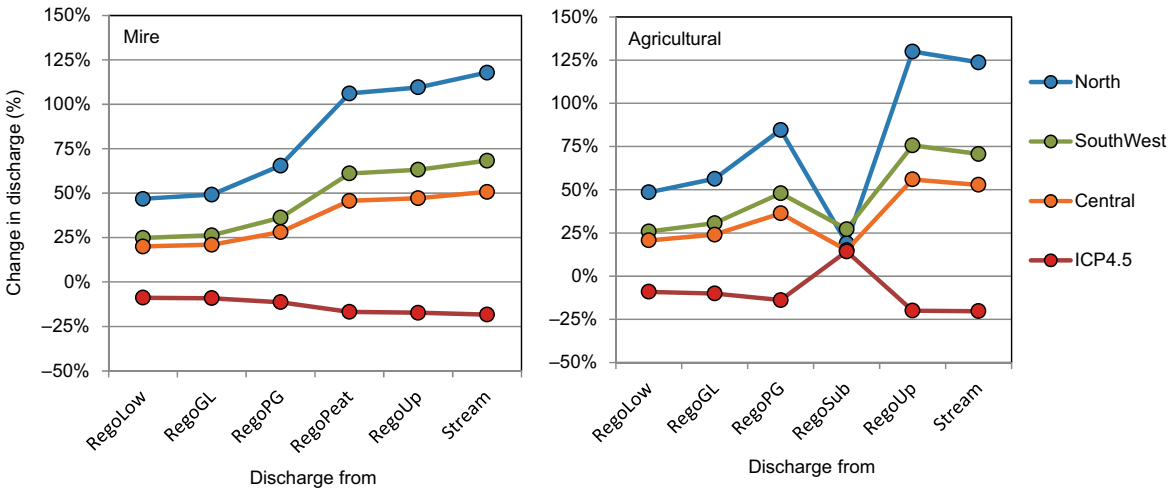

Figure 5-18. *Groundwater flow response as a function of variation in temperate climate variants. The plot displays the change in upward groundwater flux from regolith layers (RegoLow, RegoGL, RegoPG and RegoPeat), in discharge from the upper regolith layer (RegoUp) to the stream, and in the stream flow (out from the object), relative to flows given present conditions. Left) Response in mire of object 206. Right) Response in cultivated soil of object 206.*

5.9.3 Hydrology in periglacial conditions

The hydrology of periglacial environments is influenced by ice, snow and frozen ground. Permafrost controls the distribution and routing of water across the landscape and the hydrologically active period, with flows in streams and the active layer, is relatively short. The main hydrological event of the year is the snow melt period. On a landscape scale, permafrost may also reduce groundwater recharge and discharge relative to unfrozen conditions, and the exchange of deep and shallow groundwater is restricted to occurs via through-taliks. Such through-taliks may form under lakes, streams and small surface waters (e.g. ponds and peat bogs), and the extent and types of taliks that prevail in a permafrost landscape depends on the permafrost depth. Topographical differences between taliks govern the pattern of groundwater recharge and discharge, and the main groundwater discharge occurs at the most downstream through-talik (i.e. to the sea for a coastal site) (Werner et al. 2013 and references therein).

Bosson et al. (2010, 2012, 2013) studied the surface hydrology of periglacial conditions in Forsmark through simulation studies with MIKE SHE, and the results from these studies were considered relevant also for permafrost conditions at other coastal sites in Sweden. The work by Bosson and her co-workers showed that although periglacial conditions can be considered to represent a dryer climate (i.e. less precipitation and less evapotranspiration), the periglacial landscape is characterised by more ground- and surface-storage of water and an increased runoff as compared with temperate conditions (24 %).

In SR-PSU, water balances for periglacial conditions in Forsmark (100 m deep permafrost) were obtained from the MIKE SHE models developed by Bosson et al. (2010). Separate water balances were extracted for a mire located at the surface close to the location of the repository and for a lake located near the coast. As with the response on the landscape level (above), the net precipitation in both the mire and the lake increased by almost 20 % in the periglacial simulations. Moreover, there was no horizontal exchange of groundwater between the object and the local catchment below a depth of one metre.

5.9.4 Parameter values for permafrost conditions

As in the previous safety analyses SR-Site and SR-PSU, it was assumed that some lakes in the future Laxemar landscape will be connected with the unfrozen bedrock also under periglacial conditions. As no particle tracking simulations with permafrost conditions have been performed in Laxemar, Lake Frisksjön (207) was selected to represent a future talik. Given the size and depth of this lake (at isolation) it is plausible that a through-talik may form under the present waterbody in permafrost conditions (Bosson et al. 2010, 2012).

To derive hydrological parameters for the lake part of object 207, a simple conceptual model of periglacial conditions was introduced in Figure 5-17 (left panel). In this model, all horizontal exchange of water was allocated to the uppermost regolith compartment, which thus represents the active layer. Below this layer, permafrost was assumed to effectively prevent all exchange of groundwater between the object and the local catchment. However, the exchange of deep groundwater across the bedrock-till (RegoLow) boundary still occurred.

The parameters for the permafrost conditions were also calculated according to the method described in Sections 5.5 to 5.7. This was done by setting the fraction of the discharge from the local catchment that reached the object as surface discharge ($f_{disch,surf}$) to 1, and upscaling the runoff (from the basin and the watershed) and the net precipitation by 20 % (see above). The total discharge from the bedrock was assumed to be marginally affected by the permafrost (Section 5.4 in the **Radionuclide transport report**). However, as the mire part of the lake was assumed to be frozen, the area-specific discharge in the talik ($q_{bedrock,low,perm}$, m year^{-1}) increased as the discharge from the bedrock was distributed over a smaller area (corresponding to the open water):

$$q_{bedrock,low,perm} = \frac{area_{object} \times q_{bedrock,low}}{area_{obj,aqu}}$$

Where

$q_{bedrock,low,}$ is the area-specific discharge in the object under temperate conditions (m year^{-1}), and $area_{object}$ and $area_{object,aqu}$ are the surface area of the object and the open water in the object, respectively (m^2).

Moreover, when the glacial ice-front is approaching, the discharge from the bedrock may increase by more than an order of magnitude (Section 5.4 in the **Radionuclide transport report**). This increase was described by the parameter $Scalefact_{q,bedrock,IceAdv}$, and it was given the same value as used for near field and geosphere transport calculation (33, unitless).

The discharge in the regolith profile of object 207 for periglacial conditions is shown in Figure 5-19 and compared with that calculated for the lake in temperate conditions. The discharge from the bedrock increased (~50 %) as a result of the groundwater being channelled to the unfrozen area under the lake, and this increase is propagated upwards in the regolith column. However, the discharge from the bedrock is small compared with the exchange of water across the water-regolith boundary (which is presumably driven by circulation of water in the lake), and consequently the discharge across this boundary is not affected by permafrost conditions. Moreover, the discharge from the lake is 20 % higher than in the temperate case, reflecting that net precipitation and runoff (from the watershed and the catchment) were upscaled by this factor.

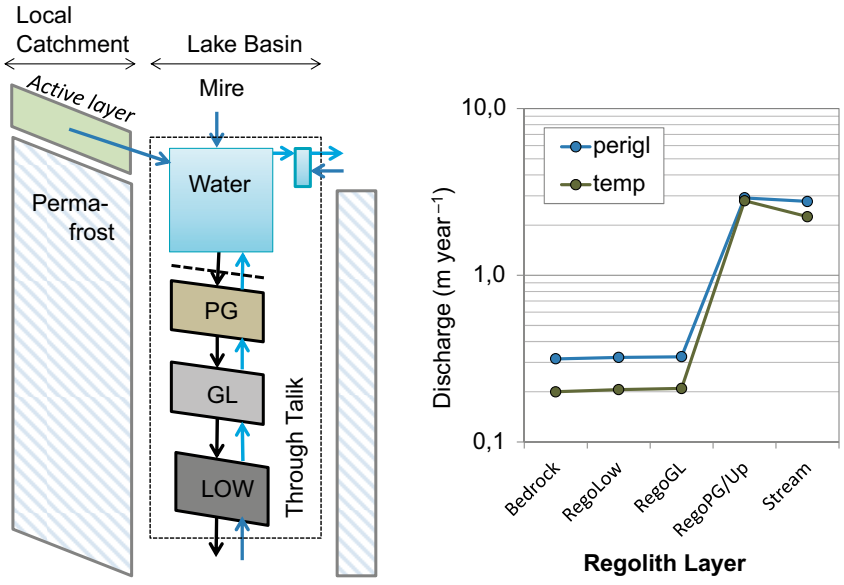

Figure 5-19. *Hydrological parameters for periglacial conditions. Left) Stylised water balance model for a lake talik surrounded by permafrost. Symbols and notation follow that in Figure 5-7. Right). Calculated upward specific flow as a function of regolith layer in object 207 under temperate (green) and periglacial (blue) conditions.*

5.10 Discussion and conclusions

In this chapter a new method for deriving groundwater parameters from MIKE SHE water balances has been developed. The method starts from a set of stylised conceptual water balance models for natural and cultivated ecosystems. Next, MIKE SHE water balances (or catchment properties) are used to derive object-specific boundary conditions, and ecosystem specific rates of percolation are calculated from empirical rules. Finally, upward groundwater flows within the object are calculated from mass balance, accounting also for the discharge of deep groundwater. The new method captures the main features of the MIKE SHE water-balances, and the calculated water flows are similar to those derived in the previous SR-PSU assessments.

The main advantage with the new method is that the vertical flow profile of the MIKE SHE water-balances can be captured by continuous, and independent, functions describing discharge from the local catchment and percolation. As these functions are scalable with the input of water (from the local catchment or in the object), and as percolation depends on the thickness of the least conductive soil layer (i.e. glacial clay), the flow profile for an object can be calculated also for alternative states (e.g. with a different regolith profile) and/or for other external conditions (e.g. with increased runoff and/or bedrock discharge). Thus, the new method can be used for systematic interpolation of water flows to other successional stages and climatic conditions.

It is important to note that the robustness of the method has not been evaluated for states lacking a MIKE SHE water balance. Moreover, at this stage it has not been possible to explain the discharge profile from the local catchment by its physical properties. Thus, the uncertainties in the calculated hydrological flows for alternative states can be considerably large. This includes the flows for the mire stage of land that is presently arable (e.g. object 206 in the main evaluation case), for future states of the aquatic objects 201, 207 and 208 (in the discharge area evaluation case), and the past development of object 206 (in the initially submerged evaluation case).

Nevertheless, the new method captures the main features of the MIKE SHE water balances and offers a systematic way for interpolation under alternative conditions. As the new method explicitly links hydrological flows to object characteristics and maintains water balance, it also allows for sensitivity analysis of variations in properties such as object and watershed areas, regolith thickness, bedrock discharge and runoff. Thus, the method strengthens SKBs assessment methodology and offers a sound platform for future development with respect to modelling transport and accumulation of radionuclides in surface ecosystems.

6 Element-specific parameters

In this Chapter the element-specific parameters are described, the parameters are listed in Table 6-1 and the definitions of the parameters are described in Section 6.1.

6.1 Parameter definitions

Sorption of radionuclides onto soil particles and particulate matter in lake and sea water are modelled by partitioning coefficients, K_d in BioTEx. K_d is defined as the ratio of the concentration of a given element in the soil solid phase to the concentration in the surrounding liquid phase (pore water or surface water) at equilibrium:

$$Kd = \frac{Conc_{soil\ solid}}{Conc_{\ liquid}}$$

where K_d is the solid/liquid distribution coefficient in $m^3\ kg_{DW}^{-1}$, $Conc_{soil\ solid}$ is the activity concentration in the solid phase of a soil in Bq kg_{DW}^{-1}. $Conc_{\ liquid}$ is the activity concentration of the liquid phase of a soil in Bq m^{-3}.

The K_d values are element specific since different elements sorb to solid materials to different degrees. The sorption of elements is also dependent on the local chemical environment and on the properties of the soils. Therefore, different K_d values are provided for every element and for every soil type in BioTEx. In the safety evaluation SE-SFL, K_d values for five soil types; till, glacial clay, postglacial claygyttja, anoxic peat and oxic peat are provided. Sorption will also be affected by agricultural practices, and therefore K_d values are also provided for soils used for agriculture, (Kd_regoUp_Drained mire, Kd_regoUp_Garden plot and Kd_regoUp_Infield outland). In addition, K_d values are provided for sorption on particulate matter in lake and sea water respectively and for deposited aquatic sediments (kD_PM_lake, kD_PM_sea). In Table 6-1 the K_d parameter names and definitions are given. More information on the different soil types and K_d parameters is given in Chapter 2 in Tröjbom et al. (2013).

Uptake of radionuclides in biota is modelled using concentration ratios, *CR*. *CR* is defined as the element concentration in biota tissues divided by the element activity concentration in the surrounding media; soil or water.

$$CR = \frac{Conc_{biota}}{Conc_{media}}$$

where *CR* is the soil to biota concentration ratio in $kg_{DW}\ kg_{DW}^{-1}$ if the medium is soil or $m^3\ kg_{DW}^{-1}$ if the medium is water. $Conc_{biota}$ is the activity concentration in tissue in Bq kg_{DW}^{-1}, $Conc_{media}$ is the activity concentration in the surrounding medium, dry soil in terms of Bq kg_{DW}^{-1} or water in Bq m^{-3}.

In BioTEx, the *CR* values used are normalised to the carbon content of biota. This gives the definition of *CR*:

$$CR = \frac{\frac{Conc_{biota}}{CC}}{Conc_{media}}$$

where *CR* is the soil to biota concentration ratio in $kg_{DW}\ kg_{C}^{-1}$, if the medium is soil or $m^3\ kg_{C}^{-1}$ if the medium is water. $Conc_{biota}$ is the activity concentration in biota tissue in Bq/kg_{DW}, CC is the carbon content of the biota sample ($kg_C\ kg_{DW}^{-1}$). $Conc_{media}$ is the activity concentration in the surrounding medium, dry soil in Bq kg_{DW}^{-1} or water Bq m^{-3}.

The uptake of radionuclides by wild herbivores from vegetation is modelled by *CR* values defined as the carbon normalised activity concentrations in animal muscle divided by the carbon normalised activity concentrations in green parts of vegetation:

$$CR = \frac{\frac{Conc_{herbivore}}{CC_{herbivore}}}{\frac{Conc_{vegetation}}{CC_{vegetation}}}$$

where, CR is the unitless soil to biota concentration ratio, $Conc_{herbivore}$ is the activity concentration in herbivore muscle in Bq kg_{DW}^{-1}, $Conc_{vegetation}$ is the activity concentration in the green parts of vegetation in Bq kg_{DW}^{-1} and CC is the carbon content of herbivores and vegetation in kg_C kg_{DW}^{-1}.

Transfer coefficients, *TC*, are used to quantify uptake of radionuclides in milk and meat in domestic animals. The transfer coefficient is defined as the ratio of the radionuclide activity concentration in meat or milk to the daily dietary radionuclide intake. In this study, cow is the only domestic animal considered. The daily intake of radionuclides is the sum of the radionuclide intake from feed, soil and water consumption.

$$TC\_Meat = \frac{Conc_{meat_i}}{Daily\_intake_i}$$

where *TC_Meat* is the transfer coefficient for cow meat (da kg_{FW}^{-1}), $Conc_{meat_i}$ is the activity concentration in cow meat (Bq kg_{FW}^{-1}) and $Daily\_intake_i$ is the total daily intake of radionuclide in (Bq day^{-1}).

$$TC\_Milk = \frac{Conc\_milk_i}{Daily\_intake_i}$$

where *TC_Milk* is the transfer coefficient for cow milk (day m^{-3}), $Conc\_milk_i$ is the activity concentration in cow milk (Bq m^{-3}) and is the total daily intake of radionuclides in (Bq day^{-1}).

CR and *TC* values are element-specific, since the properties of elements affect their uptake and retention. Uptake and retention also differ between different biota types, and therefore *CR* values are provided for each of 16 biota types included in the assessment such as crops (cereals, vegetables, tubers), other terrestrial vegetation and animals, limnic and marine algae and fish. All *CR* parameters included in this assessment are listed in Table 6-1.

Diffusivity in free solution (D_water), is a proportionality constant between the mass flux due to molecular diffusion and the gradient in the concentration of the element. The diffusivity values were used in the radionuclide transport model for calculation of the diffusion fluxes between different regolith compartments. Diffusivity is also regarded as an element-specific parameter.

Table 6-1. Description of element-specific parameters used in BioTEx for SE-SFL.

Name	Unit	Description
cR_agri_cereal	$kg_{DW}\ kg_C^{-1}$	*CR* between soil and cereals
cR_agri_fodder	$kg_{DW}\ kg_C^{-1}$	*CR* between soil and fodder
cR_agri_tuber	$kg_{DW}\ kg_C^{-1}$	*CR* between soil and potatoes
cR_agri_veg	$kg_{DW}\ kg_C^{-1}$	*CR* between soil and vegetables (edible parts above ground)
cR_food_herbiv	$kg_C\ kg_C^{-1}$	*CR* with respect to herbivores and their diet
cR_lake_cray	$m^3\ kg_C^{-1}$	*CR* for crayfish in lake water
cR_lake_fish	$m^3\ kg_C^{-1}$	*CR* for fish in lake water
cR_lake_pp_macro	$m^3\ kg_C^{-1}$	*CR* for macrophytes in lake water
cR_lake_pp_micro	$m^3\ kg_C^{-1}$	*CR* for microphytobenthos in lake water
cR_lake_pp_plank	$m^3\ kg_C^{-1}$	*CR* for plankton in lake water
cR_sea_fish	$m^3\ kg_C^{-1}$	*CR* for fish in sea water
cR_sea_pp_macro	$m^3\ kg_C^{-1}$	*CR* for macrophytes in sea water
cR_sea_pp_micro	$m^3\ kg_C^{-1}$	*CR* for microphytobenthos in sea water
cR_sea_pp_plank	$m^3\ kg_C^{-1}$	*CR* for plankton in sea water
cR_ter_mush	$kg_{DW}\ kg_C^{-1}$	*CR* between edible mushrooms and soil
cR_ter_pp	$kg_{DW}\ kg_C^{-1}$	*CR* for terrestrial primary producers and soil
D_water	$m^2\ year^{-1}$	Diffusivity of water-based radionuclide concentration
f_combust	$kg_{DW}\ kg_{DW}^{-1}$	The fraction of the fuel inventory that ends up in fly ash and gas after combustion of wood or peat
kD_PM_lake	$m^3\ kg_{DW}^{-1}$	Distribution coefficient for particulate matter in lake water
kD_PM_sea	$m^3\ kg_{DW}^{-1}$	K_d for particulate matter in sea water
kD_regoGL	$m^3\ kg_{DW}^{-1}$	K_d in glacial clay
kD_regoLow	$m^3\ kg_{DW}^{-1}$	K_d in lower regolith (till)
kD_regoPeat	$m^3\ kg_{DW}^{-1}$	K_d in anoxic layer of terrestrial regolith (peat)
kD_regoPG	$m^3\ kg_{DW}^{-1}$	K_d in postglacial sediments
kD_regoUp_aqu	$m^3\ kg_{DW}^{-1}$	K_d in upper layer of aquatic regolith
kD_regoUp_ter	$m^3\ kg_{DW}^{-1}$	K_d in upper oxic layer of terrestrial regolith (peat)
kD_regoUp_ Drained mire.	$m^3\ kg_{DW}^{-1}$	K_d in cultivated soils in Drained mire.
kD_regoUp_ Garden plot	$m^3\ kg_{DW}^{-1}$	K_d in cultivated soils in Garden plot,
kD_regoUp_ Infield outland	$m^3\ kg_{DW}^{-1}$	K_d in cultivated soils in Infield-outland agricultural systems.
TC_meat	$d\ kg_{FW}^{-1}$	Transfer coefficient from intake of radionuclides in fodder and water to cow meat
TC_milk	$day\ l^{-1}$	Transfer coefficient from intake of radionuclides in fodder and water to cow milk

6.2 Effect of site-specific properties on parameter values

The K_d, *CR* and *TC* values are affected by the local conditions, K_d, *CR* and *TC* parameters are affected by for example pH, CEC, organic matter and clay content. This applies maily to the K_d and *CR* for vegetations while the effect of site-specific condition is less promounce for *CR* for wild animals and *TC* for domestic cows. Since these properties vary between sites, the K_d, *CR* and *TC* measurements at one site will not, in general, be representative for another site with other properties. Changes in hydrological conditions, as for example a wetter climate with more precipitation and water flows can affect the K_d, *CR* and *TC* values since the chemistry of lakes, and pore waters can be affected by altered water flows. This means that site-specific data are needed to capture the site-specific sorption and uptake processes.

6.3 Comparison between Laxemar and Forsmark data

In the previous safety assessment for low level waste, SR-PSU, K_d and *CR* values were derived for the Forsmark site. Data for the Laxemar site were also derived and used in the parameterisation process as supporting data in the SR-PSU assessment, see Tröjbom et al. (2013). In this section, K_d and *CR* values from Forsmark and Laxemar are compared in order to identify differences between the data sets.

The parameters for which this comparisons are possible (meaning data are available from both sites) are limnic and marine *CR* values for fish and primary producers (cR_Lake_Fish, cR_Lake_pp, cR_Sea_Fish, cR_Sea_pp), *CR* values for terrestrial natural vegetation (cR_Ter_pp) and uptake by herbivores, (cR_foodToHerbivores). For K_d parameters comparison between the sites were possible for K_d for aquatic sediments and particulate matter in lake and sea water (kD_Aqu_regoUp, kD_Lake_PM, kD_Sea_PM). No comparisons between K_d values for the terrestrial soil types were possible since no site-specific data from Laxemar are available.

The number of samples varied between elements and parameter. For many of the parameter/element combinations the sample number is low. For *CR* for fish and aquatic vegetation in lake and sea waters the numbers of samples were between 1 and 6, the same was true for and terrestrial vegetation. For K_d values for particulate matter the number of samples varied between 1 and 5.

To compare the *CR* and K_d values from each site both the geometric mean value and the spread in the data needed to be considered. The geometric mean of each parameter/element combination from Laxemar was compared with the geometric mean and from Forsmark. The results are presented in Table 6-2 and discussed below. Because the available K_d and *CR* values in many cases consist of few samples, no statistical tests were conducted, instead the calculated ranges (5^{th} and 95^{th} percentiles) of the data were compared and the overlap between the data were evaluated. This comparison of ranges was done in Tröjbom et al. (2013) and the results from this comparison are summarised below in Table 6-3. For some cases, there is a full overlap between the data set where either the Forsmark data range lies within the Laxemar data range or the Laxemar data range lies within the Forsmark data range, this is marked as *FULL* in Table **6-3**. There can also be a partial overlap between data sets, this is marked as *PARTIAL* in the table, to assess how large the overlap is, the percentage of the data range overlap is also presented. In some cases, there was no overlap between the data sets at all, this is marked as *NO* in the table.

Table 6-2. The comparison of geometric mean values from Forsmark (FM) and Laxemar (LX) is done by looking at the ratio between FM and LX data on a logarithmic scale. Most of the values were within one order of magnitude (ratio between 0.1 and 10 in the table), marked in green. In some cases, the Laxemar *CR* or K_d values were more than one order of magnitude lower than the Forsmark values (marked in red) and some cases had a value for Laxemar that was more than one order of magnitude higher than for Forsmark (marked in yellow).

	cR_Lake_Fish	cR_Lake_pp	cR_Sea_Fish	cR_Sea_pp	cR_Ter_pp	cR_foodToHerbiv	kD_Aqu_regoUp	kD_Lake_PM	kD_Sea_PM
Ac									
Ag							0.2		
Am									
Ba	0.41	1.07	9.06	4.08	0.78	1.34	0.75	0.303	259
Be		25.26					1.13	0.745	4.25
Ca	0.18	0.905	29.1	0.53	0.17	4.62	0.88	0.599	19.6
Cd		4.181	2.13	1.45	1.04	3.28	0.19	2.165	6.93
Cl	0.87	0.041	0.74	1.22		0.84	2.6		
Cm									
Co	2.38	2.233	6.64	9.86	0.3	7.74	1.17	0.608	4.77
Cs	0.16	0.742	0.87	11.5	1.85	0.56	2.12	0.474	10.4
Eu		18.1		0.06			2.39	0.481	1.34
Gd		24.04		0.07	0.47		1.26	0.737	3.14
Ho		20.25		0.07			2.18	0.47	2.27
I	1.49	2.276	1.69	1.46			1.25	2.126	1.06
K	0.51	0.009	0.87	0.95	1.57	1.31	0.56	1.786	12.8
La	4.35	20.37			0.19	14.9	3.17	1.47	3.07
Mo	1.38	0.456	2.63	2.46	1.6	0.94	0.36	0.866	15.5
Nb	1.72	15.4			1.04	2.69	1.9	0.35	6.06
Ni		3.978	1.24	3.07	0.52	21.2	1.32	2.182	1.35
Np									
Pa									
Pb		11.29	0.35	1.7	0.99	7.35	0.63	1.369	0.56
Pd									
Po									
Pu									
Ra						14.2			
Re								3.09	0.94
Se	0.35	1.109	1.2	0.77			0.92	0.746	0.56
Si	1.38	6.856	3.76	31.4	0.002	1.65	0.19	0.714	24.7
Sm		17.35		0.05	0.64	5.78	2.7	0.719	2.59
Sn					1.12	0.69	1		
Sr	0.38	2.563			0.5	5.72	0.57	0.474	0.97
Tb	0.46	17.32		0.11			2.15	0.481	3.43
Tc									
Th		5.996	2.64	39.3			2.53	0.596	7.78
Ti	8.39	29.12	19.2	36.8		0.79	2.09	0.899	9.23
U	0.07	1.483			0.67	0.9	0.66	0.031	1.98
Zr	3.52	5.044	1.37	18.2	0.7	1.56	1.29	0.481	6.31

Table 6-3. The result of the analyses of data overlap conducted in Tröjbom et al. (2013). Green cells marked with either full or with a partial overlap of more than 50 % is considered as good agreement. Orange cells marked partial with less than 50 % agreement and red cells cases marked as no are considered to be in poor agreement.

Element	cR_Lake_Fish	cR_Lake_pp	cR_Sea_Fish	cR_Sea_pp	cR_Ter_pp	cR_foodToHerbiv	kD_Aqu_regoUp	kD_Lake_PM	kD_Sea_PM
Ag							partial (36 %)		
Ba	partial (78 %)	full	NO	partial (85 %)	full	partial (96 %)	full	partial (34 %)	partial (6 %)
Be		NO					full	partial (91 %)	NO
Ca	partial (24 %)	full	NO	partial (97 %)	partial (34 %)	partial (61 %)	full	full	partial (22 %)
Cd		partial (22 %)	partial (59 %)	full	full	partial (75 %)	partial (28 %)	full	full
Cl	full	NO	full	full		full	full		
Co	full	full	partial (50 %)	partial (65 %)	partial (45 %)	partial (43 %)	full	full	partial (6 %)
Cs	partial (43 %)	full	full	partial (19 %)	full	partial (86 %)	full	partial (76 %)	NO
Eu		partial (15 %)		partial (26 %)			partial (86 %)	partial (61 %)	partial (74 %)
Gd		partial (21 %)		partial (61 %)	partial (79 %)		full	partial (83 %)	NO
Ho		partial (22 %)		partial (42 %)			partial (97 %)	partial (63 %)	full
I	full	full	partial (56 %)	full			full	partial (53 %)	full
K	NO	NO	partial (78 %)	full	full	partial (90 %)	full	full	partial (6 %)
La	partial (42 %)	partial (17 %)			partial (54 %)	partial (46 %)	partial (34 %)	partial (78 %)	NO
Mo	full	full	partial (17 %)	partial (64 %)	partial (97 %)	full	partial (66 %)	full	partial (32 %)
Nb	full	partial (24 %)			full	partial (67 %)	full	partial (66 %)	NO
Ni		partial (32 %)	full	partial (49 %)	partial (76 %)	partial (5 %)	full	partial (47 %)	partial (45 %)
Pb		partial (35 %)		full	full	partial (37 %)	full	full	full
Ra						partial (42 %)			
Re								partial (68 %)	full
Se	partial (14 %)	full	full	full			full	full	NO
Si	partial (81 %)	partial (23 %)	partial (41 %)	partial (20 %)	NO	partial (85 %)	partial (30 %)	partial (87 %)	NO
Sm		partial (25 %)		partial (54 %)	partia l(81 %)	partial (58 %)	partial (77 %)	full	NO
Sn					partial (95 %)	full	full		
Sr	partial (73 %)	partial (43 %)			partial (67 %)	partial (64 %)	partial (95 %)	full	full
Tb		partial (26 %)		partial (64 %)			partial (99 %)	partial (72 %)	partial (21 %)
Th		full	partial (66 %)	partial (34 %)			partial (83 %)	partial (61 %)	NO
Ti	partial (38 %)	NO	partial (11 %)	partial (31 %)		partial (93 %)	full	full	NO
U	partial (30 %)	full			full	full	full	NO	full
Zr	NO	partial (41 %)	full	partial (27 %)	full	full	partial (94 %)	partial (94 %)	NO

6.3.1 Limnic *CR*s

The comparison of geometric means and ranges for *CR* for freshwater fishes and primary producers are discussed here. The sample number is between one and three, which is a small amount of data and no certain conclusions can be drawn from this comparison. For most cases, the geometric means of *CR* values for fishes from Forsmark and Laxemar are within one order of magnitude, except for the *CR*s for uranium where the *CR* values from Laxemar are almost two orders of magnitude higher than the values from Forsmark.

For primary producers the *CR*s value differ for many of the elements. The *CR* values for the lanthanides (Eu, Gd, Ho, La, Sm and Tb) are between 20–30 times lower in Laxemar compared with Forsmark. Also, the *CR* values for Ti, Be and Nb are between 20–30 times lower in Laxemar compared with Forsmark. *CR* values for K and Cl are higher in Laxemar than Forsmark.

The overlap between the data for fishes are good for about half of the compared cases and poor for half. For primary producers, most of cases show poor agreement (15 of the cases) and good for 8 of the cases.

To get a better understanding of these differences, the underlying concentration measurements from limnic biota and lake water were analysed further. The lake water concentrations from the two sites differed for many elements, see Figure 6-1. The concentrations are in general higher in Laxemar than in Forsmark, for Fe, Al, Mn and lanthanides the mean concentrations are more than ten times higher in Laxemar. Concentrations of U and Ca are ten times higher in Forsmark than in Laxemar. Even though the lake water concentrations differ, the concentrations in limnic fishes are similar in most cases, see Figure 6-2.

The sampled species of limnic primary producers (macro algae) from the two sites differ. In Forsmark the *Chara* algae were sampled whereas the samples from Laxemar are water lilies (*Nymphaeaceae*). Difference in concentrations and *CR*s might therefore be due to the differences in species. In Figure 6-3, the average concentrations of these samples are plotted. It can be concluded that the concentrations spread around the 1:1 line, for Na, Cl and Rb the concentrations are lower in Forsmark than in Laxemar.

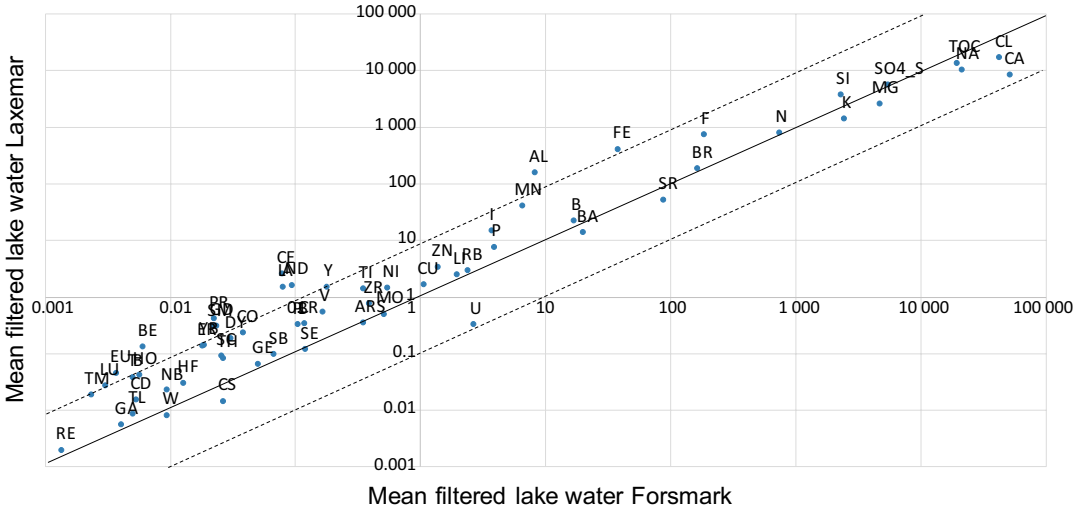

Figure 6-1. *Mean elements concentrations in lake water from Laxemar plotted against the those from Forsmark.*

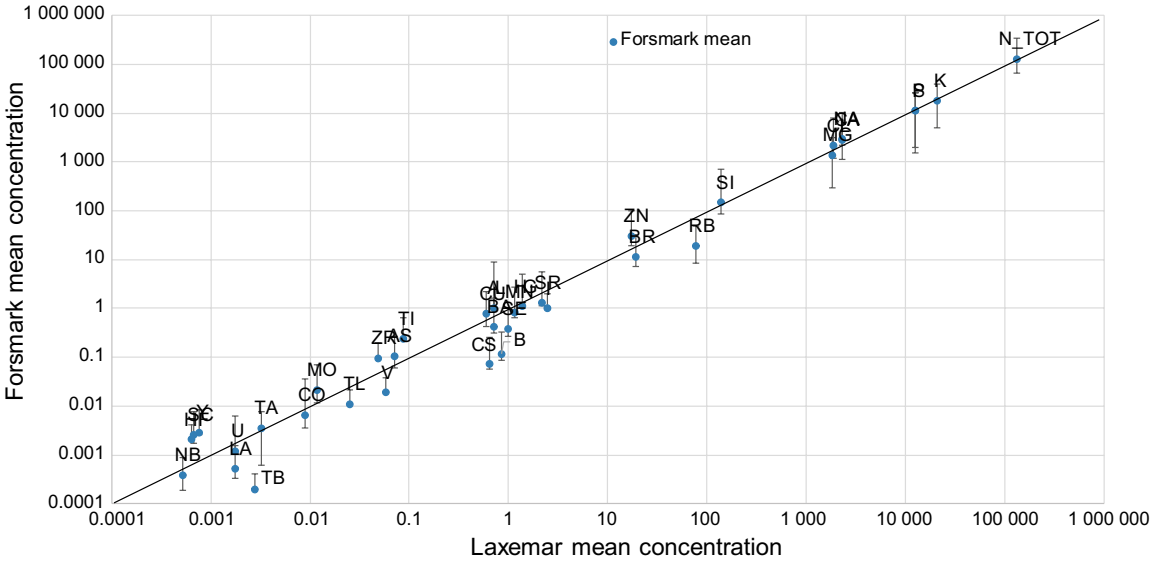

Figure 6-2. *Limnic fish sample concentrations from Forsmark are plotted against the limnic fish concentrations from Laxemar. The concentrations are similar for most elements.*

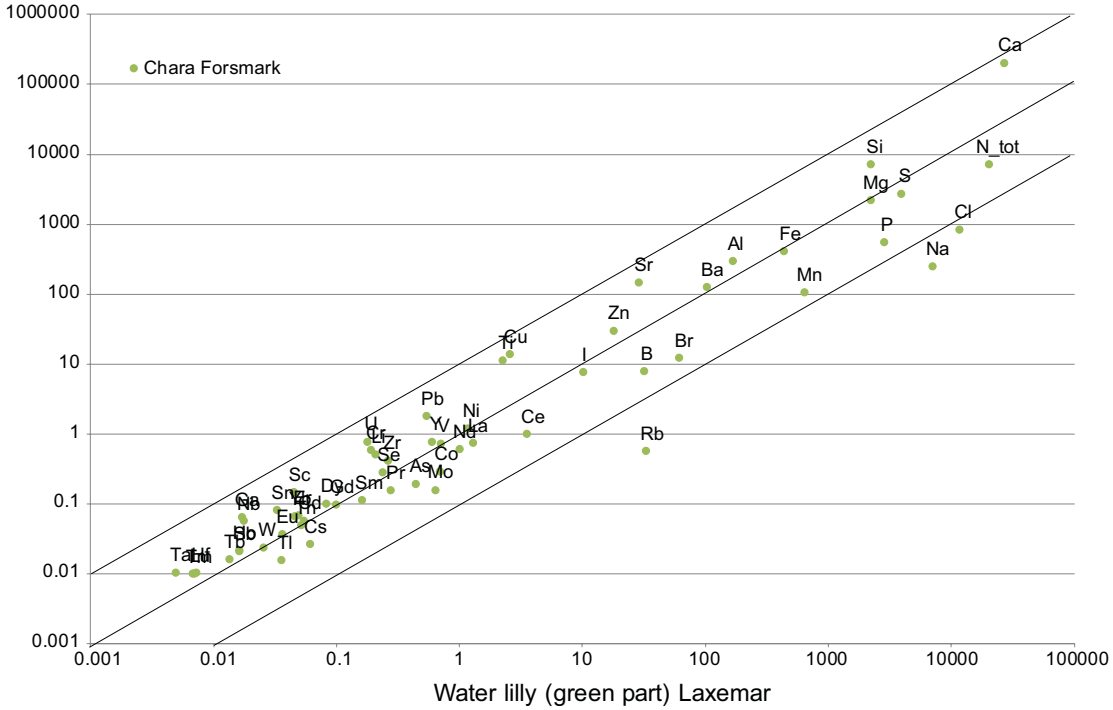

Figure 6-3. *Mean concentrations of elements in Chara from Forsmark plotted against mean element concentrations in water lily from Laxemar.*

6.3.2 Marine *CR*s

For marine fish, most of the geometric mean *CR* values from Forsmark and Laxemar are within one order of magnitude. For Ca and Ti, the *CR* values are 20–30 times lower in Laxemar compared with Forsmark. The overlap is in most cases good (10 out of 15). For Ba and Ca there is no overlap and for Ti, Si and for Mo the overlap is poor. Note that the geometric mean for Ba is within one order of magnitude but still there is no overlap, this indicates that the range is narrow, probably due to low number of samples.

Marine primary producers have 10–40 times lower geometric means in Laxemar for Cs, Si, Th, Ti and Zr compared with Forsmark. The geometric means for the lanthanides Eu, Gd, Ho and Sm are on the other hand higher in Laxemar than in Forsmark. The overlap of ranges is good for about half the cases (13 out of 25), but for 8 cases the overlap is less than 50 % (Cs, Eu, Ho, Ni, Si, Th, To and Zr).

In general, the *CR* values for marine biota could be expected to be similar since both sites are located along the Swedish east coast in the Baltic sea and the seawater concentrations can be expected to be similar. The seawater concentrations from Forsmark are plotted against the sea water concentrations in Laxemar in Figure 6-4. The concentrations correlate well for the elements with higher concentrations whereas the concentrations of elements at the lower end of the plot seem to be higher in Laxemar than in Forsmark. The concentration of Pb is ten times higher in Forsmark than in Laxemar, and the reason for this in not understood.

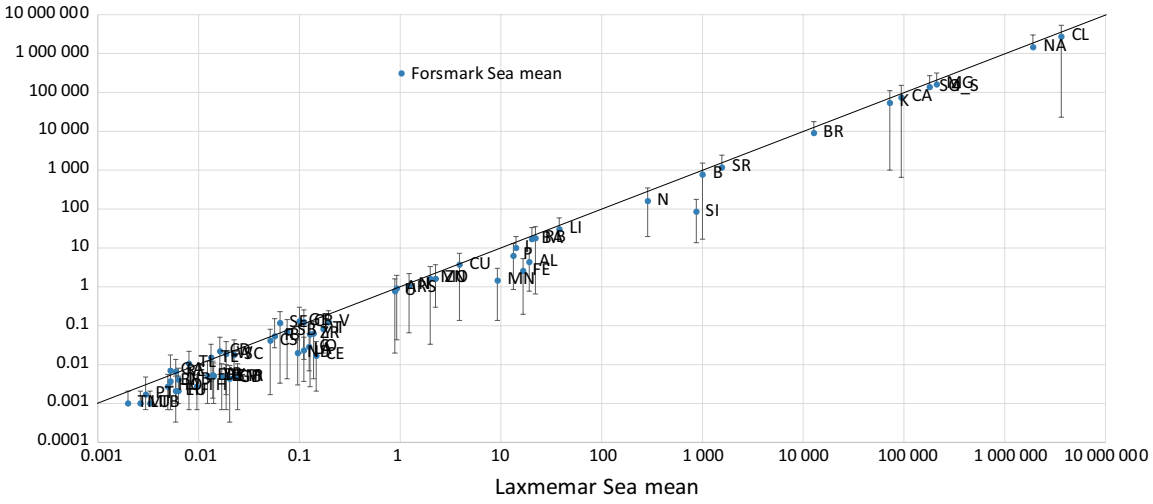

Figure 6-4. *Mean element concentrations in seawater from Laxemar plotted those from Forsmark.*

6.3.3 Terrestrial *CR*s

For terrestrial primary producers, the geometric means (GM) of CR data from Forsmark and for those from Laxemar are within one order of magnitude for all elements except for Si, for which a much higher value is reported in Laxemar. The overlap is good for most of the elements (15 out of 18), but for Si no overlap exists and for Ca and Co the overlap is less than 50 %.

The geometric means of the *CR* values for herbivores are within in order of magnitude for all elements except for La, Ti and Ra where Laxemar geometric means are 15–20 times lower. The overlap is good for most of the elements (15 out of 20) for 5 cases (Co, La, Ni, Pb and Ra) the overlap is less than 50 %.

3.3.4 K_d values

The K_d values for limnic sediments from the two sites are within one order of magnitude for all elements, and for most of the elements there is a good overlap (24 out of 28). The overlap is poor for Ag, Cd, La and Si. For the K_d values for particulate matter in lakes, the geometric means are within one order of magnitude for all except for U, where the K_d values are higher in Laxemar. There is no overlap for the U, and for Ba and Ni the overlap is poor.

The agreement between the K_d values for particulate matter in seawater in Laxemar and Forsmark is, in general, poor. For Ba, Ca, Cs, K, Mo and Si, the geometric mean differs by more than one order of magnitude. No overlap between ranges is reported for Be, Cs, Gd, La, Nb, Se, Si, Sm, Th, Ti and Zr and poor overlap exists for Tb, Ni, Mo, K, Co, Ca and Ba.

6.4 Selected data for element-specific parameters

The differences found in *CR* and K_d values are large for some parameter cases, even if there are no systematic differences to be found. The available sample numbers are low and therefore it is hard to draw any conclusions. However, it is recommended that the Laxemar data should be whenever possible to best capture the site-specific conditions at Laxemar. The data for Forsmark used in SR-PSU are not considered to be directly applicable for the Laxemar site since geochemical properties of the sites differ. Site-specific data from Laxemar have been selected for all cases where Laxemar data are available. In cases where no Laxemar data are available, the best available data are selected. Forsmark data are selected if available, since Forsmark data are representative for a site in Sweden with, in many resprects, similar conditions. In cases for which no Laxemar or Forsmark data are available, analogue data or literature data were selected. Element analogues and/or parameter analogues were selected in preference to literature data when possible. This is the same approach as in SR-PSU, for further discussion on this approach the reader is referred to Tröjbom et al. 2013, Section 4.6. Literature data are from sites around the world and consists of aggregated data from different site conditions, studies and also from different measurement methods. In cases when neither Laxemar or Forsmark data or suitable analogue data are available literature data are selected.

The methods used for deriving the *CR* and K_d data are the same as in SR-PSU, as presented in Tröjbom et al. (2013). The available data are presented per parameter in Tröjbom et al. (2013), no additional data have been made available and added in this assessment.

To evaluate available data comparisons are made among all available data in so-called sense checks. The methods used are described in Tröjbom et al. (2013, Section 4.5), and the results of the sense checks are presented per parameter in Chapters 5 to 8 in Tröjbom et al. (2013).

For *TC* for meat and milk, the same data as for SR-PSU were used, these are further described in Sections 6.4 and 6.5 in Tröjbom et al. (2013), respectively.

Data used for D_water and f_combustion was the same as in SR-PSU. Diffusivity data are described in Section 7.5 in Grolander (2013) and data for f_combust in Section 2.3 in Stenberg and Rensfeldt (2015).

The element included in the SFL assessment are: Ac, Ag, Am, Ba, Be, C, Ca, Cd, Cl, Cm, Co, Cs, Eu, Gd, H, Ho, I, K, La, Mo, Nb, Ni, Np, Pa, Pb, Pd, Po, Pu, Ra, Re, Se, Si, Sm, Sn, Sr, Tb, Tc, Th, Ti, U and Zr. Most of these elements were also included in SR-PSU assessment and K_d and *CR* values for these are presented in Tröjbom et al. (2013). Some of the listed elements were not included in SR-PSU, these are Be, Gd, La, K, Re, Si, Tb, and Ti.

After a first screening if was concluded that the dose contributions of Be and K could be significant in the SFL assessment, and therefore site-specific K_d and *CR* data for these elements were derived. The selected data for Be and K are presented in Section 6.5. For Gd, La, Re, Si, Tb and Ti the screening calculations concluded that the dose contributions were insignificant and therefore the simplified approach using element analogies for parameterisation was used for these elements. The selected element analogues for these elements are listed in Table 6-4.

For Ca, K and Cl a specific activity approach for modelling uptake in terrestrial vegetation and crops was adopted. *CR* values for terrestrial vegetation and crops (fodder, cereals, tubers and vegetables) were therefore not used for these elements. The parameters used for the specific activity approach are described in Chapter 8.

Table 6-4. Selected analogues for elements Gd, La, Re, Si, Tb, Pt and Ti.

Element	Selected analogue
Gd	Lanthanide*
La	Lanthanide*
Re	Tc
Si	Zr
Tb	Lanthanide*
Ti	Zr

*the lanthanide with the highest number of samples was selected as analogue.

In Table 6-5, an overview of selected parameterisation methods is given per parameter. For the K_d and *CR* parameters where no Laxemar data are available the same data as in SR-PSU were used. For these parameters, the data and description were presented in Tröjbom et al. (2013), see Table 6-5 below for references to the specific section in Tröjbom et al. (2013). For parameters where Laxemar data are available selected data are presented below. The selected geometric mean (GM), geometric standard deviation (GSD), minimum and maximum are all based on Laxemar data in these cases. The reported GM are used as best estimates (BE). This differs from the SR-PSU method where the GM, GSD, minimum and maximum values were based on a combination of Forsmark and Laxemar data in cases where data were available from both sites. This means that the distributions reported here for Laxemar data were based on a smaller number of data than the distributions used in the SR-PSU assessment and, therefore, there is a risk of underestimating the data range. Since no parameter distubutions were used in SFL-SE evaluation this issue has not been addressed here but this needs to be addressed in coming assessment if the parameter distributions would be used in sensitivite analysis.

Table 6-5. Overview of selected parameterisation method per parameter.

Parameter name	Laxemar data	Parameterisation method
kD_PM_lake	Yes	Updated values (Section 6.5)
kD_PM_sea	Yes	Updated values (Section 6.5)
kD_regoGL	No	PSU data used Section 5.2 in Tröjbom et al. (2013)
kD_regoLow	No	PSU data used Section 5.1 in Tröjbom et al. (2013)
kD_regoPeat	No	PSU data used Section 5.4 in Tröjbom et al. (2013)
kD_regoPG	No	PSU data used Section 5.3 in Tröjbom et al. (2013)
kD_regoUp_aqu	Yes	Updated values (Section 6.5)
kD_regoUp_drain	No	PSU data used Section 5.6 in Tröjbom et al. (2013)
kD_regoUp_garden	No	PSU data used Section 5.5 in Tröjbom et al. (2013)
kD_regoUp_io	No	PSU data used Section 5.5 in Tröjbom et al. (2013)
kD_regoUp_ter	No	PSU data used Section 5.7 in Tröjbom et al. (2013)
cR_agri_cereal	No	PSU data used Section 6.6 in Tröjbom et al. (2013)
cR_agri_fodder	Yes	Updated data from the parameter analogue cR_ter_pp are used (Section 6.5)
cR_agri_tuber	No	PSU data used Section 6.9 in Tröjbom et al. (2013)
cR_agri_veg	No	PSU data used Section 6.8 in Tröjbom et al. (2013)
cR_food_herbiv	Yes	Updated values (Section 6.5)
cR_lake_cray	No	PSU data used Section 7.8 in Tröjbom et al. (2013)
cR_lake_fish	Yes	Updated values (Section 6.5)
cR_lake_pp_macro	Yes	Updated values (Section 6.5)
cR_lake_pp_micro	Yes	Updated values from the parameter analogue cR_Lake_pp_macro are used (Section 6.5)
cR_lake_pp_plank	Yes	Updated values from the parameter analogue cR_Lake_pp_macro are used (Section 6.5)
cR_ter_mush	No	PSU data used Section 6.10 in Tröjbom et al. (2013)
cR_ter_pp	Yes	Updated values (Section 6.5)
cR_sea_fish	Yes	Updated values (Section 6.5)
cR_sea_pp_macro	Yes	Updated values (Section 6.5)
cR_sea_pp_micro	Yes	Updated values from the parameter analogue cR_Sea_pp_macro are used (Section 6.5)
cR_sea_pp_plank	Yes	Updated values from the parameter analogue cR_Sea_pp_macro are used (Section 6.5)
TC_meat	No	PSU data used Section 6.4 in Tröjbom et al. (2013)
TC_Milk	No	PSU data used Section 6.5 in Tröjbom et al. (2013)
D_water	No	PSU data used Section 7.5 in Groladner (2013)
F_combust	No	PSU data used

6.5 Updated *CR* and K_d values for Laxemar

6.5.1 *CR* for limnic fish (CR_lake_fish)

The available data for limnic fishes are described in detail in Section 7.9 and in Table 7-19 in Tröjbom et al. (2013). In cases where Laxemar data were available these data are selected here, see Table E-1 in Appendix E. In cases where Laxemar and Forsmark data were missing, Laxemar data from suitable elemental analogues were used. The selected analogues are the same as used in SR-PSU (see Section 7.9 in Tröjbom et al. 2013), that is (Ba is used for Ra; La is used for Ac, Am, Cm, Eu and Pa; Zr is used for Sn; and Ni is used for Pd). Further motivation for selected analogues are given in Section 2.7 in Tröjbom et al. (2013). In cases where no suitable analogues were available, literature data were used; the selected literature data were the same as reported in Section 7.9 in Tröjbom et al. (2013).

For the elements Gd, La, Re, Si, Tb and Ti, analogues were selected according to the list in Table 6-4.

6.5.2 *CR* for limnic primary producers (cR_lake_pp_macro, cR_ lake_ pp_ micor, cR_Lake_pp_plank)

The available data for limnic primary producers are described in detail in Section 7.1 and in Table 7-2 in Tröjbom et al. (2013). In cases where Laxemar and Forsmark data were available these data were selected, see Table E-2 in Appendix E. In cases where Laxemar and Forsmark data were missing, Laxemar data from suitable elemental analogues were used, and the selected analogues are the same as reported in Section 7.1 in Tröjbom et al. (2013), further motivation for selected analogues are given in Section 2.7 in Tröjbom et al. (2013) (Ba is used for Ra; La is used for Ac, Am, Cm, Np and Pa; Zr is used for Sn; and Ni is used for Pd). In cases where no suitable analogues were available, literature data were used; the selected literature data were the same as reported in Section 7.1 in Tröjbom et al. (2013).

For the elements Gd, La, Re, Si, Tb and Ti analogues were selected according to the list in Table 6-4.

The *CR* data for cR_lake_pp_macro are used as parameter analogues for microphytobenthos and plankton (cR_Lake_pp_micro and cR_Lake_pp_plank).

6.5.3 *CR* for marine fish (CR_sea_fish)

The available data for marine fish are described in detail in Section 8.8 and in Table 8-16 in Tröjbom et al. (2013). In cases where Laxemar data were available these data were selected, see Table E-3 in Appendix E. In cases where Laxemar data were missing, Laxamar data from suitable elemental analogues were used. The selected analogues are the same as reported in Section 8.8 in Tröjbom et al. (2013) (Ba is used for Ra; La is used for Ac, Am, Cm, Eu, Ho, Np and Pa; and Ni is used for Pd). In cases where no suitable analogues were available, literature data were used; the selected literature data were the same as reported in Section 8.8 in Tröjbom et al. (2013).

For the elements Gd, La, Re, Si, Tb and Ti analogues were selected according to the list in Table 6-4.

6.5.4 *CR* for marine primary producers (sea_pp_macro)

The available data for marine primary producers are described in detail in Section 8.1 and in Table 8-2 in Tröjbom et al. (2013). In cases where Laxemar data were available these data were selected, see Table E-4 in Appendix E. In cases where Laxemar data were missing, Laxemar data from suitable elemental analogues were used. The selected analogues are the same as reported in Section 8.1 in Tröjbom et al. (2013) (Ba is used for Ra; Nd is used for Ac, Am, Cm, Np and Pa; and Ni is used for Pd). In cases where no suitable analogues were available, literature data were used. The selected literature data were the same as reported in Section 8.1 in Tröjbom et al. (2013).

For the elements Gd, La, Re, Si, Tb and Ti analogues were selected according to the list in Table 6-4.

The *CR* data for cR_Sea_pp_macro are used as parameter analogues for microphytobenthos and plankton (cR_Sea_pp_micro and cR_Sea_pp_plank). This added uncertainty to these parameters since the *CR* values can differ substasianly between the biota types due to for difference in absorption to external surfaces as well as differences in uptake.

6.5.5 *CR* for terrestial vegetation and fodder (cR_ter_pp, cR_agri_fodder)

The available data for terrestrial primary producers are described in detail in Section 6.2 and in Table 6-4 in Tröjbom et al. (2013). In cases where Laxemar data were available these data were selected, see Table E-5 in Appendix E. In cases where Laxemar and Forsmark data were missing, Laxemar data from suitable analogues were used. The selected analogues are the same as reported in Section 6.2 of Tröjbom et al. (2013) (La is used for Ac, Am, Cm, Np and Pa. Ni is used for Pd). Data from the parameter analogue cR_agri_cereal were used for Ag and Se. For Po and Tc, data for the elemental analogues Bi and Re for the parameter analogue cR_agri_cereal were used, (both a parameter and elemental analogue). For Cl, I and Ra, Laxemar data were missing but Forsmark data were available and used here. In cases where no suitable analogues (or Forsmark data) were available, literature data were used. The selected literature data were the same as reported in Section 6.2 in Tröjbom et al. (2013).

For the elements Gd, La, Re, Si, Tb and Ti analogues were selected according to the list in Table 6-4.

These data were also used for the parameter cR_agri_fodder representing pasture since no site-specific data were available for this parameter. This is the same approach as in SR-PSU as described in Section 6.7 in Tröjbom et al. (2013).

6.5.6 *CR* for terrestial herbivores (cR_food_to_herbivore)

The available data for uptake in herbivores are described in detail in Section 6.3 and in Table 6-12 in Tröjbom et al. (2013). In cases where Laxemar data were available these data were selected, see Table E-6 in Appendix E. In cases where Laxemar data were missing, Laxemar data from suitable elemental analogues were used, the selected analogues are the same as reported in Section 6.3 of Tröjbom et al. 2013 (La is used for Ac, Am, Cm, Np, and Pa. Ni is used for Pd and Zr is used for Tc). Further motivation for selected analogues are given in Section 2.7 in Tröjbom et al. (2013). For Se and I no Laxemar data were available and Forsmark data were selected instead. In cases, where no suitable analogues (or Forsmark data) were available literature data are used, the selected literature data were the same as reported in Section 6.3 in Tröjbom et al. (2013).

For the elements Gd, La, Re, Si, Tb and Ti analogues were selected according to the list in Table 6-4.

6.5.7 K_d for particulate matter in lake water (Kd_PM_Lake)

The available K_d data for particulate matter in lake water are described in detail in Section 5.9 and in Table 5-18 in Tröjbom et al. (2013). In cases where Laxemar data were available these data were selected, see Table E-7 in Appendix E. In cases where Laxemar data were missing, Laxemar data from elemental suitable analogues were used, the selected analogues are the same as in reported in Section 5.9 of Tröjbom et al. (2013) (Sm is used for Ac, Am, Cm, Np and Pa; Br is used for Cl; Ni for Pd; Bi for Po; U for Pu; Ba for Ra; Zr for Sn; and Re for Tc). Further motivation for selected analogues are given in Section 2.7 in Tröjbom et al. (2013).

For the elements Gd, La, Re, Si, Tb and Ti analogues were selected according to the list in Table 6-4. Sm are used as an analogue for lanthanides.

6.5.8 K_d for particulate matter in seawater (Kd_PM_Sea)

The available K_d data for particulate matter in sea water are described in detail in Section 5.10 and in Table 5-20 in Tröjbom et al. (2013). In cases where Laxemar data were available these data were selected, see Table E-8 in Appendix E. In cases where Laxemar data were missing, Laxemar data from suitable elemental analogues were used, the selected analogues are the same as reported in Section 5.10 of Tröjbom et al. (2013) (Sm is used for Ac, Am, Cm, Np and Pa; Ni is used for Pd; Bi is used for Po; Pu is used for U; Ba is used for Ra; Zr is used for Si; Re is used for Tc; and K is used for Cs). For Cl no Laxemar data were available but data from Forsmark were used instead.

For the elements Gd, La, Re, Si, Tb and Ti analogues were selected according to the list in Table 6-4.

6.5.9 K_d for aquatic sediment (Kd_regoUp_aqu)

The available data aquatic sediments are described in detail in Section 5.8 and in Table 5-16 in Tröjbom et al. (2013). In cases where Laxemar data were available these data were selected, see Table E-9 in Appendix E. In cases where Laxemar data were missing, Laxemar data from suitable elemental analogues were used, the selected analogues are the same as reported in Section 5.8 of Tröjbom et al. (2013) (Ba is used for Ra; Nd is used for Ac, Am, Cm and Pa; and Ni is used for Pd). Forsmark data were used for Re and its analogue Tc, because no Laxemar data were available.

For the elements Gd, La, Re, Si, Tb and Ti analogues were selected according to the list in Table 6-4.

6.6 Selected data for Be and K

Be and K were not included in the SR-PSU assessment and therefore no K_d and *CR* values for these two elements were reported in Tröjbom et al. (2013). Site data from Laxemar and Forsmark and literature data are available for these elements, the references for these data are described in Chapter 3 in Tröjbom et al. (2013). K_d and *CR* values for Be and K were selected for each parameter based on the same parameterisation methods as used in Tröjbom et al. (2013). The selected data are presented in Tables E-10 to Tables E-13 in Appendix E.

For Be, site data for *CR* are missing for many of the parameters, and in these cases Sr was used as an elemental analogue. For crayfish, data for mussels are used as parameter analogue, and data for marine and limnic primary producers are used for phytoplankton and microphytobenthos. The selected data for *CR* and *TC* parameters are listed in Table E-10 in Appendix E.

K_d data for Be are available from Laxemar for two of the K_d parameters, kD_PM_lake, kD_PM_sea and kD_regoUp_aqu. For the rest of the K_d parameters, data from Forsmark are available and used. The selected K_d data are reported in Table E-11 in Appendix E.

Potassium (K) uptake in terrestrial plants and crops (vegetables, cereals, tubers and fodder) are modelled using the specific activity approach and therefore no *CR* values for these biota types are used or derived here. For K, Laxemar data for *CR* are available for many of the other parameters. For crayfish, data for mussels are used as parameter analogues and data for marine and limnic primary producers are used for phytoplankton and microphytobenthos. Literature data were used for *TC*. The selected data for *CR* and *TC* parameters are listed in Table E-12 in Appendix E.

K_d data for K are available from Laxemar for three of the K_d parameters, kD_PM_lake, kD_PM_sea and kD_regoUp_aqu. For the rest of the K_d parameters, data from Forsmark are available and used. The selected K_d data are reported in Table E-13 in Appendix E.

7 Aquatic ecosystem parameters

In this chapter, the parameters describing properties of the limnic and marine ecosystem in the radionuclide model for the biosphere are presented. The parameters used are listed in Table 7-1 and selected values are presented in Appendix F.

The radionuclide model for aquatic ecosystems is based on the model used in the previous safety assessment for the extension of SFR repository, SR-PSU, and therefore the parameter definitions used in this assessment are mainly the same as presented in Grolander (2013).

7.1 Effects of site-specific characteristics on parameter values

Site-specific characteristics of the aquatic ecosystem affect the parameter values for some of the parameters.

The chemistry of the lake water is affected by local geology, distance to the sea and local hydrology of the area. The temperature at the site affects the primary production, and the duration of ice-cover has implications for parameters describing water degassing and uptake. The limnic ecosystems of Laxemar are described in Andersson (2010). The lakes in the area are small and characterised as brown-water lakes. The lakes have lower levels of phosphorus, but higher concentrations of nitrogen and dissolved organic carbon than lakes in Forsmark. The brown colour of the water results in a smaller photic depth and the coverage of macrophytes is low. The lakes of the model area of Forsmark, modelled in the previous safety assessment, SR-PSU, are also described in Andersson (2010). The lakes in Forsmark are small, shallow oligotrophic hardwater lakes. High levels of calcite in the regolith layers of Forsmark results in high concentrations of Ca, high pH and low levels of phosphorus since phosphorus often co-precipitates with calcite. A thick layer of microbial mat covers the sediments of the lakes.

The marine ecosystems are affected by temperature, runoff and local geology. The marine ecosystems of Laxemar and Forsmark are described in Aquilonius (2010). The marine ecosystem at the Laxemar site is part of the Baltic Proper and Forsmark is part of the basin Bothnian Sea. The salinity is higher in Laxemar than in Forsmark, which affects the abundance and diversity of biota. The local characteristics of the shoreline affect the water exchange rates, the relative contribution of surface water to the total water pool of the marine basins, the local temperature and salinity.

The difference between the two sites will result in differences in some parameter values, as described in Section 7.4.

Table 7-1. Summary of aquatic parameters used

Name	Unit	Description
biom_pp_macro	$kg_C\ m^{-2}$	Biomass of macrobenthic community in water per unit surface area
biom_pp_micro	$kg_C\ m^{-2}$	Biomass of microbenthic community in water per unit surface area
biom_pp_plank	$kg_C\ m^{-2}$	Biomass of pelagic community in water per unit surface area
conc_DIC_lake	$kg_C\ m^{-3}$	Concentration of dissolved inorganic carbon in lake water
conc_DIC_sea	$kg_C\ m^{-3}$	Concentration of dissolved inorganic carbon in sea water
conc_PM_lake	$kg_{DW}\ m^{-3}$	Concentration of suspended matter in lakes
conc_PM_sea	$kg_{DW}\ m^{-3}$	Concentration of suspended matter in the sea
dens_water_sea	$kg\ m^{-3}$	Density of seawater (Baltic Sea)
dens_water_lake	$kg\ m^{-3}$	Density of lake water
f_C_fish	$kg_C\ kg_{DW}^{-1}$	Fraction of carbon to dry weight in fish
f_DW_FW_fish_lake	$kg_{DW}\ kg_{FW}^{-1}$	Fraction of dry weight to fresh weight for fish in lake
f_DW_FW_fish_sea	$kg_{DW}\ kg_{FW}^{-1}$	Fraction of dry weight to fresh weight in marine fish
f_H2CO3_lake	$Bq\ Bq^{-1}$	Fraction of dissolved inorganic carbon in lake water in the form of CO_2/H_2CO_3
f_H2CO3_sea	$Bq\ Bq^{-1}$	Fraction of dissolved inorganic carbon in sea water in the form of CO_2/H_2CO_3
f_inorg_Cl_PP_aqu	$kg\ kg^{-1}$	Fraction of inorganic chlorine of the total chlorine content in primary producers
f_refrac_macro_lake	$kg_C\ kg_C^{-1}$	Fraction of refractory organic matter of macrobenthic primary producers in lake water left after initial mineralization
f_refrac_macro_sea	$kg_C\ kg_C^{-1}$	Fraction of refractory organic matter of macrobenthic primary producers in seawater left after initial mineralization
f_refrac_micro_lake	$kg_C\ kg_C^{-1}$	Fraction of refractory organic matter of microbenthic primary producers in lake water left after initial mineralization
f_refrac_micro_sea	$kg_C\ kg_C^{-1}$	Fraction of refractory organic matter of microbenthic primary producers in seawater left after initial mineralization
f_refrac_plank_lake	$kg_C\ kg_C^{-1}$	Fraction of refractory organic matter of pelagic primary producers in lake water left after initial mineralization
f_refrac_plank_sea	$kg_C\ kg_C^{-1}$	Fraction of refractory organic matter of pelagic primary producers in seawater left after initial mineralization
height_L1_aqu	m	Height of first calculation layer above an open water surface area
height_L2_aqu	m	Height of second calculation layer above an open water surface area
height_ref_aqu	m	Reference height used for defining wind velocity
minRate_regoPG_lake	$kg_C\ kg_C^{-1}\ year^{-1}$	Mineralization rate in post-glacial sediments in lake
minRate_regoPG_sea	$kg_C\ kg_C^{-1}\ year^{-1}$	Mineralization rate in post-glacial sediments in sea
minRate_regoUp_lake	$kg_C\ kg_C^{-1}\ year^{-1}$	Mineralization rate in upper regolith in lake
minRate_regoUp_sea	$kg_C\ kg_C^{-1}\ year^{-1}$	Mineralization rate in upper regolith in sea
minRate_water_PM_lake	$kg_C\ kg_C^{-1}\ year^{-1}$	Mineralization rate in particulate matter in lake water
minRate_water_PM_sea	$kg_C\ kg_C^{-1}\ year^{-1}$	Mineralization rate in particulate matter in seawater
NPP_macro	$kg_C\ kg_C^{-1}\ year^{-1}$	Net primary production of macrobenthic community in water per unit surface area
NPP_micro	$kg_C\ m^{-2}\ year^{-1}$	Net primary production of microbenthic community in water per unit surface area
NPP_plank	$kg_C\ m^{-2}\ year^{-1}$	Net primary production of pelagic community in water per unit surface area
piston_vel_lake	$m\ year^{-1}$	Gas exchange coefficient for lake water in contact with the atmosphere
piston_vel_sea	$m\ year^{-1}$	Gas exchange coefficient for sea water in contact with the atmosphere
prod_edib_cray_lake	$kg_C\ m^{-2}\ year^{-1}$	Sustainable yield with respect to edible crayfish per unit area in the lake
prod_edib_fish_lake	$kg_C\ m^{-2}\ year^{-}1$	Sustainable yield with respect to edible fish per unit area in the lake
prod_edib_fish_sea	$kg_C\ m^{-2}\ year^{-1}$	Sustainable yield with respect to edible fish per unit area in the sea
solubilityCoef_lake	$(mol\ m^{-3})\cdot(mol\ m^{-3})^{-1}$	Solubility coefficient for carbon dioxide in lake water (function of temperature, salinity etc.)
solubilityCoef_sea	$(mol\ m^{-3})\cdot(mol\ m^{-3})^{-1}$	Solubility coefficient for carbon dioxide in seawater (function of temperature, salinity etc.)
vel_wind_height_ref_aqu	$m\ s^{-1}$	Wind velocity at reference height
z_min_prod_edib_cray_lake	m	Minimum water depth for production of crayfish in lake
z_min_prod_edib_fish_lake	m	Minimum water depth for production of fish in lake
z_min_prod_edib_fish_sea	m	Minimum water depth for production of fish in sea
z_regoUp_lake	m	Depth of the upper oxygenated regolith layer in lake
z_regoUp_sea	m	Depth of the upper oxygenated regolith layer in sea
z0_aqu	m	Roughness length for water surface

7.2 Selection of parameter values

The parameterisation is largely based on the parameterisations done in previous safety assessments, SR-PSU (Grolander 2013) and SR-Site (Aquilonius 2010 and Andersson 2010 for marine and limnic parameters, respectivley).

For generic parameters that are assumed to be constant for any modelled site in Sweden the data from the SR-PSU assessment presented in Chapter 8 of Grolander (2013) are used, these are described in Section 7.3 below.

Site-specific parameter values selected for the base case, with Laxemar as the reference modelling site, are presented in Section 7.4. For some of these site-specific parameters, the effect of the differences between Forsmark and Laxemar is assumed to be insignificant and therefore SR-PSU data are used for parameterisations also for the model site Laxemar. For site-specific parameters where the effect of site characteristics on parameter values are significant, site-specific data from Laxemar were used for parameterisation.

7.3 Generic parameters

The parameters assumed to be generic (not affected by the site-specific characteristics) are parameters describing properties of fish, such as carbon content and dry weight of fishes (f_C_fish, f_DW_FW_fish_lake, f_DW_FW_fish_sea). The selected parameter values are reported in Table 8-7, and on page 89 in Grolander (2013).

The minimum depth required for a fish or crayfish population to be permanent in a lake or sea basin (z_min_prod_edib_cray_lake, z_min_prod_edib_fish_lake, z_min_prod_edib_fish_sea) depends on the available oxygen and ice coverage. This depth for fish in lakes and the sea is based on test fishing conducted in Forsmark as described in Grolander (2013) in Section 8.10. It is assumed that the minimum depth of fish production (1 m) is applicable for any lake and sea basin in Sweden, including Laxemar.

The height of the first and second layer of air used in the atmosphere model (height_L1_aqu, height_L2_aqu) and the reference height used for defining the wind velocity (height_ref_aqu) are assumed to be representative for any model site. The parameter values selected for these parameters are described in Grolander (2013, Section 8.9).

The roughness length (z0_aqu), is the height in the extrapolated logarithmic wind profile at which U(z0_aqu)=0. This constant is determined based on literature studies as described in Grolander (2013, Section 8.9). It is assumed that this selected parameter value is representative for any modelled lake or sea in Sweden.

7.4 Site-dependent parameters

7.4.1 Site-specific parameters for which Forsmark data are used

Fraction of refractory carbon

To calculate the amount of carbon that is deposited in sediments the fraction of primary production that contributes to sediments, the fraction of refractory organic carbon, and the mineralisation rates in the sediments are used. The fraction of refractory carbon depends on the type of primary producers that is decomposed, phytoplankton is easily decomposed whereas macro algae are decomposed to a lower degree. Literature studies suggest that some algae decompose slower than other types. Therefore, the type of macro algae present can affect the fraction of refractory organic carbon. Also, temperature will affect the decomposition of algae. The values can therefore differ from site to site. No site-specific data are available. The data used in previous safety assessments are based on literature studies, these data are also assumed to be valid for the selected model site in Laxemar. The parameter values selected for f_refrac_macro_lake, f_refrac_micro_lake, f_refrac_plank_lake, f_refrac_macro_sea, f_refrac_micro_sea and f_refrac_plank_sea are reported in Grolander (2013, Section 8.7.2).

Mineralisation rate

The mineralisation rate in aquatic sediments (minRate_regoPG_sea, minRate_regoUP_sea, minRate_water_PM_sea, minRate_regoPG_lake, minRate_regoUP_lake, minRate_water_PM_lake) depends on bacterial biomass, the concentration and quality of organic carbon in sediments and temperature. Bacterial metabolism increases with increasing levels of autochthonous carbon sources (organic carbon produced within the aquatic system). Since the level of autochthonous production and temperature can differ between lakes, the mineralisation rate will also differ. Empirically derived mineralisation rates were calibrated using a C-12 model for the Forsmark area in SR-PSU (SKB 2015a). Similar conditions, in respect of cotrols on mineralisation rates are assumed to also be representative for the Laxemar area. The resulting parameter values are reported in Grolander (2013, Section 8.7.3).

Wind velocity

The average wind velocity at ten metres above the water surface during ice-free conditions (vel_wind_height_ref_aqu) depends on the local and regional conditions at the model site. The wind velocity is similar at both sites and therefore the Forsmark value can be used.

Solubility coefficient for CO_2

The solubility coefficient for CO_2 in lake water, (solubilityCoef_lake), depends on temperature, with a higher solubility of CO_2 at lower temperatures. Since the solubility is restricted by the ice-coverage during the winter months, the solubility coefficient is calculated based on the monthly mean temperature of the ice-free months of April to November. The solubility of CO_2 in sea water (solubilityCoef_sea) also depend on salinity as described in Section 8.8.3 in Grolander (2013). Scoping calculations suggested only small changes in the values of these parameters based on expected differences in temperature and salinity between Forsmark and Laxemar (see also Section 8.4.1), and consequently Forsmark parameters were used (Grolander 2013, Section 8.8.3).

Thickness of the oxygenated upper zone of sediments in seas

The thickness of the oxygenated upper zone of sediments in seas (z_regoUp_sea) are parameterised by a mean value for the Baltic Sea, this value is assumed to be representative for any modelled near-shore site located along the coast of the Baltic Sea. If the modelled site was located along the west cost of Sweden, this parameter might need to be updated. The corresponding value for lake sediments varies depending on the properties of the lake.

Piston velocity

The piston velocity (piston_vel_lake, piston_vel_sea) describing the gas exchange from lake water or seawater in contact with the atmosphere is dependent on temperature and wind speed. However, scoping calculations suggest only small differences and the values from Forsmark are assumed to also be representative for the Laxemar site (Grolander 2013, Section 8.8.1).

7.4.2 Site-specific data where updated data are used

Dissolved inorganic carbon in seawater

Dissolved inorganic carbon, DIC, concentrations in sea water (conc_DIC_sea) depend on runoff and precipitation in the area. The DIC concentrations in seawater for Laxemar reported in Aquilonius (2010, Section 10.13.2) is used. This value is higher than the reported value for Forsmark (Grolander 2013, Section 8.5.2.)

Dissolved inorganic carbon in lake water

The concentrations of dissolved inorganic carbon (DIC) in lake waters (conc_DIC_lake) is affected by local geochemical conditions. For example, the calcite-rich till in the Forsmark area results in high levels of DIC in lake water, with levels that are not common in Sweden. These values are not representative for the non-calcareous lakes around Laxemar. The parameter value describing the annual mean based on measurement in the Laxemar region is used, these data are presented in Andersson (2010, Section 11.4.3).

Particulate matter in sea

The value for Laxemar (conc_PM_sea) is approximately 25 % higher than the value for Forsmark and this parameter value is therefore updated to the value from Aquilonius (2010, Section 10.13.1).

Particulate matter in lake

The concentration of particulate matter (conc_PM_lake) in lake water represents a non-calcareous lake and is based on measurements from lakes in the Laxemar region (Andersson 2010, Section 11.4.3).

Fraction of DIC present as CO_2

This parameter (f_H_2CO_3_lake) describes the fractional contribution of H_2CO_3* to the total pool of dissolved inorganic carbon (DIC) in lake water and is much dependent on the pH of the water. H_2CO_3* represents the dissolved $CO_{2\,(aq)}$ and H_2CO_3 that is available for degassing from the lake water surface. A comprehensive description of this parameter is found in Grolander (2013, Section 8.8.2). The central value of f_H_2CO3_lake is calculated based on pH-measurements from three lakes in Laxemar at the water depth of 0.5 m (October 2002–May 2005) resulting in a pH of 7 (Andersson 2010, Table 4-16). The pH values of seawater in Forsmark and Laxemar are similar and therefore the SR-PSU value for f_H_2CO_3_sea is used also for Laxemar.

Production of edible fish and crayfish

The production of edible fish in lakes has been assessed in both Forsmark and Laxemar in Andersson (2010). The results show that the lake fish production was twice as high in Forsmark as compared with the Laxemar model area. This suggests that site-specific characteristics will affect the amount of edible fish that is produced in the model area. The crayfish production in Laxemar has not been estimated, but a small population has been observed in Lake Frisksjön. To avoid underestimation of the crayfish production the same value as in Forsmark was used (Andersson 2010, Section 11.4.4.). The depth of lakes in which crayfish may be found was much less in Laxemar. The parameters prod_edib_fish_lake and z_min_prod_edib_cray_lake were updated based on data for Laxemar presented in Andersson (2010, Section 11.4.4). The production of fish in the sea was estimated to be higher in Laxemar than in Forsmark, and was based on data presented in Aquilonius (2010, Section 11.4.4).

The oxygenated zone in lake sediments

The thickness of the oxygenated zone of lake sediments (z_regoUp_lake) in Laxemar is thinner than in Forsmark, where it was defined by the thickness of the microbial mat present. This microbial mat is not present in all types of lakes in Sweden e.g. in Laxemar. The depth of the oxygenated zone was estimated for Lake Frisksjön, based on the lack of lamination of the sediments indicating that the aerobic conditions are present in periods (during circulation) and was compared to literature values (Andersson 2010, Section 4.6.2).

7.4.3 Time-dependent parameters describing biomass and net primary productivity of aquatic primary producers

Biomass and net primary production (NPP) of primary producers are dependent on many factors, of which nutrient and light availability are often the most important. Nutrient concentrations in future aquatic ecosystems are assumed to be similar to those occurring at present. Light availability, on the other hand, may differ due to a different geometry (depth) of future marine and lake basins. The photic depth and/or the average basin depth of aquatic objects have been used to estimate the biomass and the net primary production in developing marine basins, lakes and streams over time.

In general, the estimates of area-specific annual mean biomasses and annual net primary production (NPP) in developing objects follow the approach by Grolander (2013) that, in turn, is based on Aquilonius (2010) for marine systems and Andersson (2010) for limnic systems. When possible, the relationships are based on site-specific data from Laxemar. The biomass and NPP were estimated for benthic macro and micro vegetation and phytoplankton separately, and different relationships were used for the marine and limnic systems. However, the estimated biomass and net primary production in streams are based on the average depth instead of the photic depth. The same functional groups found in lakes are also found in the stream ecosystems (Andersson 2010) and although other species may be present, the functions to describe biomass and NPP for lakes were also assumed to be valid for describing stream biomass and NPP.

Photic area

The photic depth is the maximum depth for net primary production by vegetation in aquatic systems. In the marine areas of Laxemar, the photic depth of pelagic primary producers was estimated to be 20 m and for bottom vegetation to be 19 m (Aquilonius 2010, Grolander 2013).

The photic depth in lakes is in general shallower than in the Baltic Sea. In contrast to the relatively large photic depth of the clear-water lakes in Forsmark (4.3 m, Andersson 2010, Grolander 2013), the photic depth in the more humic Frisksjön in Laxemar has been estimated to 2.1 m (Andersson 2010). This depth was used for all historic and future lakes in Laxemar. The photic area (area_photic), is the bottom area shallower than photic depth, i.e. bottoms with light enough for bottom vegetation to exist. Since ingrowth of reed is assumed down to 2 m depth, and that depths shallower than 2 m are, by definition therefore, part of the mire, the photic bottom area of lakes will only cover a narrow band around the lake shore, outside the reed belt. To compensate somewhat for this underestimation of the photic area, the photic area of the final stream stage was added to the bottom area between 2 and 2.1 m depth.

All current and future streams in Laxemar are shallower than the photic depth of 2.1 m and therefore the photic area equals the area of the stream.

Benthic macro vegetation biomass in the sea

Based on field observations outside Laxemar, the biomass of benthic macro vegetation (macrophytes; biom_pp_macro) per sea basin was estimated from GIS models using depth, slope, aspect, water temperature, Secchi depth, wave exposure and light conditions at the bottom as predictors (Aquilonius 2010). In agreement with the SR-PSU assessment approach (Grolander 2013), the macrophyte biomass of developing marine biosphere objects was estimated using a negative exponential relationship between GIS-modelled basin biomass in Laxemar and average depth (Figure 7-1). The biomass was set to zero in objects where the average depth was larger than the photic depth (19 m).

Benthic micro vegetation biomass in the sea (biom_pp_micro)

The biomass of benthic micro vegetation (microphytes; biom_pp_micro) per basin in Laxemar was estimated by GIS modelling (Aquilonius 2010). The microphyte biomass of developing marine biosphere objects was estimated by using a negative exponential relationship between the GIS modelled microphyte biomass and basin average depth (Figure 7-2). This is consistent with the macrophyte biomass above and gives a better fit than the linear relationship used in the SR-PSU assessment (Grolander 2013). The biomass was set to zero in objects where the average depth was larger than the photic depth (19 m).

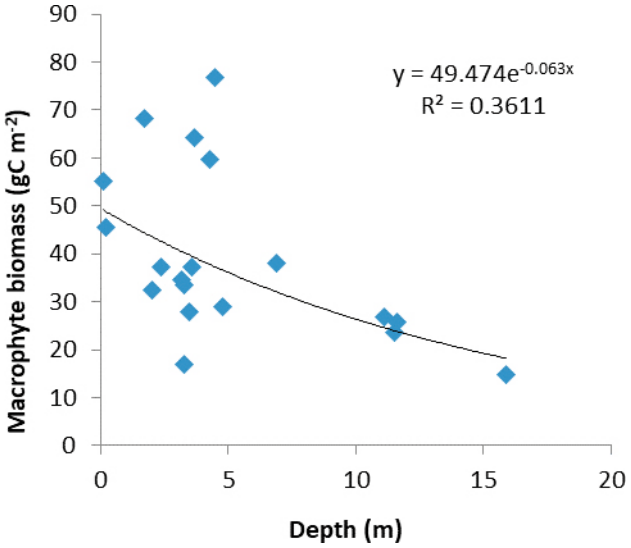

Figure 7-1. *Exponential relationship between the macrophyte biomass per basin and the average basin depth.*

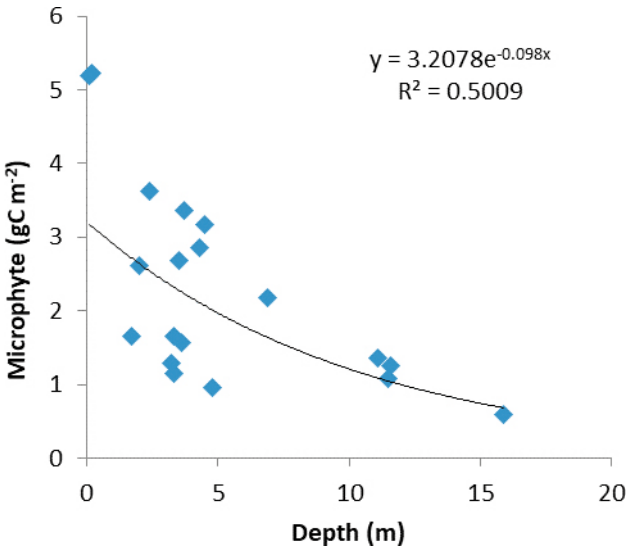

Figure 7-2. *Exponential relationship between the microphyte biomass per basin and the average basin depth.*

Phytoplankton biomass in the sea

Phytoplankton biomass in the sea area of Laxemar (biom_pp_plank), was modelled as a function of the supply of deep water nutrients (related to depth), nutrients from diffuse coastal runoff (negatively related to SWM, the Simplified Wave Model exposure index), and river nutrient runoff in Borholmsfjärden (Aquilonius 2010, Section 4.3.3). In agreement with Grolander (2013), the phytoplankton biomass of developing marine biosphere objects was based on a linear relationship through the origin between the modelled phytoplankton biomass and average basin depth (Figure 7-3).

Benthic macro vegetation biomass in lakes

All lake data in Laxemar are from Lake Frisksjön, which is assumed to be representative for the historic and future lakes in the area. The area-specific macrophyte biomass (biom_pp_macro) for each biosphere object was estimated as the area-specific mean biomass in the photic zone in Frisksjön (1.6 gC m^{-2}), multiplied by the photic area and divided by the lake area of the specific biosphere object.

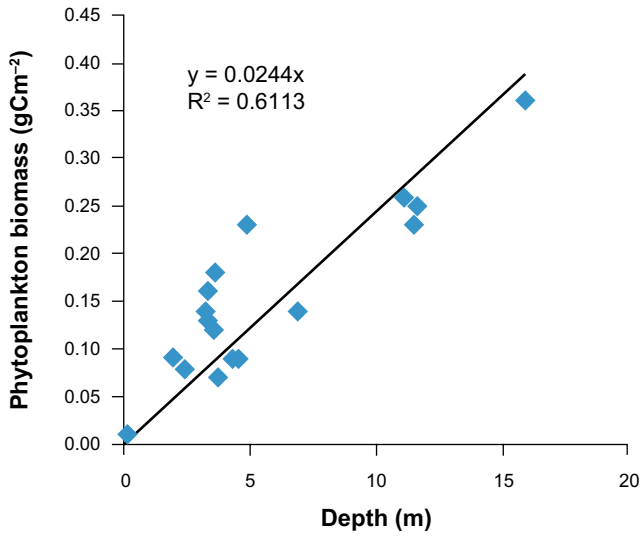

Figure 7-3. *Linear relationship between the phytoplankton biomass per basin and the average basin depth.*

Benthic micro vegetation biomass lakes

In agreement with Andersson (2010), the microbenthic vegetation (biom_pp_micro) was assumed negligible in lakes.

Phytoplankton biomass in lakes

The area-specific mean phytoplankton biomass (biom_pp_plank) was calculated as the volume-specific mean biomass in Frisksjön (0.28 gC m^{-3}) in the photic zone multiplied by the mean depth of the photic zone. Since depths shallower than 2 m (photic depth = 2.1m) are rapidly infilled by reed and thereby a part of the mire, the mean photic depth of each biosphere object was assumed to be close to the functional photic depth of 2.1 m.

Benthic macro vegetation NPP in the sea

By accounting for the productivity of specific macrophyte groups, the area-specific annual NPP in Laxemar was modelled based on irradiance, depth and their area-specific biomass (Aquilonius 2010, Chapters 4 and 6). The macrophyte NPP in developing marine objects (NPP_pp_macro) was estimated based on an exponential relationship between the modelled NPP per basin and the average basin depth (Figure 7-4). The NPP was set to zero in objects where the average depth was larger than the photic depth (19 m).

Benthic micro vegetation NPP in the sea

The area-specific annual microphyte NPP (NPP_pp_micro) in Laxemar has been modelled as being dependent on irradiance, depth and bottom substrate (Aquilonius 2010, Chapters 4 and 6). The microphyte NPP in developing marine objects was estimated based on an exponential relationship between the modelled NPP per basin and the average basin depth (Figure 7-5). This is consistent with the macrophyte NPP above and gives a better fit than the linear relationship used in the SR-PSU assessment (Grolander 2013). The NPP was set to zero in objects where the average depth was larger than the photic depth (19 m).

Phytoplankton NPP in the sea (NPP_pp_plank)

The area-specific annual phytoplankton NPP in the sea (NPP_pp_plank) was obtained by multiplying modelled areal biomass by an overall annual net primary production/biomass (P/B) ratio of 98 (Aquilonius 2010). The NPP in developing marine objects was estimated based on a linear relationship between the modelled annual NPP per basin and average depth (Figure 7-6).

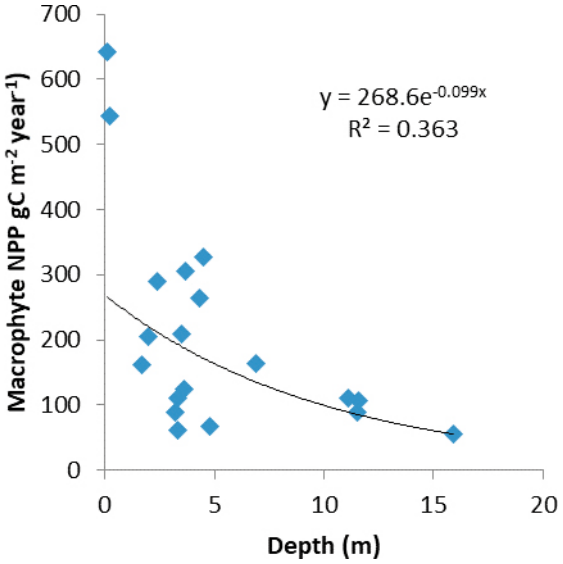

Figure 7-4. *Exponential relationship between the macrophyte NPP per basin and the average basin depth.*

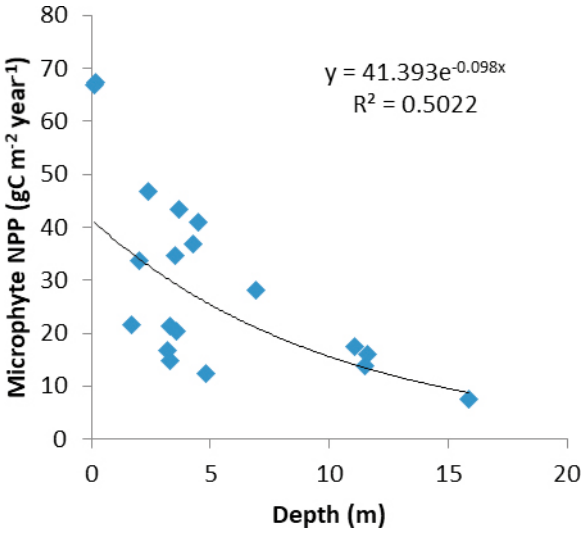

Figure 7-5. *Exponential relationship between the microphyte NPP per basin and the average basin depth.*

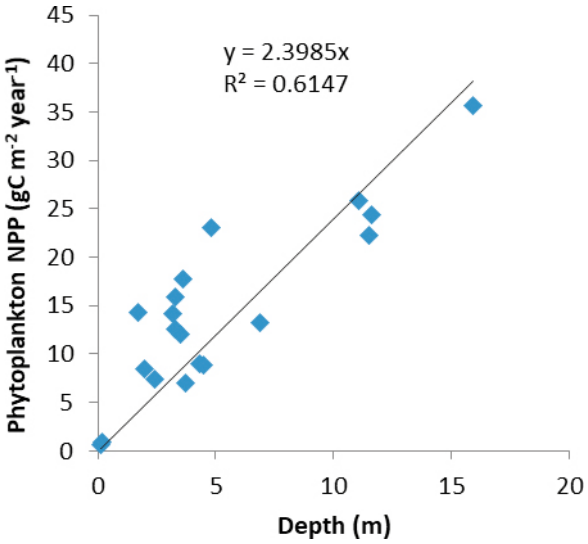

Figure 7-6. *Linear relationship between the phytoplankton NPP per basin and the average basin depth.*

Benthic macro vegetation NPP in lakes

The area-specific macrophyte annual NPP (NPP_pp_macro) was estimated as the area-specific mean annual NPP in the photic zone in Lake Frisksjön (2.05 gC m^{-2} $year^{-1}$), multiplied by the photic area of the biosphere object and divided by the biosphere object lake area.

Benthic micro vegetation NPP lakes

In agreement with Andersson (2010), the microbenthic NPP (NPP_pp_micro) was assumed negligible in lakes.

Phytoplankton NPP in lakes

The area specific annual phytoplankton NPP (NPP_pp_plank) for each biosphere object was set constant to the observed area-specific NPP of phytoplankton in Lake Frisksjön (40 gC m^{-2}).

7.4.4 Updates in BioTEx since SR-PSU

In some aspects, BioTEx has been further optimised since the SR-PSU assessment, resulting in new parameters. The new parameters used for the aquatic ecosystem are described here.

The fraction of inorganic chlorine in primary producers

This fraction of inorganic chlorine relative to the total chlorine content in primary producers (f_inorg_Cl_PP_aqu) was assumed to be similar to the value found for terrestrial primary producers, due to lack of data for aquatic primary producers (see Section 8.5, Terrestrial ecosystems).

Density of lake water

This parameter (dens_water_lake) was included in earlier versions of the model but has now been made a separate parameter that distinguishes between the sea and lake water, where the latter represent fresh water and is the standard density for water (1 000 kg m^{-3}). This is considered a generic parameter.

Density of seawater

This parameter (dens_water_sea) describes the density of the seawater for the sea outside Laxemar and is a function of the salinity and temperature. The parameter value (1 005 kg m^{-3}) is taken from Feistel et al. (2010) and represents sea water at a salinity of 7.7 PSU and a temperature of 15°C, approximately corresponding to the summer conditions somewhat south of Öland. This parameter was not defined for the SR-PSU assessment.

8 Terrestrial ecosystem parameters

In this Chapter, the selection of terrestrial ecosystem parameter values for the Laxemar model site is described. The parameters presented below are those describing terrestrial ecosystems, and, to some extent, human utilisation associated with wetlands, agricultural use of drained wetlands and garden plots. BioTEx represents a natural terrestrial ecosystem (mire), drained agricultural land, the infield-outland agricultural system and garden plot cultivation in the same way as in the recent safety assessment SR-PSU conducted for the Forsmark model area and, therefore, the parameter definitions are mainly the same. However, in some cases, parameter values have been slightly updated, in SE-SFL, radionuclide accumulation in present-day agricultural land under continuous cultivation is described by a separate model. These updates and the set of new parameters for this model are also described below.

8.1 Effects of site characteristics on parameter values

In many cases the processes and parameters are generic and do not depend on site-specific characteristics. For these parameters, the selected parameter values can be assumed to be the same for any selected model site in Sweden. For other parameters and processes, site-specific characteristics affect the parameter values.

Generally, there are several parameters that are affected by a change in temperature and/or precipitation. However, the differences between Forsmark and Laxemar is small (+1.4° C and +53 mm precipitation in Laxemar based on data from the reference period 1961–1990, Climate report) and, in some cases, the direct response to temperature and precipitation is obscured by other factors e.g. soil conditions or the data available to illustrate the relationship between climate differences and terrestrial ecosystem parameters are few or missing. It is, therefore, in most cases justified to use data collected for Forsmark also for the SE-SFL. These assumptions are valid for the Laxemar example site. However, if another example site with other site characteristics were to be selected some of these parameter values might need to be updated.

For some parameters, the parameter values are expected to differ between Laxemar and Forsmark and these are therefore updated here. These parameters would also be expected to be updated if another example site were to be selected.

In the following Sections, the parameters are evaluated based on their dependency on site-specific characteristics and the selected parameter values are described. In Chapter 10, the parameter values used in the *Alternative regional climate evaluation case* are discussed.

8.2 Selection of parameter data

In this Section, the methods for parameterisation and the selected values for terrestrial ecosystem parameters are described. Four different parameterisation methods were used:

1. For the parameters where the assumption was made that site-specific characteristics will not affect the selected parameter values in any significant way, the SR-PSU data were selected and a motivation is given as to why the assumption was made. For details of the selected data the reader is referred to the parameter report of SR-PSU (Grolander 2013), see also Section 8.3 below.
2. For parameters for which site-specific changes are likely, but the difference compared with Forsmark data is deemed small (less than 10 %), the data from SR-PSU were used.
3. For parameters where site-specific changes are likely and the difference was more than 10 %, site-specific data representing the conditions in Laxemar were used for parameterisation.
    a. In some of these cases, parameter values from the SR-Site safety assessment from Laxemar were used and the detailed information on the parameterisation is given in Löfgren (2010, Section 13.4), see Section 8.4.

b. In some cases, parameter values from the previous safety assessment SR-Site were not applicable and new parameter values were derived; the assignment of values to these parameters is described in detail in Section 8.4 of this chapter.

4. Some new parameters are used in the updated version of BioTEx for SE-SFL, as compared with SR-PSU; the assignment of values to these is described in Section 8.5

8.3 Generic parameters

The parameters assumed to be generic, i.e. they are not expected to change much as a consequence of a re-localisation of the modelling to Laxemar (or a similar locality in Sweden), are parameterised by using data from SR-PSU assessment. These parameters are described below and listed in Table 8-1 where also a reference is given to where further details on the assignment of values to each of the parameters is found. Selected parameter values are listen in Appendix G.

The parameters describing the characteristics of cattle and herbivores are assumed to be generic. Concentrations of carbon in meat and milk (conc_C_meat, conc_C_milk,) and parameters describing the habits of cows and herbivores could be assumed to be the same for any site in Sweden (ingRate_C_cattle, ingRate_soil_cattle, ingRate_water_cattle, f_mush_herbiv). The fraction of radionuclides in hay remaining when manure is applied to arable land (f_loss_orgFert) is also regarded as generic. Also, the densities of milk and water are generic (dens_milk, dens_water_lake).

Parameters used for calculation of atmospheric flows are based on generic parameters that can be assumed to be representative for any site in Sweden. This applies to the parameter drag coefficient, which represents the drag resistance of the vegetation in the canopy atmosphere (dragCoef), and to the heights of vegetation layers (height_L1_ter, height_L2_ter). The Karman constant (karman_const) is a universal constant. The concentration of carbon in the atmosphere (conc_C_atmos) can be assumed to identical regardless of selected model site. The reference height for defining wind velocity (height_ref_ter) is 10 m by definition. The only parameter describing the atmospheric flows that is assumed to be affected by site-specific characteristics is the wind velocity (vel_wind_height_ref_ter) and it is parameterised by wind velocity measurements from the Laxemar area as described below.

Also, the parameters describing the properties of crops and vegetation are assumed to be similar for any site within Sweden. These parameters include leaf width, vegetation leaf area index, leaf storage capacity, the removal of deposited radionuclides from the plant leaf surface and the height from the ground of the canopy layer (leaf_width_cereal, leaf_width_fodder, leaf_width_ter, leaf_width_tuber, leaf_width_veg, LeafStoreCapacy, LAI_cereal, LAI_fodder, LAI_ter, LAI_tuber, LAI_veg, washoffCoef,height_CA_tuber, height_CA_veg, height_CA_fodder, height_CA_ter, height_CA_ cereal). Some of these parameters could be affected by site-specific characteristics if the differences between the sites are sufficiently large. For example, the height from the ground of the canopy layer (height_CA_cereal) and leaf area index (AI) for cereals do differ between different areas of the world. However, for conditions found in Sweden, the differences are expected to be small and therefore the same parameter values can be used for Forsmark and the example site Laxemar. This is assumed to be the case for many of the properties characterising crops and vegetation.

There are also parameters that are defined by the agri- and silvicultural practices, such as the amount of resources needed to sustain a certain demand (demand_hay, demand_AlgFertil, area_support_ wood, demand_peat, fuel_cons_peat and fuel_cons_wood). The values for these parameters were originally selected to be representative for the southern part of Sweden and are thus also applicable to Laxemar.

The fraction of carbon in wood and peat (f_C_peat, f_C_wood) and in newly synthesised biomass assimilated via root uptake (f_rootUptake) are not expected to differ between sites in Sweden. The fraction of refractory organic material of mire primary producers left after initial mineralisation (f_refrac_ter) may vary due to temperature and the length of the vegetation period but is assumed to be the same in Forsmark and Laxemar.

The parameters describing the depth of oxidising layers of peat (z_regoUp_ter) and the depth of the cultivated layer of agricultural soils (z_regoUp_IO, z_regoUp_GP) are also assumed to be generic for sites within central or southern Sweden, and the value of the latter has also been applied to the constant agricultural ecosystems used in this assessment (z_regoUp_agri).

The parameters describing the concentration of dust above the agricultural fields and wetlands are also assumed to be similar at any location in Sweden (conc_Dust, conc_Dust_ter).

Table 8-1. Generic parameters for terrestrial ecosystem.

Parameter name	Unit	Description	Reference
area_support_wood	m^2	The area supporting a household's need of fire wood for heating (corresponding to 20 000 kWh $year^{-1}$) per individual	Grolander (2013, Section 9.14.8)
conc_C_atmos	$kg_C\ m^{-3}$	Concentration of carbon in the atmosphere (above the ground)	Grolander (2013, Section 9.5.7)
conc_C_meat	$kg_C\ kg_{FW}^{-1}$	Concentration of carbon in meat	Grolander (2013, Section 9.13.6)
conc_C_milk	$kg_C\ kg_{FW}^{-1}$	Concentration of carbon in milk	Grolander (2013, Section 9.13.5)
conc_Dust	$kg_{DW}\ m^{-3}$	Concentration of fine soil particles in air above agricultural land	Grolander (2013, Section 9.10)
conc_Dust_ter	$kg_{DW}\ m^{-3}$	Concentration of fine soil particles in air above wetland vegetation	Grolander (2013, Section 9.10)
demand_AlgFertil	$kg_C\ m^{-2}\ year^{-1}$	Demand for algae for used in organic fertilization in the infield-outland system	Grolander (2013, Section 9.14.7)
demand_hay	$kg_C\ m^{-2}\ year^{-1}$	Demand for winter fodder arising from areas subject to organic fertilization in the infield-outland system	Grolander (2013, Section 10.9)
demand_peat	kg_{DW}	The mass of peat needed to heat a house-hold over a 50-year period (corresponding to 20 000 kWh $year^{-1}$) per individual	Grolander (2013, 9.14.9)
dens_milk	$kg_{FW}\ l^{-1}$	Density of milk	Grolander (2013, Section 9.13.4)
dragCoef	unitless	Drag coefficient of the canopy	Grolander (2013, Section 9.5.1)
f_C_peat	$kg_C\ kg_{DW}^{-1}$	Ratio of mass of carbon to dry weight of peat (used to scale from mass to volume/ depth)	Grolander (2013, Section 9.4.3)
f_C_wood	$kg_C\ kg_{DW}^{-1}$	Ration of mass of carbon to dry weight of firewood produced by terrestrial primary producers, e.g. stem wood of Norway spruce	Grolander (2013, Section 9.14.8)
f_loss_orgFert	$Bq\ Bq^{-1}$	Fraction of the original activity concentration in hay remaining when manure is applied to arable land	Grolander (2013, Section 9.13.8)
f_mush_herbiv	$kg_C\ kg_C^{-1}$	Fraction of mushrooms in the diet of terrestrial herbivores	Grolander (2013, Section 9.13.7)
f_refrac_ter	$kg_C\ kg_C^{-1}$	Fraction of refractory organic material of mire primary producers left after initial mineralization	Grolander (2013, Section 9.9.1)
f_rootUptake	$kg_C\ kg_C^{-1}$	Fraction of carbon in newly synthesized biomass assimilated via root uptake	Grolander (2013, Section 9.4.4)
fuel_cons_peat	$kg_{DW}\ year^{-1}$	The yearly consumption of peat fuel to produce 20 000 kWh	Grolander (2013, Section 9.14.9)
fuel_cons_wood	$kg_{DW}\ year^{-1}$	The yearly consumption of wood fuel (dry weight) to produce 20 000 kWh	Grolander (2013, Section 9.14.8)
height_CA_cereal	m	Height from the ground of the canopy layer for cereals	Grolander (2013, Section 9.5.9)

Parameter name	Unit	Description	Reference
height_CA_fodder	m	Height from the ground of the canopy layer for fodder	Grolander (2013, Section 9.5.9)
height_CA_ter	m	Height from the ground of the canopy layer in a mire	Grolander (2013, Section 9.5.9)
height_CA_tuber	m	Height from the ground of the canopy layer for tubers	Grolander (2013, Section 9.5.9)
height_CA_veg	m	Height from the ground of the canopy layer for vegetables	Grolander (2013, Section 9.5.9)
height_L1_ter	m	Height from the ground of the first above-canopy layer	Grolander (2013, Section 9.5.2)
height_L2_ter	m	Height from the ground of the second above-canopy layer	Grolander (2013, Section 9.5.3)
height_ref_ter	m	Reference height used for defining wind velocity	Grolander (2013, Section 9.5.8)
ingRate_C_cattle	$kg_C\ day^{-1}$	Daily energy demand for cattle expressed in units of carbon	Grolander (2013, Section 9.13.1)
ingRate_soil_cattle	$kg_{DW}\ day^{-1}$	Daily ingestion rate of soil by cattle	Grolander (2013, Section 9.13.2)
ingRate_water_cattle	$m^3\ day^{-1}$	Daily ingestion rate of water by cattle	Grolander (2013, Section 9.13.3)
karman_const	unitless	Karman constant	Grolander (2013, Section 9.5.4)
LAI_cereal	$m^2\ m^{-2}$	Ratio of total upper leaf surface of cereals divided by the surface area of the agricultural land on which the vegetation grows (Leaf Area Index)	Grolander (2013, Section 9.5.6)
LAI_fodder	$m^2\ m^{-2}$	Ratio of total upper leaf surface of fodder divided by the surface area of the agricultural land on which the vegetation grows (Leaf Area Index)	Grolander (2013, Section 9.5.6)
LAI_ter	$m^2\ m^{-2}$	Ratio of total upper leaf surface of vegetation divided by the surface area of the mire on which the vegetation grows (Leaf Area Index)	Grolander (2013, Section 9.5.6)
LAI_tuber	$m^2\ m^{-2}$	Ratio of total upper leaf surface of tubers plants divided by the surface area of the agricultural land on which the vegetation grows (Leaf Area Index)	Grolander (2013, Section 9.5.6)
LAI_veg	$m^2\ m^{-2}$	Ratio of total upper leaf surface of leafy vegetation divided by the surface area of the agricultural land on which the vegetation grows (Leaf Area Index)	Grolander (2013, Section 9.5.6)
leaf_width_cereal	m	Leaf width of cereals	Grolander (2013, Section 9.5.5)
leaf_width_fodder	m	Leaf width of fodder	Grolander (2013, Section 9.5.5)
leaf_width_ter	m	Leaf width of terrestrial vegetation	Grolander (2013, Section 9.5.5)
leaf_width_tuber	m	Leaf width of tubers plants	Grolander (2013, Section 9.5.5)
leaf_width_veg	m	Leaf width of vegetables	Grolander (2013, Section 9.5.5)
LeafStoreCapacy	$m^3\ m^{-2}$	Leaf storage capacity	Grolander (2013, Section 9.14.3)
z_regoUp	m	Depth of upper less compacted agricultural soils in early agricultural societies and in a modern kitchen garden	Grolander (2013, Section 9.7)
z_regoUp_ter	m	Depth of oxygenated and biologically active peat layer	Grolander (2013, Section 9.7)
conc_Cl_regoUp_ter_D	$gCl\ m^{-3}$	Concentration of dissolved chlorine in the mire	Grolander (2013, Section 9.6.2)

8.4 Site-specific parameters

Generally, there are several parameters that are affected by site-specific characteristics such as temperature, hydrological properties and geochemical conditions. Here we identify the site-specific parameters for which the differences are small (less than 10 %). These are described in Section 8.4.1, whereas the parameters for which the expected differences are significant, and therefore parameter values based on site conditions at Laxemar are assigned, are described in Section 8.4.2.

8.4.1 Site-specific parameters for which Forsmark data are used

Net primary production, NPP, depends on temperature and precipitation. NPP values are used for different crops and are used in the calculation of atmospheric concentrations above the biosphere object. The atmospheric concentrations were shown to be rather insensitive to the variation in NPP parameter values (unpub. calculations). Parameter values for net primary production for agricultural crops comprising cereals, tubers and fodder (NPP_cereal, NPP_tuber, NPP_fodder) were parameterised using national figures in SR-PSU, where the mean was a best estimate representing Swedish conditions. Similarly, NPP (NPP_ter) and biomass (biom_pp_ter) for mires were based on data representing both Forsmark and Laxemar. Consequently, data from SR-PSU could be used in SE-SFL in these cases. See section below for updated descriptions of NPP for vegetables and above-ground vegetables.

Production of berries, mushrooms and meat from game (prod_edib_berry, prod_edib_mush, prod_edib_game) is also affected by temperature and precipitation. These parameters values would therefore hypothetically vary between sites in Sweden. However, no or few data are available for wetlands and the figures are based on a large geographical variation from mainly terrestrial habitats. It is therefore considered that the SR-PSU parameter values also are representative for Laxemar.

The concentration of chlorine, Cl, in mire vegetation (conc_Cl_PP_ter) and the concentration of dissolved chlorine in surface peat (conc_Cl_regoUp_ter_D) can be expected to vary between sites due to local conditions. However, data on chlorine concentrations in vegetation and pore water from mire ecosystems are scarce. In SR-PSU, the parameter value for vegetation was estimated from two Laxemar locations, and the parameter value for pore water concentration was estimated from five mires in the Forsmark area. These parameter values are deemed to be equally relevant for Laxemar conditions and reasonable to use for other wetlands in South and Central Sweden.

Mineralisation rates are also dependent on temperature and precipitation (minRate, minRate_regoPG_ter, minRate_regoUp_ter) and due to the small difference in temperature and perciptation between Forsmark and the Laxemar example site, the Forsmark values are considered as representative also in this assessment.

Water flux from the saturated to the unsaturated zone in a drained mire where cereals are grown (q_sat_unsat_agri, (earlier name Flux_water_satSoil_agri) depends on precipitation and temperature. The estimate used in SR-PSU was based on comparisons of data from three different sources covering southern Sweden and northern Germany (Grolander 2013) and is expected to also be valid for Laxemar.

The parameter piston velocity (gas exchange coefficient for peat pore water in contact with the atmosphere) depends on temperature. Scoping calculations investigating how site-specific temperature affects the ice-free conditions conditions on mires, and thereby the piston velocity (exchange of CO_2), also suggest a small difference between the Forsmark and Laxemar sites (4 %) and therefore data reported for SR-PSU are used also in this safety evaluation.

The solubility of carbon dioxide in pore water of mires, solubilityCoef_ter, depends on temperature. The solubility has been calculated using temperature measurements from Laxemar and the results has been compared with the solubility calculated from Forsmark. The difference is small (6 %) and therefore the data used for Forsmark in SR-PSU are used also in this assessment.

In Table 8-2 the parameters for which Forsmark data are used are listed and a detailed reference, the values used are listed in Appendix G.

Table 8-2. Parameters for Terrestrial Ecosystems for which the Forsmark Data are considered Representative also for Laxemar.

Name	Unit	Description	Reference
N_irrig	$year^{-1}$	Number of irrigation events	Grolander (2013, Section 9.14.5)
biom_pp_ter	$kg_C\ m^{-2}$	Biomass above- and below-ground, in a terrestrial ecosystem	Grolander (2013, Section 9.3)
conc_Cl_PP_ter	$gCl\ kg_C^{-1}$	Concentration of chlorine in vegetation	Grolander (2013, Section 9.6.1)
minRate	$kg_C\ kg_C^{-1}\ year^{-1}$	Mineralization rate for agricultural soils (drained mire, inland-outfield and garden plot)	Grolander (2013, Section 8.7.3)
minRate_regoPG_ter	$kg_C\ kg_C^{-1}\ year^{-1}$	Mineralization rate in terrestrial postglacial sediments	Grolander (2013, Section 9.9.1)
minRate_regoUp_ter	$kg_C\ kg_C^{-1}\ year^{-1}$	Mineralization rate in upper terrestrial regolith	Grolander (2013, Section 9.9.1)
NPP_cereal	$kg_C\ m^{-2}\ year^{-1}$	Total net primary production (above- and below-ground) of cereals in cultivated peat (drained mire) and sandy soils (infield-outland)	Grolander (2013, Section 9.11)
NPP_fodder	$kg_C\ m^{-2}\ year^{-1}$	Total net primary production (above- and below-ground) of fodder in cultivated peat	Grolander (2013, Section 9.11)
NPP_ter	$kg_C\ m^{-2}\ year^{-1}$	Total net primary production (above- and below-ground) in a terrestrial ecosystem	Grolander (2013, Section 9.11)
NPP_tuber	$kg_C\ m^{-2}\ year^{-1}$	Total net primary production (above- and below-ground) of tuber plant in cultivated peat (drained mire) and garden plot	Grolander (2013, Section 9.11)
piston_vel_ter	$m\ year^{-1}$	Gas-exchange coefficient for peat pore water in contact with the atmosphere	Grolander (2013, Section 9.4.5)
prod_edib_berry	$kg_C\ m^{-2}\ year^{-1}$	Sustainable yield with respect to edible berries per unit area	Grolander (2013, Section 9.12)
prod_edib_game	$kg_C\ m^{-2}\ year^{-1}$	Sustainable yield with respect to edible game per unit area	Grolander (2013, Section 9.12)
prod_edib_mush	$kg_C\ m^{-2}\ year^{-1}$	Sustainable yield with respect to edible mushrooms per unit area	Grolander (2013, Section 9.12)
solubilityCoef_ter	$(mol\ m^{-3})\ (mol\ m^{-3})^{-1}$	Solubility coefficient for carbon dioxide in pore water	Grolander (2013, Section 9.4.6)

8.4.2 Site-specific parameters where Laxemar data are assigned

The parameters for which site characteristics are expected to affect selected parameter values significantly are parameterised with new data based on site-specific conditions at Laxemar.

The parameters describing the amount of water used for irrigation (amount_irrig), the fraction of dissolved inorganic carbon in peat porewater, the length of the vegetation period and the wind velocity are site-specific and data representative for the conditions at Laxemar were estimated for these parameters as described below. The parameter values are listed in Appendix G.

Amount of water used for irrigation

This parameter describes the total annual amount of water per unit area (amount_irrig) that is used to irrigate the garden plot. The crops in this case are dominated by potatoes and therefore the amount of water needed is taken from calculations based on the water need for potatoes presented in Johansson and Klingspor (1977). They calculated the daily balance between precipitation and evapotranspiration during the vegetation period for several different regional areas in Sweden during a normal year (1976) (detailed description of methods in Johansson (1973). The deficit could either be supplied

from capillary rise or by irrigation, but for the specific safety evaluation case investigation effects of irrigation, it has cautiously been assumed that all of the deficit is covered by irrigation. Their results suggested that potatoes and fodder generally need more water than e.g. barley. The value for potatoes in the southern coastal Sweden was taken as a representative mean. The number of irrigation events (N_irrig) was, however, considered to be the same as for SR-PSU.

f_H2CO3_ter

This parameter (f_H2CO3_ter) describes the fraction of H_2CO_3* (the mixture of H_2CO_3 and $CO_{2(aq)}$) to the total pool of dissolved inorganic carbon (DIC) in peat pore water. H_2CO_3* represents the dissolved CO_2 that is available for degassing from the peat pore water surface. A comprehensive description of this parameter is found in Grolander (2013, Section 9.4.2). The central value of the f_H2CO3_ter was calculated by assuming a pH of 4.5 at a mean temperature (during the ice-free season) of 15 °C, which represents a poor fen in Laxemar.

vel_wind_height_ref_ter

Data from the local meteorological station at Äspö were used to determine the wind speed at 10 metres height for the Laxemar-Simpevarp site. The data set was obtained from the SKB database Sicada (the Sicada delivery ID is 1238587 – Data Delivery SICADA_10_057_1.pdf). The wind speed is registered every 30 minutes and calculations are based on data for the period October 2003 to October 2007. Monthly arithmetic means were calculated for the whole period, and the monthly means were used for the missing months in 2003 and 2007 so that the data set would represent five years (Löfgren 2010, Table 13-20).

Table 8-3. Site-specific parameters were Laxemar data are selected.

Name	Unit	Description
amount_irrig	m $year^{-1}$	Total amount of water used for all irrigation events during the vegetation period
f_H2CO3_ter	Bq Bq^{-1}	The fraction of H_2CO_3 and $CO_{2(aq)}$ to the total pool of dissolved inorganic carbon (DIC)
percolation_agri	m^3 m^{-2} $year^{-1}$	Downward flux of water from agricultural soils (drained mire, garden plot and infield-outland)
vel_wind_height_ref_ter	m s^{-1}	Wind velocity at reference height

8.5 Updates in the BioTEx since SR-PSU

Since SR-PSU, BioTEx has been updated in some respects, as presented in the **Biosphere synthesis** (Chapter 8). Consequently, some parameters were added to the model used for the SE-SFL as compared with the SR-PSU model. Other parameters used in the SR-PSU model were excluded from the SFL model or were given different names. The updated parameters are listen in Table 8-4. Parameters describing the translocation of irrigation water from leaves to edible parts and a wash-off coefficient were added, as well as a new approach was introduced to handle soil respiration. Parameters describing chlorine, calcium and potassium concentrations were added and parameters for biomass in crops changed name. These changes are described below. Parameter values are listed in Appendix G.

8.5.1 Water uptake in growing crops

This parameter (q_sat_unsat_agri, earlier name in SR-PSU was Flux_water_satSoil_agri) describes groundwater uptake and was calculated as in SR-PSU (Grolander 2013) using figures of additional water need apart from the precipitation (Johansson and Klingspor 1977), but was adapted to the conditions for the more southerly located Laxemar. Additionally, the uptake was weighted in accordance with the proportion of the different crops (different needs) grown on the drained mire (0.56 cereals, 0.37 fodder and 0.07 potatoes).

8.5.2 Time period of irrigation

This period covers the most sensitive occasions in plant development to water shortage (time_ irrigationPeriod) and this parameter is new since SR-PSU. This period is somewhat longer in the south of Sweden compared to central Sweden. Cabbage is a fast growing vegetable and grown during the summer, it may take between 55 and 65 days until harvest (e.g. Harvest to table 2019). Cabbage is sensitive to drought periods in the latter part of the growing period. Here it is assumed that the last 40 days represent the most sensitive period and irrigation is applied on crops during this period. This period is divided in accordance with number of irrigation events (N_irrig).

8.5.3 Fraction of inorganic chlorine in primary producers

For all other elements, except chlorine, it is assumed that radionuclides in plants and litter are incorporated into organic matter and released in proportion to the mineralisation of organic matter. However, approximately 60 % of chlorine in plant tissue is found in inorganic form (Redon et al. 2011), and this fraction can be expected to be readily released when the leaves senesce, and cell membranes are disrupted. Therefore, one parameter describing the fraction of inorganic chlorine in primary producers is added to BioTEx (f_inorg_Cl_PP_ter). This is also assumed to be valid for aquatic primary producers (f_inorg_Cl_PP_aqu, see Section 7.4.4).

8.5.4 Biomass of crops

With the *CR*-values selected for this safety evaluation, the parameters describing the biomass of cereals and fodder had no effect on calculated concentrations of radionuclides in agricultural soils. That is, the fraction of the total inventory that is expected to be stored in plant biomass was less than a few percent for all included radionuclides. Consequently, it was deemed unnecessary to account for the fraction of radionuclides stored in crops for the transport calculations, and biomass in crop as an input parameter was removed from the transport calculations.

8.5.5 Yields of tubers and vegetables

These parameters are the same as the parameters named “biomass_tuber” and “biomass_vegetables” used in SR-PSU but they have now got more intuitive and explanatory names (yield_tuber, yield_veg). These are grown on the garden plot.

8.5.6 Net primary production

The parameters that describe total net primary production (NPP_ag_veg, NPP_veg) and the above-ground NPP for cabbage were found to be wrongly calculated in the SR-PSU assessment. The parameter values are here corrected, but the description in Grolander (2013, Chapter 9) is still valid (note that NPP_ag_veg is named Biom_veg in that description, where the latter has changed to yield_veg in this assessment, see above).

8.5.7 Translocation of radionuclides during irrigation of the garden plot

Translocation of radionuclides from the plant to the tuber, f_trans_tuber, describes the fraction of a radionuclide that is deposited on the plant that ends up in the edible part of the plant (in this case the tuber). The results of empirical studies on translocation factors were presented by IAEA (2010), defined as “the ratio of the activity, on a ground area basis, of the edible part of a crop at harvest time (Bq m^{-2}) to the foliage activity of the crop at the time of deposition (Bq m^{-2}), expressed as a percentage”. For root crops, seven elements (Cs, Sr, Mn, Co, Ru, Te and Ba) were studied and for tubers two elements were studied (Cs and Sr). However, plant growth stages were not given, and it was assumed that the translocation factors were for mature plants. Overall the highest translocation factors have been found for ^{134}Cs, but this radionuclide is of limited importance in the calculations (see **Biosphere synthesis**). Nevertheless, this radionuclide was included due to the few radionuclides studied. Here it is assumed that tubers also can be represented by root crops in general and a mean value was used from all nine studies.

8.5.8 Soil respiration in different types of regolith

The soil respiration parameters (SoilResp (GP, IO), SoilResp_gyttja (DM), SoilResp_peat (DM), SoilResp_ter) are used to calculate the dissolved inorganic carbon (DIC) concentration (C-12) in the peat pore water of the mire and the organic soils used for agricultural purposes (drained mire, garden plot and infield-outland farming). In the earlier safety analyses, DIC concentration was a parameter on its own, but it is now expressed with a dependency on several other parameters in BioTEx. The transport of DIC into a surficial soil volume from below is negligible in comparison with the autotrophic and heterotrophic respiration (two orders of magnitude lower), which are the main contributors to the overall DIC concentration in combination with the fraction of DIC that is hidden in the carbonate equilibrium (pH dependent).

Lindroth et al. (2007) described the soil respiration for four Nordic boreal mires showing a range between 214 and 456 gCm^{-2} $year^{-1}$, where the highest values were from a southerly located bog and the lowest from a northern mire. The mean value corresponds to two oligotrophic mires, which are assumed to be representative for an oligotrophic boreal mire on the southeast coast of Sweden. They also found that temperature sensitivity was higher for productivity than for respiration.

Lohila et al. (2003) estimated the respiration from cultivated peaty soil growing barley, grass and potatoes to be between 0.11 and 0.36 mg CO_2 m^{-2} s^{-1}. These figures were also put in a wider perspective in the review by Oertel et al. (2016), and they are regarded as applicable for peaty soils in temperate climates and for Laxemar.

8.5.9 Removal of deposited radionuclides from the plant leaf surface

This parameter (washoffCoef_veg) describes the removal of deposited radionuclides from the plant leaf surface of vegetables and has been added to the model, with the value being taken from SR-PSU to represent cereals, grass and rice based on eight studies identified in a compilation by IAEA (2010) (see Grolander 2013).

8.5.10 Diffusivity of CO_2 in air

In SR-PSU the diffusivity of CO_2 in regolith was calculated as a parameter for different regolith types (see Grolander 2013), now this is done in the model based on regolith porosity, degree of water saturation in the soil and the diffusivity of CO_2 in air (D_{CO2_air}). Field and laboratory experiments show that the loss of inorganic carbon by degassing is driven primarily by gaseous diffusion in unsaturated soils (Sheppard et al. 1994). The molecular diffusivity or diffusion coefficient is a proportionality constant between the molar flux due to molecular diffusion and the gradient in the concentration of the molecules of interest. A compound's diffusion coefficient is typically four orders of magnitude greater in air than in water (Haynes 2012), and the molecular diffusivity of carbon dioxide in soil depends on temperature. We used a linear relationship to describe this at a temperature of 10 °C, which is the approximate mean soil temperature during the period that lacks ground frost in Forsmark (Heneryd 2007), as

$$D_{CO2\_air} = 0.1325 + T \times \beta_T$$

where the coefficient for temperature response of CO_2 was taken from Lerman (1979) ($\beta_T = 0.0009$) and is expressed in 10^{-4} m^2 s^{-1}. The diffusivity of CO_2 in air (D_CO2_air) is expressed as m^2 $year^{-1}$ in the model. The response of diffusivity to temperature is relatively small (approximately a 4 % change in the diffusivity of CO_2 in air for a change of 6 °C).

8.5.11 Concentration in air after combustion of peat and wood in a small household

The ground-level activity concentrations in air per unit activity concentration in peat or wood (Bqm^{-3} per $Bqkg_{DW}^{-1}$) are used for calculation of exposure of radionuclides by combustion of peat or wood (conc_air_combPeat, conc_air_combWood). The parameters are presented in Section 3.2.2. and in Table 3-2 in Stenberg and Rensfeldt (2015). The values for a household calculated in the cavity zone and as an average over downwind distances of 0–200 m for a house of height 3 metres and 60 m^2 wall area are used in this assessment. It is assumed that a person will move around outside

the house and a mean value for the distance of 0–200 metres was therefore assumed to be the most representative value. The dimensions of the house affect the activity concentrations, and therefore different heights (3 or 5 metres) and wall areas (30 or 60 m^2) of a one-story house were used in the calculations in Stenberg and Rensfeldt (2015). The calculated activity concentration was highest for a 3 metres high house with a 60 m^2 wall area, and this case was therefore selected here. The same approach and the same basic calculations were used in SR-PSU.

8.5.12 Stable element concentrations in vegetation and regolith layers

Essential elements for vegetation have a regulated uptake and for these elements plant uptake was modelled as a function of NPP, the concentration in the plant and specific activity of the radionuclide in the regolith layer (see **Biosphere synthesis**, Chapter 8). The specific activity approach in radionuclide modelling and dose calculations relates the quantity of the radionuclide to the quantity of the stable element present. Therefore, the calculations need information on the natural concentrations of the stable elements in the plant and also in the available pore water for uptake.

Chlorine in vegetation

The concentration of chlorine in cereals from Forsmark was described by Sheppard et al. (2011). A mean was used to describe the concentration of the whole plant among four different sites. This estimate was similar to that from other investigations on cereals in Sweden (e.g. Williamsson et al. 2004) and could therefore be assumed to also represent non-calcite rich soils. There were no differences in concentrations between the grain, straw and roots. The data from cereals were assumed to also be representative for other crops and for mushrooms (conc_Cl_cereal, conc_Cl_fodder, conc_Cl_tuber, conc_Cl_veg and conc_Cl_mush).

Chlorine in regolith

The concentration of chlorine in pore water of different types of regolith (conc_Cl_regoUp_peat_D, conc_Cl_regoUp_gyttja_D, conc_Cl_regoUp_D in infield and outland, and garden plot) was based on the different regolith types associated with the cereals from the study referenced above (Sheppard et al. 2011). They described the concentration of chlorine in pore water of cultivated peat, gyttja and glacial clay at a depth of 0.2 m in Forsmark. Only four values among three regolith types were available for Laxemar (Sheppard et al. 2009) and these were therefore disregarded. The related parameter conc_Cl_regoUp_ter_D is described in Grolander (2013) and is from the same study above, representing five mires in Forsmark.

Calcium in vegetation

The concentrations of calcium in cereals, fodder, vegetables and tuber (conc_Ca_cereal, conc_Ca_fodder, conc_Ca_veg. conc_Ca_tuber) were based on data from measurements on cereals in Forsmark (Sheppard et al. 2011), due to lack of data from Laxemar. No data for fodder, vegetables and tubers were, however not available from Forsmark. Therefore, concentrations of Ca in cereals were matched according to concentrations in the grain for cereals, above-ground parts for fodder and vegetables, and roots for tubers. The data on crops from Sheppard et al. (2011) were approximately 2 times higher than the national mean of spring wheat (Miljödata 2018), suggesting an overestimation (see also below for forest vegetation). The Ca concentration in fungi, (conc_Ca_mush) where the carbon concentration was 0.46 $kg_C\ kg_{DW}^{-1}$, was based on measurements by Johanson et al. (2004) in Forsmark due to a lack of data from other sites. The calcium concentration in mire vegetation (conc_Ca_PP_ter) was assumed to be similar to measurements on field and bottom layers from three forest ecosystems in Laxemar. These values were approximately half the Forsmark values for similar ecosystems suggesting that there might be regional differences associated with high concentrations in the regolith.

Calcium in regolith

The concentration of calcium in the pore water of different soils is known to vary among regions, due to the $CaCO_3$ content in the soil. Therefore, one geometrical mean based on only three values from Laxemar were used for this estimate. These three values described the concentration in the pore water of two clay gyttja samples and one peat sample (Sheppard et al. 2009), which together represented organic soils (conc_Ca_regoUp_D, conc_Ca_regoUp_gyttja_D, conc_Ca_regoUp_peat_D, conc_Ca_regoUp_ter_D).

Potassium in vegetation

The concentration of potassium in cereals, fodder, vegetables and tubers (conc_K_cereal, conc_K_fodder, conc_K_veg and conc_K_tuber) were based on data from measurements on cereals in Forsmark (Sheppard et al. 2011), where a mean for the axe, stem and root was used to represent the plant. This value was similar to national estimates of the concentration of potassium in spring wheat (Miljödata 2018). The concentrations of potassium and carbon (0.46 $kg_C\ kg_{DW}^{-1}$) in fungi (conc_K_mush) was based on measurements by Johansson et al. (2004) in Forsmark. The potassium concentration in mire vegetation (conc_K_ter) was assumed to be similar to concentrations obtained from measurements on field and bottom layers from three forest ecosystems in Laxemar.

Potassium in regolith

The concentration of potassium in pore water of different types of regolith layers was described by Sheppard et al. (2011) for Forsmark. They described the concentration of potassium in pore water of peat, cultivated peat, and clay gyttja (conc_K_regoUp_D, conc_K_regoUp_gyttja_D, conc_K_regoUp_peat_D, conc_K_regoUp_ter_D) at a depth of 0.2 m. Only four values among three regolith types were available for Laxemar (Sheppard et al. 2009) and these were therefore disregarded.

Table 8-4. New or updated parameters used in the SFL evaluation.

Name	Unit	Description	Comment
yield_tuber	$kg_C\ m^{-2}\ year^{-1}$	Yearly edible yield of tubers	updated name
yield_veg	$kg_C\ m^{-2}\ year^{-1}$	The above-ground net primary production for vegetables in the garden plot	updated name
q_sat_unsat_agri	$m^2\ m^{-2}\ year^{-1}$	Water flux from saturated to unsaturated zone growing cereals	Updated name and data
conc_air_combPeat	$(Bq\ m^{-3})\cdot(Bq\ kg_{DW}^{-1})^{-1}$	The ground level activity concentration in air per unit activity concentration in peat	updated
conc_air_combWood	$(Bq\ m^{-3})\cdot(Bq\ kg_{DW}^{-1})^{-1}$	The ground level activity concentration in air per unit activity concentration in wood	updated
D_CO2_air	$m^2\ year^{-1}$	Diffusivity of radionuclides incorporated in gases in air	updated
f_trans_tuber	Unitless	Translocation of elements deposited on aerial parts of the plant to the edible parts of the plant	updated
NPP_veg	$kg_C\ m^{-2}\ year^{-1}$	Total net primary production (above- and below-ground) of vegetables	Corrected data (Specific but no large diff)
conc_Ca_cereal	$gCa\ kg_C^{-1}$	Concentration of calcium in cereals	new
conc_Ca_fodder	$gCa\ kg_C^{-1}$	Concentration of calcium in fodder	new
conc_Ca_mush	$gCa\ kg_C^{-1}$	Concentration of calcium in mushrooms	new
conc_Ca_PP_ter	$gCa\ kg_C^{-1}$	Concentration of calcium in vegetation	new
conc_Ca_regoUp_D	$gCa\ m^{-3}$	Concentration of dissolved calcium in clay gyttja	new
conc_Ca_regoUp_gyttja_D	$gCa\ m^{-3}$	Concentration of dissolved calcium in clay gyttja	new
conc_Ca_regoUp_peat_D	$gCa\ m^{-3}$	Concentration of dissolved calcium in cultivated peat	new

Name	Unit	Description	Comment
conc_Ca_regoUp_ter_D	gCa m^{-3}	Concentration of dissolved calcium in the mire	new
conc_Ca_tuber	gCa kg_C^{-1}	Concentration of calcium in tubers	new
conc_Ca_veg	gCa kg_C^{-1}	Concentration of calcium in vegetables	new
conc_Cl_cereal	gCl kg_C^{-1}	Concentration of chlorine in cereals	new
conc_Cl_fodder	gCl kg_C^{-1}	Concentration of chlorine in fodder	new
conc_Cl_mush	gCl kg_C^{-1}	Concentration of chlorine in mushrooms	new
conc_Cl_regoUp_D	gCl m^{-3}	Concentration of dissolved chlorine in clay gyttja	new
conc_Cl_regoUp_gyttja_D	gCl m^{-3}	Concentration of dissolved chlorine in clay gyttja	new
conc_Cl_regoUp_peat_D	gCl m^{-3}	Concentration of dissolved chlorine in cultivated peat	new
conc_Cl_tuber	gCl kg_C^{-1}	Concentration of chlorine in tubers	new
conc_Cl_veg	gCl kg_C^{-1}	Concentration of chlorine in vegetables	new
conc_K_cereal	gK kg_C^{-1}	Concentration of potassium in cereals	new
conc_K_fodder	gK kg_C^{-1}	Concentration of potassium in fodder	new
conc_K_mush	gK kg_C^{-1}	Concentration of potassium in mushrooms	new
conc_K_PP_ter	gK kg_C^{-1}	Concentration of potassium in vegetation	new
conc_K_regoUp_D	gK m^{-3}	Concentration of dissolved potassium in clay gyttja	new
conc_K_regoUp_gyttja_D	gK m^{-3}	Concentration of dissolved potassium in clay gyttja	new
conc_K_regoUp_peat_D	gK m^{-3}	Concentration of dissolved potassium in cultivated peat	new
conc_K_regoUp_ter_D	gK m^{-3}	Concentration of dissolved potassium in the mire	new
conc_K_tuber	gK kg_C^{-1}	Concentration of potassium in tubers	new
conc_K_veg	gK kg_C^{-1}	Concentration of potassium in vegetables	new
f_inorg_Cl_PP_ter	kg kg^{-1}	Fraction of inorganic chlorine of the total chlorine content	new
SoilResp	kg_C m^{-2} $year^{-1}$	Soil respiration including autotroph and heterotroph respiration	new
SoilResp_gyttja	kg_C m^{-2} $year^{-1}$	Soil respiration including autotroph and heterotroph respiration in drained clay gyttja	new
SoilResp_peat	kg_C m^{-2} $year^{-1}$	Soil respiration including autotroph and heterotroph respiration in peaty soil of a drained mire	new
SoilResp_ter	kg_C m^{-2} $year^{-1}$	Soil respiration including autotroph and heterotroph respiration in a mire	new
time_irrigationPeriod	days	The period during which irrigation is applied starting from the day of harvest counted backwards to the first irrigation event. The irrigation events are distributed evenly within this period	new
washoffCoef_veg	$year^{-1}$	Removal of deposited radionuclides from the plant leaf surface	new

9 Human characteristics

In this chapter the parameters describing the characteristics of humans are presented, these parameters are needed to assess the potential dose to the most exposed group of human. The parameters listed in Table 9-1 include ingestion rates of food and water, inhalation rates and parameters describing the four types of land use. These parameters are identical to the parameters used in the SR-PSU assessment. Parameter values are presented in Appendix H.

9.1 Parameters and dependencies of exposure route

Four potential most highly exposed populations were included in the analysis. These groups were considered credible to use as bounding cases for the most exposed groups with respect to exposure through all major exposure pathways in SR-PSU (SKB 2014b) and in the SE-SFL assessment. When characterising the potentially most exposed groups, physical and biological characteristics of the biosphere objects, human requirements for energy and nutrients, and habits from historical and present societies were considered (Chapter 6 of the **Biosphere synthesis**, Saetre et al. 2013a, SKB 2014b). These were; 1) hunter-gatherers foraging discharge areas by fishing, hunting, and collecting berries and mushrooms, 2) infield-outland farmers having a self-sustained agriculture with infield crops and dependent on outfield nutrients from wetlands (outland), 3) family farmers self-sustained on agriculture on former lakes or wetlands (drained mire), 4) garden-plot households that are self-sustained with respect to vegetables and root crops produced through small-scale horticulture and having drinking water from a dug well. Depending on which exposed group that is modelled, some parameters may have different values, and this is indicated in the tables below describing the parameters.

9.2 Effects of site characteristics on parameter values

The parameters describing the properties of humans are assumed to be generic. This is because, even though the respiration rate and water ingestion rate can be affected by changes in climate, as stated in Grolander (2013, Section 10.2), these effects of changes in climate are expected to be limited.

The exposure analysis conducted for SR-PSU is assumed to be valid also for the site-specific conditions prevailing at Laxemar but for sites with substantially different conditions these parameters might have to be re-evaluated. For example, if a site in northern Sweden was to be evaluated some of the agricultural practices might not be feasible due to the cold climate.

Table 9-1. Summary of human characteristics parameters used.

Name	Unit	Description
area	m^2	Area of agricultural land used to support one individual of the most exposed group (infield-outland) and Area of agricultural land used to support one individual's need for vegetables (Garden plot)
area_support	m^2	Drained wetland area required to support the energy demand of an individual of the most exposed group (drained mire) and Mire area required to support winter fodder for the livestock associated with an individual of the most exposed group (Infield-outland).
f_area_cereal	$m^2\ m^{-2}$	Fraction of area used for cereal
f_area_fodder	$m^2\ m^{-2}$	Fraction of area used for fodder
f_area_tuber	$m^2\ m^{-2}$	Fraction of area used for tuber crops
f_area_veg	$m^2\ m^{-2}$	Fraction of area used for vegetables
f_diet_cereal	$kg_C\ kg_C^{-1}$	Fraction of the annual energy demand that is covered by consumption of cereal
f_diet_fish_max	$kg_C\ kg_C^{-1}$	Fraction of fish in diet corresponding to the maximum healthy protein consumption

Name	Unit	Description
f_diet_meat	$kg_C\ kg_C^{-1}$	Fraction of the annual energy demand that is covered by consumption of meat
f_diet_milk	$kg_C\ kg_C^{-1}$	Fraction of the annual energy demand that is covered by consumption of milk
f_diet_tuber	$kg_C\ kg_C^{-1}$	Fraction of the annual energy demand that is covered by consumption of tuber
f_diet_veg	$kg_C\ kg_C^{-1}$	Fraction of the annual energy demand that is covered by consumption of vegetables
f_meadow	unitless	Fraction of the annual fodder demand that is covered by hay
f_time_agri	year $year^{-1}$	Fraction of time spent working on arable land in an infield-outland agricultural system
f_time_hay	year $year^{-1}$	Fraction of time spent working on collecting hay in wetland in an infield-outland agricultural system
ingRate_C	$kg_C\ year^{-1}$	Annual energy demand for an adult individual in units of carbon
ingRate_water	$m^3\ year^{-1}$	Human ingestion rate of water
inhRate	$m^3\ hour^{-1}$	Human inhalation rate of air
N_group	unitless	Number of individuals in the most exposed group for each type of land-use
q_well	$m^3\ year^{-1}$	Water extraction rate from a drilled well
time_exposure	hours $year^{-1}$	Exposure time for an individual working outside a house
time_exposure_comb	hours $year^{-1}$	Exposure time for an individual spending time outside a house in which combustion of peat or wood takes place.

9.3 Selection of parameter values

The model site in Laxemar is similar to the site in Forsmark in regard to the possibility for humans to utilise the area for agricultural practises. It is therefore assumed that that parameter values describing the human behaviour in the SR-PSU assessment are representative also for the Laxemar model site. The parameterisation of human characteristics is described in the SR-PSU Parameter report Grolander (2013, Chapter 10). In Table 9-2, detailed references are given to the section in Grolander (2013) were the selected data are described. For some parameters, updated parameter values were selected in the SE-SFL assessment (area_Garden plot, f_area_veg, f_area_tuber, time_exposure_comb), as described below.

Area of the garden plot

The area of a garden plot that may support a family group was recalculated due to an error that was discovered in the estimate of cabbage production (see Section 8.4). Therefore, the garden plot area, which is the area that may feed a family group of 5 members increased. The garden plot is assumed to supply the family group with potatoes and cabbage summing up to a fraction of 8 % of the total diet (Grolander 2013, Section 10.9). The updated value of the garden plot area is 54 m^2, describing the needed garden plot area per individual.

Fraction of the area of the garden plot that is cultivated with tubers and vegetables

The updated value for cabbage production value also have implications for the fraction of the garden plot that is cultivated with cabbage and tubers, respectively. The updated fraction cabbage (f_area_veg) is 0.54 and the fraction of potatoes (f_area_tuber) is 0.46.

Time period of exposure

The parameter time_exposure_comb defines the exposure time for an individual outside a house in which combustion of peat or wood takes place. This parameter was not used in the SR-PSU assessment. In this assessment it is assumed that an individual spends all their time outside the house (8 760 hours per year).

Table 9-2. References to where the parameter data are described, given for each parameter.

Parameter name	Land use	Reference
area	Infield-outland	Grolander (2013, Section 10.9)
area	Garden plot	Updated in Section 9.3
area_support	Drained mire	Grolander (2013, Section 10.8)
area_support	Infield-outland	Grolander (2013, Section 10.8)
f_area_cereal	Drained mire	Grolander (2013, Section 10.7)
f_area_fodder	Drained mire	Grolander (2013, Section 10.7)
f_area_tuber	Drained mire	Updated in Section 9.3
f_area_tuber	Garden plot	Grolander (2013, Section 9.14.1)
f_area_veg	Garden plot	Updated in Section 9.3
f_diet_cereal	Drained mire	Grolander (2013, Section 10.6)
f_diet_cereal	Infield-outland	Grolander (2013, Section 10.6)
f_diet_fish_max	Forager	Grolander (2013, Section 10.11)
f_diet_meat	Drained mire	Grolander (2013, Section 10.6)
f_diet_meat	Infield-outland	Grolander (2013, Section 10.6)
f_diet_milk	Drained mire	Grolander (2013, Section 10.6)
f_diet_milk	Infield-outland	Grolander (2013, Section 10.6)
f_diet_tuber	Drained mire	Grolander (2013, Section 10.6)
f_diet_tuber	Garden plot	Grolander (2013, Section 10.6)
f_diet_veg	Garden plot	Grolander (2013, Section 10.6)
f_meadow	Infield-outland	Grolander (2013, Section 10.9)
f_time_agri	Infield-outland	Grolander (2013, Section 10.12)
f_time_hay	Infield-outland	Grolander (2013, Section 10.12)
ingRate_C	All land uses	Grolander (2013, Section 10.4)
ingRate_water	All land uses	Grolander (2013, Section 10.3)
inhRate	All land uses	Grolander (2013, Section 10.5)
N_group	Forager	Grolander (2013, Section 10.10)
N_group	Drained mire	Grolander (2013, Section 10.10)
N_group	Infield-outland	Grolander (2013, Section 10.10)
N_group	Garden plot	Grolander (2013, Section 10.10)
time_exposure	Forager	Grolander (2013, Section 10.12)
time_exposure	Drained mire	Grolander (2013, Section 10.12)
time_exposure	Infield-outland	Grolander (2013, Section 10.12)
time_exposure	Garden plot	Grolander (2013, Section 10.12)
time_exposure_comb	Garden plot	Define in Section 9.3

10 Alternative regional climate evaluation case

This biosphere evaluation case considers the effects of the local climate (e.g. precipitation and temperature) on external conditions, and consequences for dose calculations. The variations in local climate are represented by three additional sites in terms of hydrology. The properties of biosphere object 206 are in this evaluation, thus allowing the comparison of the results with the results of the base case. The ecosystems represented are constant agricultural land use based on properties existing today, and a mire that is drained for agricultural purposes.

Three additional sites were chosen to represent other climate types of coastal sites in Sweden. A northern (Örnsköldsvik municipality), central (Forsmark) and a southwestern location (Varberg municipality) were chosen besides Laxemar (Figure 10-1).

Seasonal temperature and precipitation are presented in the **Climate report,** SKB (2014b) and based on these regional differences, parameters that related to surface and groundwater hydrology were updated (see Section 5.9 and below). The reason for this is that earlier studies suggested that climate-related changes in surface hydrology had a much larger influence on the calculated dose than changes in plant-related parameters (such as biomass, net primary production and leaf area index) (SBK 2014a, Section 10.6).

Factors such as the length of the vegetation growth period, yield of crops, rate of mineralisation and leaf area index, which all to some extent are dependent on climatic characteristics, e.g. temperature, were held constant. Future evaluations also have to include differences in these aspects to estimate the full potential of climate effects on calculated doses, even though these are currently regarded as less important.

The uptake of groundwater by crops on agricultural land (drained mire, garden plot and infield and outland) was assumed to change in accordance to the change in calculated potential water requirement on a national scale calculated by Johansson and Klingspor (1977). The percolation was adjusted in accordance with the expected increase or decrease in runoff as compared with the Laxemar site (see also 8.4.2). The need for irrigation on the garden plots was based on the calculations made by Johansson and Klingspor (1977).

Figure 10-1. *Illustration of the four localities that were chosen to represent four regional climate zones in Sweden.*

10.1 Parameters changed in the Alternative regional climate evaluation case

The parameters that were changed for this evaluation case are listed in Table 10-1. In addition, the hydrological parameters for this case are changes as described in Section 5.9.

The selected parameter values for the three alternative locations are listed in Appendix I.

Table 10-1. Parameter that are changed in the Alternative regional climate evaluation case (in addition to the hydrological parameters presented in Section 5.9).

Name	Unit	Description
q_sat_unsat_agri	m $year^{-1}$	Water flux from saturated to unsaturated zone growing cereals
amount_irrig	m $year^{-1}$	Total amount of water used for all irrigation events during the vegetation period
percolation_agri	m^3 m^{-2} $year^{-1}$	Downward flux of water from agricultural soils (drained mire, garden plot and inland-outfield)

10.1.1 Water uptake in crops

This parameter (q_sat_unsat_agri) describes the upward flux of groundwater into the unsaturated zone of the agricultural land, where the roots are found. This groundwater flux is driven by evapotranspiration and is affected by the amount of water originating from precipitation that is available in the root zone. The parameter values for the different climate regions were estimated in the same way as for Laxemar (Section 8.5.1) and Forsmark (Grolander 2013, Section 9.8.2), which was based on the central value of the water deficit in a normal year and a dry year for the applicable region. The water deficit for a normal year and a dry year were based on calculations by Johansson and Klingspor (1977) who described six regions in Sweden. The calculated need for additional water input could be provided either by irrigation or by capillary rise from deeper soil layers and was here assumed to be provided by capillary rise.

10.1.2 Amount of irrigation

This parameter (amount_irrig) describes the total amount of water per unit area of land that is used to irrigate the garden plot, as described in Grolander (2013). Johansson and Klingspor (1977) calculated the daily balance between precipitation and evapotranspiration during the vegetation period for several different regional areas in Sweden. The deficit for potatoes during a normal year was assumed to be supplied by irrigation water in the garden plot.

10.1.3 Percolation

The percolation in the agricultural (percolation_agri) land types of the drained mire and the infield-outland system were calculated as the sum of the net precipitation (precipitation decreased by evapotranspiration, see hydrological parameter in Section 0) and the upward transport of water under drier periods during the vegetation period. (q_up_satSoil_agri, see Section 10.1.1 above). The percolation in the garden plot was calculated as the sum of the net precipitation and the irrigation water (amount_irig, above, see Section 10.1.2 above).

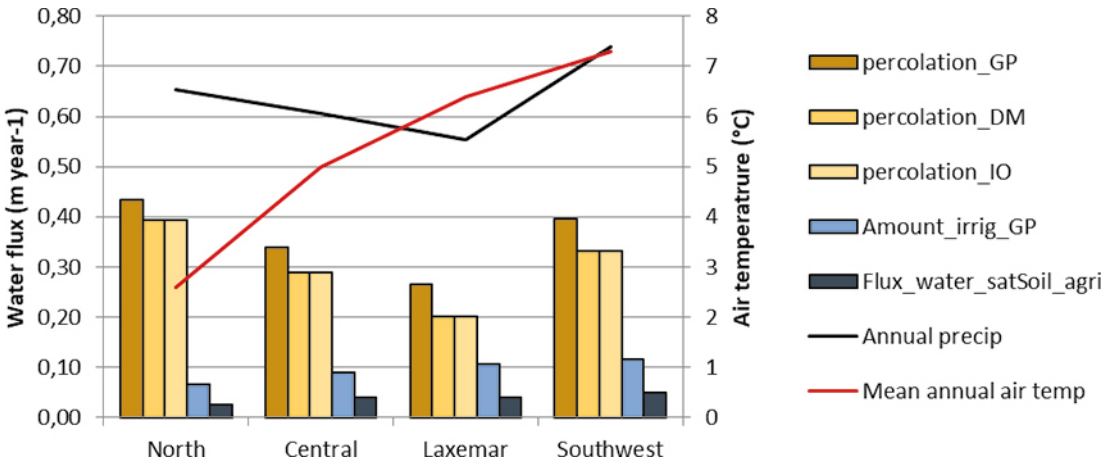

Figure 10-2. *Percolation, irrigation and flux of water into the root zone (Flux_water_satSoil_agri) for Laxemar and three alternative localities (Figure 10-1) representing regional climate conditions along the Swedish coast. Temperature and precipitation are from the reference period 1961–1990 (Alexandersson and Eggertsson Karlström 2001).*

11 Increased greenhouse effect evaluation case

This biosphere evaluation case investigates potential effects on dose to humans in a warmer climate in accordance with the *increased greenhouse effect climate case, IGE climate case* **(Climate report**, SKB 2014b**).** This evaluation case investigates the potential effects from utilising natural resources from a mire ecosystem, (including cultivation after draining), and from continuous cultivation of crops on soils similar to those presently existing in Laxemar.

In the *IGE climate case*, it is assumed that the climate in Laxemar will be warmer for an initial period of 23 000 years after closure (**Biosphere synthesis**, Chapter 4, Table 4-1). After this period, the climate will return to the present-day climate (as described in *the present day evaluation case*). The description of the warmer climate reflects IPCC's intermediate emissions scenario RCP4.5, where the global atmospheric CO_2 level stabilises at 543 ppm. This corresponds to a mean annual temperature and an annual precipitation that are 2.6°C and 12 % higher than in the present conditions.

Most properties of the mire and the agricultural ecosystems are expected to be marginally affected by this climatic change (Löfgren 2010, Chapter 11), and changes in plant- and crop-related parameters (e.g. biomass, net primary production and leaf area index) due to a warmer climate are expected to have small effects on the calculated dose (SKB 2015a, Section 10.6). Therefore, these parameter values were the same as in the *Present-day evaluation case.*

However, in a warmer climate where precipitation dose not compensate for higher evapotranspiration during the vegetation period, the plant water deficit will increase. The increased demand of water can either be supplied by an increased groundwater uptake through capillary rise, or it can be supplied by irrigation water. Such changes have a potential to affect the release to and accumulation of radionuclides in cultivated soils, and consequently parameters reflecting surface hydrology and irrigation are updated in this evaluation case (see section 5.9 and below).

Moreover, the atmospheric concentration of stable CO_2 in the atmosphere affects the specific activity of C-14 in carbon resulting from atmospheric plant fixation (Saetre et al. 2013) and thus this parameter is also updated in the warmer climate.

11.1 Water deficit and irrigation practice

11.1.1 The drained mire

Today irrigation of crops is not common in Sweden, and only 3–4 % of the total agricultural area is irrigated. The irrigated areas are mainly located in the very south of Sweden (Brundell et al. 2008). In a warmer climate where precipitation dose not compensate for higher evapotranspiration, the plant water deficit may increase and full-scale irrigation with surface water could be a reasonable option to cover this deficit when the depth to the groundwater table is large.

In SE-SFL regions that have a present-day climate that is similar to that expected in Laxemar in a future warmer climate have been identified (Appendix B2 in the **Climate report,** SKB 2014b). Taking the projected change in near-surface temperature and precipitation during the central vegetation season (June–August) for RCP4.5, western Poland is identified as a reasonable regional analogue to Laxemar (Figure C-3 in the **Climate report**, SKB 2014b). Labędzki (2007) described the status of irrigation in Poland and estimated the net irrigation requirements for rye and oats to be between 0 and 50 mm per harvest, and between 60 and 80 mm for winter wheat. The corresponding irrigation requirements for tubers ("Late potatoes") and fodder ("Pasture") were 100–150 mm and 90–120 mm, respectively.

Similarly, a dry year in southern Sweden is a reasonable analogue to Laxemar under a warmer climate. Johansson and Klingspor (1977) have calculated the water deficit for different crop types during the vegetation period based on the daily balance between precipitation and evapotranspiration in Sweden. For agricultural land in southern coastal Sweden they estimated the water deficit for a dry year to be 65 mm for spring barley, 120 mm for fodder and 125 mm for tubers.

11.1.2 The garden plot

The garden plot is a small area for gardening close to a house, where additional crops are cultivated for the household, such as tubers, vegetables or herbs. These crops need more intensive management and are therefore irrigated more frequently and in smaller amounts per event than is the case for large-scale agricultural land.

11.2 Parameters changed or added in the increased greenhouse effect climate case

The parameters for which data values were changed in *the increased greenhouse* evaluation case are listed in Table 11-1 and described in the text below. Parameter valueas are presented in Appendix J.

The hydrological fluxes that were changed in this evaluation case are described in Section 5.9

Table 11-1. Parameter that were changed in the increased greenhouse evaluation case.

Name	Unit	Description
amount_irrig_IGE	$m^3\ m^{-2}\ year^{-1}$	Volume of water used for irrigation
conc_C_atmos_IGE	$kg_C\ m^{-3}$	The concentration of C in the atmosphere
f_trans_cereal_IGE	Unitless	Translocation is the process of redistributing elements deposited on aerial parts of the plant to the edible parts of the plant
N_irrig_IGE	$year^{-1}$	Number of irrigation events per vegetation period
percolation_agri_IGE	$m\ year^{-1}$	Downward flux of water from agricultural soils (Garden plot, Drained mire and Infield-outland agricultural systems)
q_sat_unsat_agri_IGE	$m\ year^{-1}$	Water flux from the saturated to unsaturated zone in the area growing cereals
threshold_IGE	Year	The year when when the increased greenhouse climate is back to “normal” temperate climate
time_irrigationPeriod_IGE	days	The period during which irrigation is applied starting from the day of harvest counted backwards to the first irrigation event. The irrigation events are applied at uniform intervals within this period
washoffCoef_fodder_IGE	$year^{-1}$	Removal of deposited radionuclides from the plant leaf surface
LeafStoreCapacy	$m^3\ m^{-2}$	Thickness of the water layer from which the radionuclides has been removed by sorption and other processes to the leaf surface

11.2.1 Number of irrigation events for large scale agriculture

Cereals are especially sensitive to drought during three different life stages; germination, spike development and early seed development (Wesström and Joel 2014). Here we assume that the total irrigation need is divided between the latter two periods of the growing season (N_irrig_IGE = 2). This is a cautious assumption, as translocation to the grains after irrigation is higher later in the growing season (see below). This is also consistent with the fact that irrigation rations smaller than 10 mm are rarely applied in large-scale irrigation practices (Malm and Berglund 2007).

11.2.2 Number of irrigation events for a garden plot

The garden plot is assumed to require more frequent irrigation and this is approximated as irrigation occurring ten times during the vegetation season. This corresponds to a watering event every ninth day.

11.2.3 Time period for irrigation for large-scale agriculture

Barley is ready for harvest approximately 49–56 days in Sweden after the start of spike development (Pedersen 2004). Accordingly, it is assumed that the first irrigation ration is given 60 days before harvest (approximately coinciding with the spike development) and the second 30 days before harvest (at the earing/flowering). The period during which irrigation is applied (time_irrigationPeriod_IGE) is thus set to 60 days, which includes both spike development and early seed development.

11.2.4 Time period for irrigation of the garden plot

The time period for irrigation is assumed to include the whole growing period, which is approximately 90 days for tubers (time_irrigationPeriod_IGE =90 days).

11.2.5 Amount of irrigation

Three different crops are assumed to be cultivated on the drained mire; barley, fodder and tubers, and the tuber crop is the one that has the greatest water deficit (see above). The water deficit during the vegetation period in southern coastal Sweden in a dry year is taken as an upper estimate for sustainable irrigation in the *Increased greenhouse effect evaluation case*. Thus, the the amount of water used for large scale irrigation (amount_irrig_IGE), is set to 0.125 m per year. This figure is in the middle of the span presented for tuber crops in Poland (see above). As the same amount of water is applied to all crops in the biosphere model, the approach is cautious for crops that have a smaller requirement for water. For simplicity, the same amount of irrigation water (amount_irrig_IGE) is assumed to be applicable also to the cultivation of fodder and vegetables on the garden plot.

11.2.6 Water uptake in crops

In the *Present-day evaluation case* it is assumed that groundwater uptake in the drained mire during the central part of the vegetation season is 69 mm (see Section 8.5.1). This value is based on a weighted average over the three crops grown on the drained mire (weightings of 0.56 for cereals, 0.37 for fodder and 0.07 for potatoes). In the *Increased greenhouse effect evaluation case*, it is assumed that the modest increase in precipitation will not be enough to compensate for the increased evapotranspiration associated with higher temperatures, and therefore a plant water deficit of 90 mm is assumed in the warmer climate based on the same approach as in the base case, but with a higher water demand (see above).

The agricultural lands that are of interest for the safety assessment are those with a history of deep groundwater inflow. Today, these are situated in topographically low-lying areas in the landscape. Historically, these locations were occupied by lakes or wetlands, and subsequent cultivation is still dependent on effective draining by ditches. As the groundwater level presently is relatively close to the soil surface (ca 0.5–1 m, Morosini et al. 2007), it is likely that groundwater uptake will be a pathway to cover plant water deficient in a warmer climate. Thus, in variant A of this evaluation case the plant water deficit during the vegetation season is assumed to be completely covered by uptake of groundwater through capillary rise (q_sat_unsat_agri_IGE = 0.09 m year^{-1}). Conversely, in variant B where the water deficit is covered by irrigation, no uptake of groundwater is assumed to occur (q_sat_unsat_agri_IGE = 0 m year^{-1}).

11.2.7 Percolation

To estimate the percolation in the drained mire in a warmer climate (percolation_agri_IGE) the parameter value from the present-day evaluation case was scaled by the same factor as the runoff (i.e. it was assumed to decrease by 20 %, see Section 5.6). This decrease was further assumed to affect the percolation by the same amount in the drained mire and it was consequently set to 0.160 m year^{-1}.

11.2.8 Concentration of CO_2 in the atmosphere

The CO_2 concentration in the atmosphere, conc_C_atmos_IGE, in the RCP4.5 climate modelling case is 543 ppm (**Climate report**, SKB 2014b). The carbon concentration in the atmosphere is calculated at the mean temperature of 18°C, which represents the air temperature during the central part of the vegetation period in the *increased greenhouse effect climate case* (June–August, **Climate report**, SKB 2014b).

11.2.9 Wash off coefficient for fodder

This and the following two parameters are described here as a consequence of introducing large scale irrigation on certain crops in this specific evaluation case. The activity of radionuclides deposited on a crop with irrigation water will decrease with time due to wash-off. The rate of decrease is described by a weathering half-life or a first-order rate constant (IAEA 2010, Saetre et al. 2013, Grolander 2013). In SE-SFL, a translocation factor is used to describe to what extent radionuclides that are deposited on crops will end up in the edible parts (see Section 11.2.11 below). However, for fodder (which is consumed by livestock) the wash-off coefficient remains applicable.

Empirically determined wash-off coefficients are reasonably similar for different elements but may vary with crop type (IAEA 2010). Thus, in SE-SFL, one value is selected for the wash-off coefficient for fodder, and this value is based on studies on grass only (n = 3, IAEA 2010), which also is the same used for cereals in SR-PSU (Grolander 2013): washoffCoef_fodder_IGE = 16.1 $year^{-1}$.

11.2.10 Leaf storage capacity for fodder

The leaf storage capacity parameter describes the thickness of the water layer from which the radionuclide has been removed by sorption and other processes, LeafStoreCapacy, and data from Grolander (2013) were used. The value for fodder that was used in this case was assumed to be equal to the one used for leafy vegetables (Grolander 2013).

11.2.11 Translocation of radionuclides to cereals

Translocation of radionuclides from the plant to the grain, f_trans_cereal, describes the fractions of radionuclides deposited on the plant that ends up in the edible part of the plant (in this case the grain). The translocation factors depends on the developmental stage of the crop, and radionuclides (Cs, Sr, Mn, Co, Fe and Sb) deposited during late developmental stages (flowering and grain growth) show the highest rate of translocation to the seed (average 2.3 and 2.9 %, respectively; IAEA 2010).

Bengtson et al. (2012) studied translocation of Cs-134 and Sr-85 wet deposited on spring wheat over two growing seasons in central Sweden. They confirmed that the rates close to harvest (i.e. seed growth/ripening) were consistently higher than those for other developmental stages but found no significant difference between the two studied radionuclides. Assuming that the studied fields had a yield similar to the average of Uppland (0.42 kg dw m^{-2}, Swedish Board of Agriculture 2017), the translocation factor for the two radionuclides during ripening (days 70–92) corresponded to 6 % of the intercepted radionuclides.

Due to lack of data, one value for f_trans_cereal was used for all elements in SE-SFL. We selected the value from the study in central Sweden (6 %). This value is similar to the IAEA recommended value for Cs for late developmental stages (5.5–6.1 %) and above the typical value for other radionuclides (see above). As irrigation is assumed to occur also at earlier developmental stages (see section 8.5.2), this is a cautious simplification.

11.2.12 Threshold describing the length of the “greenhouse” climate (threshold_IGE)

The greenhouse climate is assumed to prevail from closure to 23 000 years after closure (**Biosphere synthesis**, Chapter 4, Table 4-1).

12 Simplified glacial cycle

This biosphere *Simplified glacial cycle evaluation case* is part of the glaciation evaluation case, which has been designed to illustrate how, 1) an early period of periglacial climate domain, and 2) early succession, different climate conditions and the transitions between stages, affects the calculated dose. In this case a 100 000-year glaciation cycle is repeated ten times. The glaciation cycle contains three different climatic domains corresponding to temperate, periglacial and glacial conditions. Temperate conditions are described by the present-day conditions (*Present-day evaluation case*). The periglacial conditions include permafrost, which are characterised as perennially frozen ground, whereas glacial conditions occur when the area is covered by an ice-sheet. When the ice sheet retreats during the end of the glaciation climate domain most unconsolidated regolith layers on top of the till are expected to be removed by glacial erosion. Moreover, the remaining regolith is assumed to be flushed out by large quantities of surface water when the ice sheet melts. Thus, the radionuclide inventory in all regolith layers is assumed to be negligible at the start of the submerged period in each interglacial-glacial cycle.

During permafrost conditions the annual average near-surface air temperatures are estimated as −1° and −4° for the two periods in each glacial cycle when permafrost conditions occur (see below; **Climate report,** SKB 2014b). Because extensive permafrost generally acts as an impermeable layer, groundwater recharge and discharge are reduced relative to unfrozen soil conditions, and, in areas with continuous permafrost, groundwater recharge and discharge are restricted to taliks (**Climate report,** SKB 2014b). In this landscape, no agricultural use of mires is possible. In this biosphere evaluation case, the periglacial conditions are based on the SR-PSU climate description (**Climate report,** SKB 2014b).

The first periglacial period starts around 17 500 AD (Figure 12-1), in agreement with the early periglacial climate case in SR-PSU (SKB 2014b, **Climate report**). Permafrost is assumed to develop from non-existing to a continuous cover at the repository site during the first 100 years of the periglacial period. Similarly, the transition from the periglacial to the temperate climate domain at 20 500 AD is assumed to occur during the last 100 years of the periglacial period. For the second periglacial period that ends at 57 000 AD, the permafrost is assumed to thaw during the initial 100 years of the period of glacial climate domain. The terrestrial and aquatic ecosystems of the biosphere objects 206 (mire) and 208 (lake) are used in the modelling with most of the parameters having the same values as in temperate conditions with the exception of the parameters listed in Table 12-1. These parameters were also used in the SR-PSU assessment and are described in Grolander (2013). Parameter values are presented in Appendix K.

In periods of temperate climate, radionuclides from the repository are discharged to the same biosphere object as in the present-day evaluation case, namely biosphere object 206. During periods of periglacial climate, the mire in object 206 is assumed to be frozen, and consequently not connected to flowing bedrock groundwater. During this period, releases are instead assumed to reach a lake via a through talik that is represented by Lake Frisksjön (object 207). Given the size and average water depth of this lake (190 m radius and 4 m, respectively) it is plausible that a through talik may form under the waterbody even when permafrost reaches a depth of 300 m (Hartikainen et al. 2010).

When Laxemar is in the glacial climate domain, radionuclides from the geosphere are assumed to be discharged to a sea basin beyond the ice margin. The location of the ice margin is expected to vary and it will be located far away from the repository for much of this period. Instead of a detailed description of the fate of radionuclides under this period, a simplifying assumption is used in the biosphere calculations. Thus, the release is assumed to reach one sea basin during the complete period of glacial conditions. The turnover time of an offshore basin is expected to be short. However, it cannot be excluded that radionuclides may at times discharge to a coastal location, and thus the recipient is cautiously assumed to be a semi-enclosed coastal basin (with a relatively small water depth and low rate of turnover), represented by the present state of object 208.

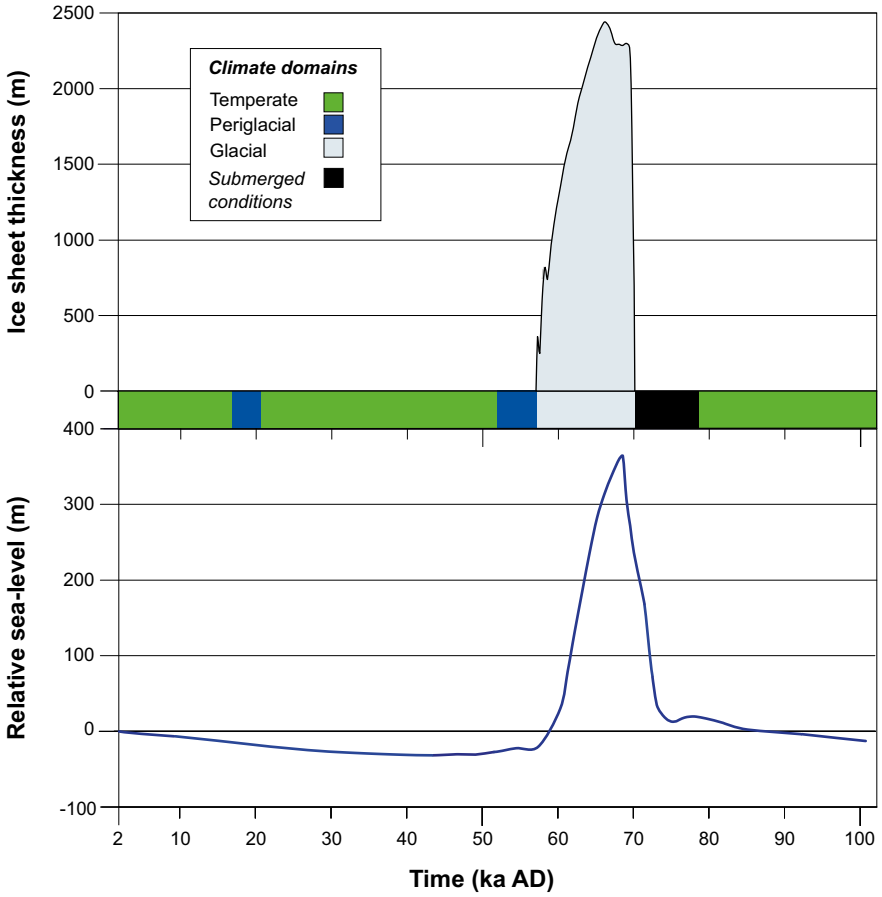

Figure 12-1. *Development of climate and climate domains, ice sheet thickness, and shoreline displacement for the glaciation evaluation case. The development of climate domains and submerged periods is shown on the colored axis. The submerged period (black) shows the duration of sea water-covered conditions for the area immediately above the repository and for biosphere object 206. The relative sea-level curve has its zero line at the present sea level. The development from 2000 AD to 102 000 AD is repeated every 100 000 years until one million years after repository closure to represent the effects of repeated glacial-interglacial cycles. Figure from the Climate report, SKB (2014b).*

Table 12-1. The parameters that were changed when going from temperate to permafrost conditions for a mire and a lake in the Glaciation evaluation case. The calculation of these parameters is described in Grolander (2013).

Name	Unit	Description	Reference
biom_pp_ter_perm	$kg_C\ m^{-2}$	Total biomass of terrestrial primary producers per unit area	Grolander (2013, Section 9.3)
conc_C_atmos_perm	$kg_C\ m^{-3}$	Concentration of carbon in the atmosphere (above the ground)	Grolander (2013, Section 9.5.7)
minRate_regoUp_ter_perm	$kg_C\ kg_C^{-1}\ year^{-1}$	Water flux from the upper peat layer to the water column for limnic phase in periglacial conditions	Grolander (2013, Section 9.9)
NPP_ter_perm	$kg_C\ m^{-2}\ year^{-1}$	Total net primary production (above and below ground) in the terrestrial ecosystem	Grolander (2013, Section 9.3)
piston_vel_ter_perm	$m\ year^{-1}$	Gas exchange coefficient for peat pore water in contact with the atmosphere	Grolander (2013, Section 9.4.5)
prod_edib_cray_lake_perm	$kg_C\ m^{-2}\ year^{-1}$	Sustainable yield with respect to edible crayfish per unit area in the lake in periglacial conditions	Grolander (2013, Section 8.10.2)
prod_edib_fish_lake_perm	$kg_C\ m^{-2}\ year^{-1}$	Sustainable yield with respect to edible fish per unit area in the lake in periglacial conditions	Grolander (2013, Section 8.10.1)
solubilityCoef_ter_perm	$(mol\ m^{-3})\ (mol\ m^{-3})^{-1}$	Solubility coefficient for carbon dioxide in pore water of the upper peat layer	Grolander (2013, Section 9.4.6)

Object 206 starts as mire in this evaluation case. After the glaciation the area will be submerged, and it is assumed that the groundwater flows will reach the central parts of the basin (which will later become the lake basin) during this period. Two parameters are used to describe when the object becomes submerged for the first time and for how long (Table 12-2, Figure 12-1). As the land rises, the sea basin will develop into a bay, which finally gets isolated from the sea. The development of the object, i.e. the change in bathymetry and the accumulation of post-glacial sediments during the submerged period is described with the coupled regolith-lake development model (RLDM, Brydsten and Strömgren 2010). The original size of the lake is estimated from present-day conditions (area and regolith stratigraphy) and the development of the lake is described as a function of mire vegetation ingrowth and net sediment accumulation. According to the projected development the mire ingrowth is completed 4 400 years after isolation. For details on the landscape development see Chapter 3 of this report, and Chapter 5 in the **Biosphere synthesis**. The biosphere objects used to assess consequences of a release during permafrost and glacial conditions do not change during the simulations of these periods.

In the simulations, the maximum increase of groundwater flow during ice-sheet advance is taken to be 35 times the groundwater flow during temperate conditions. This maximum occurs 50 years after the ice sheet margin has passed the repository location. The maximum groundwater flow increase during ice-sheet retreat varies in the range 3 to 20 times the magnitude simulated for present-day conditions. To not overestimate the amounts of radionuclides that are flushed out in the submerged period (when dose consequences are expected to be small) the maximum groundwater flow increase during ice-sheet retreat is taken to be 3. For more information of the groundwater flow parameters used see Section 5.9.

Table 12-2. New parameters describing the development and duration of ice-sheet impact on modelled biosphere objects (defined in the Biosphere synthesis).

Parameter	Unit	Description	Ecosystem	Reference
threshold_submerged	year	Time when the submerged period starts in the first interglacial (Time AD)	Mire	Biosphere synthesis,Table 4-2
time_submerged	year	Length of the submerged period	Mire	Biosphere synthesis, Table 4-2
f_glaciation	unitless	Fraction of release that reaches the sea basin (in front of the ice)	Sea	Biosphere synthesis, Section 7.7.2
f_permafrost	unitless	Fraction of release that reaches the lake talik	Lake	Biosphere synthesis, Section 7.7.2

13 Concluding summary

The parameters used in BioTEx reflect important processes related to transport and accumulation of, and human exposure to, radionuclides. In total, the model relies on approximately 620 input parameters, of which more than half represent radionuclide- or element-specific properties (for the 10 dominating radionuclides). For each parameter, a best estimate was derived from site or literature data, and these were used for deterministic calculations of human exposure.

Since the last safety assessment, SR-PSU (Saetre et al. 2013), BioTEx has been somewhat further developed in order to increase its fitness for purpose (see Chapter 8 in the **Biosphere synthesis).** In some cases, this means that parameters have been slightly modified or replaced, or new parameters have been added. In SR-PSU, fluxes of ground and surface water were estimated from MIKE SHE water balances for three different successional stages for each biosphere object separately. However, in SE-SFL, water-balances were only available for present-day conditions. Therefore, a new methodology for deriving groundwater flow parameters was developed (Chapter 5). This was used for systematic extrapolations to other successional stages, which made it possible for a coherent derivation of hydrological parameters for other additional evaluation cases, e.g. for studying the effects of different local climatic conditions. In addition, parameters for eight new elements (Be, Gd, K, La, Re, Si, Tb, and Ti) were included in SE-SFL, and parameter values for these elements were approximated based on elemental analogues (Chapter 6). New parameters introduced in BioTEx are soil respiration in unsaturated soil, the fraction of inorganic chlorine in primary producers, the concentrations of some nutrients in mire vegetation, fungi and crops, and the corresponding concentrations in the pore water of soils (Chapter 8). These nutrients are Cl, Ca and K, which are used to calculate tissue concentration of Cl-36, Ca-41 and K-40 in fungi, higher plants including crops, and thus these parameters replace the *CR*s for these elements in terrestrial plants including crops and fungi.

SFL-SE is not yet restricted to a specific location of the repository and is evaluated in a broad context with the aim of identifying circumstances more or less favourable to long-term safety by using Laxemar as an example site. Some parameters values can be expected to be valid for any selected model site within Sweden, whereas other parameter values are dependent on site-characteristics such as air temperature, precipitation, hydrology, Quaternary geology and geochemical conditions and will differ between sites, as well as changing over time. Therefore, the sensitivity of the parameter values to site-specific conditions was evaluated and the parameters were divided into a site-specific or generic group based on their sensitivity to site-specific conditions. The evaluation of sensitivity to site conditions was done by expert judgement and considered the spatial boundaries of whole Sweden, excluding the mountain range in the north. In total, approximately 450 out of 620 parameters were judged to be site-specific and thereby regarded as being sensitive to the choice of site. This means that if the model site is changed, these parameter values will need to be updated to select parameter values representative for the selected site.

In Table 13-1, the parameter classification into site-specific and generic is shown for every parameter group. The parameters describing the geometries and development of the landscape are by definition site-specific and the same applies to the hydrological flows and the properties of the regolith layers. The parameters describing terrestrial and aquatic ecosystem properties can be either site-specific or generic. The generic parameters are properties like carbon content of milk, ingestion rate for cows and height of the canopy of crops, whereas the site-specific often depend on temperature and precipitation, as in the cases of net primary production, production of berries, concentration of dissolved inorganic carbon and mineralisation rate etc. This is described in detail in Chapters 7 and 8. K_d and *CR* values are site-specific since they are expected to change with changing geochemical conditions and regolith properties (for example pH, organic matter content and clay content etc). It can be expected that the site-specific K_d and *CR* values will differ significantly between sites within Sweden, however, few data are available. The data for the dose coefficients and half-lives of radionuclides are by definition not dependent on the modelled site. The parameters describing the properties and habits of the exposed human population are based on an exposure pathway analysis that is regarded to be valid for most sites in Sweden.

Table 13-1. The parameters in the radionuclide transport model for the biosphere are categorised into two categories, "site-specific" and "generic" based on whether or not they are expected to vary with location across Sweden. Evaluations of sensitivity to temperature, precipitation, Quaternary geology and geochemical conditions were based on expert judgement.

Parameters	Site-specific	Generic	Comment
Landscape geometries	27	0	Landscape geometrics are by definition site-specific as these describe the size of objects etc.
Regolith properties	23	3	Regolith properties can differ depending on the genesis of the regolith layers which might differ between sites.
Hydrological fluxes	33	0	Hydrological flows are dependent on local conditions, such as topography, soil properties, climate (temperature and precipitation).
Terrestrial ecosystem	45	65	Many of the site-specific parameters depend on climate conditions (temperature and precipitation). Details are given in Sections 8.3 and 8.4.
Aquatic ecosystem	30	10	Many of the site-specific parameters, for example primary production, depend on climate conditions (temperature and precipitation). Details are given in Sections 7.3 and 7.4.
Element-specific K_d, *CR* and *TC CR*	$31 \times N_e$[1]	0	K_d and *CR* values depend on the local geochemical condition and the variation between sites can be expected to be large.
Human characteristics	0	22	The human habits are based on an exposure analysis that is assumed to be valid for any site in Sweden.
Radionuclide-specific properties	0	$7 \times N_r$[2]	Dose coefficients and half-lives are generic as these describe properties of the radionuclides that are not affected by site conditions

1) K_d (11), *CR* (18) and *TC* (2) for each analysed radionuclide (N_e).

2) Dose coefficients for ingestion, inhalation and combustion, half-life and the effect of ingrowth for each analysed radionuclide (Nr).

For generic parameters, data from SR-PSU were used. These data were quality assured within the previous assessment and can therefore be used without an additional quality assurance procedure. For many of the site-specific parameters, the difference in values between Laxemar and Forsmark was judged to be small (less than 10 %), and in these cases data used in the previous safety assessment, SR-PSU, were used also for Laxemar. This means that even if the parameter is site-specific, the difference in parameter values can be small between sites in Sweden (in this case between Laxemar and Forsmark). This is valid for the parameters of regolith properties and many of the terrestrial and aquatic parameters. If the model site were to change from Laxemar to another location in Sweden, an updated evaluation of the differences would be needed and the data from either Laxemar or Forsmark might not be regarded as representative. For some of the site-specific parameters the differences in parameter values between Laxemar and Forsmark were judged to be significant (more than 10 %) and data from Laxemar were used for parameterisation. For K_d and *CR*, the differences in values between the sites are expected to be significant and Laxemar data were used when available, but due to lack of data, parameters from Forsmark were used. In the end, 14 out of 27 parameters describing K_d (3/11) and *CR* (11/16) could be populated with Laxemar data (Chapter 6). This means that the K_d and *CR* values used in many cases do not represent the geochemical conditions at Laxemar. This adds additional uncertainty to the calculations. However, this was investigated in a separate sensitivity case where the effects of alternative K_d and *CR* values were evaluated by benchmarking against a generic data set (Section 13.3 in the **Biosphere synthesis**).

Of the 620 parameter values, 290 are K_d and *CR* for the ten most dose contributing radionuclides. In a sensitivity analysis of the contribution of parameter distributions to the variation in final dose result for three dose contributing radionuclides (Cl-36, Ni-59 and Mo-93) for Forsmark in SR-PSU (SKB 2014b), showed that nearly all parameters with a high impact on the uncertainty of the results were found in the category "element-specific K_d and *CR*". For C-14, which does not require a K_d value, and where plant uptake is described by specific activity and net primary production, it were the root uptake, water transport from the saturated soil to the crop and soil respiration, which were the three most important parameters explaining the variation in dose in the SR-PSU safety assessment (SKB 2014b). All these are regarded as site-specific, which highlights that good quality of site-specific data are important to obtain a reliable evaluation of a potential repository site.

At the same time, an evaluation of site-specific data can also be done by including a broad span of different biosphere objects with different properties, different long-term development and different successional stages during their long-term development, in this case from Laxemar and Forsmark (e.g. *Alternative* d*ischarge area evaluation case*). Similarly, an evaluation of differences in hydrology, based on climate was done in a first attempt to study the sensitivity of the results to specific important parameters. However, the effects of some important dose-contributing element-specific parameters on the resulting dose could not be evaluated in the context of a generic site in Sweden, as studied in this safety evaluation.

In order to broaden the context, a number of additional evaluation cases were added (Chapter 10 to 12). Two other coastal sites were added as an additional evaluation case (Chapter 10) to study the effects of alternative regional climate conditions and the resulting change in hydrological parameter values holding all other parameters constant (Section 5 and 10.1). To fully evaluate the consequence of altered regional location, all site-specific parameters need to be re-evaluated and updated when significant differences are expected.

In conclusion, parameter values representing the example site of Laxemar and a number of additional evaluation cases are described in this report. The approach has been to identify the parameters that can be regarded as site-specific. This information is important since the change of model site will require an update of all site-specific parameters. It was shown that most of the parameter values depend on site-specific conditions, but also that many of them might not change significantly between sites in Sweden (here the differences between Laxemar and Forsmark were evaluated). Nevertheless, in order to be able to undertake a safety evaluation or safety assessment and minimise the uncertainty in the results, extensive site-specific information is required.

References

SKB's (Svensk Kärnbränslehantering AB) publications can be found at www.skb.com/publications.

References with abbreviated names

Main report, 2019. Post-closure safety for a proposed repository concept for SFL. Main report for the safety evaluation SE-SFL. SKB TR-19-01, Svensk Kärnbränslehantering AB.

Biosphere synthesis, 2019. Biosphere synthesis for the safety evaluation SE-SFL. SKB TR-19-05, Svensk Kärnbränslehantering AB.

Climate report, 2019. Climate and climate-related issues for the safety evaluation SE-SFL. SKB TR-19-04, Svensk Kärnbränslehantering AB.

Radionuclide transport report, 2019. Radionuclide transport and dose calculations for the safety evaluation SE-SFL. SKB TR-19-06, Svensk Kärnbränslehantering AB.

FEP report, 2019. Features, events and processes for the safety evaluation SE-SFL. SKB TR-19-02, Svensk Kärnbränslehantering AB.

Initial state report, 2019. Initial state for the repository for the safety evaluation SE-SFL. SKB TR-19-03, Svensk Kärnbränslehantering AB.

Other references

Alexandersson H, Eggertsson Karlström C, 2001. Temperaturen och nederbörden i Sverige 1961–1990: referensnormaler. 2nd ed. Norrköping: SMHI. (Meteorologi 99) (In Swedish.)

Andersson E, 2010. The limnic ecosystems at Forsmark and Laxemar-Simpevarp. SR-Site Biosphere. SKB TR-10-02, Svensk Kärnbränslehantering AB.

Aquilonius K (ed), 2010. The marine ecosystems at Forsmark and Laxemar-Simpevarp. SR-Site Biosphere. SKB TR-10-03, Svensk Kärnbränslehantering AB.

Bengtsson S, Eriksson J, Gärdenäs A, Rosén K, 2012. Influence of development stage of spring oilseed rape and spring wheat on interception of wet-deposited radiocaesium and radiostrontium. Atmospheric Environment 60, 227–233.

Bosson E, Gustafsson L-G, Sassner M, 2008. Numerical modeling of surface hydrology and near-surface hydrogeology at Forsmark. Site descriptive modeling, SDM-Site Forsmark. SKB R-08-09, Svensk Kärnbränslehantering AB.

Bosson E, Sassner M, Gustafsson L-G, 2009. Numerical modeling of surface hydrology and near-surface hydrogeology at Laxemar-Simpevarp. Site descriptive modeling SDM-Site Laxemar. SKB R-08-72, Svensk Kärnbränslehantering AB.

Bosson E, Sassner M, Sabel U, Gustafsson L-G, 2010. Modelling of present and future hydrology and solute transport at Forsmark. SR-Site Biosphere. SKB R-10-02, Svensk Kärnbränslehantering AB.

Bosson E, Sabel U, Gustafsson L-G, Sassner M, Destouni G, 2012. Influences of shifts in climate, landscape, and permafrost on terrestrial hydrology. Journal of Geophysical Research 117. doi:10.1029/2011JD016429.

Bosson E, Selroos J-O, Stigsson M, Gustafsson L-G, Destouni G, 2013. Exchange and pathways of deep and shallow groundwater in different climate and permafrost conditions using the Forsmark site, Sweden, as an example catchment. Hydrogeology Journal 21, 225–237.

Brundell P, Kanlén F, Westö A-K, 2008. Water use for irrigation. Report on Grant Agreement No 71301.2006.002–2006.470, Statistiska centralbyrån (Statistics Sweden).

Brydsten L, 2006. A model for landscape development in terms of shoreline displacement, sediment dynamics, lake formation, and lake choke-up processes. SKB TR-06-40, Svensk Kärnbränslehantering AB.

Brydsten L, Strömgren M, 2010. A coupled regolith-lake development model applied to the Forsmark site. SKB TR-10-56, Svensk Kärnbränslehantering AB.

Brydsten L, Strömgren M, 2013. Landscape development in the Forsmark area from the past into the future (8500 BC – 40 000 AD). SKB R-13-27, Svensk Kärnbränslehantering AB.

Eckerman K F, Leggett R W, 1996. DCFPAK: Dose coefficient data file package for Sandia National Laboratory. ORNL/TM-13347, Oak Ridge National Laboratory, Oak Ridge, TN.

Eckerman K F, Ryman J C, 1993. External exposure to radionuclides in air, water, and soil. Federal Guidance Report 12. EPA-402-R-93-081, U.S. Environmental Protection Agency, Washington, DC.

Engqvist A, 2006. Coastal oceanography of the Laxemar area. In Lindborg T (ed). Description of surface systems. Preliminary site description Laxemar subarea – version 1.2. SKB R-06-11, Svensk Kärnbränslehantering AB, Chapter 3.5, 113–139.

Engqvist A, 2010. Estimation of residence times of coastal basins in the Laxemar-Simpevarp area between 3000 BC and 9000 AD. SKB R-10-57, Svensk Kärnbränslehantering AB.

Elfwing M, Evins L Z, Gontier M, Grahm P, Mårtensson P, Tunbrant S, 2013. SFL concept study. Main report. SKB TR-13-14, Svensk Kärnbränslehantering AB.

Evins L, 2013. Progress report on evaluation of long term safety of proposed SFL concepts. SKB R-13-41, Svensk Kärnbränslehantering AB

Feistel R, Weinreben S, Wolf H, Seitz S, Spitzer P, Adel B, Nausch G, Schneider B, Wright D G. 2010. Density and absolute salinity of the Baltic Sea 2006–2009. Ocean Science 6, 3–24.

Firestone R B, Baglin C M (ed), Chu S Y F (ed), 1998. Table of isotopes: 1998 update. 8th ed. New York: Wiley.

Grolander S, 2013. Biosphere parameters used in radionuclide transport modelling and dose calculations in SR-PSU. SKB R-13-18, Svensk Kärnbränslehantering AB.

Harrison J D, Leggett R W, 2016. Appropriate selection of dose coefficients in radiological assessments: C-14 and Cl-36: response to the letter of G Smith and M Thorne (2015 J. Radiol. Prot. 35 737-40). Journal of Radiological Protection 36, 388–390.

Hartikainen J, Kouhia R, Wallroth T, 2010. Permafrost simulations at Forsmark using a numerical 2D thermo-hydro-chemical model. SKB TR-09-17, Svensk kärnbränslehantering AB.

Harvest to table, 2019. Quick-maturing vegetable varieties. Available at: https://harvesttotable.com/quick-maturing_vegetable_varie/ [20 December 2019].

Haynes W H (ed), 2012. CRC handbook of chemistry and physics: a ready-reference book of chemical and physical data. 93rd ed. Boca Raton, FL: CRC Press.

Heneryd N, 2007. Forsmark site investigation. Measurements of ground respiration, primary production and NEE in terrestrial habitats. SKB P-07-23, Svensk Kärnbränslehantering AB.

IAEA, 2010. Handbook of parameter values for the prediction of radionuclide transfer in terrestrial and freshwater environments. Vienna: International Atomic Energy Agency. (Technical Reports Series 472)

ICRP, 2008. Nuclear decay data for dosimetric calculations. Oxford: Elsevier. (ICRP Publication 107, Annals of the ICRP 38(3))

ICRP, 2009. Environmental protection: transfer parameters for reference animals and plants. Oxford: Elsevier. (ICRP Publication 114, Annals of the ICRP 39(6))

ICRP, 2012. Compendium of dose coefficients based on ICRP Publication 60: Corrected version. Oxford: Elsevier. (ICRP Publication 119, Annals of the ICRP, 41(1))

Johanson K, Nikolova I, Taylor A F S, Vinichuk M, 2004. Uptake of elements by fungi in the Forsmark area. SKB TR-04-26, Svensk Kärnbränslehantering AB.

Johansson E, Sassner M, 2019. Development of methodology for flow path analysis in the Surface system – Numerical modelling in MIKE SHE for Laxemar. A report for the safety evaluation SE-SFL. SKB R-19-04, Svensk Kärnbränslehantering AB.

Johansson W, 1973. Metod för beräkning av vatteninnehåll och vattenomsättning i odlad jord med ledning av meteorologiska data (Method using meteorological data for estimation of soil moisture content and soil moisture changes in cultivated land). Grundförbättring 26, 57–153. (In Swedish with summary in English)

Johansson W, Klingspor P, 1977. Bevattning inom lantbruket 1976: bevattnad areal, vattenåtgång och vattentäkter. Uppsala: Institutionen för markvetenskap, avdelningen för lantbrukets hydroteknik. (Stenciltryck 100) (In Swedish.)

Jörg G, Bühnemann R, Hollas S, Kivel N, Kossert K, Van Winckel S, Gostomski C L, 2010. Preparation of radiochemically pure ^{79}Se and highly precise determination of its half-life. Applied Radiation and Isotopes 68, 2339–2351.

Kłos R, 2015. GEMA-Site 1: Model description and example application. SSM Report 2015:47, Swedish Radiation Safety Authority.

Labędzki L, 2007. Irrigation in Poland – current status after reforms in agriculture and future development. Journal of Water and Land Development 11, 3–16.

Leggett R W, 2004. A biokinetic model for carbon dioxide and bicarbonate. Radiation Protection Dosimetry 108, 203–213.

Lerman A, 1979. Geochemical processes: water and sediment environments. New York: Wiley.

Lindborg T (ed), 2006. Description of surface systems. Preliminary site description Laxemar subarea – version 1.2 SKB R-06-11, Svensk Kärnbränslehantering AB.

Lindborg T, 2010. Landscape Forsmark – data, methodology and results for SR-Site. SKB TR-10-05, Svensk Kärnbränslehantering AB.

Lindroth A, Lund M, Nilsson M, Aurela M, Christensen T R, Laurila T, Rinne J, Riutta T, Sagerfors J, Ström L, Tuovinen J-P, Vesala T, 2007. Environmental controls on the CO_2 exchange in north European mires. Tellus B 59, 812–825.

Lohila A, Aurela M, Regina K, Laurila T, 2003. Soil and total ecosystem respiration in agricultural fields: effect of soil and crop type. Plant and Soil 251, 303–317.

Losjö K, Johansson B, Bringfelt B, Oleskog I, Bergström S, 1999. Groundwater recharge – climatic and vegetation induced variations. Simulations in the Emån and Äspö areas in southern Sweden. SKB TR-99-01, Svensk Kärnbränslehantering AB.

Lundin L, Stendahl J, Lode E, 2005. Forsmark site investigation. Soils in two large trenches. SKB P-05-166, Svensk Kärnbränslehantering AB.

Löfgren A (ed), 2010. The terrestrial ecosystems at Forsmark and Laxemar-Simpevarp. SR-Site Biosphere. SKB TR-10-01, Svensk Kärnbränslehantering AB.

Malm P, Berglund P, 2007. Bevattning och växtnäringsutnyttjande. Jönköping: Jordbruksverket. (Jordbruksinformation 5) (In Swedish.)

Miljödata, 2018. Sök data - Åkermarksinventeringen.. http://miljodata.slu.se/mvm/aker?epslanguage=sv?submenu=open [1 October 2018]. (In Swedish)

Morosini M, Jenkins C, Simson S, Albrecht J, Zetterlund M, 2007. Oskarshamn site investigation. Hydrogeological characterization of deepest valley soil aquifers and soil-rock transition zone at Laxemar, 2006. Subarea Laxemar. SKB P-07-91, Svensk Kärnbränslehantering AB.

Nyman H, Sohlenius G, Strömgren M, Brydsten L, 2008. Depth and stratigraphy of regolith. Site descriptive modeling SDM-Site Laxemar. SKB R-08-06, Svensk Kärnbränslehantering AB.

Odén M, Follin S, Öhman J, Vidstrand P, 2014. SR-PSU bedrock hydrogeology. Groundwater flow modelling methodology, setup and results. SKB R-13-25, Svensk Kärnbränslehantering AB.

Oertel C, Matschullat J, Zurba K, Zimmermann F, Erasmi S, 2016. Greenhouse gas emissions from soils – A review. Geochemistry 76, 327–352.

Pedersen T R, 2004. Odlingsbeskrivningar – Spannmål. Jönköping: Jordbruksverket. (In Swedish.)

Påsse T, 2001. An empirical model of glacio-isostatic movements and shore-level displacement in Fennoscandia. SKB R-01-41, Svensk Kärnbränslehantering AB.

Redon P-O, Abdelouas A, Bastviken D, Cecchini S, Nicolas M, Thiry Y, 2011. Chloride and organic chlorine in forest soils: storage, residence times, and influence of ecological conditions. Environmental Science & Technology 45, 7202–7208.

Saetre P, Nordén S, Keesmann S, Ekström P-A, 2013. The biosphere model for radionuclide transport and dose assessment in SR-PSU. SKB R-13-46, Svensk Kärnbränslehantering AB.

Sassner M, Sabel U, Bosson E, Berglund S, 2011. Numerical modelling of present and future hydrology at Laxemar-Simpevarp. SKB R-11-05, Svensk Kärnbränslehantering AB

Schrader H, 2004. Half-life measurements with ionization chambers – a study of systematic effects and results. Applied Radiation and Isotopes 60, 317–323.

Shahkarami P, 2019. Input data report for near-field and geosphere radionuclide transport modelling. Report for the safety evaluation SE-SFL. SKB R-19-09, Svensk Kärnbränslehantering AB.

Sheppard M I, Ewing L L, Hawkins J L, 1994. Soil degassing of carbon-14 dioxide: rates and factors. Journal of Environmental Quality 23, 461–468.

Sheppard S, Long J, Sanipelli B, Sohlenius G, 2009. Solid/liquid partition coefficients (K_d) for selected soils and sediments at Forsmark and Laxemar-Simpevarp. SKB R-09-27, Svensk Kärnbränslehantering AB.

Sheppard S, Sohlenius G, Omberg L-G, Borgiel M, Grolander S, Nordén S, 2011. Solid/liquid partition coefficients (K_d) and plant/soil concentration ratios (CR) for selected soils, tills and sediments at Forsmark. SKB R-11-24, Svensk Kärnbränslehantering AB.

Sjöfartsverket, 1992. Svensk lots. Del A: allmänna upplysningar. Norrköping: Sjöfartsverket. (In Swedish.)

SKB, 1999. Deep repository for long-lived low- and intermediate-level waste. Preliminary safety assessment. SKB TR-99-28, Svensk Kärnbränslehantering AB.

SKB, 2008. Safety analysis SFR 1. Long-term safety. SKB R-08-130, Svensk Kärnbränslehantering AB.

SKB, 2010a. Comparative analysis of safety related site characteristics. SKB TR-10-54, Svensk Kärnbränslehantering AB.

SKB, 2010b. Biosphere analyses for the safety assessment SR-Site – synthesis and summary of results. SKB TR-10-09, Svensk Kärnbränslehantering AB.

SKB, 2011a. Long-term safety for the final repository for spent nuclear fuel at Forsmark. Main report of the SR-Site project. SKB TR-11-01, Svensk Kärnbränslehantering AB.

SKB, 2011b. Site selection – siting of the final repository for spent nuclear fuel. SKB R-11-07, Svensk Kärnbränslehantering AB.

SKB, 2014a. Geosphere process report for the safety assessment SR-PSU. SKB TR-14-05, Svensk Kärnbränslehantering AB.

SKB, 2014b. Biosphere synthesis report for the safety assessment SR-PSU. SKB TR-14-06, Svensk Kärnbränslehantering AB.

SKB, 2014c. Engineered barrier process report for the safety assessment SR-PSU. SKB TR-14-04, Svensk Kärnbränslehantering AB.

SKB, 2014d. Waste form and packaging process report for the safety assessment SR-PSU. SKB TR-14-03, Svensk Kärnbränslehantering AB.

SKB, 2015a. Safety analysis for SFR. Long-term safety. Main report for the safety assessment SR-PSU. Revised edition. SKB TR-14-01, Svensk Kärnbränslehantering AB.

SKB, 2015b. Handling of biosphere FEPs and recommendations for model development in SR-PSU. SKB R-14-02, Svensk Kärnbränslehantering AB.

SKI/SSI, 2001. SKI:s och SSI:s gemensamma granskning av SKB:s preliminära säkerhetsanalys för slutförvar för långlivat låg- och medelaktivt avfall. Granskningsrapport. SKI rapport 01:14, Statens kärnkraftinspektion (Swedish Nuclear Power Inspectorate), SSI-rapport 2001:10, Statens strålskyddsinstitut (Swedish Radiation Protection Authority). (In Swedish.)

Smith G M, Thorne M C, 2015. Appropriate selection of dose coefficients in radiological assessments: C-14 and Cl-36. Journal of Radiological Protection 35, 737–740.

Sohlenius G, Hedenström A, 2008. Description of regolith at Laxemar-Simpevarp. Site descriptive modeling SDM-Site Laxemar. SKB R-08-05, Svensk Kärnbränslehantering AB.

Sohlenius G, Hedenström A, Nyman H, 2006. Oskarshamn site investigation. Characterisation of Quaternary deposits in Lake Frisksjön and Skettkärret. SKB P-06-144, Svensk Kärnbränslehantering AB.

Stenberg K, Rensfeldt V, 2015. Estimating doses from exposure to contaminated air when burning peat or wood. SKB R-14-33, Svensk Kärnbränslehantering AB.

Strömgren M, Brydsten L, Lindgren F, 2006. Oskarshamn site investigation. Measurements of brook gradients. SKB P-06-05, Svensk Kärnbränslehantering AB.

Swedish Board of Agriculture, 2017. Statistical database (In Swedish). Available at: http://statistik.sjv.se/PXWeb/pxweb/sv/?rxid=6485b66a-c6ca-47c6-9aee-9ca558faa6a0 [12 March 2017].

Tröjbom M, Grolander S, Rensfeldt V, Nordén S, 2013. K_d and CR used for transport calculations in the biosphere in SR-PSU. SKB R-13-01, Svensk Kärnbränslehantering AB.

Werner K, Sassner M, Johansson E, 2013. Hydrology and near-surface hydrogeology at Forsmark – synthesis for the SR-PSU project. SKB R-13-19, Svensk Kärnbränslehantering AB.

Wesström I, Joel A, 2014. Bevattning och dränering. In Elmquist H, Arvidsson (eds). J Höstvete mot nya höjder. Uppsala: Swedish University of Agricultural Sciences. (Rapporter från jordbearbetningen 129) (In Swedish.)

Williamsson U, Gunnarsson A, Djurle A, Kirchmann H. 2004. Klorbrist orsakar fysiologiska fläckar i höstvete. Uppsala: Swedish University of Agricultural Sciences. (Fakta Jordbruk 15) (In Swedish.)

Appendix A

Radionuclide-specifc parameters

Table A-1. Dose coefficient for ^{14}C in drinking water.

Parameter	Unit	Description	Value
doseCoef_ing_water_14C	Sv Bq^{-1}	Dose coefficient for ^{14}C in drinking water	2.90E-11

Table A-2. Dose coefficient for external exposure (doseCoef_ext, (Sv h^{-1})/(Bq m^{-3})), inhalation (doseCoef_inh (Sv Bq^{-1})) and ingestion (doseCoef_ing, (Sv Bq^{-1})). The dose cefficents for external exposure are based on homogeneous distribution of the radionuclides in a soil layer of infinite depth and infinite lateral extent. (svn://svn.skb.se/SFL/SFL-SAK/Arbetsmaterial/RadionuclideTransport/GemensammaIndata/Radionuclides/DCC.xlsm)

Radionuclides	doseCoef_ext 1)	doseCoef_inh 2)	doseCoef_ing 2)
Ac-227	3.6E−14	5.7E−04	1.2E−06
Ag-108m	1.7E−13	3.7E−08	2.3E−09
Am-241	7.2E−16	9.6E−05	2.0E−07
Am-242m	1.2E−15	9.2E−05	1.9E−07
Am-243	1.6E−14	9.6E−05	2.0E−07
Ar-39	1.5E−17	0.0E+00	0.0E+00
Ba-133	3.5E−14	1.0E−08	1.5E−09
Be-10	1.9E−17	3.5E−08	1.1E−09
C-14-ind	2.1E−19	6.2E−12	5.8E−10
C-14-inorg	2.1E−19	6.2E−12	5.8E−10
C-14-org	2.1E−19	6.2E−12	5.8E−10
Ca-41	0.0E+00	1.8E−10	1.9E−10
Cd-113m	1.2E−17	1.1E−07	2.3E−08
Cl-36	4.8E−17	7.3E−09	9.3E−10
Cm-242	2.5E−18	5.9E−06	1.2E−08
Cm-243	1.0E−14	6.9E−05	1.5E−07
Cm-244	1.7E−18	5.7E−05	1.2E−07
Cm-245	5.9E−15	9.9E−05	2.1E−07
Cm-246	1.6E−18	9.8E−05	2.1E−07
Co-60	3.0E−13	3.1E−08	3.4E−09
Cs-135	6.2E−19	8.6E−09	2.0E−09
Cs-137	6.2E−14	3.9E−08	1.3E−08
Eu-150	1.6E−13	5.3E−08	1.3E−09
Eu-152	1.3E−13	4.2E−08	1.4E−09
Gd-148	0.0E+00	2.6E−05	5.6E−08
H-3	0.0E+00	2.6E−10	1.8E−11
Ho-166m	1.9E−13	1.2E−07	2.0E−09
I-129	1.8E−16	3.6E−08	1.1E−07
K-40	1.9E−14	2.1E−09	6.2E−09
La-137	2.0E−16	8.7E−09	8.1E−11
Mo-93	8.0E−18	2.3E−09	3.1E−09
Nb-93m	1.4E−18	1.8E−09	1.2E−10
Nb-94	1.8E−13	4.9E−08	1.7E−09
Ni-59	0.0E+00	4.4E−10	6.3E−11
Ni-63	0.0E+00	1.3E−09	1.5E−10
Np-237	1.9E−14	5.0E−05	1.1E−07
Pa-231	3.4E−15	1.4E−04	7.1E−07
Pb-210	1.4E−16	5.7E−06	6.9E−07
Pd-107	0.0E+00	5.9E−10	3.7E−11
Po-210	9.5E−19	4.3E−06	1.2E−06

Radionuclides	doseCoef_ext 1)	doseCoef_inh 2)	doseCoef_ing 2)
Pu-238	2.2E−18	1.1E−04	2.3E−07
Pu-239	5.1E−18	1.2E−04	2.5E−07
Pu-240	2.2E−18	1.2E−04	2.5E−07
Pu-241	3.3E−19	2.3E−06	4.8E−09
Pu-242	1.9E−18	1.1E−04	2.4E−07
Ra-226	2.0E−13	9.5E−06	2.8E−07
Ra-228	1.1E−13	1.6E−05	6.9E−07
Re-186m	1.8E−15	1.3E−08	3.7E−09
Se-79	2.9E−19	6.8E−09	2.9E−09
Si-32	3.9E−16	1.1E−07	3.0E−09
Sm-151	1.3E−20	4.0E−09	9.8E−11
Sr-90	7.9E−16	1.6E−07	3.1E−08
Tb-157	4.5E−17	1.2E−09	3.4E−11
Tb-158	8.6E−14	4.6E−08	1.1E−09
Tc-99	2.1E−18	1.3E−08	6.4E−10
Th-228	1.9E−13	4.4E−05	1.4E−07
Th-229	2.8E−14	2.6E−04	6.1E−07
Th-230	2.1E−17	1.0E−04	2.1E−07
Th-232	8.8E−18	1.1E−04	2.3E−07
Ti-44	2.5E−13	1.2E−07	6.2E−09
U-232	1.5E−17	3.7E−05	3.3E−07
U-233	2.4E−17	9.6E−06	5.1E−08
U-234	6.6E−18	9.4E−06	4.9E−08
U-235	1.3E−14	8.5E−06	4.7E−08
U-236	3.4E−18	8.7E−06	4.7E−08
U-238	2.6E−15	8.0E−06	4.8E−08
Zr-93	0.0E+00	2.5E−08	1.1E−09

1) *Eckerman and Ryman 1993*
2) ICRP 2012

Table A-3. Average relative contribution from radionuclides including daughter radionuclides in agricultural lands for external exposure (dose_ingrowth_agri_ext), ingestion (dose_ingrowth_agri_ing) and inhalation (dose_ingrowth_agri_inh) (unitless). (svn://svn.skb.se/projekt/SFLsurface/Synthesis/Parameters/RN.xlsm)

Radionuclide	dose_ingrowth_agri_ext	dose_ingrowth_agri_ing	dose_ingrowth_agri_inh
Ac-227	1	1	1
Ag-108m	1	1	1
Am-241	1	1	1
Am-242m	1.00	1.23	1.23
Am-243	1	1.00	1.00
Ar-39	1	1	1
Ba-133	1	1	1
Be-10	1	1	1
C-14-ind	1	1	1
C-14-inorg	1	1	1
C-14-org	1	1	1
Ca-41	1	1	1
Cd-113m	1	1	1
Cl-36	1	1	1
Cm-242	1.15	4.16	4.07
Cm-243	1	1.00	1.00
Cm-244	1.00	1.01	1.01
Cm-245	1.00	1.03	1.03
Cm-246	1	1	1
Co-60	1	1	1
Cs-135	1	1	1
Cs-137	1	1	1
Eu-150	1	1	1
Eu-152	1	1	1
Gd-148	1	1	1
H-3	1	1	1
Ho-166m	1	1	1
I-129	1	1	1
K-40	1	1	1
La-137	1	1	1
Mo-93	1.10	1.02	1.46
Nb-93m	1	1	1
Nb-94	1	1	1
Ni-59	1	1	1
Ni-63	1	1	1
Np-237	1	1	1
Pa-231	6.27	1.85	2.96
Pb-210	1.01	2.68	1.75
Pd-107	1	1	1
Po-210	1	1	1
Pu-238	1	1	1
Pu-239	1	1	1
Pu-240	1	1	1
Pu-241	114.87	3.18	3.19
Pu-242	1	1	1
Ra-226	1	4.28	1.51
Ra-228	2.60	1.19	3.55
Re-186m	1	1	1
Se-79	1	1	1
Si-32	1	1	1
Sm-151	1	1	1
Sn-126	1	1	1

Radionuclide	dose_ingrowth_agri_ext	dose_ingrowth_agri_ing	dose_ingrowth_agri_inh
Sr-90	1	1	1
Tb-157	1	1	1
Tb-158	1	1	1
Tc-99	1	1	1
Th-228	1	1	1
Th-229	1	1	1
Th-230	107.65	1.05	1.00
Th-232	26700.28	3.97	1.43
Ti-44	1	1	1
U-232	11528.04	1.41	2.11
U-233	3.76	1.03	1.06
U-234	1.05	1.00	1.00
U-235	1.00	1.01	1.02
U-236	1	1	1
U-238	1	1	1
Zr-93	1	1.06	1.04

Appendix B

Landscape geometries

Table B-1. Biosphere object-specific parameter values for the biosphere objects in Laxemar. (svn://svn.skb.se/projekt/SFLsurface/Synthesis/Parameters/OS.xlsm)

Name	Unit	Object 201	Object 203	Object 204	Object 206	Object 207	Object 208	Object 210	Object 212	Object 213
area_obj	m^2	5.11E+05	3.68E+05	9.40E+04	7.80E+04	1.74E+05	8.03E+05	1.16E+05	2.53E+05	1.36E+05
area_obj_ter_init	m^2	0.00E+00	0.00E+00	0.00E+00	0.00E+00	0.00E+00	0.00E+00	0.00E+00	0.00E+00	0.00E+00
threshold_end	year	2.11E+04	4.40E+03	8.00E+02	3.00E+02	9.80E+03	1.32E+04	2.20E+03	6.20E+03	4.40E+03
threshold_isolation	year	5.10E+03	−1.50E+03	−3.60E+03	−4.10E+03	−4.00E+02	2.50E+03	−4.30E+03	−1.00E+02	−1.90E+03
threshold_start	year	4.10E+03	−2.00E+03	−3.90E+03	−4.40E+03	−9.00E+02	1.70E+03	−4.70E+03	−6.00E+02	−2.20E+03
threshold_stop	year	6.80E+03	−8.00E+02	−3.10E+03	−3.50E+03	4.00E+02	3.70E+03	−3.90E+03	1.30E+03	−1.20E+03
threshold_well	year	6.80E+03	−8.00E+02	−3.10E+03	−3.50E+03	4.00E+02	3.70E+03	−3.90E+03	1.30E+03	−1.20E+03
z_regoGL	m	2.00E+00	1.13E+00	5.40E−01	8.40E−01	7.90E−01	1.23E+00	7.50E−01	2.60E−01	6.70E−01
z_regoLow	m	3.25E+00	2.29E+00	1.54E+00	2.79E+00	2.81E+00	2.85E+00	2.99E+00	2.14E+00	2.64E+00
z_regoPeat_equlib	m	1.89E+00	1.50E+00	1.32E+00	1.69E+00	1.78E+00	1.69E+00	1.49E+00	1.46E+00	1.37E+00
z_regoPeat_init	m	0.00E+00	0.00E+00	0.00E+00	0.00E+00	0.00E+00	0.00E+00	0.00E+00	0.00E+00	0.00E+00
timeshift	year	0.00E+00				0.00E+00	0.00E+00			

Table B-2. Biosphere object-specific parameter values assigned to time-independent sea biosphere objects in Laxemar. These are representing; an early time point (9 500 BC), representing a sea basin with a high rate of water exchange (201) and a semi-enclosed embayment with a low water exchange (208). (svn://svn.skb.se/projekt/SFLsurface/Synthesis/Parameters/Sea_constant.xlsm)

Parameter	Unit	Object 201	Object 208
area_obj_aqu	m^2	6.50E+06	1.22E+06
biom_pp_macro	kgC m^{-2}	0.00E+00	4.09E−02
biom_pp_micro	kgC m^{-2}	0.00E+00	2.39E−03
biom_pp_plank	kgC m^{-2}	4.88E−04	7.39E−05
NPP_macro	kgC m^{-2} $year^{-1}$	0.00E+00	1.99E−01
NPP_micro	kgC m^{-2} $year^{-1}$	0.00E+00	3.08E−02
NPP_plank	kgC m^{-2} $year^{-1}$	4.80E−02	7.27E−03
res_rate	m^3 m^{-2} $year^{-1}$	9.60E−04	4.21E−04
sed_rate	m^3 m^{-2} $year^{-1}$	9.60E−04	3.13E−04
wat_ret	Year	1.10E−02	8.31E−02
z_regoPG_aqu	m	6.90E−01	1.73E+00
z_water	m	5.20E+01	3.03E+00

Table B-3. Biosphere object-specific parameter values assigned to time-independent lake biosphere objects in Laxemar. These are describing the biosphere objects at the time for lake isolation, which is 5 100 AD, 2 000 AD and 2 500 AD for biosphere objects 201, 207 and 208, respectively. (svn://svn.skb.se/projekt/SFLsurface/Synthesis/Parameters/Lake_constant.xlsm)

Parameter	Unit	Object 201	Object 207	Object 208
area_obj_aqu	m^2	4.73E+05	1.10E+05	5.98E+05
biom_pp_macro	kgC m^{-2}	1.33E−04	3.25E−05	6.68E−04
biom_pp_micro	kgC m^{-2}	0	0	0
biom_pp_plank	kgC m^{-2}	5.88E−04	5.88E−04	5.88E−04
NPP_macro	kgC m^{-2} $year^{-1}$	1.70E−04	4.16E−05	8.55E−04
NPP_micro	kgC m^{-2} $year^{-1}$	0	0	0
NPP_plank	kgC m^{-2} $year^{-1}$	4.00E−02	4.00E−02	4.00E−02
res_rate	m^3 m^{-2} $year^{-1}$	4.93E−04	4.60E−04	4.48E−04
sed_rate	m^3 m^{-2} $year^{-1}$	1.21E−03	1.16E−03	1.01E−03
z_regoPG_aqu	m	4.11E+00	3.94E+00	2.28E+00
z_water	m	6.79E+00	3.69E+00	4.44E+00

Table B-4. Biosphere object-specific parameter values for time-independent mire biosphere objects in Laxemar. The present-day lake and sea biosphere objects (201, 207 and 208) were parameterized by using the available landscape development data (time-dependent) for a late period when the biosphere object is a mire. (svn://svn.skb.se/projekt/SFLsurface/Synthesis/Parameters/Mire_constant.xlsm)

Parameter	Unit	Object 203	Object 204	Object 206	Object 210	Object 212	Object 213
area_basin	m^2	2.67E+06	4.50E+05	6.15E+05	1.92E+06	1.74E+06	7.73E+06
area_obj_aqu	m^2	1.88E+03	1.07E+03	9.47E+02	2.04E+03	2.81E+03	4.23E+03
area_obj_ter	m^2	3.66E+05	9.29E+04	7.71E+04	1.14E+05	2.50E+05	1.32E+05
area_watershed	m^2	3.11E+06	4.50E+05	6.15E+05	1.92E+06	1.48E+07	1.31E+07
z_regoPeat_equlib	m	7.50E−01	1.32E+00	1.69E+00	1.49E+00	1.46E+00	1.37E+00
z_regoPG_ter	m	2.03E+00	1.95E+00	2.21E+00	2.26E+00	1.39E+00	2.01E+00
z_water	m	1.80E−01	1.80E−01	1.60E−01	2.51E−01	1.15E−01	2.43E−01

Table B-5. Biosphere object-specific parameter values for time-independent agricultural biosphere objects in Laxemar. These biosphere objects are agricultural land in the present-day landscape. (svn://svn.skb.se/projekt/SFLsurface/Synthesis/Parameters/agr_constant.xlsm)

Parameter	Unit	Object 204	Object 206	Object 210	Object 212	Object 213
area_basin	m^2	4.50E+05	6.15E+05	1.92E+06	1.74E+06	7.73E+06
area_obj_aqu_agri	m^2	1.07E+03	9.47E+02	2.04E+03	2.81E+03	4.23E+03
area_obj_ter_agri	m^2	9.29E+04	7.71E+04	1.14E+05	2.50E+05	1.32E+05
area_watershed	m^2	4.50E+05	6.15E+05	1.92E+06	1.48E+07	1.31E+07
z_regoPG_agri	m	1.02E+00	1.40E+00	1.39E+00	3.30E−01	1.24E+00
z_regoSub_agri	m	2.40E−01	4.10E−01	3.50E−01	3.10E−01	3.80E−01
z_water_agri	m	1.80E-01	1.65E−01	2.51E−01	1.15E−01	2.43E−01

Appendix C

Regolith parameters

Table C-1. Regolith parameters data. (svn://svn.skb.se/projekt/SFLsurface/Synthesis/Parameters/Regolith.xlsm)

Name	Unit	Land use	Value	Reference
compact_gyttja	$m\ m^{-1}$	Drained mire.	0.25	Grolander (2013, Section 5.4.3)
compact_peat	$m\ m^{-1}$	Drained mire.	0.34	Grolander (2013, Section 5.4.3)
dens_regoCoarseSed	$kg_{DW}\ m^{-3}$		1650	Sohlenius et al. (2006)
dens_regoGL	$kg_{DW}\ m^{-3}$		673	Grolander (2013, Section 5.3.2)
dens_regoLow	$kg_{DW}\ m^{-3}$		2115	Grolander (2013, Section 5.3.1)
dens_regoPeat	$kg_{DW}\ m^{-3}$		100	Grolander (2013, Section 5.3.4)
dens_regoPG	$kg_{DW}\ m^{-3}$		182	Grolander (2013, Section 5.3.3)
dens_regoUp	$kg_{DW}\ m^{-3}$	Infield-outland.	771	Grolander (2013, Section 5.3.5)
dens_regoUp	$kg_{DW}\ m^{-3}$	Garden plot.	771	Grolander (2013, Section 5.3.5)
dens_regoUp_gyttja	$kg_{DW}\ m^{-3}$	Drained mire.	771	Grolander (2013, Section 5.4.1)
dens_regoUp_lake	$kg_{DW}\ m^{-3}$		61	Grolander (2013, Section 5.3.6)
dens_regoUp_peat	$kg_{DW}\ m^{-3}$	Drained mire.	274	Grolander (2013, Section 5.4.1)
dens_regoUp_sea	$kg_{DW}\ m^{-3}$		179	Grolander (2013, Section 5.3.6)
dens_regoUp_ter	$kg_{DW}\ m^{-3}$		100	Grolander (2013, Section 5.3.5)
poro_regoCoarseSed	$m^3\ m^{-3}$		0.37	Sohlenius et al. (2006)
poro_regoGL	$m^3\ m^{-3}$		0.75	Grolander (2013, Section 5.3.2)
poro_regoLow	$m^3\ m^{-3}$		0.21	Grolander (2013, Section 5.3.1)
poro_regoPeat	$m^3\ m^{-3}$		0.9	Grolander (2013, Section 5.3.4)
poro_regoPG	$m^3\ m^{-3}$		0.92	Grolander (2013, Section 5.3.3)
poro_regoUp	$m^3\ m^{-3}$	Infield-outland.	0.63	Grolander (2013, Section 5.3.5)
poro_regoUp	$m^3\ m^{-3}$	Garden plot.	0.63	Grolander (2013, Section 5.3.5)
poro_regoUp_gyttja	$m^3\ m^{-3}$	Drained mire.	0.63	Grolander (2013, Section 5.4.1)
poro_regoUp_lake	$m^3\ m^{-3}$		0.97	Grolander (2013, Section 5.3.6)
poro_regoUp_peat	$m^3\ m^{-3}$	Drained mire.	0.75	Grolander (2013, Section 5.4.1)
poro_regoUp_sea	$m^3\ m^{-3}$		0.92	Grolander (2013, Section 5.3.6)
poro_regoUp_ter	$m^3\ m^{-3}$		0.9	Grolander (2013, Section 5.3.5)
S_w_regoUp	$m^3\ m^{-3}$	Infield-outland.	0.6	Grolander (2013, Sections 5.1 and 5.4.4)
S_w_regoUp	$m^3\ m^{-3}$	Garden plot.	0.6	Grolander (2013, Sections 5.1 and 5.4.4)
S_w_regoUp_gyttja	$m^3\ m^{-3}$	Drained mire.	0.6	Grolander (2013, Table F-1)
S_w_regoUp_peat	$m^3\ m^{-3}$	Drained mire.	0.63	Grolander (2013, Table A-3)
z_drain_agri	m	Drained mire.	0.5	Grolander (2013, Section 9.7)

Appendix D

Hydrological fluxes

Table D-1. Hydrological fluxes for sea, lake and mire biosphere objects in Laxemar (m year^{-1}). The biosphere object 206 was modelled in the base case. Object 203 was only modelled in a mire stage not preceded by sea or lake. (svn://svn.skb.se/projekt/SFLsurface/Synthesis/Parameters/q.xlsm)

Name	Object 201	Object 203	Object 206	Object 207	Object 208
q_bedrock_low_lake	1.02E−01		2.60E−01	2.00E−01	4.55E−02
q_bedrock_low_sea	7.52E−02		2.60E−02	0.00E+00	4.35E−02
q_bedrock_low_ter	1.02E−01	7.00E−02	2.60E−01	2.00E−01	4.55E−02
q_downstream	5.67E+00	1.74E+00	1.86E+00	2.24E+00	5.06E+00
q_gl_low_lake	1.42E−03		1.04E−02	9.54E−03	6.89E−03
q_gl_low_sea	1.27E−04		3.64E−03	0.00E+00	6.45E−04
q_gl_low_ter	5.23E−04	1.26E−02	2.10E−02	1.04E−02	6.18E−03
q_gl_pg_lake	1.05E−01		2.70E−01	2.09E−01	5.40E−02
q_gl_pg_sea	7.61E−02		3.51E−02	0.00E+00	4.57E−02
q_gl_pg_ter	1.03E−01	8.58E−02	2.85E−01	2.10E−01	5.24E−02
q_low_bedrock_lake	4.27E−04		3.71E−03	3.37E−03	2.40E−03
q_low_bedrock_sea	5.09E−06		2.08E−04	0.00E+00	3.84E−05
q_low_bedrock_ter	1.85E−04	6.10E−03	8.61E−03	4.22E−03	2.48E−03
q_low_gl_lake	1.03E−01		2.67E−01	2.06E−01	5.00E−02
q_low_gl_sea	7.53E−02		2.94E−02	0.00E+00	4.41E−02
q_low_gl_ter	1.03E−01	7.75E−02	2.75E−01	2.06E−01	4.93E−02
q_peat_pg_ter	1.44E−02	3.83E−02	4.90E−02	4.90E−02	3.28E−02
q_peat_up_ter	5.60E−01	9.67E−01	8.10E−01	7.11E−01	3.20E−01
q_pg_gl_lake	2.98E−03		1.42E−02	1.28E−02	1.09E−02
q_pg_gl_sea	9.21E−04		9.33E−03	0.00E+00	2.18E−03
q_pg_gl_ter	9.92E−04	1.81E−02	2.75E−02	1.34E−02	9.16E−03
q_pg_peat_ter	1.57E−01	1.66E−01	3.50E−01	2.89E−01	1.03E−01
q_pg_up_lake	1.80E+00		1.96E+00	2.80E+00	1.74E+00
q_pg_up_sea	8.09E−02		4.18E−02	0.00E+00	5.56E−02
q_up_peat_ter	7.04E−02	5.18E−01	1.77E−01	1.99E−01	7.04E−02
q_up_pg_lake	1.70E+00		1.70E+00	2.60E+00	1.70E+00
q_up_pg_sea	5.66E−03		1.60E−02	0.00E+00	1.21E−02
q_up_wat_lake	1.80E+00		1.96E+00	2.80E+00	1.74E+00
q_up_wat_sea	8.09E−02		4.18E−02	0.00E+00	5.56E−02
q_up_wat_ter	1.81E+00	1.33E+00	1.11E+00	1.38E+00	1.03E+00
q_wat_up_lake	1.70E+00		1.70E+00	2.60E+00	1.70E+00
q_wat_up_sea	5.66E−03		1.60E−02	0.00E+00	1.21E−02
q_wat_up_ter	0.00E+00	0.00E+00	0.00E+00	0.00E+00	0.00E+00

Table D-2. Hydrological fluxes for biosphere objects that today are a mire (203) or agricultural land in Laxemar. Biosphere object 206 was used in the base case. svn://svn.skb.se/projekt/SFLsurface/Synthesis/Parameters/mire_constant.xlsm and agr_constant xlsm)

Name	Unit	Object 203	Object 204	Object 206	Object 210	Object 212	Object 213
delta_disch	m^{-1}	1.20	1.00	1.20	1.20	1.60	0.90
f_disch_stream_agri	m^{-1}		0.00	0.52	0.39	0.29	0.53
f_disch_stream_ter	m^{-1}	0.16	0.00	0.52	0.39	0.29	0.53
f_disch_surf	unitless	0.65	0.86	0.45	0.80	0.84	0.93
f_surfperc_LC	unitless	0.50	0.06	0.06	0.06	0.06	0.06
f_surfperc_obj_agri	unitless		0.78	0.78	0.78	0.78	0.78
f_surfperc_obj_ter	unitless	1.00	1.00	1.00	1.00	1.00	1.00
m_percol_agri	unitless		0.34	0.34	0.34	0.34	0.34
m_percol_ter	unitless	0.32	0.32	0.32	0.32	0.32	0.32
q_bedrock_ter	m^{-1}	0.07	0.15	0.26	0.18	0.11	0.09

Table D-3. Site-specific hydrological fluxes for mire and agricultural biosphere objects in Laxemar (Obejct 201, 203, 204, 206, 207, 208, 210, 212, 213). svn://svn.skb.se/projekt/SFLsurface/Synthesis/Parameters/mire_constant.xlsm and agr_constant xlsm)

Name	Unit	Value
b_percol_agri	m^{-1}	0.00
b_percol_ter	m^{-1}	0.98
k_percol_agri	m^{-2}	0.82
k_percol_ter	m^{-2}	0.00

Table D-4. Site-specific hydrological fluxes for the constant sea bay of biosphere object 201 ($m\,year^{-1}$) at approximately 9 500 BC in Laxemar (see Section 3.5). (svn://svn.skb.se/projekt/SFLsurface/Synthesis/Parameters/sea_constant.xlsm)

Name	Value
q_bedrock_low_sea	1.02E-02
q_gl_low_sea	3.95E-04
q_gl_pg_sea	1.31E-02
q_low_bedrock_sea	1.58E-05
q_low_gl_sea	1.06E-02
q_pg_gl_sea	2.86E-03
q_pg_up_sea	1.59E-02
q_up_wat_sea	1.59E-02

Appendix E

Element-specific parameter values

Updated *CR* and K_d values for Laxemar

All the tabulated values in Appendix E are from svn://svn.skb.se/projekt/SFLsurface/Synthesis/Parameters/ElementSpecific.xlsm.

Table E-1. Selected data, properties and comments for limnic fish (cR_Lake_fish) $m^3\ kg_C^{-1}$. The abbreviations used in the table are; EA = element analogue, PA = parameter analogue, N= number of sampeles, Min= minimum, Max= maximum, GM= gemometic mean.

Element	EA	PA	N	Min	GM	Max	GSD	Reference
Ac	La		3	4.92E−04	3.00E−03	1.83E−02	2.2	Laxemar
Ag			27	1.55E−01	9.42E−01	5.74E+00	3.0	IAEA 2010
Am	La		3	4.92E−04	3.00E−03	1.83E−02	2.2	Laxemar
Ba			3	1.35E−02	8.24E−02	5.02E−01	2.9	Laxemar
Ca			3	9.02E−02	5.49E−01	3.35E+00	1.8	Laxemar
Cd			4	1.71E−01	1.49E+00	9.06E+00	3.0	ERICA
Cl			3	4.06E−02	2.48E−01	1.51E+00	1.4	Laxemar
Cm	La		3	4.92E−04	3.00E−03	1.83E−02	2.2	Laxemar
Co			3	1.80E−02	1.41E−01	1.11E+00	3.5	Laxemar
Cs			3	1.28E+01	7.80E+01	4.75E+02	2.5	Laxemar
Eu	La		3	4.92E−04	3.00E−03	1.83E−02	2.2	Laxemar
Gd	La		3	4.92E−04	3.00E−03	1.83E−02	2.2	Laxemar
Ho			1	8.76E−03	1.24E−01	1.75E+00	2.2	Laxemar
I			3	7.15E−02	4.36E−01	2.66E+00	2.6	Laxemar
La			3	4.92E−04	3.00E−03	1.83E−02	2.2	Laxemar
Mo			3	1.17E−02	7.16E−02	4.36E−01	2.6	Laxemar
Nb			3	9.15E−03	5.58E−02	3.40E−01	2.3	Laxemar
Ni			1	4.63E−03	6.54E−02	9.23E−01	1.5	Laxemar
Np	La		3	4.92E−04	3.00E−03	1.83E−02	2.2	Laxemar
Pa	La		3	4.92E−04	3.00E−03	1.83E−02	2.2	Laxemar
Pb			39	8.57E−04	2.14E−01	2.31E+00	3.0	IAEA 2010
Pd	Ni		1	4.63E−03	6.54E−02	9.23E−01	1.5	Laxemar
Po			5	2.80E−02	3.08E−01	3.40E+00	4.3	IAEA 2010
Pu			3	1.27E+01	1.80E+02	2.54E+03	5.0	IAEA 2010
Ra	Ba		3	1.35E−02	8.24E−02	5.02E−01	2.9	Laxemar
Re	Tc		3	1.83E−02	2.58E−01	3.64E+00	5.0	ERICA
Se			3	3.13E+00	1.90E+01	1.16E+02	1.3	Laxemar
Si	Zr		3	2.74E−02	1.67E−01	1.02E+00	2.1	Laxemar
Sm			1	1.84E−03	2.60E−02	3.67E−01	2.6	Laxemar
Sn	Zr		3	2.74E−02	1.67E−01	1.02E+00	2.1	Laxemar
Sr			3	7.19E−03	7.43E−02	4.53E−01	2.7	Laxemar
Tb	La		3	4.92E−04	3.00E−03	1.83E−02	2.2	Laxemar
Tc			3	1.83E−02	2.58E−01	3.64E+00	5.0	ERICA
Th			5	1.09E−01	6.66E−01	4.80E+00	2.3	ERICA
Ti	Zr		3	2.74E−02	1.67E−01	1.02E+00	2.1	Laxemar
U			3	1.23E−03	8.63E−03	5.51E−02	3.1	Laxemar
Zr			3	2.74E−02	1.67E−01	1.02E+00	2.1	Laxemar

Table E-2. Selected data, properties and comments for limnic primary producers (cR_Lake_pp_ macro, cR_lake_pp_micor, cR_Lake_pp_plank) m^3 kg_C^{-1}. The abbreviations used in the table are; EA = element analogue, PA = parameter analogue, N= number of sampeles, Min= minimum, Max= maximum, GM= gemometic mean.

Element	EA	PA	N	Min	GM	Max	GSD	Reference
Ac	La		3	2.17E−01	2.12E+00	2.08E+01	2.5	Laxemar
Ag			1	8.14E−01	2.00E+01	4.91E+02	7.0	ERICA
Am	La		3	2.17E−01	2.12E+00	2.08E+01	2.5	Laxemar
Ba			3	1.26E+00	1.24E+01	1.21E+02	3.1	Laxemar
Ca			3	7.83E−01	7.66E+00	7.49E+01	1.1	Laxemar
Cd			3	8.77E−01	8.58E+00	8.39E+01	1.6	Laxemar
Cl			3	1.66E−01	1.62E+00	1.59E+01	1.2	Laxemar
Cm	La		3	2.17E−01	2.12E+00	2.08E+01	2.5	Laxemar
Co			3	1.13E+00	1.11E+01	1.08E+02	3.7	Laxemar
Cs			3	1.08E+00	1.06E+01	1.03E+02	1.4	Laxemar
Eu			3	2.36E−01	2.31E+00	2.26E+01	2.5	Laxemar
Gd	La		3	2.17E−01	2.12E+00	2.08E+01	2.5	Laxemar
Ho			3	9.94E−02	9.72E−01	9.51E+00	2.5	Laxemar
I			3	2.03E−01	1.99E+00	1.94E+01	2.5	Laxemar
La			3	2.17E−01	2.12E+00	2.08E+01	2.5	Laxemar
Mo			3	4.22E−01	4.13E+00	4.04E+01	2.6	Laxemar
Nb			3	2.09E−01	2.05E+00	2.00E+01	2.3	Laxemar
Ni			3	1.97E−01	1.92E+00	1.88E+01	1.8	Laxemar
Np	La		3	2.17E−01	2.12E+00	2.08E+01	2.5	Laxemar
Pa	La		3	2.17E−01	2.12E+00	2.08E+01	2.5	Laxemar
Pb			3	5.82E−01	5.69E+00	5.57E+01	3.2	Laxemar
Pd	Ni		3	1.97E−01	1.92E+00	1.88E+01	1.8	Laxemar
Po			6	2.46E+00	2.41E+01	2.36E+02	4.0	ERICA
Pu			40	2.98E+00	6.45E+02	1.22E+06	14.0	IAEA 2010
Ra	Ba		3	1.26E+00	1.24E+01	1.21E+02	3.1	Laxemar
Re	Tc		9	7.20E−03	1.36E−01	2.46E+00	4.9	IAEA 2010
Se			3	4.93E−01	4.82E+00	4.72E+01	1.2	Laxemar
Si	Zr		3	9.55E−02	9.34E−01	9.14E+00	2.1	Laxemar
Sm			3	1.46E−01	1.43E+00	1.40E+01	2.7	Laxemar
Sn	Zr		3	9.55E−02	9.34E−01	9.14E+00	2.1	Laxemar
Sr			3	1.29E−01	1.26E+00	1.23E+01	1.6	Laxemar
Tb	La		3	2.17E−01	2.12E+00	2.08E+01	2.5	Laxemar
Tc			9	5.56E−03	1.36E−01	3.35E+00	7.0	IAEA 2010
Th			3	1.51E−01	1.48E+00	1.45E+01	1.7	Laxemar
Ti	Zr		3	9.55E−02	9.34E−01	9.14E+00	2.1	Laxemar
U			3	1.26E−01	1.23E+00	1.20E+01	1.6	Laxemar
Zr			3	9.55E−02	9.34E−01	9.14E+00	2.1	Laxemar

Table E-3. Selected data, properties and comments for marine fish (CR_sea_fish) $m^3\ kg_C^{-1}$. The abbreviations used in the table are; EA = element analogue, PA = parameter analogue, N= number of sampeles, Min= minimum, Max= maximum, GM= gemometic mean.

Element	EA	PA	N	Min	GM	Max	GSD	Reference
Ac	La		3	1.92E−03	2.63E−02	9.95E−01	4.9	Laxemar
Ag			4	2.35E+00	1.43E+01	8.74E+01	3.0	ERICA
Am	La		3	1.92E−03	2.63E−02	9.95E−01	4.9	Laxemar
Ba			3	2.82E−03	1.72E−02	1.05E−01	1.5	Laxemar
Ca			3	4.52E−03	2.76E−02	1.68E−01	2.0	Laxemar
Cd			3	1.29E−01	7.84E−01	4.77E+00	1.8	Laxemar
Cl			3	2.32E−04	1.41E−03	8.61E−03	1.6	Laxemar
Cm	La		3	1.92E−03	2.63E−02	9.95E−01	4.9	Laxemar
Co			3	4.22E−02	2.77E−01	2.01E+00	3.1	Laxemar
Cs			3	3.78E−01	2.30E+00	1.40E+01	1.8	Laxemar
Eu	La		3	1.92E−03	2.63E−02	9.95E−01	4.9	Laxemar
Gd	La		3	1.87E−03	2.63E−02	9.95E−01	5.0	Laxemar
Ho	La		3	1.92E−03	2.63E−02	9.95E-01	4.9	Laxemar
I			3	2.30E−02	1.40E−01	8.53E−01	1.5	Laxemar
La			3	1.87E−03	2.63E−02	9.95E−01	5.0	Laxemar
Mo			3	2.14E−03	1.30E−02	7.94E−02	1.4	Laxemar
Nb			3	2.46E−02	1.50E−01	9.12E−01	1.5	Laxemar
Ni			2	2.71E−02	1.65E−01	1.01E+00	2.6	Laxemar
Np	La		3	1.87E−03	2.63E−02	9.95E−01	5.0	Laxemar
Pa	La		3	1.92E−03	2.63E−02	9.95E−01	4.9	Laxemar
Pb			1	1.34E−01	1.90E+00	2.68E+01	1.0	Laxemar
Pd	Ni		2	2.71E−02	1.65E−01	1.01E+00	2.6	Laxemar
Po			16	1.20E+01	1.16E+02	7.05E+02	3.0	ERICA
Pu			25	1.71E−02	1.78E−01	3.34E+00	3.8	ICRP 2009
Ra	Ba		3	2.82E−03	1.72E−02	1.05E−01	1.5	Laxemar
Re	Tc		92	1.77E−02	1.29E−01	3.43E+00	3.3	ERICA
Se			3	5.23E+00	3.18E+01	1.94E+02	1.2	Laxemar
Si	Zr		3	6.12E−02	1.17E+00	2.67E+01	6.0	Laxemar
Sm			1	9.65E−03	1.36E−01	1.92E+00	4.5	Laxemar
Sn			3	6.47E−01	3.94E+00	2.40E+01	1.5	Laxemar
Sr			3	3.48E−04	3.00E−03	2.81E−02	3.7	Laxemar
Tb	La		3	1.87E−03	2.63E−02	9.95E−01	5.0	Laxemar
Tc			92	1.77E−02	1.29E−01	3.43E+00	3.3	ERICA
Th			3	4.30E−01	2.62E+00	1.59E+01	2.0	Laxemar
Ti	Zr		3	6.12E−02	1.17E+00	2.67E+01	6.0	Laxemar
U			3	2.56E−04	1.56E−03	9.49E−03	1.5	Laxemar
Zr			3	6.12E−02	1.17E+00	2.67E+01	6.0	Laxemar

Table E-4. Selected data, properties and comments for marine primary producers (cR_sea_pp_macro) m^3 kg_C^{-1}. The abbreviations used in the table are; EA = element analogue, PA = parameter analogue, N= number of sampeles, Min= minimum, Max= maximum, GM= gemometic mean.

Element	EA	PA	N	Min	GM	Max	GSD	Reference
Ac	Nd		3	2.25E+00	8.27E+01	3.41E+03	7.7	Laxemar
Ag			10	3.78E+00	2.53E+01	1.97E+02	3.2	ICRP 2009
Am	Nd		3	2.25E+00	8.27E+01	3.41E+03	7.7	Laxemar
Ba			3	3.19E−01	4.61E+00	6.25E+01	4.9	Laxemar
Ca			3	1.08E−01	8.99E−01	9.33E+00	3.6	Laxemar
Cd			3	1.54E+01	9.41E+01	8.44E+02	2.5	Laxemar
Cl			3	4.94E−03	3.01E−02	1.84E−01	1.5	Laxemar
Cm	Nd		3	2.25E+00	8.27E+01	3.41E+03	7.7	Laxemar
Co			3	1.38E+00	3.19E+01	1.17E+03	6.0	Laxemar
Cs			3	4.39E−01	2.68E+00	1.63E+01	2.3	Laxemar
Eu			2	4.07E+00	2.99E+01	2.19E+02	3.4	Laxemar
Gd	Nd		3	2.25E+00	8.27E+01	3.41E+03	7.7	Laxemar
Ho			3	1.69E+00	2.17E+01	2.80E+02	4.7	Laxemar
I			3	1.71E+00	1.04E+01	6.35E+01	2.1	Laxemar
La	Nd		3	2.25E+00	8.27E+01	3.41E+03	7.7	Laxemar
Mo			3	8.21E−02	5.00E−01	3.05E+00	2.4	Laxemar
Nb			3	1.86E+00	2.93E+01	3.60E+02	4.6	Laxemar
Ni			3	1.95E+00	1.19E+01	7.25E+01	2.0	Laxemar
Np	Nd		3	2.25E+00	8.27E+01	3.41E+03	7.7	Laxemar
Pa	Nd		3	2.25E+00	8.27E+01	3.41E+03	7.7	Laxemar
Pb			3	5.82E+00	3.84E+01	2.53E+02	3.1	Laxemar
Pd	Ni		3	1.95E+00	1.19E+01	7.25E+01	2.0	Laxemar
Po			13	9.21E−01	1.05E+01	6.41E+01	3.0	ERICA
Pu			146	4.34E+00	3.22E+01	1.97E+02	3.0	ICRP 2009
Ra	Ba		3	3.19E−01	4.61E+00	6.25E+01	4.9	Laxemar
Re	Tc		166	8.00E+01	4.87E+02	5.62E+03	3.0	ICRP 2009
Se			3	2.67E+00	1.63E+01	9.90E+01	1.3	Laxemar
Si	Zr		3	2.83E+00	3.97E+01	3.86E+02	3.7	Laxemar
Sm			3	2.23E+00	6.76E+01	2.75E+03	7.6	Laxemar
Sn			3	2.67E+00	1.63E+01	9.92E+01	2.3	Laxemar
Sr			3	9.32E−02	9.77E−01	1.02E+01	4.2	Laxemar
Tb	Nd		3	2.25E+00	8.27E+01	3.41E+03	7.7	Laxemar
Tc			166	8.00E+01	4.87E+02	5.62E+03	3.0	ICRP 2009
Th			3	1.43E+00	3.50E+01	7.41E+02	6.4	Laxemar
Ti	Zr		3	2.83E+00	3.97E+01	3.86E+02	3.7	Laxemar
U			3	1.82E−01	1.84E+00	1.12E+01	2.9	Laxemar
Zr			3	2.83E+00	3.97E+01	3.86E+02	3.7	Laxemar

Table E-5. Selected data, properties and comments for primary producers (cR_ter_pp) and fodder (cR_agri_fodder) kg_{DW} kg_C^{-1}. The abbreviations used in the table are; EA = element analogue, PA = parameter analogue, N= number of sampeles, Min= minimum, Max= maximum, GM= gemometic mean.

Element	EA	PA	N	Min	GM	Max	GSD	Reference
Ac	La		8	4.21E−04	1.16E−02	1.13E−01	3.1	Laxemar
Ag		cR_agri_cereal	10	1.71E−03	4.19E−02	1.03E+00	7.0	Forsmark
Am	La		8	4.21E−04	1.16E−02	1.13E−01	3.1	Laxemar
Ba			8	5.50E−02	1.19E+00	1.17E+01	2.7	Laxemar
Cd			8	4.41E−02	6.31E−01	1.76E+01	3.7	Laxemar
Cm	La		8	4.21E−04	1.16E−02	1.13E−01	3.1	Laxemar
Co			8	1.20E−02	1.17E−01	1.15E+00	1.8	Laxemar
Cs			8	8.96E−03	2.06E−01	9.38E+00	4.1	Laxemar
Eu			8	6.13E−04	6.49E−03	6.34E−02	3.0	Laxemar
Gd	La		8	4.21E−04	1.16E−02	1.13E−01	3.1	Laxemar
Ho			6	6.66E−04	6.51E−03	6.37E−02	2.8	Laxemar
I			5	6.75E−03	1.56E−01	1.30E+01	5.8	Forsmark
La			8	4.21E−04	1.16E−02	1.13E−01	3.1	Laxemar
Mo			8	6.97E−03	2.02E−01	4.86E+00	5.1	Laxemar
Nb			8	8.49E−04	8.30E−03	8.12E−02	2.1	Laxemar
Ni			8	2.48E−02	2.42E−01	2.37E+00	2.4	Laxemar
Np	La		8	4.21E−04	1.16E−02	1.13E−01	3.1	Laxemar
Pa	La		8	4.21E−04	1.16E−02	1.13E−01	3.1	Laxemar
Pb			8	3.66E−03	3.58E−02	3.50E−01	2.1	Laxemar
Pd	Ni		8	2.48E−02	2.42E−01	2.37E+00	2.4	Laxemar
Po	Bi	cR_agri_cereal	10	2.66E−04	6.54E−03	1.61E−01	7.0	Forsmark
Pu	U		8	1.49E−04	1.67E−03	2.01E−02	3.3	Laxemar
Ra			6	6.13E−03	5.99E−02	9.76E−01	4.0	Forsmark
Re		cR_agri_cereal	9	9.04E−04	6.41E−02	4.55E+00	7.0	Forsmark
Se		cR_agri_cereal	6	2.30E−03	5.65E−02	1.39E+00	7.0	Forsmark
Si	Zr		8	3.79E−03	3.70E−02	5.38E−01	3.8	Laxemar
Sm			8	2.76E−04	4.73E−03	5.38E−02	3.2	Laxemar
Sn			3	1.14E−02	1.11E−01	1.09E+00	1.8	Laxemar
Sr			8	2.05E−01	2.01E+00	1.96E+01	1.9	Laxemar
Tb	La		8	4.21E−04	1.16E−02	1.13E−01	3.1	Laxemar
Tc	Re	cR_agri_cereal	9	9.04E−04	6.41E−02	4.55E+00	7.0	Forsmark
Th			1	1.19E−03	1.16E−02	1.14E−01	2.2	Laxemar
Ti	Zr		8	3.79E−03	3.70E−02	5.38E−01	3.8	Laxemar
U			8	1.49E−04	1.67E−03	2.01E−02	3.3	Laxemar
Zr			8	3.79E−03	3.70E−02	5.38E−01	3.8	Laxemar

Table E-6. Selected data, properties and comments for herbivores (cR_food_to_herbiv) $kg_C\ kg_C^{-1}$. The abbreviations used in the table are; EA = element analogue, PA = parameter analogue, N= number of sampeles, Min= minimum, Max= maximum, GM= gemometic mean.

Element	EA	PA	N	Min	GM	Max	GSD	GSD Ref	Reference
Ac	La		13	3.72E−04	2.86E−02	1.10E+00	4.5	GSD	Laxemar
Ag			1	1.41E−05	4.30E−04	1.32E−02	8.0	GSDmax	IAEA 2010
Am	La		13	3.72E−04	2.86E−02	1.10E+00	4.5	GSD	Laxemar
Ba			12	5.92E−04	3.03E−02	1.52E+00	4.0	GSD	Laxemar
Ca			13	3.22E−03	1.24E−01	1.53E+00	3.4	GSD	Laxemar
Cd			13	6.85E−03	5.21E−01	2.63E+01	5.0	GSD	Laxemar
Cl			13	2.79E−01	7.10E+00	7.54E+01	3.8	GSD	Laxemar
Cm	La		13	3.72E−04	2.86E−02	1.10E+00	4.5	GSD	Laxemar
Co			13	6.00E−03	3.32E−01	3.43E+00	2.8	GSD	Laxemar
Cs			13	1.92E−01	3.57E+01	8.77E+02	5.7	GSD	Laxemar
Eu			1	3.81E−02	3.73E−01	3.65E+00	1.6	GSD	Laxemar
Gd	La		13	3.72E−04	2.86E−02	1.10E+00	4.5	GSD	Laxemar
Ho			1	7.92E−02	7.74E−01	7.57E+00	2.0	GSD	Laxemar
I			1	9.22E−02	1.00E+01	3.06E+02	8.0	GSDmax	Forsmark
La			13	3.72E−04	2.86E−02	1.10E+00	4.5	GSD	Laxemar
Mo			13	1.41E−02	6.40E−01	1.23E+01	4.7	GSD	Laxemar
Nb			13	1.79E−02	4.11E−01	4.02E+00	3.0	GSD	Laxemar
Ni			8	1.38E−02	1.47E−01	1.44E+00	2.2	GSD	Laxemar
Np	La		13	3.72E−04	2.86E−02	1.10E+00	4.5	GSD	Laxemar
Pa	La		13	3.72E−04	2.86E−02	1.10E+00	4.5	GSD	Laxemar
Pb			4	8.83E−02	1.17E+00	1.15E+01	2.5	GSD	Laxemar
Pd	Ni		8	1.38E−02	1.47E−01	1.44E+00	2.2	GSD	Laxemar
Po			1	4.58E−03	1.40E−01	4.28E+00	8.0	GSDmax	IAEA 2010
Pu			1	1.27E−06	3.90E−05	1.19E−03	8.0	GSDmax	IAEA 2010
Ra			2	2.60E−03	2.66E−02	2.61E−01	4.0	GSD	Laxemar
Re	Zr		13	2.41E−02	1.56E+00	2.04E+01	4.3	GSD	Laxemar
Se			6	1.58E+00	1.54E+01	1.51E+02	4.0	GSDmean	Forsmark
Si	Zr		13	2.41E−02	1.56E+00	2.04E+01	4.3	GSD	Laxemar
Sm			7	6.71E−03	1.77E−01	1.79E+00	3.5	GSD	Laxemar
Sn			4	5.67E−01	5.55E+00	5.43E+01	2.7	GSD	Laxemar
Sr			13	4.88E−04	2.05E−02	2.00E−01	3.9	GSD	Laxemar
Tb	La		13	3.72E−04	2.86E−02	1.10E+00	4.5	GSD	Laxemar
Tc	Zr		13	2.41E−02	1.56E+00	2.04E+01	4.3	GSD	Laxemar
Th			1	3.25E−01	3.18E+00	3.11E+01	2.0	GSD	Laxemar
Ti	Zr		13	2.41E−02	1.56E+00	2.04E+01	4.3	GSD	Laxemar
U			10	4.18E−02	5.93E−01	2.15E+01	3.4	GSD	Laxemar
Zr			13	2.41E−02	1.56E+00	2.04E+01	4.3	GSD	Laxemar

Table E-7. Selected data, properties and comments for K_d for particulate matter in lakes (Kd_PM_lake) $m^3\ kg_{DW}^{-1}$. The abbreviations used in the table are; EA = element analogue, PA = parameter analogue, N= number of sampeles, Min= minimum, Max= maximum, GM= gemometic mean.

Element	EA	PA	N	Min	GM	Max	GSD	GSD Ref	Reference
Ac	Sm		3	7.63E+00	1.08E+02	1.52E+03	2.0	GSD	Laxemar
Ag			2	2.57E+00	3.62E+01	5.12E+02	2.0	GSD	Laxemar
Am	Sm		3	7.63E+00	1.08E+02	1.52E+03	2.0	GSD	Laxemar
Ba			3	1.49E+00	2.10E+01	2.97E+02	1.7	GSD	Laxemar
Ca			3	9.82E−02	1.39E+00	1.96E+01	1.3	GSD	Laxemar
Cd			2	1.09E+01	1.54E+02	2.17E+03	2.7	GSD	Laxemar
Cl	Br		3	6.12E−02	8.64E−01	1.22E+01	3.6	GSD	Laxemar
Cm	Sm		3	7.63E+00	1.08E+02	1.52E+03	2.0	GSD	Laxemar
Co			3	3.96E+00	1.12E+02	3.18E+03	7.6	GSD	Laxemar
Cs			3	1.08E+01	1.52E+02	2.15E+03	2.8	GSD	Laxemar
Eu			3	7.60E+00	1.07E+02	1.51E+03	1.9	GSD	Laxemar
Gd	Sm		3	7.63E+00	1.08E+02	1.52E+03	2.0	GSD	Laxemar
Ho			3	7.79E+00	1.10E+02	1.55E+03	1.9	GSD	Laxemar
I			3	8.31E−01	1.17E+01	1.66E+02	1.7	GSD	Laxemar
La	Sm		3	7.63E+00	1.08E+02	1.52E+03	2.0	GSD	Laxemar
Mo			3	9.20E−01	1.30E+01	1.83E+02	1.3	GSD	Laxemar
Nb			3	3.26E+01	4.61E+02	6.51E+03	2.3	GSD	Laxemar
Ni			3	1.34E+00	1.89E+01	2.67E+02	1.5	GSD	Laxemar
Np	Sm		3	7.63E+00	1.08E+02	1.52E+03	2.0	GSD	Laxemar
Pa	Sm		3	7.63E+00	1.08E+02	1.52E+03	2.0	GSD	Laxemar
Pb			3	3.24E+01	4.58E+02	6.46E+03	3.2	GSD	Laxemar
Pd	Ni		3	1.34E+00	1.89E+01	2.67E+02	1.5	GSD	Laxemar
Po	Bi		2	1.25E+01	1.76E+02	2.49E+03	1.7	GSD	Laxemar
Pu	U		3	3.37E+00	4.75E+01	6.71E+02	1.7	GSD	Laxemar
Ra	Ba		3	1.49E+00	2.10E+01	2.97E+02	1.7	GSD	Laxemar
Re			2	1.54E−02	2.17E−01	3.06E+00	2.9	GSD	Laxemar
Se			3	8.10E−01	1.14E+01	1.62E+02	2.1	GSD	Laxemar
Si	Zr		3	8.67E+00	1.22E+02	1.73E+03	2.7	GSD	Laxemar
Sm			3	7.63E+00	1.08E+02	1.52E+03	2.0	GSD	Laxemar
Sn	Zr		3	8.67E+00	1.22E+02	1.73E+03	2.7	GSD	Laxemar
Sr			3	1.30E−01	1.84E+00	2.60E+01	1.2	GSD	Laxemar
Tb	Sm		3	7.63E+00	1.08E+02	1.52E+03	2.0	GSD	Laxemar
Tc	Re		2	1.54E−02	2.17E−01	3.06E+00	2.9	GSD	Laxemar
Th			3	1.73E+01	2.44E+02	3.44E+03	1.6	GSD	Laxemar
Ti	Zr		3	8.67E+00	1.22E+02	1.73E+03	2.7	GSD	Laxemar
U			3	3.37E+00	4.75E+01	6.71E+02	1.7	GSD	Laxemar
Zr			3	8.67E+00	1.22E+02	1.73E+03	2.7	GSD	Laxemar

Table E-8. Selected data, properties and comments K_d particulate matter in sea water (Kd_PM_sea) $m^3\ kg_{DW}^{-1}$. The abbreviations used in the table are; EA = element analogue, PA = parameter analogue, N= number of sampeles, Min= minimum, Max= maximum, GM= gemometic mean.

Element	EA	PA	N	Min	GM	Max	GSD	GSD Ref	Reference
Ac	Sm		3	2.22E+01	3.13E+02	4.42E+03	1.4	GSD	Laxemar
Ag		kD_Lake_PM	2	2.57E+00	3.62E+01	5.12E+02	5.0	GSDmax	Laxemar
Am	Sm		3	2.22E+01	3.13E+02	4.42E+03	1.4	GSD	Laxemar
Ba			3	1.65E−01	2.33E+00	3.30E+01	1.5	GSD	Laxemar
Ca			3	3.05E−03	4.31E−02	6.09E−01	1.8	GSD	Laxemar
Cd			3	4.13E+00	5.84E+01	8.24E+02	1.3	GSD	Laxemar
Cl			1	4.51E−05	6.37E−04	9.00E−03	5.0	GSDmax	Forsmark
Cm	Sm		3	2.22E+01	3.13E+02	4.42E+03	1.4	GSD	Laxemar
Co			3	2.24E+00	3.17E+01	4.47E+02	1.4	GSD	Laxemar
Cs			3	5.32E−01	7.51E+00	1.06E+02	2.0	GSD	Laxemar
Eu			2	1.60E+01	2.26E+02	3.19E+03	1.7	GSD	Laxemar
Gd	Sm		3	2.22E+01	3.13E+02	4.42E+03	1.4	GSD	Laxemar
Ho			3	7.66E+00	1.08E+02	1.53E+03	3.4	GSD	Laxemar
I			3	3.64E−01	5.14E+00	7.26E+01	2.1	GSD	Laxemar
La			3	3.20E+01	4.51E+02	6.37E+03	1.4	GSD	Laxemar
Mo			3	2.89E−02	4.08E−01	5.76E+00	2.3	GSD	Laxemar
Nb			3	1.30E+01	1.83E+02	2.59E+03	1.9	GSD	Laxemar
Ni			3	8.05E−01	1.14E+01	1.61E+02	1.2	GSD	Laxemar
Np	Sm		3	2.22E+01	3.13E+02	4.42E+03	5.0	GSDmax	Laxemar
Pa	Sm		3	2.22E+01	3.13E+02	4.42E+03	1.4	GSD	Laxemar
Pb			3	2.66E+01	3.75E+02	5.30E+03	1.5	GSD	Laxemar
Pd	Ni		3	8.05E−01	1.14E+01	1.61E+02	1.2	GSD	Laxemar
Po	Bi		3	1.49E+00	2.10E+01	2.97E+02	2.2	GSD	Laxemar
Pu	U		3	6.54E−02	9.23E−01	1.30E+01	5.0	GSDmax	Laxemar
Ra	Ba		3	1.65E−01	2.33E+00	3.30E+01	1.5	GSD	Laxemar
Re			3	8.13E−03	1.15E−01	1.62E+00	1.6	GSD	Laxemar
Se			3	7.76E−01	1.10E+01	1.55E+02	1.2	GSD	Laxemar
Si	Zr		3	1.18E+01	1.66E+02	2.35E+03	1.6	GSD	Laxemar
Sm			3	2.22E+01	3.13E+02	4.42E+03	1.4	GSD	Laxemar
Sn			3	3.39E+00	4.79E+01	6.76E+02	1.4	GSD	Laxemar
Sr			3	6.71E−03	9.47E−02	1.34E+00	1.5	GSD	Laxemar
Tb	Sm		3	2.22E+01	3.13E+02	4.42E+03	1.4	GSD	Laxemar
Tc	Re		3	8.13E−03	1.15E−01	1.62E+00	1.6	GSD	Laxemar
Th			3	2.43E+01	3.43E+02	4.84E+03	1.7	GSD	Laxemar
Ti	Zr		3	1.18E+01	1.66E+02	2.35E+03	1.6	GSD	Laxemar
U			3	6.54E−02	9.23E−01	1.30E+01	2.4	GSD	Laxemar
Zr			3	1.18E+01	1.66E+02	2.35E+03	1.6	GSD	Laxemar

Table E-9. Selected data, properties and comments Kd of aquatic sediments (kd_regoUp_aqu) m^3 kg_{DW}^{-1}. The abbreviations used in the table are; EA = element analogue, PA = parameter analogue, N= number of sampeles, Min= minimum, Max= maximum, GM= gemometic mean.

Element	EA	PA	N	Min	GM	Max	GSD	GSD Ref	Reference
Ac	Sm		4	5.36E+00	3.26E+01	1.99E+02	2.2	GSD	Laxemar
Ag			3	7.20E+00	1.37E+02	2.61E+03	2.1	GSD	Laxemar
Am	Sm		4	5.36E+00	3.26E+01	1.99E+02	2.2	GSD	Laxemar
Ba			4	6.91E−01	4.21E+00	2.57E+01	1.3	GSD	Laxemar
Ca			4	2.84E−02	1.73E−01	1.06E+00	2.7	GSD	Laxemar
Cd			4	5.66E+01	3.45E+02	2.10E+03	1.6	GSD	Laxemar
Cl			2	1.81E−04	3.44E−03	6.56E−02	1.2	GSD	Laxemar
Cm	Sm		4	5.36E+00	3.26E+01	1.99E+02	2.2	GSD	Laxemar
Co			4	2.21E+00	1.35E+01	8.22E+01	1.9	GSD	Laxemar
Cs			4	3.59E+00	2.18E+01	1.33E+02	1.2	GSD	Laxemar
Eu			4	5.40E+00	3.29E+01	2.01E+02	2.4	GSD	Laxemar
Gd	Sm		4	5.36E+00	3.26E+01	1.99E+02	2.2	GSD	Laxemar
Ho			4	4.57E+00	2.78E+01	1.70E+02	2.1	GSD	Laxemar
I			4	4.61E−02	2.81E−01	1.71E+00	1.8	GSD	Laxemar
La	Sm		4	5.36E+00	3.26E+01	1.99E+02	2.2	GSD	Laxemar
Mo			4	2.74E−01	1.67E+00	1.02E+01	2.5	GSD	Laxemar
Nb			4	7.03E+00	7.92E+01	8.92E+02	4.4	GSD	Laxemar
Ni			4	1.80E+00	1.09E+01	6.67E+01	1.4	GSD	Laxemar
Np	Sm		4	5.36E+00	3.26E+01	1.99E+02	2.2	GSD	Laxemar
Pa	Sm		4	5.36E+00	3.26E+01	1.99E+02	2.2	GSD	Laxemar
Pb			4	3.78E+01	2.30E+02	1.40E+03	1.5	GSD	Laxemar
Pd	Ni		4	1.80E+00	1.09E+01	6.67E+01	1.4	GSD	Laxemar
Po	Bi		4	4.15E+00	2.53E+01	1.54E+02	1.7	GSD	Laxemar
Pu	U		4	8.12E−01	6.90E+00	5.86E+01	3.7	GSD	Laxemar
Ra	Ba		4	6.91E−01	4.21E+00	2.57E+01	1.3	GSD	Laxemar
Re			1	9.25E−03	1.76E−01	3.36E+00	6.0	GSDmax	Forsmark
Se			4	7.68E−01	4.83E+00	3.04E+01	3.1	GSD	Laxemar
Si	Zr		4	6.07E+00	6.90E+01	7.84E+02	4.4	GSD	Laxemar
Sm			4	5.36E+00	3.26E+01	1.99E+02	2.2	GSD	Laxemar
Sn			4	1.57E+00	9.58E+00	5.84E+01	2.1	GSD	Laxemar
Sr			4	3.15E−02	2.37E−01	1.79E+00	3.4	GSD	Laxemar
Tb	Sm		4	5.36E+00	3.26E+01	1.99E+02	2.2	GSD	Laxemar
Tc	Re		1	9.25E−03	1.76E−01	3.36E+00	6.0	GSDmax	Forsmark
Th			4	1.39E+01	8.45E+01	5.15E+02	2.4	GSD	Laxemar
Ti	Zr		4	6.07E+00	6.90E+01	7.84E+02	4.4	GSD	Laxemar
U			4	8.12E−01	6.90E+00	5.86E+01	3.7	GSD	Laxemar
Zr			4	6.07E+00	6.90E+01	7.84E+02	4.4	GSD	Laxemar

Selected data for Be and K

Table E-10. *CR* and *TC* data selected for Be. For many of the parameters no Be Laxemar data were available, instead Sr data are used as element analogue (EA). The abbreviations used in the table are; EA = element analogue, PA = parameter analogue, Min = minimum, Max = maximum, GM = gemometic mean.

Parameter	Unit	EA	PA	GM	GSD	Min	Max	Comment
cR_agri_cereal	$kg_{DW}\ kg_C^{-1}$			8.85E−03	4.8	4.41E−04	7.87E−01	Be FM data used'
cR_agri_fodder	$kg_{DW}\ kg_C^{-1}$	Sr		2.01E+00	1.9	2.05E−01	1.96E+01	Be site data missing. Sr used as EA.
cR_agri_tuber	$kg_{DW}\ kg_C^{-1}$	Sr		3.88E−01	4.0	1.80E−02	3.88E+00	Be site data missing. Sr used as EA.
cR_agri_veg	$kg_{DW}\ kg_C^{-1}$	Sr		2.03E+00	6.0	1.04E−02	3.86E+01	Be site data missing. Sr used as EA.
cR_food_herbiv	$kg_C\ kg_C^{-1}$	Sr		2.05E−02	3.9	4.88E−04	2.00E−01	Be site data missing. Sr used as EA.
cR_lake_cray	$m^3\ kg_C^{-1}$		cR_lake_bivalve	2.57E+01	5.0	1.05E+01	4.37E+01	Be LX data for bivalve used as PA.
cR_lake_fish	$m^3\ kg_C^{-1}$	Sr		7.43E−02	2.7	7.19E−03	4.53E−01	Be site data missing. Sr used as EA.
cR_lake_pp_macro	$m^3\ kg_C^{-1}$			2.23E+00	7.0	8.49E−01	3.95E+00	Be LX data used.
cR_lake_pp_micro	$m^3\ kg_C^{-1}$		cR_lake_pp_macro	2.23E+00	7.0	8.49E−01	3.95E+00	Be LX data for macro algae used as PA
cR_lake_pp_plank	$m^3\ kg_C^{-1}$		cR_lake_pp_macro	2.23E+00	7.0	8.49E−01	3.95E+00	Be LX data for macro algae used as PA
cR_sea_fish	$m^3\ kg_C^{-1}$	Sr		3.00E−03	3.7	3.48E−04	2.81E−02	Be site data missing. Sr used as EA.
cR_sea_pp_macro	$m^3\ kg_C^{-1}$			6.01E+01	3.6	1.64E+01	4.08E+02	Be LX data used (N=3). High reported value.
cR_sea_pp_micro	$m^3\ kg_C^{-1}$		cR_sea_pp_macro	6.01E+01	3.6	1.64E+01	4.08E+02	Be LX data for macro algae used
cR_sea_pp_plank	$m^3\ kg_C^{-1}$		cR_sea_pp_macro	6.01E+01	3.6	1.64E+01	4.08E+02	Be LX data for macro algae used
cR_ter_mush	$kg_{DW}\ kg_C^{-1}$	Sr		6.90E−02	3.2	5.82E−03	1.54E+00	Be site data missing. Sr used as EA.
cR_ter_pp	$kg_{DW}\ kg_C^{-1}$	Sr		2.01E+00	1.9	2.05E−01	1.96E+01	Be site data missing. Sr used as EA.
TC_meat	$day\ kg_{FW}^{-1}$	Sr		1.30E−02	30	4.83E−05	3.50E+00	Sr used as EA
TC_milk	$day\ l^{-1}$	Sr		1.30E−03	4.0	1.33E−04	1.27E−02	Sr used as EA

Table E-11. K_d values ($m^3\ kg_{DW}^{-1}$) selected for Be. For most of the K_d parameters Be data for Forsmark were used since no Kd data from Laxemar are available. For kD_PM_lake and kD_regoUp_aqu Laxemar data (LX) are used. No element or parameter analogue are used. The abbreviations used in the table are; EA = element analogue, PA = parameter analogue, Min= minimum, Max= maximum, GM= gemometic mean.

Parameter	EA	PA	GM	GSD	Min	Max	Comment
kD_PM_lake			7.25E+01	3.0	4.08E+01	1.23E+02	Be LX data used
kD_PM_sea			6.32E+01	3.0	4.69E+01	8.90E+01	Be LX data used.
kD_regoGL			9.64E+00	3.0	4.02E+00	1.58E+01	Be FM data used
kD_regoLow			7.14E+00	3.0	4.46E+00	1.10E+01	Be FM data used
kD_regoPeat			6.24E−01	3.0	2.80E−01	1.55E+00	Be FM data used
kD_regoPG			1.42E+00	4.3	3.28E−01	1.49E+01	Be FM data used
kD_regoUp (Garden plot)			1.37E+00	2.0	3.49E−01	2.47E+00	Be FM data used
kD_regoUp (Drained mire)			6.69E+00	3.0	6.10E+00	7.38E+00	Be FM data used
kD_regoUp (Infield outland)			5.23E+00	2.0	9.79E−01	8.46E+00	Be FM data used
kD_regoUp_aqu			1.93E+01	3.0	9.53E+00	6.36E+01	Be LX data used.
kD_regoUp_ter			5.06E−01	3.0	3.58E−01	8.47E−01	Be FM data used

Table E-12. *CR* and *TC* data for K. For many of the parameters Laxemar data (LX) were available and used. The abbreviations used in the table are; EA = element analogue, PA = parameter analogue, Min = minimum, Max = maximum, GM = gemometic mean.

Parameter	Unit	EA	PA	N	GM	GDS	Min	Max	Comment
cR_food_herbiv	$kg_C\ kg_C^{-1}$			13	4.86E+00	2.8	4.73E−01	3.82E+01	K data from LX used
cR_lake_cray	$m^3\ kg_C^{-1}$		cR_lake_bivalve	3	6.06E+00	1.1	5.77E+00	6.68E+00	cR_lake_bivalve data from LX used as PA
cR_lake_fish	$m^3\ kg_C^{-1}$			3	3.43E+01	1.1	3.08E+01	4.11E+01	K data from LX used
cR_lake_pp_macro	$m^3\ kg_C^{-1}$			3	3.36E+01	1.1	3.36E+01	4.10E+01	K data from LX used
cR_lake_pp_micro	$m^3\ kg_C^{-1}$		cR_lake_pp_ macro	3	3.36E+01	1.1	3.36E+01	4.10E+01	K data from LX used
cR_lake_pp_plank	$m^3\ kg_C^{-1}$			3	3.36E+01	1.1	3.36E+01	4.10E+01	K data from LX used
cR_sea_fish	$m^3\ kg_C^{-1}$		cR_lake_pp_ macro	3	6.32E−01	1.3	3.13E−01	9.17E−01	K data from LX used
cR_sea_pp_macro	$m^3\ kg_C^{-1}$			3	9.01E−01	2.1	2.65E−01	3.01E+00	K data from LX used
cR_sea_pp_micro	$m^3\ kg_C^{-1}$		cR_sea_pp_ macro	3	9.01E−01	2.1	2.65E−01	3.01E+00	K data from LX used
cR_sea_pp_plank	$m^3\ kg_C^{-1}$		cR_sea_pp_ macro	3	9.01E−01	2.1	2.65E−01	3.01E+00	K data from LX used
cR_ter_mush	$kg_{DW}\ kg_C^{-1}$			13	8.69E+01	3.0	1.10E+01	5.41E+02	K data from FM used. LX data missing.
cR_ter_pp	$kg_{DW}\ kg_C^{-1}$				1.84E+01	2.6	2.16E+00	1.05E+02	K data from LX used
TC_meat	$day\ kg_{FW}^{-1}$	Cs			2.20E−02	4.0	2.25E−03	2.15E−01	K data missing. Cs used as EA.
TC_milk	$day\ l^{-1}$	Cs			4.60E−03	4.0	4.70E−04	6.80E−02	K data missing. Cs used as EA.

Table E-13. K_d values ($m^3\ kg_{DW}^{-1}$) selected for K. For most of the K_d parameters K data for Forsmark were used since no K_d data from Laxemar are available. For kD_PM_lake and kD_regoUp_aqu Laxemar data are used. No element or parameter analogues were used. The abbreviations used in the table are; EA = element analogue, PA = parameter analogue, Min = minimum, Max = maximum, GM = gemometic mean.

Parameter	EA	PA	GM	GSD	Min	Max	Comment
kD_PM_lake			5.04E+00	3.0	2.58E+00	9.52E+00	Laxemar data
kD_PM_sea			5.39E−02	2.2	2.21E−02	1.05E−01	Laxemar data
kD_regoGL			2.00E+00	3.0	3.29E−01	1.22E+01	FM data used
kD_regoLow			3.62E−02	3.0	5.95E−03	2.21E−01	FM data used
kD_regoPeat			5.56E−02	3.0	9.13E−03	3.39E−01	FM data used
kD_regoPG			6.24E−01	5.0	4.49E−02	8.67E+00	FM data used
kD_regoUp			4.65E−01	3.5	5.80E−02	4.76E+00	FM data used
kD_regoUp			4.28E−01	2.0	1.14E−01	1.34E+00	FM data used
kD_regoUp			5.22E−01	3.0	8.57E−02	3.18E+00	FM data used
kD_regoUp_aqu			5.63E−01	6.0	1.03E−01	3.35E+00	Laxemar data
kD_regoUp_ter			4.55E−02	3.0	7.46E−03	2.77E−01	FM data used

Data for element-specific parameter that were not updated

The parameter values for those parameters were data have not been updated in comparison to SR-PSU are presented in the tables below.

Table E-14. *CR* for cerals (cR_agri_cereal) kg_{DW} kg_C^{-1}.

Elements	Value	GSD	Minimum	Maximum	Comment
Ac	5.29E−03	6.5	1.96E−04	6.65E−01	FM data
Ag	4.19E−02	3.0	6.30E−03	2.55E−01	FM data
Am	5.29E−03	6.5	1.96E−04	6.65E−01	FM data
Ba	2.83E−01	3.0	3.60E−02	4.39E+00	FM data
Be	8.85E−03	4.8	4.41E−04	7.87E−01	
Ca	0.00E+00	0.0	0.00E+00	0.00E+00	FM data
Cd	2.41E−01	4.0	2.47E−02	2.73E+00	FM data
Cl	0.00E+00	0.0	0.00E+00	0.00E+00	FM data
Cm	5.29E−03	6.5	1.96E−04	6.65E−01	FM data
Co	1.09E−02	5.2	3.21E−04	6.41E−01	FM data
Cs	2.46E−02	7.6	8.75E−04	2.11E+00	FM data
Eu	5.66E−03	7.0	2.31E−04	1.69E−01	FM data
Gd	5.29E−03	6.5	1.96E−04	6.65E−01	PSU data
Ho	4.04E−03	5.4	2.48E−04	4.23E−01	FM data
I	2.71E−02	3.6	1.46E−03	6.64E−01	FM data
K	2.46E−02	7.6	8.75E−04	2.11E+00	PSU data
La	5.29E−03	6.5	1.96E−04	6.65E−01	PSU data
Mo	1.23E+00	3.2	7.16E−02	1.25E+01	FM data
Nb	9.78E−03	6.3	4.77E−04	1.88E+00	FM data
Ni	1.65E−02	3.1	1.46E−03	5.25E−01	FM data
Np	5.29E−03	6.5	1.96E−04	6.65E−01	FM data
Pa	5.29E−03	6.5	1.96E−04	6.65E−01	FM data
Pb	6.54E−03	3.0	9.87E−04	3.99E−02	FM data
Pd	1.65E−02	3.1	1.46E−03	5.25E−01	FM data
Po	6.54E−03	3.0	4.87E−04	6.98E−02	FM data
Pu	3.90E−03	10.4	2.80E−05	1.92E+00	FM data
Ra	3.84E−02	12.0	1.81E−04	2.29E+00	Literature data (L1)
Re	6.41E−02	5.1	9.04E−04	4.55E+00	PSU data
Se	5.65E−02	4.0	5.77E−03	5.52E−01	FM data
Si	7.53E−02	3.7	7.32E−03	4.89E+00	PSU data
Sm	4.03E−03	6.4	1.84E−04	4.42E−01	FM data
Sn	3.71E−02	3.0	5.42E−03	2.33E−01	FM data
Sr	2.77E−01	3.0	3.35E−02	3.26E+00	FM data
Tb	5.29E−03	6.5	1.96E−04	6.65E−01	PSU data
Tc	6.41E−02	5.1	9.04E−04	4.55E+00	FM data
Th	8.24E−03	6.4	3.90E−04	1.62E+00	FM data
Ti	7.53E−02	3.7	7.32E−03	4.89E+00	PSU data
U	3.90E−03	10.4	2.80E−05	1.92E+00	FM data
Zr	7.53E−02	3.7	7.32E−03	4.89E+00	FM data

Table E-15. *CR* for fodder (cR_agri_fodder) kg_{DW} kg_C^{-1}.

Elements	Value	GSD	Minimum	Maximum	Comment
Ac	1.16E−02	3.1	4.21E−04	1.13E−01	Forsmark site data
Ag	4.19E−02	7.0	1.71E−03	1.03E+00	Forsmark site data
Am	1.16E−02	3.1	4.21E−04	1.13E−01	Forsmark site data
Ba	1.19E+00	2.7	5.50E−02	1.17E+01	Forsmark site data
Cd	6.31E−01	3.7	4.41E−02	1.76E+01	Forsmark site data
Cm	1.16E−02	3.1	4.21E−04	1.13E−01	Forsmark site data
Co	1.17E−01	1.8	1.20E−02	1.15E+00	Forsmark site data
Cs	2.06E−01	4.1	8.96E−03	9.38E+00	Forsmark site data
Eu	6.49E−03	3.0	6.13E−04	6.34E−02	Laxemar site data
Gd	1.16E−02	3.1	4.21E−04	1.13E−01	PSU data used
Ho	6.51E−03	2.8	6.66E−04	6.37E−02	Laxemar site data
I	1.56E−01	5.8	6.75E−03	1.30E+01	Forsmark site data
La	1.16E−02	3.1	4.21E−04	1.13E−01	PSU data used
Mo	2.02E−01	5.1	6.97E−03	4.86E+00	Forsmark site data
Nb	8.30E−03	2.1	8.49E−04	8.12E−02	Forsmark site data
Ni	2.42E−01	2.4	2.48E−02	2.37E+00	Forsmark site data
Np	1.16E−02	3.1	4.21E−04	1.13E−01	Forsmark site data
Pa	1.16E−02	3.1	4.21E−04	1.13E−01	Forsmark site data
Pb	3.58E−02	2.1	3.66E−03	3.50E−01	Forsmark site data
Pd	2.42E−01	2.4	2.48E−02	2.37E+00	Forsmark site data
Po	6.54E−03	7.0	2.66E−04	1.61E−01	Forsmark site data
Pu	1.67E−03	3.3	1.49E−04	2.01E−02	Forsmark site data
Ra	5.99E−02	4.0	6.13E−03	9.76E−01	Forsmark site data
Re	6.41E−02	7.0	9.04E−04	4.55E+00	PSU data used
Se	5.65E−02	7.0	2.30E−03	1.39E+00	Forsmark site data
Si	3.70E−02	3.8	3.79E−03	5.38E−01	PSU data used
Sm	4.73E−03	3.2	2.76E−04	5.38E−02	Forsmark site data
Sn	1.11E−01	1.8	1.14E−02	1.09E+00	Forsmark site data
Sr	2.01E+00	1.9	2.05E−01	1.96E+01	Forsmark site data
Tb	1.16E−02	3.1	4.21E−04	1.13E−01	PSU data used
Tc	6.41E−02	7.0	9.04E−04	4.55E+00	Forsmark site data
Th	1.16E−02	2.2	1.19E−03	1.14E−01	Laxemar site data
Ti	3.70E−02	3.8	3.79E−03	5.38E−01	PSU data used
U	1.67E−03	3.3	1.49E−04	2.01E−02	Forsmark site data
Zr	3.70E−02	3.8	3.79E−03	5.38E−01	Forsmark site data

Table E-16. *CR* for tubers (cR_agri_tuber) kg_{DW} kg_C^{-1}.

Elements	Value	GSD	Minimum	Maximum	Comment
Ac	9.47E−04	4.0	9.68E−05	9.71E−03	Literature data
Ag	3.67E−03	4.0	3.76E−04	3.59E−02	Literature data
Am	5.10E−04	6.0	2.67E−05	8.25E−02	Literature data
Ba	3.88E−01	4.0	1.80E−02	3.88E+00	Literature data
Cd	7.28E−01	4.0	7.44E−02	7.12E+00	Literature data
Cm	3.64E−04	4.0	2.67E−05	5.10E−03	Literature data
Co	1.31E−01	4.0	1.34E−02	1.63E+00	Literature data
Cs	1.36E−01	4.0	9.71E−03	1.46E+00	Literature data
Eu	9.47E−04	4.0	9.68E−05	9.71E−03	Literature data
Gd	9.47E−04	4.0	9.68E−05	9.71E−03	PSU data used
Ho	9.47E−04	4.0	9.68E−05	9.71E−03	Literature data
I	2.18E−02	3.0	2.22E−03	2.13E−01	Literature data
La	9.47E−04	4.0	9.68E−05	9.71E−03	PSU data used
Mo	9.04E−01	7.0	3.68E−02	2.22E+01	Literature data
Nb	9.71E−03	7.0	3.95E−04	2.38E−01	Literature data
Ni	1.16E−01	7.0	5.73E−03	3.46E+00	Forsmark site data
Np	1.38E−02	4.0	1.41E−03	1.35E−01	Literature data
Pa	9.47E−04	4.0	9.68E−05	9.71E−03	Literature data
Pb	3.64E−03	7.4	1.35E−04	6.31E+00	Literature data
Pd	1.16E−01	7.0	5.73E−03	3.46E+00	Forsmark site data
Po	6.55E−03	5.8	3.40E−04	1.18E−01	Literature data
Pu	2.67E−04	5.5	9.22E−06	1.21E−02	Literature data
Ra	2.67E−02	6.8	5.83E−04	9.47E+00	Literature data
Re	5.58E−01	4.0	3.16E−02	5.46E+00	PSU data used
Se	5.65E−02	7.0	2.30E−03	1.39E+00	Forsmark site data
Si	2.42E−02	7.0	1.13E−03	6.82E−01	PSU data used
Sm	9.47E−04	4.0	9.68E−05	9.71E−03	Literature data
Sn	4.85E−04	9.9	1.12E−05	4.37E−02	Literature data
Sr	3.88E−01	4.0	1.80E−02	3.88E+00	Literature data
Tb	9.47E−04	4.0	9.68E−05	9.71E−03	PSU data used
Tc	5.58E−01	4.0	3.16E−02	5.46E+00	Literature data
Th	4.85E−04	9.9	1.12E−05	4.37E−02	Literature data
Ti	2.42E−02	7.0	1.13E−03	6.82E−01	PSU data used
U	1.21E−02	6.4	4.37E−04	2.57E−01	Literature data
Zr	2.42E−02	7.0	1.13E−03	6.82E−01	Forsmark site data

Table E-17. *CR* for vegetables (cR_agri_veg) kg_{DW} kg_C^{-1}.

Elements	Value	GSD	Minimum	Maximum	Comment
Ac	1.52E−02	4.0	1.55E−03	1.49E−01	Literature data
Ag	4.80E−04	4.0	4.91E−05	4.69E−03	Literature data
Am	7.20E−04	4.0	7.36E−05	7.04E−03	Literature data
Ba	2.43E−01	6.7	4.80E−03	3.47E+02	Literature data
Cd	6.40E+00	4.0	2.67E−01	6.26E+01	Literature data
Cm	3.73E−03	4.5	3.14E−04	4.43E−02	Literature data
Co	4.53E−01	4.0	3.47E−02	4.43E+00	Literature data
Cs	1.60E−01	6.0	8.00E−04	3.05E+00	Literature data
Eu	1.52E−02	4.0	1.55E−03	1.49E−01	Literature data
Gd	1.52E−02	4.0	1.55E−03	1.49E−01	PSU data used
Ho	1.52E−02	4.0	1.55E−03	1.49E−01	Literature data
I	1.73E−02	4.0	1.77E−03	2.67E−01	Literature data
La	1.52E−02	4.0	1.55E−03	1.49E−01	PSU data used
Mo	1.36E+00	7.0	5.54E−02	3.34E+01	Literature data
Nb	4.53E−02	7.0	1.85E−03	1.11E+00	Literature data
Ni	1.16E−01	7.0	5.73E−03	3.46E+00	Forsmark site data
Np	7.20E−02	4.0	7.36E−03	7.04E−01	Literature data
Pa	1.52E−02	4.0	1.55E−03	1.49E−01	Literature data
Pb	2.13E−01	13.0	3.14E−03	6.67E+01	Literature data
Pd	1.16E−01	7.0	5.73E−03	3.46E+00	Forsmark site data
Po	1.97E−02	6.9	6.67E−04	4.73E−01	Literature data
Pu	2.21E−04	4.0	2.26E−05	2.16E−03	Literature data
Ra	2.43E−01	6.7	4.80E−03	3.47E+02	Literature data
Re	6.41E−02	7.0	9.04E−04	4.55E+00	PSU data used
Se	5.65E−02	7.0	2.30E−03	1.39E+00	Forsmark site data
Si	1.07E−02	7.0	4.34E−04	2.62E−01	PSU data used
Sm	1.52E−02	4.0	1.55E−03	1.49E−01	Literature data
Sn	3.20E−03	6.0	1.68E−04	5.60E−01	Literature data
Sr	2.03E+00	6.0	1.04E−02	3.86E+01	Literature data
Tb	1.52E−02	4.0	1.55E−03	1.49E−01	PSU data used
Tc	6.41E−02	7.0	9.04E−04	4.55E+00	Forsmark site data
Th	3.20E−03	6.0	1.68E−04	5.60E−01	Literature data
Ti	1.07E−02	7.0	4.34E−04	2.62E−01	PSU data used
U	5.33E−02	7.3	2.08E−04	2.35E+01	Literature data
Zr	1.07E−02	7.0	4.34E−04	2.62E−01	Literature data

Table E-18. *CR* for terrestrial herbivores (cR_food_herbiv) $kg_C\ kg_C^{-1}$

Elements	Value	GSD	Minimum	Maximum	Comment
Ac	2.86E−02	4.5	3.72E−04	1.10E+00	Laxemar site data
Ag	4.30E−04	8.0	1.41E−05	1.32E−02	Literature data
Am	2.86E−02	4.5	3.72E−04	1.10E+00	Laxemar site data
Ba	3.03E−02	4.0	5.92E−04	1.52E+00	Laxemar site data
Ca	1.24E−01	3.4	3.22E−03	1.53E+00	Laxemar site data
Cd	5.21E−01	5.0	6.85E−03	2.63E+01	Laxemar site data
Cl	7.10E+00	3.8	2.79E−01	7.54E+01	Laxemar site data
Cm	2.86E−02	4.5	3.72E−04	1.10E+00	Laxemar site data
Co	3.32E−01	2.8	6.00E−03	3.43E+00	Laxemar site data
Cs	3.57E+01	5.7	1.92E−01	8.77E+02	Laxemar site data
Eu	3.73E−01	1.6	3.81E−02	3.65E+00	Laxemar site data
Gd	2.86E−02	4.5	3.72E−04	1.10E+00	Laxemar site data
Ho	7.74E−01	2.0	7.92E−02	7.57E+00	Laxemar site data
I	1.00E+01	8.0	9.22E−02	3.06E+02	Forsmark site data
La	2.86E−02	4.5	3.72E−04	1.10E+00	Laxemar site data
Mo	6.40E−01	4.7	1.41E−02	1.23E+01	Laxemar site data
Nb	4.11E−01	3.0	1.79E−02	4.02E+00	Laxemar site data
Ni	1.47E−01	2.2	1.38E−02	1.44E+00	Laxemar site data
Np	2.86E−02	4.5	3.72E−04	1.10E+00	Laxemar site data
Pa	2.86E−02	4.5	3.72E−04	1.10E+00	Laxemar site data
Pb	1.17E+00	2.5	8.83E−02	1.15E+01	Laxemar site data
Pd	1.47E−01	2.2	1.38E−02	1.44E+00	Laxemar site data
Po	1.40E−01	8.0	4.58E−03	4.28E+00	Literature data
Pu	3.90E−05	8.0	1.27E−06	1.19E−03	Literature data
Ra	2.66E−02	4.0	2.60E−03	2.61E−01	Laxemar site data
Re	1.56E+00	4.3	2.41E−02	2.04E+01	Laxemar site data
Se	1.54E+01	4.0	1.58E+00	1.51E+02	Forsmark site data
Si	1.56E+00	4.3	2.41E−02	2.04E+01	Laxemar site data
Sm	1.77E−01	3.5	6.71E−03	1.79E+00	Laxemar site data
Sn	5.55E+00	2.7	5.67E−01	5.43E+01	Laxemar site data
Sr	2.05E−02	3.9	4.88E−04	2.00E−01	Laxemar site data
Tb	2.86E−02	4.5	3.72E−04	1.10E+00	Laxemar site data
Tc	1.56E+00	4.3	2.41E−02	2.04E+01	Laxemar site data
Th	3.18E+00	2.0	3.25E−01	3.11E+01	Laxemar site data
Ti	1.56E+00	4.3	2.41E−02	2.04E+01	Laxemar site data
U	5.93E−01	3.4	4.18E−02	2.15E+01	Laxemar site data
Zr	1.56E+00	4.3	2.41E−02	2.04E+01	Laxemar site data

Table E-19. *CR* for limnic cray fish (cR_lake_cray) m^3 kg_C^{-1}.

Elements	Value	GSD	Minimum	Maximum	Comment
Ac	2.47E+01	5.0	3.26E+00	6.50E+02	Forsmark site data
Ag	3.94E+01	5.0	2.79E+00	5.57E+02	Laxemar site data
Am	2.47E+01	5.0	3.26E+00	6.50E+02	Forsmark site data
Ba	5.23E+01	5.0	4.95E+00	9.87E+02	Forsmark site data
Ca	7.89E+00	5.0	5.59E−01	1.11E+02	Forsmark site data
Cd	1.89E+03	5.0	8.67E+01	1.73E+04	Forsmark site data
Cl	8.33E−01	5.0	4.36E−02	1.18E+01	Forsmark site data
Cm	2.47E+01	5.0	3.26E+00	6.50E+02	Forsmark site data
Co	5.66E+01	5.0	2.80E+00	5.58E+02	Forsmark site data
Cs	5.11E+00	5.0	5.31E−01	1.06E+02	Forsmark site data
Eu	4.52E+01	5.0	2.77E+00	5.52E+02	Forsmark site data
Gd	2.47E+01	5.0	3.26E+00	6.50E+02	PSU data used
Ho	4.27E+00	5.0	4.86E−01	9.69E+01	Forsmark site data
I	3.55E+00	5.0	1.68E−01	3.35E+01	Forsmark site data
La	2.47E+01	5.0	3.26E+00	6.50E+02	PSU data used
Mo	2.38E+00	5.0	3.14E−01	6.26E+01	Forsmark site data
Nb	1.15E+01	5.0	5.73E−01	1.14E+02	Forsmark site data
Ni	4.62E+00	5.0	2.74E−01	5.45E+01	Forsmark site data
Np	2.47E+01	5.0	3.26E+00	6.50E+02	Forsmark site data
Pa	2.47E+01	5.0	3.26E+00	6.50E+02	Forsmark site data
Pb	9.94E+01	5.0	3.83E+00	7.63E+02	Forsmark site data
Pd	4.62E+00	5.0	2.74E−01	5.45E+01	Forsmark site data
Po	8.42E+01	5.0	5.97E+00	1.19E+03	Literature data
Pu	8.80E+00	5.0	6.24E−01	1.24E+02	Literature data
Ra	9.74E+00	3.0	1.29E+00	5.94E+01	Literature data
Re	1.12E−01	5.0	7.91E−03	1.58E+00	PSU data used
Se	4.93E+01	5.0	3.24E+00	6.46E+02	Forsmark site data
Si	1.68E+00	5.0	1.62E−01	3.23E+01	PSU data used
Sm	7.72E+00	5.0	1.04E+00	2.08E+02	Forsmark site data
Sn	1.68E+00	5.0	1.62E−01	3.23E+01	Forsmark site data
Sr	4.14E+00	5.0	4.01E−01	7.99E+01	Forsmark site data
Tb	2.47E+01	5.0	3.26E+00	6.50E+02	PSU data used
Tc	1.12E−01	5.0	7.91E−03	1.58E+00	Literature data
Th	4.46E+00	5.0	4.21E−01	8.40E+01	Forsmark site data
Ti	1.68E+00	5.0	1.62E−01	3.23E+01	PSU data used
U	3.15E−01	5.6	1.08E−01	2.15E+01	Forsmark site data
Zr	1.68E+00	5.0	1.62E−01	3.23E+01	Forsmark site data

Table E-20. *CR* for limnic fish (cR_lake_fish) $m^3\ kg_c^{-1}$.

Elements	Value	GSD	Minimum	Maximum	Comment
Ac	3.00E−03	2.2	4.92E−04	1.83E−02	Laxemar site data
Ag	9.42E−01	3.0	1.55E−01	5.74E+00	Literature data
Am	3.00E−03	2.2	4.92E−04	1.83E−02	Laxemar site data
Ba	8.24E−02	2.9	1.35E−02	5.02E−01	Laxemar site data
Ca	5.49E−01	1.8	9.02E−02	3.35E+00	Laxemar site data
Cd	1.49E+00	3.0	1.71E−01	9.06E+00	Literature data
Cl	2.48E−01	1.8	4.06E−02	1.51E+00	Laxemar site data
Cm	3.00E−03	2.2	4.92E−04	1.83E−02	Laxemar site data
Co	1.41E−01	3.5	1.80E−02	1.11E+00	Laxemar site data
Cs	7.80E+01	2.5	1.28E+01	4.75E+02	Laxemar site data
Eu	3.00E−03	2.2	4.92E−04	1.83E−02	Laxemar site data
Gd	3.00E−03	2.2	4.92E−04	1.83E−02	Laxemar site data
Ho	1.24E−01	2.2	8.76E−03	1.75E+00	Laxemar site data
I	4.36E−01	2.6	7.15E−02	2.66E+00	Laxemar site data
La	3.00E−03	2.2	4.92E−04	1.83E−02	Laxemar site data
Mo	7.16E−02	2.6	1.17E−02	4.36E−01	Laxemar site data
Nb	5.58E−02	2.3	9.15E−03	3.40E−01	Laxemar site data
Ni	6.54E−02	1.5	4.63E−03	9.23E−01	Laxemar site data
Np	3.00E−03	2.2	4.92E−04	1.83E−02	Laxemar site data
Pa	3.00E−03	2.2	4.92E−04	1.83E−02	Laxemar site data
Pb	2.14E−01	3.0	8.57E−04	2.31E+00	Literature data
Pd	6.54E−02	1.5	4.63E−03	9.23E−01	Laxemar site data
Po	3.08E−01	4.3	2.80E−02	3.40E+00	Literature data
Pu	1.80E+02	5.0	1.27E+01	2.54E+03	Literature data
Ra	8.24E−02	2.9	1.35E−02	5.02E−01	Laxemar site data
Re	2.58E−01	5.0	1.83E−02	3.64E+00	Literature data
Se	1.90E+01	1.3	3.13E+00	1.16E+02	Laxemar site data
Si	1.67E−01	2.1	2.74E−02	1.02E+00	Laxemar site data
Sm	2.60E−02	2.6	1.84E−03	3.67E−01	Laxemar site data
Sn	1.67E−01	2.1	2.74E−02	1.02E+00	Laxemar site data
Sr	7.43E−02	2.7	7.19E−03	4.53E−01	Laxemar site data
Tb	3.00E−03	2.2	4.92E−04	1.83E−02	Laxemar site data
Tc	2.58E−01	5.0	1.83E−02	3.64E+00	Literature data
Th	6.66E−01	2.3	1.09E−01	4.80E+00	Literature data
Ti	1.67E−01	2.1	2.74E−02	1.02E+00	Laxemar site data
U	8.63E−03	3.1	1.23E−03	5.51E−02	Laxemar site data
Zr	1.67E−01	2.1	2.74E−02	1.02E+00	Laxemar site data

Table E-21. CR for limnic macroalgae, plankton and microphytobenthos (cR_lake_pp_macro, cR_lake_pp_plank and cR_lake_pp_micro_) m^3 kg_C^{-1}.

Elements	Value	GSD	Minimum	Maximum	Comment
Ac	2.12E+00	2.5	2.17E−01	2.08E+01	Laxemar site data
Ag	2.00E+01	7.0	8.14E−01	4.91E+02	Literature data
Am	2.12E+00	2.5	2.17E−01	2.08E+01	Laxemar site data
Ba	1.24E+01	3.1	1.26E+00	1.21E+02	Laxemar site data
Ca	7.66E+00	1.1	7.83E−01	7.49E+01	Laxemar site data
Cd	8.58E+00	1.6	8.77E−01	8.39E+01	Laxemar site data
Cl	1.62E+00	1.2	1.66E−01	1.59E+01	Laxemar site data
Cm	2.12E+00	2.5	2.17E−01	2.08E+01	Laxemar site data
Co	1.11E+01	3.7	1.13E+00	1.08E+02	Laxemar site data
Cs	1.06E+01	1.4	1.08E+00	1.03E+02	Laxemar site data
Eu	2.31E+00	2.5	2.36E−01	2.26E+01	Laxemar site data
Gd	2.12E+00	2.5	2.17E−01	2.08E+01	Laxemar site data
Ho	9.72E−01	2.5	9.94E−02	9.51E+00	Laxemar site data
I	1.99E+00	2.5	2.03E−01	1.94E+01	Laxemar site data
La	2.12E+00	2.5	2.17E−01	2.08E+01	Laxemar site data
Mo	4.13E+00	2.6	4.22E−01	4.04E+01	Laxemar site data
Nb	2.05E+00	2.3	2.09E−01	2.00E+01	Laxemar site data
Ni	1.92E+00	1.8	1.97E−01	1.88E+01	Laxemar site data
Np	2.12E+00	2.5	2.17E−01	2.08E+01	Laxemar site data
Pa	2.12E+00	2.5	2.17E−01	2.08E+01	Laxemar site data
Pb	5.69E+00	3.2	5.82E−01	5.57E+01	Laxemar site data
Pd	1.92E+00	1.8	1.97E−01	1.88E+01	Laxemar site data
Po	2.41E+01	4.0	2.46E+00	2.36E+02	Literature data
Pu	6.45E+02	14.0	2.98E+00	1.22E+06	Literature data
Ra	1.24E+01	3.1	1.26E+00	1.21E+02	Laxemar site data
Re	1.36E−01	7.0	5.56E−03	3.35E+00	Literature data
Se	4.82E+00	1.2	4.93E−01	4.72E+01	Laxemar site data
Si	9.34E−01	2.1	9.55E−02	9.14E+00	Laxemar site data
Sm	1.43E+00	2.7	1.46E−01	1.40E+01	Laxemar site data
Sn	9.34E−01	2.1	9.55E−02	9.14E+00	Laxemar site data
Sr	1.26E+00	1.6	1.29E−01	1.23E+01	Laxemar site data
Tb	2.12E+00	2.5	2.17E−01	2.08E+01	Laxemar site data
Tc	1.36E−01	7.0	5.56E−03	3.35E+00	Literature data
Th	1.48E+00	1.7	1.51E−01	1.45E+01	Laxemar site data
Ti	9.34E−01	2.1	9.55E−02	9.14E+00	Laxemar site data
U	1.23E+00	1.6	1.26E−01	1.20E+01	Laxemar site data
Zr	9.34E−01	2.1	9.55E−02	9.14E+00	Laxemar site data

Table E-22. *CR* for marine fish (cR_sea_fish) m^3 kg_c^{-1}.

Elements	Value	GSD	Minimum	Maximum	Comment
Ac	2.63E−02	4.9	1.92E−03	9.95E−01	Laxemar site data
Ag	1.43E+01	3.0	2.35E+00	8.74E+01	Literature data
Am	2.63E−02	4.9	1.92E−03	9.95E−01	Laxemar site data
Ba	1.72E−02	1.5	2.82E−03	1.05E−01	Laxemar site data
Ca	2.76E−02	2.0	4.52E−03	1.68E−01	Laxemar site data
Cd	7.84E−01	1.8	1.29E−01	4.77E+00	Laxemar site data
Cl	1.41E−03	1.6	2.32E−04	8.61E−03	Laxemar site data
Cm	2.63E−02	4.9	1.92E−03	9.95E−01	Laxemar site data
Co	2.77E−01	3.1	4.22E−02	2.01E+00	Laxemar site data
Cs	2.30E+00	1.8	3.78E−01	1.40E+01	Laxemar site data
Eu	2.63E−02	4.9	1.92E−03	9.95E−01	Laxemar site data
Gd	2.63E−02	5.0	1.87E−03	9.95E−01	Laxemar site data
Ho	2.63E−02	4.9	1.92E−03	9.95E−01	Laxemar site data
I	1.40E−01	1.5	2.30E−02	8.53E−01	Laxemar site data
La	2.63E−02	5.0	1.87E−03	9.95E−01	Laxemar site data
Mo	1.30E−02	1.4	2.14E−03	7.94E−02	Laxemar site data
Nb	1.50E−01	1.5	2.46E−02	9.12E−01	Laxemar site data
Ni	1.65E−01	2.6	2.71E−02	1.01E+00	Laxemar site data
Np	2.63E−02	5.0	1.87E−03	9.95E−01	Laxemar site data
Pa	2.63E−02	4.9	1.92E−03	9.95E−01	Laxemar site data
Pb	1.90E+00	1.0	1.34E−01	2.68E+01	Laxemar site data
Pd	1.65E−01	2.6	2.71E−02	1.01E+00	Laxemar site data
Po	1.16E+02	3.0	1.20E+01	7.05E+02	Literature data
Pu	1.78E−01	3.8	1.71E−02	3.34E+00	Literature data
Ra	1.72E−02	1.5	2.82E−03	1.05E−01	Laxemar site data
Re	1.29E−01	3.3	1.77E−02	3.43E+00	Literature data
Se	3.18E+01	1.2	5.23E+00	1.94E+02	Laxemar site data
Si	1.17E+00	6.0	6.12E−02	2.67E+01	Laxemar site data
Sm	1.36E−01	4.5	9.65E−03	1.92E+00	Laxemar site data
Sn	3.94E+00	1.5	6.47E−01	2.40E+01	Laxemar site data
Sr	3.00E−03	3.7	3.48E−04	2.81E−02	Laxemar site data
Tb	2.63E−02	5.0	1.87E−03	9.95E−01	Laxemar site data
Tc	1.29E−01	3.3	1.77E−02	3.43E+00	Literature data
Th	2.62E+00	2.0	4.30E−01	1.59E+01	Laxemar site data
Ti	1.17E+00	6.0	6.12E−02	2.67E+01	Laxemar site data
U	1.56E−03	1.5	2.56E−04	9.49E−03	Laxemar site data
Zr	1.17E+00	6.0	6.12E−02	2.67E+01	Laxemar site data

Table E-23. CR for marine macroalgae, plankton and microphytobentos (cR_sea_pp_macro, cR_sea_pp_plank and cR_sea_pp_micro) $m^3\ kg_C^{-1}$.

Elements	Value	GSD	Minimum	Maximum	Comment
Ac	8.27E+01	7.7	2.25E+00	3.41E+03	Laxemar site data
Ag	2.53E+01	3.2	3.78E+00	1.97E+02	Literature data
Am	8.27E+01	7.7	2.25E+00	3.41E+03	Laxemar site data
Ba	4.61E+00	4.9	3.19E−01	6.25E+01	Laxemar site data
Ca	8.99E−01	3.6	1.08E−01	9.33E+00	Laxemar site data
Cd	9.41E+01	2.5	1.54E+01	8.44E+02	Laxemar site data
Cl	3.01E−02	1.5	4.94E−03	1.84E−01	Laxemar site data
Cm	8.27E+01	7.7	2.25E+00	3.41E+03	Laxemar site data
Co	3.19E+01	6.0	1.38E+00	1.17E+03	Laxemar site data
Cs	2.68E+00	2.3	4.39E−01	1.63E+01	Laxemar site data
Eu	2.99E+01	3.4	4.07E+00	2.19E+02	Laxemar site data
Gd	8.27E+01	7.7	2.25E+00	3.41E+03	Laxemar site data
Ho	2.17E+01	4.7	1.69E+00	2.80E+02	Laxemar site data
I	1.04E+01	2.1	1.71E+00	6.35E+01	Laxemar site data
La	8.27E+01	7.7	2.25E+00	3.41E+03	Laxemar site data
Mo	5.00E−01	2.4	8.21E−02	3.05E+00	Laxemar site data
Nb	2.93E+01	4.6	1.86E+00	3.60E+02	Laxemar site data
Ni	1.19E+01	2.0	1.95E+00	7.25E+01	Laxemar site data
Np	8.27E+01	7.7	2.25E+00	3.41E+03	Laxemar site data
Pa	8.27E+01	7.7	2.25E+00	3.41E+03	Laxemar site data
Pb	3.84E+01	3.1	5.82E+00	2.53E+02	Laxemar site data
Pd	1.19E+01	2.0	1.95E+00	7.25E+01	Laxemar site data
Po	1.05E+01	3.0	9.21E−01	6.41E+01	Literature data
Pu	3.22E+01	3.0	4.34E+00	1.97E+02	Literature data
Ra	4.61E+00	4.9	3.19E−01	6.25E+01	Laxemar site data
Re	4.87E+02	3.0	8.00E+01	5.62E+03	Literature data
Se	1.63E+01	1.3	2.67E+00	9.90E+01	Laxemar site data
Si	3.97E+01	3.7	2.83E+00	3.86E+02	Laxemar site data
Sm	6.76E+01	7.6	2.23E+00	2.75E+03	Laxemar site data
Sn	1.63E+01	2.3	2.67E+00	9.92E+01	Laxemar site data
Sr	9.77E−01	4.2	9.32E−02	1.02E+01	Laxemar site data
Tb	8.27E+01	7.7	2.25E+00	3.41E+03	Laxemar site data
Tc	4.87E+02	3.0	8.00E+01	5.62E+03	Literature data
Th	3.50E+01	6.4	1.43E+00	7.41E+02	Laxemar site data
Ti	3.97E+01	3.7	2.83E+00	3.86E+02	Laxemar site data
U	1.84E+00	2.9	1.82E−01	1.12E+01	Laxemar site data
Zr	3.97E+01	3.7	2.83E+00	3.86E+02	Laxemar site data

Table E-24. *CR* for mushroom (cR_ter_mush) kg_{DW} kg_C^{-1}.

Elements	Value	GSD	Minimum	Maximum	Comment
Ac	2.03E−03	7.0	1.11E−04	1.45E−01	Forsmark site data
Ag	5.76E+00	3.0	4.45E−01	3.51E+01	Forsmark site data
Am	2.03E−03	7.0	1.11E−04	1.45E−01	Forsmark site data
Ba	6.90E−02	3.2	5.82E−03	1.54E+00	Forsmark site data
Cd	1.09E+01	3.4	2.31E−01	2.20E+02	Forsmark site data
Cm	2.03E−03	7.0	1.11E−04	1.45E−01	Forsmark site data
Co	1.07E−01	5.0	5.91E−03	7.02E+00	Forsmark site data
Cs	3.31E+01	4.7	2.34E−01	1.16E+03	Forsmark site data
Eu	6.49E−03	7.0	2.64E−04	1.59E−01	Laxemar site data
Gd	2.03E−03	7.0	1.11E−04	1.45E−01	PSU data used
Ho	6.51E−03	7.0	2.65E−04	1.60E−01	Laxemar site data
I	6.48E−02	3.0	1.06E−02	3.03E+00	Forsmark site data
La	2.03E−03	7.0	1.11E−04	1.45E−01	PSU data used
Mo	1.03E−01	4.4	6.38E−03	1.15E+01	Forsmark site data
Nb	7.99E−03	7.0	3.29E−04	4.86E−01	Forsmark site data
Ni	3.26E−01	3.0	1.53E−02	3.45E+00	Forsmark site data
Np	2.03E−03	7.0	1.11E−04	1.45E−01	Forsmark site data
Pa	2.03E−03	7.0	1.11E−04	1.45E−01	Forsmark site data
Pb	3.22E−02	3.0	4.20E−03	3.36E−01	Forsmark site data
Pd	3.26E−01	3.0	1.53E−02	3.45E+00	Forsmark site data
Po	6.54E−03	7.0	2.66E−04	1.61E−01	Forsmark site data
Pu	9.05E−03	9.8	1.18E−04	1.53E+01	Forsmark site data
Ra	6.90E−02	3.2	5.82E−03	1.54E+00	Forsmark site data
Re	6.41E−02	7.0	9.04E−04	4.55E+00	PSU data used
Se	5.65E−02	7.0	2.30E−03	1.39E+00	Forsmark site data
Si	2.42E−02	7.0	1.13E−03	6.82E−01	PSU data used
Sm	2.81E−03	7.0	1.38E−04	9.82E−02	Forsmark site data
Sn	1.03E−02	3.9	7.12E−04	6.13E−01	Forsmark site data
Sr	6.90E−02	3.2	5.82E−03	1.54E+00	Forsmark site data
Tb	2.03E−03	7.0	1.11E−04	1.45E−01	PSU data used
Tc	6.41E−02	7.0	9.04E−04	4.55E+00	Forsmark site data
Th	1.03E−02	3.9	7.12E−04	6.13E−01	Forsmark site data
Ti	2.42E−02	7.0	1.13E−03	6.82E−01	PSU data used
U	9.05E−03	9.8	1.18E−04	1.53E+01	Forsmark site data
Zr	2.42E−02	7.0	1.13E−03	6.82E−01	Forsmark site data

Table E-25. *CR* for terestrial primapry producers (cR_ter_pp) kg_{DW} kg_C^{-1}.

Elements	Value	GSD	Minimum	Maximum	Comment
Ac	1.16E−02	3.1	4.21E−04	1.13E−01	Laxemar site data
Ag	4.19E−02	7.0	1.71E−03	1.03E+00	Forsmark site data
Am	1.16E−02	3.1	4.21E−04	1.13E−01	Laxemar site data
Ba	1.19E+00	2.7	5.50E−02	1.17E+01	Laxemar site data
Cd	6.31E−01	3.7	4.41E−02	1.76E+01	Laxemar site data
Cm	1.16E−02	3.1	4.21E−04	1.13E−01	Laxemar site data
Co	1.17E−01	1.8	1.20E−02	1.15E+00	Laxemar site data
Cs	2.06E−01	4.1	8.96E−03	9.38E+00	Laxemar site data
Eu	6.49E−03	3.0	6.13E−04	6.34E−02	Laxemar site data
Gd	1.16E−02	3.1	4.21E−04	1.13E−01	Laxemar site data
Ho	6.51E−03	2.8	6.66E−04	6.37E−02	Laxemar site data
I	1.56E−01	5.8	6.75E−03	1.30E+01	Forsmark site data
La	1.16E−02	3.1	4.21E−04	1.13E−01	Laxemar site data
Mo	2.02E−01	5.1	6.97E−03	4.86E+00	Laxemar site data
Nb	8.30E−03	2.1	8.49E−04	8.12E−02	Laxemar site data
Ni	2.42E−01	2.4	2.48E−02	2.37E+00	Laxemar site data
Np	1.16E−02	3.1	4.21E−04	1.13E−01	Laxemar site data
Pa	1.16E−02	3.1	4.21E−04	1.13E−01	Laxemar site data
Pb	3.58E−02	2.1	3.66E−03	3.50E−01	Laxemar site data
Pd	2.42E−01	2.4	2.48E−02	2.37E+00	Laxemar site data
Po	6.54E−03	7.0	2.66E−04	1.61E−01	Forsmark site data
Pu	1.67E−03	3.3	1.49E−04	2.01E−02	Laxemar site data
Ra	5.99E−02	4.0	6.13E−03	9.76E−01	Forsmark site data
Re	6.41E−02	7.0	9.04E−04	4.55E+00	Forsmark site data
Se	5.65E−02	7.0	2.30E−03	1.39E+00	Forsmark site data
Si	3.70E−02	3.8	3.79E−03	5.38E−01	Laxemar site data
Sm	4.73E−03	3.2	2.76E−04	5.38E−02	Laxemar site data
Sn	1.11E−01	1.8	1.14E−02	1.09E+00	Laxemar site data
Sr	2.01E+00	1.9	2.05E−01	1.96E+01	Laxemar site data
Tb	1.16E−02	3.1	4.21E−04	1.13E−01	Laxemar site data
Tc	6.41E−02	7.0	9.04E−04	4.55E+00	Forsmark site data
Th	1.16E−02	2.2	1.19E−03	1.14E−01	Laxemar site data
Ti	3.70E−02	3.8	3.79E−03	5.38E−01	Laxemar site data
U	1.67E−03	3.3	1.49E−04	2.01E−02	Laxemar site data
Zr	3.70E−02	3.8	3.79E−03	5.38E−01	Laxemar site data

Table E-26. K_d for partcualte matter in lake water (kD_PM_lake) m^3 kg_{DW}^{-1}.

Elements	Value	GSD	Minimum	Maximum	Comment
Ac	1.08E+02	2.0	7.63E+00	1.52E+03	Laxemar site data
Ag	3.62E+01	2.0	2.57E+00	5.12E+02	Laxemar site data
Am	1.08E+02	2.0	7.63E+00	1.52E+03	Laxemar site data
Ba	2.10E+01	1.7	1.49E+00	2.97E+02	Laxemar site data
Ca	1.39E+00	1.3	9.82E−02	1.96E+01	Laxemar site data
Cd	1.54E+02	2.7	1.09E+01	2.17E+03	Laxemar site data
Cl	8.64E−01	3.6	6.12E−02	1.22E+01	Laxemar site data
Cm	1.08E+02	2.0	7.63E+00	1.52E+03	Laxemar site data
Co	1.12E+02	7.6	3.96E+00	3.18E+03	Laxemar site data
Cs	1.52E+02	2.8	1.08E+01	2.15E+03	Laxemar site data
Eu	1.07E+02	1.9	7.60E+00	1.51E+03	Laxemar site data
Gd	1.08E+02	2.0	7.63E+00	1.52E+03	Laxemar site data
Ho	1.10E+02	1.9	7.79E+00	1.55E+03	Laxemar site data
I	1.17E+01	1.7	8.31E−01	1.66E+02	Laxemar site data
La	1.08E+02	2.0	7.63E+00	1.52E+03	Laxemar site data
Mo	1.30E+01	1.3	9.20E−01	1.83E+02	Laxemar site data
Nb	4.61E+02	2.3	3.26E+01	6.51E+03	Laxemar site data
Ni	1.89E+01	1.5	1.34E+00	2.67E+02	Laxemar site data
Np	1.08E+02	2.0	7.63E+00	1.52E+03	Laxemar site data
Pa	1.08E+02	2.0	7.63E+00	1.52E+03	Laxemar site data
Pb	4.58E+02	3.2	3.24E+01	6.46E+03	Laxemar site data
Pd	1.89E+01	1.5	1.34E+00	2.67E+02	Laxemar site data
Po	1.76E+02	1.7	1.25E+01	2.49E+03	Laxemar site data
Pu	4.75E+01	1.7	3.37E+00	6.71E+02	Laxemar site data
Ra	2.10E+01	1.7	1.49E+00	2.97E+02	Laxemar site data
Re	2.17E−01	2.9	1.54E−02	3.06E+00	Laxemar site data
Se	1.14E+01	2.1	8.10E−01	1.62E+02	Laxemar site data
Si	1.22E+02	2.7	8.67E+00	1.73E+03	Laxemar site data
Sm	1.08E+02	2.0	7.63E+00	1.52E+03	Laxemar site data
Sn	1.22E+02	2.7	8.67E+00	1.73E+03	Laxemar site data
Sr	1.84E+00	1.2	1.30E−01	2.60E+01	Laxemar site data
Tb	1.08E+02	2.0	7.63E+00	1.52E+03	Laxemar site data
Tc	2.17E−01	2.9	1.54E−02	3.06E+00	Laxemar site data
Th	2.44E+02	1.6	1.73E+01	3.44E+03	Laxemar site data
Ti	1.22E+02	2.7	8.67E+00	1.73E+03	Laxemar site data
U	4.75E+01	1.7	3.37E+00	6.71E+02	Laxemar site data
Zr	1.22E+02	2.7	8.67E+00	1.73E+03	Laxemar site data

Table E-27. K_d for particulate matter in seawater (kD_PM_sea) $m^3\ kg_{DW}^{-1}$.

Elements	Value	GSD	Minimum	Maximum	Comment
Ac	3.13E+02	1.4	2.22E+01	4.42E+03	Laxemar site data
Ag	3.62E+01	5.0	2.57E+00	5.12E+02	Laxemar site data
Am	3.13E+02	1.4	2.22E+01	4.42E+03	Laxemar site data
Ba	2.33E+00	1.5	1.65E−01	3.30E+01	Laxemar site data
Ca	4.31E−02	1.8	3.05E−03	6.09E−01	Laxemar site data
Cd	5.84E+01	1.3	4.13E+00	8.24E+02	Laxemar site data
Cl	6.37E−04	5.0	4.51E−05	9.00E−03	Forsmark site data
Cm	3.13E+02	1.4	2.22E+01	4.42E+03	Laxemar site data
Co	3.17E+01	1.4	2.24E+00	4.47E+02	Laxemar site data
Cs	7.51E+00	2.0	5.32E−01	1.06E+02	Laxemar site data
Eu	2.26E+02	1.7	1.60E+01	3.19E+03	Laxemar site data
Gd	3.13E+02	1.4	2.22E+01	4.42E+03	Laxemar site data
Ho	1.08E+02	3.4	7.66E+00	1.53E+03	Laxemar site data
I	5.14E+00	2.1	3.64E−01	7.26E+01	Laxemar site data
La	4.51E+02	1.4	3.20E+01	6.37E+03	Laxemar site data
Mo	4.08E−01	2.3	2.89E−02	5.76E+00	Laxemar site data
Nb	1.83E+02	1.9	1.30E+01	2.59E+03	Laxemar site data
Ni	1.14E+01	1.2	8.05E−01	1.61E+02	Laxemar site data
Np	3.13E+02	5.0	2.22E+01	4.42E+03	Laxemar site data
Pa	3.13E+02	1.4	2.22E+01	4.42E+03	Laxemar site data
Pb	3.75E+02	1.5	2.66E+01	5.30E+03	Laxemar site data
Pd	1.14E+01	1.2	8.05E−01	1.61E+02	Laxemar site data
Po	2.10E+01	2.2	1.49E+00	2.97E+02	Laxemar site data
Pu	9.23E−01	5.0	6.54E−02	1.30E+01	Laxemar site data
Ra	2.33E+00	1.5	1.65E−01	3.30E+01	Laxemar site data
Re	1.15E−01	1.6	8.13E−03	1.62E+00	Laxemar site data
Se	1.10E+01	1.2	7.76E−01	1.55E+02	Laxemar site data
Si	1.66E+02	1.6	1.18E+01	2.35E+03	Laxemar site data
Sm	3.13E+02	1.4	2.22E+01	4.42E+03	Laxemar site data
Sn	4.79E+01	1.4	3.39E+00	6.76E+02	Laxemar site data
Sr	9.47E−02	1.5	6.71E−03	1.34E+00	Laxemar site data
Tb	3.13E+02	1.4	2.22E+01	4.42E+03	Laxemar site data
Tc	1.15E−01	1.6	8.13E−03	1.62E+00	Laxemar site data
Th	3.43E+02	1.7	2.43E+01	4.84E+03	Laxemar site data
Ti	1.66E+02	1.6	1.18E+01	2.35E+03	Laxemar site data
U	9.23E−01	2.4	6.54E−02	1.30E+01	Laxemar site data
Zr	1.66E+02	1.6	1.18E+01	2.35E+03	Laxemar site data

Table E-28. K_d for glacial clay (kD_regoGL) m^3 kg_{DW}^{-1}.

Elements	Value	GSD	Minimum	Maximum	Comment
Ac	1.0E+02	3.1	1.60E+01	6.81E+02	Forsmark site data
Ag	3.5E−01	3.0	5.75E−02	2.13E+00	Forsmark site data
Am	1.0E+02	3.1	1.60E+01	6.81E+02	Forsmark site data
Ba	3.6E+00	3.0	5.94E−01	2.21E+01	Forsmark site data
Ca	9.5E−01	3.0	1.56E−01	5.78E+00	Forsmark site data
Cd	1.7E+01	3.0	2.87E+00	1.06E+02	Forsmark site data
Cl	5.1E−03	3.0	8.35E−04	3.10E−02	Forsmark site data
Cm	1.0E+02	3.1	1.60E+01	6.81E+02	Forsmark site data
Co	8.4E+01	3.0	1.37E+01	5.09E+02	Forsmark site data
Cs	3.3E+02	3.0	5.33E+01	1.98E+03	Forsmark site data
Eu	9.2E+01	6.0	4.84E+00	1.76E+03	Forsmark site data
Gd	1.0E+02	3.1	1.60E+01	6.81E+02	PSU data used
Ho	8.0E+01	3.0	1.31E+01	4.87E+02	Forsmark site data
I	2.3E−01	3.0	3.76E−02	1.40E+00	Forsmark site data
La	1.0E+02	3.1	1.60E+01	6.81E+02	PSU data used
Mo	2.2E−01	4.6	1.81E−02	2.99E+00	Forsmark site data
Nb	1.5E+02	3.0	2.47E+01	9.18E+02	Forsmark site data
Ni	1.7E+01	3.0	2.82E+00	1.05E+02	Forsmark site data
Np	9.3E+01	3.0	1.53E+01	5.67E+02	Forsmark site data
Pa	1.0E+02	3.1	1.60E+01	6.81E+02	Forsmark site data
Pb	2.1E+02	3.0	3.46E+01	1.29E+03	Forsmark site data
Pd	1.7E+01	3.0	2.82E+00	1.05E+02	Forsmark site data
Po	1.3E+02	3.0	2.14E+01	7.95E+02	Forsmark site data
Pu	1.0E+02	3.1	1.60E+01	6.81E+02	Forsmark site data
Ra	1.0E+01	3.0	1.67E+00	6.20E+01	Forsmark site data
Re	5.4E+01	3.0	8.82E+00	3.27E+02	PSU data used
Se	9.2E−01	6.0	4.82E−02	1.75E+01	Forsmark site data
Si	5.4E+01	3.0	8.82E+00	3.27E+02	PSU data used
Sm	1.0E+02	3.1	1.60E+01	6.81E+02	Forsmark site data
Sn	1.3E+01	3.0	2.10E+00	7.81E+01	Forsmark site data
Sr	7.0E−01	3.0	1.14E−01	4.24E+00	Forsmark site data
Tb	1.0E+02	3.1	1.60E+01	6.81E+02	PSU data used
Tc	5.4E+01	3.0	8.82E+00	3.27E+02	Forsmark site data
Th	9.3E+01	3.0	1.53E+01	5.67E+02	Forsmark site data
Ti	5.4E+01	3.0	8.82E+00	3.27E+02	PSU data used
U	4.3E−01	8.4	1.30E−02	1.78E+01	Forsmark site data
Zr	5.4E+01	3.0	8.82E+00	3.27E+02	Forsmark site data

Table E-29. K_d for till (kD_regoLow) m^3 kg_{DW}^{-1}.

Elements	Value	GSD	Minimum	Maximum	Comment
Ac	1.1E+01	3.0	1.75E+00	6.48E+01	Forsmark site data
Ag	1.1E+00	3.0	1.83E−01	6.99E+00	Forsmark site data
Am	1.1E+01	3.0	1.75E+00	6.48E+01	Forsmark site data
Ba	2.1E−01	3.0	3.47E−02	1.29E+00	Forsmark site data
Ca	2.9E−01	3.0	4.76E−02	1.77E+00	Forsmark site data
Cd	1.1E+00	8.4	3.26E−02	3.53E+01	Forsmark site data
Cl	5.4E−04	3.0	8.80E−05	3.27E−03	Forsmark site data
Cm	1.1E+01	3.0	1.75E+00	6.48E+01	Forsmark site data
Co	2.5E+00	3.0	4.08E−01	1.52E+01	Forsmark site data
Cs	1.2E+01	3.0	2.04E+00	7.57E+01	Forsmark site data
Eu	9.1E+00	3.0	1.49E+00	5.54E+01	Forsmark site data
Gd	1.1E+01	3.0	1.75E+00	6.48E+01	PSU data used
Ho	5.6E+00	3.0	9.26E−01	3.44E+01	Forsmark site data
I	1.4E−02	3.0	2.31E−03	8.59E−02	Forsmark site data
La	1.1E+01	3.0	1.75E+00	6.48E+01	PSU data used
Mo	2.1E−02	3.0	2.61E−03	1.26E−01	Forsmark site data
Nb	3.1E+01	3.0	5.05E+00	1.87E+02	Forsmark site data
Ni	7.9E−01	3.0	1.30E−01	4.83E+00	Forsmark site data
Np	2.4E+01	3.0	3.86E+00	1.43E+02	Forsmark site data
Pa	1.1E+01	3.0	1.75E+00	6.48E+01	Forsmark site data
Pb	1.7E+01	3.0	2.74E+00	1.02E+02	Forsmark site data
Pd	7.9E−01	3.0	1.30E−01	4.83E+00	Forsmark site data
Po	1.5E+01	3.6	1.81E+00	1.18E+02	Forsmark site data
Pu	1.1E+01	3.0	1.75E+00	6.48E+01	Forsmark site data
Ra	1.4E+00	3.0	2.30E−01	8.55E+00	Forsmark site data
Re	3.6E+00	3.0	5.86E−01	2.18E+01	PSU data used
Se	1.4E−01	3.0	2.27E−02	8.43E−01	Forsmark site data
Si	3.6E+00	3.0	5.86E−01	2.18E+01	PSU data used
Sm	1.1E+01	3.0	1.75E+00	6.48E+01	Forsmark site data
Sn	1.1E+01	3.0	1.76E+00	6.54E+01	Forsmark site data
Sr	1.1E−01	3.0	1.80E−02	6.70E−01	Forsmark site data
Tb	1.1E+01	3.0	1.75E+00	6.48E+01	PSU data used
Tc	3.6E+00	3.0	5.86E−01	2.18E+01	Forsmark site data
Th	2.4E+01	3.0	3.86E+00	1.43E+02	Forsmark site data
Ti	3.6E+00	3.0	5.86E−01	2.18E+01	PSU data used
U	2.2E−02	3.1	2.95E−03	1.41E−01	Forsmark site data
Zr	3.6E+00	3.0	5.86E−01	2.18E+01	Forsmark site data

Table E-30. K_d for anoxic peat (kD_regoPeat) $m^3\ kg_{DW}^{-1}$.

Elements	Value	GSD	Minimum	Maximum	Comment
Ac	1.0E+01	3.0	1.64E+00	6.09E+01	Forsmark site data
Ag	2.6E+00	3.0	4.33E−01	1.61E+01	Forsmark site data
Am	1.0E+01	3.0	1.64E+00	6.09E+01	Forsmark site data
Ba	5.6E−01	4.9	2.46E−02	7.57E+00	Forsmark site data
Ca	3.8E−01	3.0	6.29E−02	2.34E+00	Forsmark site data
Cd	1.7E+01	7.1	6.06E−01	4.18E+02	Forsmark site data
Cl	2.7E−02	3.9	2.84E−03	2.49E−01	Forsmark site data
Cm	1.0E+01	3.0	1.64E+00	6.09E+01	Forsmark site data
Co	3.0E+00	3.0	4.90E−01	1.82E+01	Forsmark site data
Cs	4.7E−01	3.0	7.64E−02	2.84E+00	Forsmark site data
Eu	1.3E+01	6.0	6.77E−01	2.46E+02	Forsmark site data
Gd	1.0E+01	3.0	1.64E+00	6.09E+01	PSU data used
Ho	1.3E+01	3.0	2.06E+00	7.64E+01	Forsmark site data
I	7.3E−01	3.0	1.19E−01	4.43E+00	Forsmark site data
La	1.0E+01	3.0	1.64E+00	6.09E+01	PSU data used
Mo	3.9E+00	3.0	6.46E−01	2.40E+01	Forsmark site data
Nb	1.2E+01	3.0	1.93E+00	7.15E+01	Forsmark site data
Ni	2.6E+00	3.0	4.29E−01	1.59E+01	Forsmark site data
Np	3.2E+00	3.4	4.20E−01	3.61E+01	Forsmark site data
Pa	1.0E+01	3.0	1.64E+00	6.09E+01	Forsmark site data
Pb	1.4E+01	3.0	2.38E+00	8.82E+01	Forsmark site data
Pd	4.3E+00	6.0	2.23E−01	8.10E+01	Forsmark site data
Po	1.5E+01	3.0	2.44E+00	9.05E+01	Forsmark site data
Pu	1.0E+01	3.0	1.64E+00	6.09E+01	Forsmark site data
Ra	2.1E+00	3.0	3.42E−01	1.27E+01	Forsmark site data
Re	2.6E+00	3.0	4.25E−01	1.58E+01	PSU data used
Se	4.4E−01	6.0	2.30E−02	8.35E+00	Forsmark site data
Si	2.6E+00	3.0	4.25E−01	1.58E+01	PSU data used
Sm	1.0E+01	3.0	1.64E+00	6.09E+01	Forsmark site data
Sn	1.0E+01	3.5	1.27E+00	8.16E+01	Forsmark site data
Sr	3.9E−01	3.0	6.48E−02	2.41E+00	Forsmark site data
Tb	1.0E+01	3.0	1.64E+00	6.09E+01	PSU data used
Tc	2.6E+00	3.0	4.25E−01	1.58E+01	Forsmark site data
Th	3.2E+00	3.4	4.20E−01	3.61E+01	Forsmark site data
Ti	2.6E+00	3.0	4.25E−01	1.58E+01	PSU data used
U	1.3E+01	3.1	1.82E+00	8.13E+01	Forsmark site data
Zr	2.6E+00	3.0	4.25E−01	1.58E+01	Forsmark site data

Table E-31. K_d for postglacial sediments (kD_regoPG) m^3 kg_{DW}^{-1}.

Elements	Value	GSD	Minimum	Maximum	Comment
Ac	3.5E+00	3.0	6.43E−01	2.42E+01	Forsmark site data
Ag	4.1E+00	4.3	3.73E−01	5.21E+01	Forsmark site data
Am	3.5E+00	3.0	6.43E−01	2.42E+01	Forsmark site data
Ba	2.0E+00	11.7	7.15E−03	2.37E+01	Forsmark site data
Ca	3.7E−02	3.0	6.83E−03	2.54E−01	Forsmark site data
Cd	7.3E−02	3.0	1.68E−02	6.24E−01	Forsmark site data
Cl	8.4E−03	3.0	1.38E−03	5.13E−02	Forsmark site data
Cm	3.5E+00	3.0	6.43E−01	2.42E+01	Forsmark site data
Co	1.3E+00	3.8	8.70E−02	7.21E+00	Forsmark site data
Cs	4.3E+01	3.0	6.36E+00	2.36E+02	Forsmark site data
Eu	3.8E+00	3.2	5.14E−01	3.28E+01	Forsmark site data
Gd	3.5E+00	3.0	6.43E−01	2.42E+01	PSU data used
Ho	3.0E+00	3.0	5.55E−01	2.12E+01	Forsmark site data
I	4.8E−01	3.0	7.94E−02	2.95E+00	Forsmark site data
La	3.5E+00	3.0	6.43E−01	2.42E+01	PSU data used
Mo	3.4E+00	5.5	2.01E−01	5.40E+01	Forsmark site data
Nb	3.1E+01	3.0	4.06E+00	1.51E+02	Forsmark site data
Ni	1.1E+00	3.1	1.22E−01	6.19E+00	Forsmark site data
Np	1.3E+01	3.0	2.11E+00	7.84E+01	Forsmark site data
Pa	3.5E+00	3.0	6.43E−01	2.42E+01	Forsmark site data
Pb	7.7E+00	3.0	1.59E+00	5.90E+01	Forsmark site data
Pd	1.1E+00	3.1	1.22E−01	6.19E+00	Forsmark site data
Po	3.7E+01	3.0	6.08E+00	2.26E+02	Forsmark site data
Pu	3.5E+00	3.0	6.43E−01	2.42E+01	Forsmark site data
Ra	2.6E+00	3.0	4.35E−01	1.61E+01	Forsmark site data
Re	4.1E+00	4.3	1.97E−01	5.75E+01	PSU data used
Se	1.5E+00	4.2	3.24E−02	3.57E+00	Forsmark site data
Si	4.1E+00	4.3	1.97E−01	5.75E+01	PSU data used
Sm	3.5E+00	3.0	6.43E−01	2.42E+01	Forsmark site data
Sn	2.7E+01	9.6	6.55E−01	1.13E+03	Forsmark site data
Sr	5.8E−02	3.0	9.38E−03	3.48E−01	Forsmark site data
Tb	3.5E+00	3.0	6.43E−01	2.42E+01	PSU data used
Tc	4.1E+00	4.3	1.97E−01	5.75E+01	Forsmark site data
Th	1.3E+01	3.0	2.11E+00	7.84E+01	Forsmark site data
Ti	4.1E+00	4.3	1.97E−01	5.75E+01	PSU data used
U	3.8E+00	3.0	9.55E−01	3.55E+01	Forsmark site data
Zr	4.1E+00	4.3	1.97E−01	5.75E+01	Forsmark site data

Table E-32. K_d for cultivated drain mire (kD_regoUp_drained mire) $m^3\ kg_{DW}^{-1}$.

Element	GM	GSD	minimum	maximum	Comment
Ac	5.5E+00	3.3	4.81E−01	3.96E+01	FM_GM
Ag	2.8E+00	2.5	5.96E−01	1.29E+01	FM_GM
Am	5.5E+00	3.3	4.81E−01	3.96E+01	FM_GM
Ba	8.0E−01	2.0	2.55E−01	2.49E+00	FM_GM
Ca	1.1E−01	2.9	1.88E−02	6.17E−01	FM_GM
Cd	1.9E+00	7.2	7.43E−02	5.03E+01	FM_GM
Cl	2.1E−02	2.7	4.15E−03	1.04E−01	FM_GM
Cm	5.5E+00	3.3	4.81E−01	3.96E+01	FM_GM
Co	8.0E−01	2.4	1.00E−01	3.36E+00	FM_GM
Cs	1.1E+01	3.6	1.27E+00	9.87E+01	FM_GM
Eu	2.9E+00	3.5	3.71E−01	2.32E+01	FM_GM
Gd	5.5E+00	3.3	4.81E−01	3.96E+01	PSU data
Ho	4.4E+00	3.5	3.20E−01	3.52E+01	FM_GM
I	1.4E−01	2.7	1.33E−02	7.03E−01	FM_GM
La	5.5E+00	3.3	4.81E−01	3.96E+01	PSU data
Mo	7.4E−01	3.2	1.11E−01	6.30E+00	FM_GM
Nb	3.9E+00	2.9	4.80E−01	2.65E+01	FM_GM
Ni	8.3E−01	2.5	1.28E−01	3.81E+00	FM_GM
Np	5.5E+00	3.3	4.81E−01	3.96E+01	FM_GM
Pa	5.5E+00	3.3	4.81E−01	3.96E+01	FM_GM
Pb	8.0E+00	3.8	5.31E−01	7.16E+01	FM_GM
Pd	6.4E−01	6.0	3.34E−02	1.21E+01	FM_GM
Po	7.3E+00	3.4	5.98E−01	5.42E+01	FM_GM
Pu	5.9E+00	3.4	6.06E−01	4.50E+01	FM_GM
Ra	2.1E+00	2.0	6.83E−01	6.68E+00	FM_GM
Re	6.7E−02	7.4	2.49E−03	2.68E+00	PSU data
Se	1.3E+00	3.0	2.14E−01	7.94E+00	FM_GM
Si	8.9E−01	4.4	5.99E−02	1.01E+01	PSU data
Sm	5.5E+00	3.3	4.81E−01	3.96E+01	FM_GM
Sn	5.5E+00	2.4	1.33E+00	3.83E+01	FM_GM
Sr	1.4E−01	2.5	3.07E−02	6.55E−01	FM_GM
Tb	5.5E+00	3.3	4.81E−01	3.96E+01	PSU data
Tc	6.7E−02	7.4	2.49E−03	2.68E+00	FM_GM
Th	4.0E+00	2.9	3.67E−01	2.38E+01	FM_GM
Ti	8.9E−01	4.4	5.99E−02	1.01E+01	PSU data
U	5.9E+00	3.4	6.06E−01	4.50E+01	FM_GM
Zr	8.9E−01	4.4	5.99E−02	1.01E+01	FM_GM

Table E-33. K_d for garden plot (kD_regoUp_gaden_plot) m^3 kg_{DW}^{-1}.

Element	GM	GSD	minimum	maximum	Comment
Ac	2.1E+01	6.0	8.46E−01	3.07E+02	FM_GM
Ag	2.6E+00	6.0	1.39E−01	5.03E+01	FM_GM
Am	2.1E+01	6.0	8.46E−01	3.07E+02	FM_GM
Ba	1.1E+00	6.0	3.00E−02	1.54E+01	FM_GM
Ca	1.2E−01	6.0	7.09E−03	2.58E+00	FM_GM
Cd	6.8E+00	6.0	2.07E−01	8.42E+01	FM_GM
Cl	5.8E−03	6.0	3.05E−04	1.11E−01	FM_GM
Cm	2.1E+01	6.0	8.46E−01	3.07E+02	FM_GM
Co	1.1E+01	6.0	4.76E−01	1.73E+02	FM_GM
Cs	2.5E+02	6.0	5.71E+00	3.81E+03	FM_GM
Eu	1.7E+01	6.0	6.25E−01	2.27E+02	FM_GM
Gd	2.1E+01	4.2	1.28E+00	1.72E+02	PSU data
Ho	1.6E+01	6.0	7.02E−01	2.55E+02	FM_GM
I	2.0E−01	6.0	1.04E−02	3.76E+00	FM_GM
La	2.1E+01	4.2	1.28E+00	1.72E+02	PSU data
Mo	1.6E−01	6.0	9.47E−03	3.44E+00	FM_GM
Nb	2.2E+01	6.0	7.97E−01	3.39E+02	FM_GM
Ni	2.6E+00	6.0	1.19E−01	4.33E+01	FM_GM
Np	2.1E+01	6.0	8.46E−01	3.07E+02	FM_GM
Pa	2.1E+01	6.0	8.46E−01	3.07E+02	FM_GM
Pb	6.1E+01	6.9	1.15E+00	8.51E+02	FM_GM
Pd	4.6E+00	6.0	2.40E−01	8.71E+01	FM_GM
Po	3.2E+01	6.0	7.53E−01	6.12E+02	FM_GM
Pu	3.8E−01	6.0	2.28E−02	8.27E+00	FM_GM
Ra	6.0E+00	6.0	3.17E−01	1.15E+02	FM_GM
Re	1.1E−01	2.0	3.63E−02	3.55E−01	PSU data
Se	9.8E−01	6.0	3.46E−02	1.26E+01	FM_GM
Si	2.2E+00	2.7	1.89E−01	9.83E+00	PSU data
Sm	2.1E+01	6.0	8.46E−01	3.07E+02	FM_GM
Sn	8.3E+00	6.0	4.36E−01	1.58E+02	FM_GM
Sr	1.2E−01	6.0	7.77E−03	2.82E+00	FM_GM
Tb	2.1E+01	4.2	1.28E+00	1.72E+02	PSU data
Tc	1.1E−01	6.0	5.96E−03	2.17E+00	FM_GM
Th	2.5E+01	6.0	7.01E−01	4.11E+02	FM_GM
Ti	2.2E+00	2.7	1.89E−01	9.83E+00	PSU data
U	3.8E−01	6.0	2.28E−02	8.27E+00	FM_GM
Zr	2.2E+00	6.0	9.99E−02	3.63E+01	FM_GM

Table E-34. K_d for infield-outland cultivated soil (kD_regoUp_infield_outland) $m^3\ kg_{DW}^{-1}$.

Element	Value	GSD	minimum	maximum	Comment
Ac	2.1E+01	4.2	1.28E+00	1.72E+02	FM_GM
Ag	2.6E+00	2.0	8.44E−01	8.26E+00	FM_GM
Am	2.1E+01	4.2	1.28E+00	1.72E+02	FM_GM
Ba	1.1E+00	3.1	3.00E−02	5.31E+00	FM_GM
Ca	1.2E−01	2.3	3.54E−02	5.16E−01	FM_GM
Cd	6.8E+00	5.8	2.07E−01	7.90E+01	FM_GM
Cl	5.8E−03	2.0	1.86E−03	1.82E−02	FM_GM
Cm	2.1E+01	4.2	1.28E+00	1.72E+02	FM_GM
Co	1.1E+01	2.8	1.71E+00	4.81E+01	FM_GM
Cs	2.5E+02	4.7	5.71E+00	2.51E+03	FM_GM
Eu	1.7E+01	5.0	8.42E−01	1.68E+02	FM_GM
Gd	2.1E+01	4.2	1.28E+00	1.72E+02	PSU data used
Ho	1.6E+01	3.6	1.21E+00	1.11E+02	FM_GM
I	2.0E−01	2.0	4.44E−02	6.17E−01	FM_GM
La	2.1E+01	4.2	1.28E+00	1.72E+02	PSU data used
Mo	1.6E−01	2.0	5.77E−02	5.64E−01	FM_GM
Nb	2.2E+01	4.3	7.97E−01	1.95E+02	FM_GM
Ni	2.6E+00	2.0	5.72E−01	7.11E+00	FM_GM
Np	2.1E+01	4.2	1.28E+00	1.72E+02	FM_GM
Pa	2.1E+01	4.2	1.28E+00	1.72E+02	FM_GM
Pb	6.1E+01	6.9	1.15E+00	1.08E+03	FM_GM
Pd	4.6E+00	6.0	2.40E−01	8.71E+01	FM_GM
Po	3.2E+01	4.8	7.53E−01	4.21E+02	FM_GM
Pu	3.8E−01	2.0	1.38E−01	1.57E+00	FM_GM
Ra	6.0E+00	3.0	9.92E−01	3.69E+01	FM_GM
Re	1.1E−01	2.0	3.63E−02	3.55E−01	PSU data used
Se	9.8E−01	3.4	4.08E−02	4.97E+00	FM_GM
Si	2.2E+00	2.7	1.89E−01	9.83E+00	PSU data used
Sm	2.1E+01	4.2	1.28E+00	1.72E+02	FM_GM
Sn	8.3E+00	2.2	2.26E+00	3.21E+01	FM_GM
Sr	1.2E−01	2.4	3.62E−02	1.19E+00	FM_GM
Tb	2.1E+01	4.2	1.28E+00	1.72E+02	PSU data used
Tc	1.1E−01	2.0	3.63E−02	3.55E−01	FM_GM
Th	2.5E+01	4.7	7.01E−01	2.76E+02	FM_GM
Ti	2.2E+00	2.7	1.89E−01	9.83E+00	PSU data used
U	3.8E−01	2.0	1.38E−01	1.57E+00	FM_GM
Zr	2.2E+00	2.7	1.89E−01	9.83E+00	FM_GM

Table E-35. K_d aquatic sediemnt (kD_regoUp_aqu) m^3 kg_{DW}^{-1}.

Elements	Value	GSD	Minimum	Maximum	Comment
Ac	3.26E+01	2.2	5.36E+00	1.99E+02	Laxemar site data
Ag	1.37E+02	2.1	7.20E+00	2.61E+03	Laxemar site data
Am	3.26E+01	2.2	5.36E+00	1.99E+02	Laxemar site data
Ba	4.21E+00	1.3	6.91E−01	2.57E+01	Laxemar site data
Ca	1.73E−01	2.7	2.84E−02	1.06E+00	Laxemar site data
Cd	3.45E+02	1.6	5.66E+01	2.10E+03	Laxemar site data
Cl	3.44E−03	1.2	1.81E−04	6.56E−02	Laxemar site data
Cm	3.26E+01	2.2	5.36E+00	1.99E+02	Laxemar site data
Co	1.35E+01	1.9	2.21E+00	8.22E+01	Laxemar site data
Cs	2.18E+01	1.2	3.59E+00	1.33E+02	Laxemar site data
Eu	3.29E+01	2.4	5.40E+00	2.01E+02	Laxemar site data
Gd	3.26E+01	2.2	5.36E+00	1.99E+02	Laxemar site data
Ho	2.78E+01	2.1	4.57E+00	1.70E+02	Laxemar site data
I	2.81E−01	1.8	4.61E−02	1.71E+00	Laxemar site data
La	3.26E+01	2.2	5.36E+00	1.99E+02	Laxemar site data
Mo	1.67E+00	2.5	2.74E−01	1.02E+01	Laxemar site data
Nb	7.92E+01	4.4	7.03E+00	8.92E+02	Laxemar site data
Ni	1.09E+01	1.4	1.80E+00	6.67E+01	Laxemar site data
Np	3.26E+01	2.2	5.36E+00	1.99E+02	Laxemar site data
Pa	3.26E+01	2.2	5.36E+00	1.99E+02	Laxemar site data
Pb	2.30E+02	1.5	3.78E+01	1.40E+03	Laxemar site data
Pd	1.09E+01	1.4	1.80E+00	6.67E+01	Laxemar site data
Po	2.53E+01	1.7	4.15E+00	1.54E+02	Laxemar site data
Pu	6.90E+00	3.7	8.12E−01	5.86E+01	Laxemar site data
Ra	4.21E+00	1.3	6.91E−01	2.57E+01	Laxemar site data
Re	1.76E−01	6.0	9.25E−03	3.36E+00	Forsmark site data
Se	4.83E+00	3.1	7.68E−01	3.04E+01	Laxemar site data
Si	6.90E+01	4.4	6.07E+00	7.84E+02	Laxemar site data
Sm	3.26E+01	2.2	5.36E+00	1.99E+02	Laxemar site data
Sn	9.58E+00	2.1	1.57E+00	5.84E+01	Laxemar site data
Sr	2.37E−01	3.4	3.15E−02	1.79E+00	Laxemar site data
Tb	3.26E+01	2.2	5.36E+00	1.99E+02	Laxemar site data
Tc	1.76E−01	6.0	9.25E−03	3.36E+00	Forsmark site data
Th	8.45E+01	2.4	1.39E+01	5.15E+02	Laxemar site data
Ti	6.90E+01	4.4	6.07E+00	7.84E+02	Laxemar site data
U	6.90E+00	3.7	8.12E−01	5.86E+01	Laxemar site data
Zr	6.90E+01	4.4	6.07E+00	7.84E+02	Laxemar site data

Table E-36. K_d for upper oxic peat (kD_regoUp_ter) m^3 kg_{DW}^{-1}.

Elements	Value	GSD	Minimum	Maximum	Comment
Ac	1.2E+01	3.0	1.91E+00	7.08E+01	Forsmark site data
Ag	1.2E+01	3.0	1.99E+00	7.37E+01	Forsmark site data
Am	1.2E+01	3.0	1.91E+00	7.08E+01	Forsmark site data
Ba	8.2E−01	3.0	1.34E−01	4.99E+00	Forsmark site data
Ca	3.1E−01	3.0	5.01E−02	1.86E+00	Forsmark site data
Cd	1.3E+01	5.6	7.51E−01	2.13E+02	Forsmark site data
Cl	2.1E−02	3.0	3.37E−03	1.25E−01	Forsmark site data
Cm	1.2E+01	3.0	1.91E+00	7.08E+01	Forsmark site data
Co	1.7E+00	3.0	2.80E−01	1.04E+01	Forsmark site data
Cs	4.6E−01	3.0	7.61E−02	2.83E+00	Forsmark site data
Eu	4.0E+00	6.0	2.10E−01	7.62E+01	Forsmark site data
Gd	1.2E+01	3.0	1.91E+00	7.08E+01	PSU data used
Ho	9.6E+00	3.0	1.58E+00	5.88E+01	Forsmark site data
I	2.0E−01	3.0	3.34E−02	1.24E+00	Forsmark site data
La	1.2E+01	3.0	1.91E+00	7.08E+01	PSU data used
Mo	4.4E+00	3.0	7.22E−01	2.68E+01	Forsmark site data
Nb	7.3E+00	3.0	1.19E+00	4.43E+01	Forsmark site data
Ni	1.9E+00	3.0	3.19E−01	1.18E+01	Forsmark site data
Np	1.2E+01	3.0	1.91E+00	7.08E+01	Forsmark site data
Pa	1.2E+01	3.0	1.91E+00	7.08E+01	Forsmark site data
Pb	1.8E+01	3.2	2.56E+00	1.23E+02	Forsmark site data
Pd	1.9E+00	3.0	3.19E−01	1.18E+01	Forsmark site data
Po	1.2E+01	3.0	2.01E+00	7.48E+01	Forsmark site data
Pu	1.0E+01	3.0	1.64E+00	6.08E+01	Forsmark site data
Ra	2.1E+00	3.0	3.47E−01	1.29E+01	Forsmark site data
Re	4.1E−01	3.0	6.81E−02	2.53E+00	PSU data used
Se	1.0E+00	6.0	5.27E−02	1.91E+01	Forsmark site data
Si	2.3E+00	3.0	3.84E−01	1.43E+01	PSU data used
Sm	1.2E+01	3.0	1.91E+00	7.08E+01	Forsmark site data
Sn	5.2E+00	3.9	5.66E−01	4.85E+01	Forsmark site data
Sr	3.2E−01	3.0	5.28E−02	1.96E+00	Forsmark site data
Tb	1.2E+01	3.0	1.91E+00	7.08E+01	PSU data used
Tc	4.1E−01	3.0	6.81E−02	2.53E+00	Forsmark site data
Th	2.8E+00	3.0	4.53E−01	1.68E+01	Forsmark site data
Ti	2.3E+00	3.0	3.84E−01	1.43E+01	PSU data used
U	1.0E+01	3.0	1.64E+00	6.08E+01	Forsmark site data
Zr	2.3E+00	3.0	3.84E−01	1.43E+01	Forsmark site data

Table E-37. *TC* for meat (TC_meat) d kg_{FW}^{-1}

Elements	Value	GSD	Minimum	Maximum	Comment
Ac	1.30E−04	7.0	5.29E−06	3.19E−03	Literature data
Ag	1.60E−01	4.0	1.64E−02	1.56E+00	Literature data
Am	5.00E−04	7.0	2.04E−05	1.23E−02	Literature data
Ba	1.40E−04	7.0	5.70E−06	3.44E−03	Literature data
Ca	1.30E−02	30.0	4.83E−05	3.50E+00	Literature data
Cd	5.80E−03	7.8	1.50E−04	1.70E−01	Literature data
Cl	1.70E−02	7.0	6.92E−04	4.17E−01	Literature data
Cm	5.40E−03	7.0	5.29E−06	3.19E−03	Literature data
Co	4.30E−04	4.0	4.40E−05	4.21E−03	Literature data
Cs	2.20E−02	4.0	2.25E−03	2.15E−01	Literature data
Eu	1.30E−04	7.0	5.29E−06	3.19E−03	Literature data
Gd	1.30E−04	7.0	5.29E−06	3.19E−03	PSU data used
Ho	1.30E−04	7.0	5.29E−06	3.19E−03	Literature data
I	6.70E−03	4.0	6.85E−04	6.55E−02	Literature data
La	1.30E−04	7.0	5.29E−06	3.19E−03	PSU data used
Mo	1.00E−03	7.0	4.07E−05	2.46E−02	Literature data
Nb	2.60E−07	7.0	1.06E−08	6.38E−06	Literature data
Ni	1.60E−01	4.0	1.64E−02	1.56E+00	Literature data
Np	1.30E−04	7.0	5.29E−06	3.19E−03	Literature data
Pa	1.30E−04	7.0	5.29E−06	3.19E−03	Literature data
Pb	7.00E−04	4.0	7.16E−05	6.85E−03	Literature data
Pd	1.60E−01	4.0	1.64E−02	1.56E+00	Literature data
Po	7.00E−04	4.0	7.16E−05	6.85E−03	Literature data
Pu	1.10E−06	24.8	5.59E−09	3.00E−04	Literature data
Ra	1.70E−03	7.0	6.92E−05	4.17E−02	Literature data
Re	1.20E−06	7.0	4.89E−08	2.95E−05	PSU data used
Se	7.00E−03	7.0	2.85E−04	1.72E−01	Literature data
Si	1.20E−06	7.0	4.89E−08	2.95E−05	PSU data used
Sm	1.30E−04	7.0	5.29E−06	3.19E−03	Literature data
Sn	1.20E−06	7.0	4.89E−08	2.95E−05	Literature data
Sr	1.30E−03	2.9	2.00E−04	9.20E−03	Literature data
Tb	1.30E−04	7.0	5.29E−06	3.19E−03	PSU data used
Tc	1.20E−06	7.0	4.89E−08	2.95E−05	Literature data
Th	2.30E−04	4.0	2.35E−05	2.25E−03	Literature data
Ti	1.20E−06	7.0	4.89E−08	2.95E−05	PSU data used
U	3.90E−04	7.0	1.59E−05	9.58E−03	Literature data
Zr	1.20E−06	7.0	4.89E−08	2.95E−05	Literature data

Table E-38. *TC* for milk (TC_milk) d l^{-1}

Elements	Value	GSD	Minimum	Maximum	Comment
Ac	4.20E−07	7.0	1.71E−08	1.03E−05	Literature data
Ag	2.70E−03	4.0	1.30E−04	2.64E−02	Literature data
Am	4.20E−07	7.0	1.71E−08	1.03E−05	Literature data
Ba	1.60E−04	4.0	1.64E−05	1.56E−03	Literature data
Ca	1.00E−02	4.0	1.02E−03	9.78E−02	Literature data
Cd	1.90E−04	15.0	1.80E−06	1.63E−02	Literature data
Cl	5.40E−03	4.0	4.00E−04	5.28E−02	Literature data
Cm	4.20E−07	7.0	1.71E−08	1.03E−05	Literature data
Co	1.10E−04	4.0	1.12E−05	1.08E−03	Literature data
Cs	4.60E−03	4.0	4.70E−04	6.80E−02	Literature data
Eu	4.20E−07	7.0	1.71E−08	1.03E−05	Literature data
Gd	4.20E−07	7.0	1.71E−08	1.03E−05	PSU data used
Ho	4.20E−07	7.0	1.71E−08	1.03E−05	Literature data
I	5.40E−03	4.0	4.00E−04	5.28E−02	Literature data
La	4.20E−07	7.0	1.71E−08	1.03E−05	PSU data used
Mo	1.10E−03	4.0	1.12E−04	1.08E−02	Literature data
Nb	4.10E−07	7.0	1.67E−08	1.01E−05	Literature data
Ni	9.50E−04	7.0	3.87E−05	2.33E−02	Literature data
Np	4.20E−07	7.0	1.71E−08	1.03E−05	Literature data
Pa	4.20E−07	7.0	1.71E−08	1.03E−05	Literature data
Pb	1.90E−04	4.0	7.30E−06	1.86E−03	Literature data
Pd	9.50E−04	7.0	3.87E−05	2.33E−02	Literature data
Po	2.10E−04	4.0	2.15E−05	2.05E−03	Literature data
Pu	1.00E−05	7.0	4.07E−07	2.46E−04	Literature data
Ra	3.80E−04	4.0	3.89E−05	3.72E−03	Literature data
Re	3.60E−06	4.3	3.27E−07	3.97E−05	PSU data used
Se	4.00E−03	4.0	4.09E−04	3.91E−02	Literature data
Si	3.60E−06	4.3	3.27E−07	3.97E−05	PSU data used
Sm	4.20E−07	7.0	1.71E−08	1.03E−05	Literature data
Sn	3.60E−06	4.3	3.27E−07	3.97E−05	Literature data
Sr	1.30E−03	1.7	3.40E−04	4.30E−03	Literature data
Tb	4.20E−07	7.0	1.71E−08	1.03E−05	PSU data used
Tc	3.60E−06	4.3	3.27E−07	3.97E−05	Literature data
Th	3.60E−06	4.3	3.27E−07	3.97E−05	Literature data
Ti	3.60E−06	4.3	3.27E−07	3.97E−05	PSU data used
U	1.80E−03	7.0	7.33E−05	4.42E−02	Literature data
Zr	3.60E−06	4.3	3.27E−07	3.97E−05	Literature data

Table E-39. Diffusivity for water (D_water) m^2 $year^{-1}$.

Element	Value
Ac	3.15E−02
Ag	5.36E−02
Am	3.15E−02
Ba	3.15E−02
Be	2.49E−02
C	3.78E−02
Ca	3.15E−02
Cd	2.27E−02
Cl	6.31E−02
Cm	3.15E−02
Co	3.78E−02
Cs	6.62E−02
Eu	3.15E−02
Gd	3.15E−02
H	3.78E−02
Ho	3.15E−02
I	6.31E−02
K	6.62E−02
La	3.15E−02
Mo	3.15E−02
Nb	3.15E−02
Ni	2.14E−02
Np	3.15E−02
Pa	3.15E−02
Pb	3.15E−02
Pd	3.15E−02
Po	3.15E−02
Pu	3.15E−02
Ra	2.81E−02
Re	3.15E−02
Se	3.15E−02
Si	3.15E−02
Sm	3.15E−02
Sn	3.15E−02
Sr	2.49E−02
Tb	3.15E−02
Tc	3.15E−02
Th	4.73E−03
Ti	3.15E−02
U	3.15E−02
Zr	3.15E−02

Table E-40. Fraction combust (f_combust) kg_{DW} kg_{DW}^{-1}.

Elements	Value	Minimum	Maximum
Ac	0.5	0.25	0.75
Ag	0.5	0.25	0.75
Am	0.5	0.25	0.75
Ba	0.5	0.25	0.75
C	0.95	0.9	0.99
Ca	0.5	0.25	0.75
Cd	0.5	0.25	0.75
Cl	0.5	0.25	0.75
Cm	0.5	0.25	0.75
Co	0.5	0.25	0.75
Cs	0.5	0.25	0.75
Eu	0.5	0.25	0.75
Gd	0.5	0.25	0.75
H	1		
Ho	0.5	0.25	0.75
I	0.5	0.25	0.75
La	0.5	0.25	0.75
Mo	0.5	0.25	0.75
Nb	0.5	0.25	0.75
Ni	0.5	0.25	0.75
Np	0.5	0.25	0.75
Pa	0.5	0.25	0.75
Pb	0.5	0.25	0.75
Pd	0.5	0.25	0.75
Po	0.5	0.25	0.75
Pu	0.5	0.25	0.75
Ra	0.5	0.25	0.75
Re	0.5	0.25	0.75
Se	0.5	0.25	0.75
Si	0.5	0.25	0.75
Sm	0.5	0.25	0.75
Sn	0.5	0.25	0.75
Sr	0.5	0.25	0.75
Tb	0.5	0.25	0.75
Tc	0.5	0.25	0.75
Th	0.5	0.25	0.75
Ti	0.5	0.25	0.75
U	0.5	0.25	0.75
Zr	0.5	0.25	0.75

Appendix F

Aquatic ecosystem parameters

Table F-1. Aquatic ecosystem parameter data. (svn://svn.skb.se/projekt/SFLsurface/Synthesis/Parameters/AquaticEcosystem.xlsm)

Name	Unit	Value	Reference
conc_DIC_lake	$kg_C\ m^{-3}$	3.00E−03	Andersson (2010, Section 11.4.3)
conc_DIC_sea	$kg_C\ m^{-3}$	1.50E−02	Grolander (2013, Section 8.5.2)
conc_PM_lake	$kg_{DW}\ m^{-3}$	4.00E−03	Andersson (2010, Section 11.4.3)
conc_PM_sea	$kg_{DW}\ m^{-3}$	3.76E−03	Grolander (2013, Section 8.5.1)
dens_water_sea	$kg\ m^{-3}$	1.01E+03	Chapter 7
f_C_fish	$kg_C\ kg_{DW}^{-1}$	4.42E−01	Grolander (2013, Section 8.10.1)
f_DW_FW_fish_lake	$kg_{DW}\ kg_{FW}^{-1}$	2.08E−01	Grolander (2013, Section 8.10.1)
f_DW_FW_fish_sea	$kg_{DW}\ kg_{FW}^{-1}$	2.08E−01	Grolander (2013, Section 8.10.1)
f_H2CO3_lake	$Bq\ Bq^{-1}$	1.70E−01	Chapter 7
f_H2CO3_sea	$Bq\ Bq^{-1}$	9.31E−03	Grolander (2013, Section 8.8.2)
f_inorg_Cl_PP_aqu	$kg\ kg^{-1}$	6.00E−01	Chapter 7
f_refrac_macro_lake	$kg_C\ kg_C^{-1}$	3.00E−01	Grolander (2013, Section 8.7.2)
f_refrac_macro_sea	$kg_C\ kg_C^{-1}$	3.00E−01	Grolander (2013, Section 8.7.2)
f_refrac_micro_lake	$kg_C\ kg_C^{-1}$	1.00E−01	Grolander (2013, Section 8.7.2)
f_refrac_micro_sea	$kg_C\ kg_C^{-1}$	1.00E−01	Grolander (2013, Section 8.7.2)
f_refrac_plank_lake	$kg_C\ kg_C^{-1}$	1.00E−01	Grolander (2013, Section 8.7.2)
f_refrac_plank_sea	$kg_C\ kg_C^{-1}$	1.00E−01	Grolander (2013, Section 8.7.2)
height_L1_aqu	m	1.00E+00	Grolander (2013, Section 8.8)
height_L2_aqu	m	1.00E+01	Grolander (2013, Section 8.8)
height_ref_aqu	m	1.00E+01	Grolander (2013, Section 8.9)
minRate_regoPG_lake	$kg_C\ kg_C^{-1}\ year^{-1}$	6.50E−05	Grolander (2013, Section 8.7.3)
minRate_regoPG_sea	$kg_C\ kg_C^{-1}\ year^{-1}$	6.50E−05	Grolander (2013, Section 8.7.3)
minRate_regoUp_lake	$kg_C\ kg_C^{-1}\ year^{-1}$	3.00E−02	Grolander (2013, Section 8.7.3)
minRate_regoUp_sea	$kg_C\ kg_C^{-1}\ year^{-1}$	3.00E−02	Grolander (2013, Section 8.7.3)
minRate_water_PM_lake	$kg_C\ kg_C^{-1}\ year^{-1}$	3.00E−02	Grolander (2013, Section 8.7.3)
minRate_water_PM_sea	$kg_C\ kg_C^{-1}\ year^{-1}1$	3.00E−02	Grolander (2013, Section 8.7.3)
piston_vel_lake	$m\ year^{-1}$	2.01E+02	Grolander (2013, Section 8.8.1)
piston_vel_sea	$m\ year^{-1}$	1.87E+02	Grolander (2013, Secton 8.8.1)
prod_edib_cray_lake	$kg_C\ m^{-2}\ year^{-1}$	3.14E−05	Grolander (2013, Section 8.10.2)
prod_edib_fish_lake	$kg_C\ m^{-2}\ year^{-1}$	1.30E−04	Andersson (2010, Section 11.4.4)
prod_edib_fish_sea	$kg_C\ m^{-2}\ year^{-1}$	3.26E−04	Aquilonius 2010 Section 11.4.4)
solubilityCoef_lake	$(mol\ m^{-3})\cdot(mol\ m^{-3})^{-1}$	1.14E+00	Grolander (2013, Section 8.8.3)
solubilityCoef_sea	$(mol\ m^{-3})\cdot(mol\ m^{-3})^{-1}$	1.36E+00	Grolander (2013, Section 8.9)
vel_wind_height_ref_aqu	$m\ s^{-1}$	1.78E+00	Grolander (2013, Section 8.9)
z_min_prod_edib_cray_lake	m	3.00E−01	Andersson (2010, Section 11.4.4)
z_min_prod_edib_fish_lake	m	1.00E+00	Grolander (2013, Section 8.10.1)
z_min_prod_edib_fish_sea	m	1.00E+00	Grolander (2013, Section 8.10.1)
z_regoUp_lake	m	1.00E−02	Andersson (2010, Section 4.6.2)
z_regoUp_sea	m	1.00E−01	Grolander (2013, Section 8.7.1)
z0_aqu	m	5.00E−04	Grolander (2013, Sections 8.8–8.9)

Appendix G

Terrestrial ecosystem parameters

Table G-1. Terrestrail ecosystem parameter data. (svn://svn.skb.se/projekt/SFLsurface/Synthesis/Parameters/TerrestrialEcosystem.xlsm)

Name	Unit	Land use	Value	Reference
amount_irrig	m $year^{-1}$	Garden plot	1.05E−01	Chapter 8
area_support_wood	m^2	Garden plot	3.52E+03	Grolander (2013, Section 9.14.8)
biom_pp_ter	$kg_C\ m^{-2}$		2.30E+00	Grolander (2013, Section 9.3)
conc_air_combPeat	(Bq m^{-3})·(Bq kg_{DW}^{-1})$^{-1}$	Garden plot	2.16E−07	Chapter 8
conc_air_combWood	(Bq m^{-3})·(Bq kg_{DW}^{-1})$^{-1}$	Garden plot	2.49E−07	Chapter 8
conc_C_atmos	$kg_C\ m^{-3}$		2.00E−04	Grolander (2013, Section 9.5.7)
conc_C_meat	$kg_C\ kg_{FW}^{-1}$		1.20E−01	Grolander (2013, Section 9.13.6)
conc_C_milk	$kg_C\ kg_{FW}^{-1}$		6.40E−02	Grolander (2013, Section 9.13.5)
conc_Ca_cereal	gCa kg_C^{-1}		1.46E+00	Chapter 8
conc_Ca_fodder	gCa kg_C^{-1}		4.31E+00	Chapter 8
conc_Ca_mush	gCa kg_C^{-1}		4.70E−01	Chapter 8
conc_Ca_PP_ter	gCa kg_C^{-1}		1.16E+01	Chapter 8
conc_Ca_regoUp_D	gCa m^{-3}	Infield-outland	4.64E+01	Chapter 8
conc_Ca_regoUp_D	gCa m^{-3}	Garden plot	4.64E+01	Chapter 8
conc_Ca_regoUp_gyttja_D	gCa m^{-3}	Drained mire	4.64E+01	Chapter 8
conc_Ca_regoUp_peat_D	gCa m^{-3}	Drained mire	4.64E+01	Chapter 8
conc_Ca_regoUp_ter_D	gCa m^{-3}		4.64E+01	Chapter 8
conc_Ca_tuber	gCa kg_C^{-1}		7.34E+00	Chapter 8
conc_Ca_veg	gCa kg_C^{-1}	Garden plot	4.31E+00	Chapter 8
conc_Cl_cereal	gCl kg_C^{-1}		5.67E−01	Chapter 8
conc_Cl_fodder	gCl kg_C^{-1}		5.67E−01	Chapter 8
conc_Cl_mush	gCl kg_C^{-1}		5.67E−01	Chapter 8
conc_Cl_PP_ter	gCl kg_C^{-1}		2.10E+00	Grolander (2013, Section 9.6.1)
conc_Cl_regoUp_D	gCl m^{-3}	Infield-outland	5.28E+00	Chapter 8
conc_Cl_regoUp_D	gCl m^{-3}	Garden plot	5.28E+00	Chapter 8
conc_Cl_regoUp_gyttja_D	gCl m^{-3}	Drained mire	5.28E+00	Chapter 8
conc_Cl_regoUp_peat_D	gCl m^{-3}	Drained mire	2.53E+00	Chapter 8
conc_Cl_regoUp_ter_D	gCl m^{-3}		1.39E+01	Grolander (2013, Section 9.6.2)
conc_Cl_tuber	gCl kg_C^{-1}		5.67E−01	Chapter 8
conc_Cl_veg	gCl kg_C^{-1}	Garden plot	5.67E−01	Chapter 8
conc_Dust	$kg_{DW}\ m^{-3}$	Infield-outland	5.00E−08	Grolander (2013, Section 9.10)
conc_Dust	$kg_{DW}\ m^{-3}$	Garden plot	5.00E−08	Grolander (2013, Section 9.10)
conc_Dust	$kg_{DW}\ m^{-3}$	Drained mire	5.00E−08	Grolander (2013, Section 9.10)
conc_Dust_ter	$kg_{DW}\ m^{-3}$		1.40E−08	Grolander (2013, Section 9.10)
conc_K_cereal	gK kg_C^{-1}		1.06E+01	Chapter 8
conc_K_fodder	gK kg_C^{-1}		1.15E+01	Chapter 8
conc_K_mush	gK kg_C^{-1}		8.66E+01	Chapter 8
conc_K_PP_ter	gK kg_C^{-1}		1.16E+01	Chapter 8
conc_K_regoUp_D	gK m^{-3}	Infield-outland	1.66E+00	Chapter 8
conc_K_regoUp_D	gK m^{-3}	Garden plot	1.66E+00	Chapter 8
conc_K_regoUp_gyttja_D	gK m^{-3}	Drained mire	1.66E+00	Chapter 8
conc_K_regoUp_peat_D	gK m^{-3}	Drained mire	7.28E−01	Chapter 8
conc_K_regoUp_ter_D	gK m^{-3}		6.00E+00	Chapter 8
conc_K_tuber	gK kg_C^{-1}		1.06E+01	Chapter 8
conc_K_veg	gK kg_C^{-1}	Garden plot	1.15E+01	Chapter 8
D_CO2_air	$m^2\ year^{-1}$		4.35E+02	Chapter 8
demand_AlgFertil	$kg_C\ m^{-2}\ year^{-1}$	Garden plot	2.18E−01	Grolander (2013, Section 9.14.7)
demand_hay	$kg_C\ m^{-2}\ year^{-1}$	Infiel-outland	2.30E−01	Grolander (2013, Section 10.9)

Name	Unit	Land use	Value	Reference
demand_peat	kg_{DW}	Garden plot	3.40E+04	Grolander (2013) 9.14.9)
dens_milk	$kg_{FW}\ l^{-1}$		1.03E+00	Grolander (2013, Section 9.13.4)
dens_water_lake	kg m^{-3}		1.00E+03	Chapter 8
dragCoef	unitless		2.00E−01	Grolander (2013, Section 9.5.1)
f_C_peat	$kg_C\ kg_{DW}^{-1}$		4.60E−01	Grolander (2013, Section 9.4.3)
f_C_wood	$kg_C\ kg_{DW}^{-1}$	Garden plot	4.80E−01	Grolander (2013, Section 9.14.8)
f_H2CO3_ter	Bq Bq^{-1}		9.88E−01	Chapter 8
f_inorg_Cl_PP_ter	kg kg^{-1}		6.00E−01	Chapter 8
f_loss_orgFert	Bq Bq^{-1}	Infield-outland	1.00E+00	Grolander (2013, Section 9.13.8)
f_mush_herbiv	$kg_C\ kg_C^{-1}$		6.00E−02	Grolander (2013, Section 9.13.7)
f_refrac_ter	$kg_C\ kg_C^{-1}$		3.00E−01	Grolander (2013, Section 9.9.1)
f_rootUptake	$kg_C\ kg_C^{-1}$		2.00E−02	Grolander (2013, Section 9.4.4)
f_trans_tuber	unitless		3.13E−02	Chapter 8
fuel_cons_peat	$kg_{DW}\ year^{-1}$	Garden plot	3.45E+03	Grolander (2013, Section 9.14.9)
fuel_cons_wood	$kg_{DW}\ year^{-1}$	Garden plot	3.97E+03	Grolander (2013, Section 9.14.8)
height_CA_cereal	m		9.00E−01	Grolander (2013, Section 9.5.9)
height_CA_fodder	m		4.00E−01	Grolander (2013, Section 9.5.9)
height_CA_ter	m		3.00E−01	Grolander (2013, Section 9.5.9)
height_CA_tuber	m		4.00E−01	Grolander (2013, Section 9.5.9)
height_CA_veg	m	Garden plot	2.50E−01	Grolander (2013, Section 9.5.9)
height_L1_ter	m		2.50E+00	Grolander (2013, Section 9.5.2)
height_L2_ter	m		1.00E+01	Grolander (2013, Section 9.5.3)
height_ref_ter	m		1.00E+01	Grolander (2013, Section 9.5.8)
ingRate_C_cattle	$kg_C\ day^{-1}$		4.00E+00	Grolander (2013, Section 9.13.1)
ingRate_soil_cattle	$kg_{DW}\ day^{-1}$		3.00E−01	Grolander (2013, Section 9.13.2)
ingRate_water_cattle	$m^3\ day^{-1}$		4.00E−02	Grolander (2013, Section 9.13.3)
karman_const	unitless		4.10E−01	Grolander (2013, Section 9.5.4)
LAI_cereal	$m^2\ m^{-2}$	Drained mire	4.00E+00	Grolander (2013, Section 9.5.6)
LAI_fodder	$m^2\ m^{-2}$	Infield-outland	6.00E+00	Grolander (2013, Section 9.5.6)
LAI_ter	$m^2\ m^{-2}$		1.20E+00	Grolander (2013, Section 9.5.6)
LAI_tuber	$m^2\ m^{-2}$	Drained mire	4.00E+00	Grolander (2013, Section 9.5.6)
LAI_veg	$m^2\ m^{-2}$	Garden plot	5.00E+00	Grolander (2013, Section 9.5.6)
leaf_width_cereal	m		1.50E−02	Grolander (2013, Section 9.5.5)
leaf_width_fodder	m		2.00E−02	Grolander (2013, Section 9.5.5)
leaf_width_ter	m		5.00E−03	Grolander (2013, Section 9.5.5)
leaf_width_tuber	m		6.00E−02	Grolander (2013, Section 9.5.5)
leaf_width_veg	m	Garden plot	1.50E−01	Grolander (2013, Section 9.5.5)
LeafStoreCapacy	$m^3\ m^{-2}$	Garden plot	3.00E−04	Grolander (2013, Section 9.14.3)
minRate	$kg_C\ kg_C^{-1}\ year^{-1}$	Infield-outland	2.90E−03	Grolander (2013, Section 8.7.3)
minRate	$kg_C\ kg_C^{-1}\ year^{-1}$	Garden plot	2.90E−03	Grolander (2013, Section 8.7.3)
minRate	$kg_C\ kg_C^{-1}\ year^{-1}$	Drained mire	7.00E−03	Grolander (2013, Section 8.7.3)
minRate_regoPG_ter	$kg_C\ kg_C^{-1}\ year^{-1}$		6.50E−05	Grolander (2013, Section 9.9.1)
minRate_regoUp_ter	$kg_C\ kg_C^{-1}\ year^{-1}$		2.90E−03	Grolander (2013, Section 9.9.1)
N_irrig	$year^{-1}$	Garden plot	4.00E+00	Grolander (2013, Section 9.14.5)
NPP_cereal	$kg_C\ m^{-2}\ year^{-1}$	Infield-outland	1.00E−01	Grolander (2013, Section 9.11)
NPP_cereal	$kg_C\ m^{-2}\ year^{-1}$	Drained mire	1.17E−01	Grolander (2013, Section 9.11)
NPP_fodder	$kg_C\ m^{-2}\ year^{-1}$	Drained mire	2.13E−01	Grolander (2013, Section 9.11)
NPP_ter	$kg_C\ m^{-2}\ year^{-1}$		3.20E−01	Grolander (2013, Section 9.11)
NPP_tuber	$kg_C\ m^{-2}\ year^{-1}$	Drained mire	1.58E−01	Grolander (2013, Section 9.11)
NPP_tuber	$kg_C\ m^{-2}\ year^{-1}$	Garden plot	3.61E−01	Grolander (2013, Section 9.11)
NPP_veg	$kg_C\ m^{-2}\ year^{-1}$	Garden plot	1.50E−01	Chapter 8
percolation_agri	$m^3\ m^{-2}\ year^{-1}$	Drained mire	1.60E−01	Chapter 8
percolation_agri	$m^3\ m^{-2}\ year^{-1}$	Infield-outland	1.60E−01	Chapter 8
percolation_agri	$m^3\ m^{-2}\ year^{-1}$	Garden plot	1.60E−01	Chapter 8
piston_vel_ter	m $year^{-1}$		5.00E+01	Grolander (2013, Section 9.4.5)
prod_edib_berry	$kg_C\ m^{-2}\ year^{-1}$		1.10E−04	Löfgren (2010, Section 13.4.5)

Name	Unit	Land use	Value	Reference
prod_edib_game	$kg_C\ m^{-2}\ year^{-1}$		7.80E−06	Löfgren (2010, Section 13.4.5)
prod_edib_mush	$kg_C\ m^{-2}\ year^{-1}$		3.00E−05	Löfgren (2010, Section 13.4.5)
q_sat_unsat_agri	$m^3\ m^{-2}\ year^{-1}$	Drained mire	6.90E−02	Chapter 8
SoilResp	$kg_C\ m^{-2}$ year−1	Garden plot	1.46E+00	Chapter 8
SoilResp	$kg_C\ m^{-2}$ year−1	Infield-outland	1.46E+00	Chapter 8
SoilResp_gyttja	$kg_C\ m^{-2}$ year−1	Drained mire	1.46E+00	Chapter 8
SoilResp_peat	$kg_C\ m^{-2}$ year−1	Drained mire	1.46E+00	Chapter 8
SoilResp_ter	$kg_C\ m^{-2}$ year−1		3.35E−01	Chapter 8
solubilityCoef_ter	$(mol\ m^{-3})\cdot(mol\ m^{-3})^{-1}$		1.23E+00	Grolander (2013, Section 9.4.6)
time_irrigationPeriod	days	Garden plot	4.00E+01	Chapter 8
washoffCoef_veg	$year^{-1}$	Garden plot	1.53E+01	Grolander (2013, Section 9.14.4)
vel_wind_height_ref_ter	$m\ s^{-1}$		1.70E+00	Chapter 8
yield_tuber	$kg_C\ m^{-2}\ year^{-1}$	Garden plot	2.19E−01	Chapter 8
yield_veg	$kg_C\ m^{-2}\ year^{-1}$	Garden plot	1.13E−01	Chapter 8
z_regoUp	m	Infield-outland	2.50E−01	Grolander (2013, Section 9.7)
z_regoUp	m	Garden plot	2.50E−01	Grolander (2013, Section 9.7)
z_regoUp_ter	m		3.00E−01	Grolander (2013, Section 9.7)

Appendix H

Human characteristics

Table H-1. Human characteristics parameter data. (svn://svn.skb.se/projekt/SFLsurface/Synthesis/Parameters/HumanCharac.xlsm)

Name	Unit	Land use	Value	Reference
area	m^2	Infield-outland	5 000	Grolander (2013, Section 10.9)
area	m^2 individual^{-1}	Garden plot	54	
area_support	m^2	Drained mire	6 200	Grolander (2013, Section 10.8)
area_support	m^2	Infield-outland	10 000	Grolander (2013, Section 10.8)
f_area_cereal	m^2 m^{-2}	Drained mire	0.48	Grolander (2013, Section 10.7)
f_area_fodder	m^2 m^{-2}	Drained mire	0.33	Grolander (2013, Section 10.7)
f_area_tuber	m^2 m^{-2}	Drained mire	0.06	Grolander (2013, Section 10.7)
f_area_tuber	m^2 m^{-2}	Garden plot.	0.46	
f_area_veg	m^2 m^{-2}	Garden plot.	0.54	
f_diet_cereal	kg_C kg_C^{-1}	Drained mire	0.6	Grolander (2013, Section 10.6)
f_diet_cereal	kg_C kg_C^{-1}	Infield-outland	0.71	Grolander (2013, Section 10.6)
f_diet_fish_max	kg_C kg_C^{-1}	Forager	0.35	Grolander (2013, Section 10.11)
f_diet_meat	kg_C kg_C^{-1}	Drained mire	0.04	Grolander (2013, Section 10.6)
f_diet_meat	kg_C kg_C^{-1}	Infield-outland	0.05	Grolander (2013, Section 10.6)
f_diet_milk	kg_C kg_C^{-1}	Drained mire	0.25	Grolander (2013, Section 10.6)
f_diet_milk	kg_C kg_C^{-1}	Infield-outland	0.24	Grolander (2013, Section 10.6)
f_diet_tuber	kg_C kg_C^{-1}	Drained mire	0.11	Grolander (2013, Section 10.6)
f_diet_tuber	kg_C kg_C^{-1}	Garden plot	0.05	Grolander (2013, Section 10.6)
f_diet_veg	kg_C kg_C^{-1}	Garden plot	0.03	Grolander (2013, Section 10.6)
f_meadow	unitless	Infield-outland	0.5	Grolander (2013, Section 10.9)
f_time_agri	year year^{-1}	Infield-outland	0.55	Grolander (2013, Section 10.12)
f_time_hay	year year^{-1}	Infield-outland	0.45	Grolander (2013, Section 10.12)
ingRate_C	kg_C year^{-1}	All	110	Grolander (2013, Section 10.4)
ingRate_water	m^3 year^{-1}	All	0.73	Grolander (2013, Section 10.3)
inhRate	m^3 h^{-1}	All	1	Grolander (2013, Section 10.5)
N_group	unitless	Forager	30	Grolander (2013, Section 10.10)
N_group	unitless	Drained mire	10	Grolander (2013, Section 10.10)
N_group	unitless	Infield-outland	10	Grolander (2013, Section 10.10)
N_group	unitless	Garden plot	5	Grolander (2013, Section 10.10)
q_well	m^3 year^{-1}	Garden plot	256	
time_exposure	h year^{-1}	Forager	8 760	Grolander (2013, Section 10.12)
time_exposure	h year^{-1}	Drained mire	54	Grolander (2013, Section 10.12)
time_exposure	h year^{-1}	Infield-outland	220	Grolander (2013, Section 10.12)
time_exposure	h year^{-1}	Garden plot	54	Grolander (2013, Section 10.12)
time_exposure_comb	h year^{-1}	Garden plot	8 760	New

Appendix I

Alternative regional climate

Table I-1. Parameter data used in the alternative regional climate evaluation case. (svn://svn.skb.se/projekt/SFLsurface/Synthesis/Parameters/BCC5*_local_climate_*.xlsm)

Name	Unit	Central location	North location	Western location
NetPrec	m year^{-1}	0.25	0.37	0.28
Runoff_basin	m year^{-1}	0.33	0.48	0.37
Runoff_watershed	m year^{-1}	0.27	0.39	0.30
q_bedrock_ter	m year^{-1}	0.30	0.37	0.32
q_sat_unsat_agri	m year^{-1}	0.07	0.05	0.07
amount_irrig	m year^{-1}	0.09	0.07	0.12
percolation_agri	m^3 m^{-2} year^{-1}	0.25	0.37	0.28

Appendix J

An increased greenhouse effect

Table J-1. Parameter data used in the increased greenhouse effect evaluation case. (svn://svn.skb.se/projekt/SFLsurface/Synthesis/Parameters/BCC10*_increased_greenhouse.xlsm)

Name	Unit	Land use	Value
amount_irrig_IGE	m $year^{-1}$	Drained mire.	9.00E−02
amount_irrig_IGE	m $year^{-1}$	Garden plot.	1.25E−01
conc_C_atmos_IGE	kg_C m^{-3}		2.73E−04
f_trans_cereal_IGE	unitless		2.87E−02
N_irrig_IGE	$year^{-1}$	Garden plot.	1.00E+01
N_irrig_IGE	$year^{-1}$	Drained mire.	2.00E+00
NetPrec_IGE	m $year^{-1}$		1.28E−01
percolation_agri_IGE	m^3 m^{-2} $year^{-1}$	Drained mire.	1.30E−01
q_bedrock_ter_IGE	m $year^{-1}$	lobj206.	2.38E−01
q_sat_unsat_agri_IGE	m $year^{-1}$	Drained mire.	0.00E+00
Runoff_basin_IGE	m $year^{-1}$		1.68E−01
Runoff_watershed_IGE	m $year^{-1}$		1.36E−01
threshold_IGE	year		2.51E+04
time_irrigationPeriod_IGE	days	Drained mire.	6.00E+01
time_irrigationPeriod_IGE	days	Garden plot.	9.00E+01
washoffCoef_fodder_IGE	$year^{-1}$		1.61E+01
yield_cereal_IGE	kg_C m^{-2} $year^{-1}$	Drained mire.	6.00E−02
yield_fodder_IGE	kg_C m^{-2} $year^{-1}$	Drained mire.	6.00E−02
yield_tuber_IGE	kg_C m^{-2} $year^{-1}$1	Drained mire.	9.60E−02

Appendix K

Simplified glacial cycle

Table K-1. Parameter data used in the simplified glaciation evaluation case. (svn://svn.skb.se/projekt/SFLsurface/Synthesis/Parameters/BCC51_glaciation.xlsm)

Name	Unit	Value
area_obj_ter_init	m^2	7.71E+04
biom_pp_ter_perm	$kg_C\ m^{-2}$	8.20E−01
conc_C_atmos_perm	$kg_C\ m^{-3}$	1.10E−04
minRate_regoUp_ter_perm	$kg_C\ kg_C^{-1}\ year^{-1}$	8.10E−04
NPP_ter_perm	$kg_C\ m^{-2}\ year^{-1}$	9.00E−02
piston_vel_ter_perm	$m\ year^{-1}$	4.70E+01
prod_edib_cray_lake_perm	$kg_C\ m^{-2}\ year^{-1}$	0.00E+00
prod_edib_fish_lake_perm	$kg_C\ m^{-2}\ year^{-1}$	3.22E−05
solubilityCoef_ter_perm	$(mol\ m^{-3})\ (mol\ m^{-3})^{-1}$	1.34E+00

Table K-2. Hydological fluxes used in the simplified glaciation evaluation case. (svn://svn.skb.se/projekt/SFLsurface/Synthesis/Parameters/BCC51_glaciation.xlsm)

Name	Unit	Object	Value
q_bedrock_low_ter_perm	$m\ year^{-1}$	lobj206.	0.00
q_downstream_perm	$m\ year^{-1}$	lobj206.	1.93
q_gl_low_ter_perm	$m\ year^{-1}$	lobj206.	0.00
q_gl_pg_ter_perm	$m\ year^{-1}$	lobj206.	0.00
q_low_bedrock_ter_perm	$m\ year^{-1}$	lobj206.	0.00
q_low_gl_ter_perm	$m\ year^{-1}$	lobj206.	0.00
q_peat_pg_ter_perm	$m\ year^{-1}$	lobj206.	0.00
q_peat_up_ter_perm	$m\ year^{-1}$	lobj206.	0.00
q_pg_gl_ter_perm	$m\ year^{-1}$	lobj206.	0.00
q_pg_peat_ter_perm	$m\ year^{-1}$	lobj206.	0.00
q_up_peat_ter_perm	$m\ year^{-1}$	lobj206.	0.00
q_up_wat_ter_perm	$m\ year^{-1}$	lobj206.	1.03
q_bedrock_low_lake_perm	$m\ year^{-1}$	lobj207.	0.32
q_downstream_perm	$m\ year^{-1}$	lobj207.	2.77
q_gl_low_lake_perm	$m\ year^{-1}$	lobj207.	0.01
q_gl_pg_lake_perm	$m\ year^{-1}$	lobj207.	0.32
q_low_bedrock_lake_perm	$m\ year^{-1}$	lobj207.	0.00
q_low_gl_lake_perm	$m\ year^{-1}$	lobj207.	0.32
q_pg_gl_lake_perm	$m\ year^{-1}$	lobj207.	0.01
q_pg_up_lake_perm	$m\ year^{-1}$	lobj207.	2.91
q_up_pg_lake_perm	$m\ year^{-1}$	lobj207.	2.60
q_up_wat_lake_perm	$m\ year^{-1}$	lobj207.	2.91
q_wat_up_lake_perm	$m\ year^{-1}$	lobj207.	2.60

Table K-3. Parameters used to define times of thresholds in the simplified glaciation evaluation case. (svn://svn.skb.se/projekt/SFLsurface/Synthesis/Parameters/BCC51_glaciation.xlsm)

Name	Unit	Value
threshold_submerged	year	70 000
time_submerged	year	8 742
z_regoPeat_init[1]	m	1.69

[1] Used for object 206

Arkitektkopia AB, Bromma, 2020

SKB is responsible for managing spent nuclear fuel and radioactive waste produced by the Swedish nuclear power plants such that man and the environment are protected in the near and distant future.

skb.se